

TECHNICAL REPORT STANDARD TITLE PAGE

1. Report No. TX - 99 1780 - 2		2. Government Accession No.		3. Recipient's Catalog No.	
4. Title and Subtitle A SENSITIVITY STUDY OF PARAMETERS INVOLVED IN DESIGN WITH SEISMIC MODULI				5. Report Date January 2002	
				6. Performing Organization Code	
7. Authors L. Ke, S. Nazarian, I. Abdallah, and D. Yuan				8. Performing Organization Report No. Research Report 1780-2	
9. Performing Organization Name and Address Center for Highway Materials Research The University of Texas at El Paso El Paso, Texas 79968-0516				10. Work Unit No.	
				11. Contract or Grant No. Project No. 0-1780	
12. Sponsoring Agency Name and Address Texas Department of Transportation Construction Division, Research and Technology Transfer Division P.O. Box 5080 Austin, Texas 78763-5080				13. Type of Report and Period Covered Interim Report 9/98 -8/99	
				14. Sponsoring Agency Code	
15. Supplementary Notes Research Performed in Cooperation with TxDOT Research Study Title: Feasibility Study for Determining Design Modulus Values Using Seismic Data Collection					
16. Abstract <p>Currently, one of the most popular approaches for evaluating the structural adequacy of a flexible pavement involves analyzing the measured deflections collected with a Falling Weight Deflectometer (FWD). The benefit is that the moduli backcalculated from this approach can be conveniently used in pavement design and analysis since a load similar to a traffic load is applied in the FWD test. Another nondestructive device, the Seismic Pavement Analyzer (SPA), can be used to obtain seismic moduli of pavement layers. In order to incorporate seismic moduli into pavement design and analysis, models should be developed to consider the load-induced nonlinear behavior of pavement materials</p> <p>In this report, a constitutive model that relates the modulus of a pavement material with its state of stress is adopted. To carry out this constitutive model, an equivalent-linear model has been developed based on the multi-layer program BISAR. The nonlinear static model and the nonlinear dynamic model have also been studied with the same constitutive model using the finite element software ABAQUS</p> <p>By analyzing the responses of the typical pavement, the degree of material nonlinearity considered in different models and the influence of dynamic effects on pavement response are investigated. The nonlinear static model and the nonlinear dynamic model yield similar results as long as the bedrock is not at a shallow depth. However, implementing these two models in everyday design may be time-consuming. The pavement response from the equivalent-linear model can be rapidly obtained, and the results are generally acceptable.</p>					
17. Key Words Falling Weight Deflectometer, Seismic Pavement Analyzer, Seismic Nondestructive Testing, flexible pavement			18. Distribution Statement No restrictions. This document is available to the public through the National Technical Information Service, 5285 Port Royal Road, Springfield, Virginia 22161		
19. Security Classified (of this report) Unclassified		20. Security Classified (of this page) Unclassified		21. No. of Pages 232	22. Price

A Sensitivity Study of Parameters Involved in Design with Seismic Moduli

by

**Liqun Ke, MSCE
Soheil Nazarian, Ph.D., P.E.
Imad Abdallah, MSCE
and
Deren Yuan, Ph.D.**

Research Project 0-1780

Conducted for

Texas Department of Transportation

Research Report 1780-2

January 2002

**The Center for Highway Materials Research
The University of Texas at El Paso
El Paso, TX 79968-0516**

The contents of this report reflect the view of the authors, who are responsible for the facts and the accuracy of the data presented herein. The contents do not necessarily reflect the official views or policies of the Texas Department of Transportation or the Federal Highway Administration. This report does not constitute a standard, specification, or regulation.

The material contained in this report is experimental in nature and is published for informational purposes only. Any discrepancies with official views or policies of the Texas Department of Transportation or the Federal Highway Administration should be discussed with the appropriate Austin Division prior to implementation of the procedures or results.

NOT INTENDED FOR CONSTRUCTION, BIDDING, OR PERMIT PURPOSES

Liqun Ke, MSCE
Soheil Nazarian, Ph.D., P.E. (69263)
Imad Abdallah, MSCE
Deren Yuan, Ph.D.

Acknowledgments

The authors would like to express their sincere appreciation to Mark McDaniel of the TxDOT Design Division and Joe Thompson of the Dallas District for their ever-present support.

We would also like to thank the hardworking people from districts that generously offered their time. Especially, we would like to thank Raymond Guerra of the El Paso District for arranging the logistics for the field tests.

The authors would also like to thank undergraduates who worked on this project. Specifically, recognition is extended to Susana Facio and Ruben Williams for their enthusiasm in performing all the necessary tests for this project. Rachel Vidal assisted us with the editorial aspects of this report.

ABSTRACT

Currently, one of the most popular approaches for evaluating the structural adequacy of a flexible pavement involves analyzing the measured deflections collected with a Falling Weight Deflectometer (FWD). The benefit is that the moduli backcalculated from this approach can be conveniently used in pavement design and analysis since a load similar to a traffic load is applied in the FWD test. Another nondestructive device, the Seismic Pavement Analyzer (SPA), can be used to obtain seismic moduli of pavement layers. Seismic moduli are similar to linear elastic ones since they correspond to very small strain levels. In order to incorporate seismic moduli into pavement design and analysis, models should be developed to consider the load-induced nonlinear behavior of pavement materials.

In this report, a constitutive model that relates the modulus of a pavement material with its state of stress is adopted. To carry out this constitutive model, an equivalent-linear model has been developed based on the multi-layer program BISAR. The nonlinear static model and the nonlinear dynamic model have also been studied with the same constitutive model using the finite element software ABAQUS.

A typical pavement section was assumed. By comparing responses of this typical pavement section, the sensitivity of critical strains and remaining lives of the typical pavement to variations in pavement parameters was studied. It is shown that in the equivalent-linear model and nonlinear models, the parameters of the pavement layers affect the response in much the same way.

By analyzing the responses of the typical pavement, the degree of material nonlinearity considered in different models and the influence of dynamic effects on pavement response are investigated. The nonlinear static model and the nonlinear dynamic model yield similar results as long as the bedrock is not at a shallow depth. However, implementing these two models in everyday design may be time-consuming. The pavement response from the equivalent-linear model can be rapidly obtained, and the results are generally acceptable.

Implementation Statement

With the initiation of "AASHTO 2002" program, which aims towards a mechanistic pavement design implementable by all highway agencies, this project may have significant impact. To develop a mechanistic pavement design that can contain performance-based specifications, the same engineering properties that are used to design a pavement should be used to determine the suitability of a material for construction and should be specified as criteria for accepting the material placed at the site. The only practical and available method at this time is based on seismic testing. Furthermore, it seems that with proper laboratory testing technique and proper simulation one can develop remaining life models that are more realistic.

Some of the software and protocols being developed can also be applied in pavement design with the FWD.

TABLE OF CONTENTS

	Page
ACKNOWLEDGEMENTS.....	iii
ABSTRACT.....	iv
IMPLEMENTATION STATEMENT.....	v
TABLE OF CONTENTS	vi
LIST OF FIGURES	ix
LIST OF TABLES.....	xi
CHAPTER 1 INTRODUCTION	
1.1 Problem Statement.....	1
1.2 Objective and Approaches.....	1
1.3 Organization.....	2
CHAPTER 2 LITERATURE REVIEW	
2.1 General.....	5
2.2 Falling Weight Deflectometer.....	5
2.3 Seismic Pavement Analyzer	8
2.4 Pavement Material Characterization.....	11
2.4.1 Base and Subgrade Materials.....	13
2.4.2 Bituminous Materials.....	13
2.5 Pavement Remaining Life.....	15
CHAPTER 3 DESCRIPTION OF PAVEMENT ANALYSIS MODELS	
3.1 Introduction.....	17
3.2 Constitutive Models Used.....	17
3.2.1 Linear Elastic Model.....	18
3.2.2 Equivalent-Linear Model.....	18
3.2.3 Nonlinear Models	24
3.3 Description of Algorithms	24
3.3.1 Multi-Layer Linear System.....	24
3.3.2 Multi-Layer Equivalent-Linear System.....	26
3.3.3 Finite Element Analysis.....	28
3.4 Typical Pavement Section.....	29

CHAPTER 4 PAVEMENT RESPONSE UNDER LINEAR ELASTIC MODEL	
4.1 Introduction.....	35
4.2 Sensitivity Study of “3-12 PAVE”	35
4.2.1 Thickness of AC Layer	38
4.2.2 Depth to Bedrock	39
4.2.3 Other Properties	41
4.3 Summary of the Sensitivity Study for the Linear Elastic Models	43
CHAPTER 5 PAVEMENT RESPONSE UNDER EQUIVALENT-LINEAR MODEL	
5.1 Introduction.....	55
5.2 Effects of Number of Sublayers on Response from Equivalent-Linear Model	55
5.3 Sensitivity Study for “3-12 PAVE”	56
5.3.1 AC Layer.....	59
5.3.2 Base Layer	59
5.3.3 Upper Subgrade	63
5.3.4 Depth to Bedrock	67
5.3.5 Summary	69
5.4 Sensitivity Study Results for the Four Pavements.....	70
CHAPTER 6 PAVEMENT RESPONSE UNDER NONLINEAR STATIC MODEL	
6.1 Introduction.....	77
6.2 Sensitivity Study for Typical Section	77
6.2.1 AC Layer.....	77
6.2.2 Base Layer	78
6.2.3 Upper Subgrade	78
6.2.4 Conclusions of Sensitivity Study.....	85
6.3 Sensitivity Study Results for the Four Pavements.....	85
CHAPTER 7 DYNAMIC RESPONSES OF PAVEMENT	
7.1 Introduction.....	95
7.2 Approaches to Modeling of Dynamic Effects	95
7.3 Dynamic Responses of One Typical Pavement Section	98
7.3.1 Response Under Linear Dynamic Model.....	98
7.3.2 Response Under Nonlinear Dynamic Model	99
7.4 Sensitivity Study for “3-12 PAVE”	99
7.4.1 Linear Dynamic Model	99
7.4.2 Nonlinear Dynamic Model	102
7.4.2.1 Nonlinear Parameters of Base Layer	105
7.4.2.2 Nonlinear Parameters of Upper Subgrade	105
7.4.3 Conclusions of Sensitivity Study for “3-12 PAVE’	106
7.5 Sensitivity Study Results for the Four Pavements.....	106
CHAPTER 8 ANALYSIS OF RESULTS	
8.1 Introduction.....	115
8.2 Linear Static Models	115

8.3 Approximation in Models	117
8.3.1 Linear Static Model	117
8.3.2 Linear Dynamic Model.....	119
8.3.3 Equivalent-Linear Model.....	120
8.3.4 Nonlinear Static Model.....	120
8.3.5 Summary.....	120
8.4 Parameters to Be Considered.....	121
CHAPTER 9 SUMMARY, CONCLUSIONS AND RECOMMENDATIONS	
9.1 Summary.....	127
9.2 Conclusions.....	128
9.3 Recommendations.....	130
REFERENCES	131
APPENDIX A: Results of Sensitivity Study Under Linear Static Model	135
APPENDIX B: Results of Sensitivity Study Under Equivalent-Linear Model.....	155
APPENDIX C: Results of Sensitivity Study Under Nonlinear Static Model.....	171
APPENDIX D: Responses of Typical Pavement Section Under Linear Dynamic Model.....	187
APPENDIX E: Responses of Typical Pavement Section Under Nonlinear Dynamic Model	195

LIST OF FIGURES

Figure	Page
2.1 Geometrical Configuration of Falling Weight Deflectometer Test (Uddin et al., 1983).....	6
2.2 Schematic of Seismic Pavement Analyzer	9
2.3 Typical Stress-Strain Curve for a Pavement Material	12
2.4 Variation in AC Modulus with Frequency and Temperature (from Aouad et al., 1993).....	14
2.5 Frequency Dependency of AC Modulus (from Daniel and Kim, 1998).....	15
2.6 Impact of Air Void Content on Modulus of AC (from Rojas, 1999)	16
3.1 State of Stress under Seismic Test.....	21
3.2 State of Stress under FWD Test.....	21
3.3 A Typical n-layer System	25
3.4 Flow Chart of Implementation of Equivalent-Linear Model.....	27
3.5 Optimal Mesh Used to Analyze Typical Pavement in ABAQUS	30
3.6 Two Types of Elements Used in Finite Element Analysis	31
3.7 Profile of Pavement Section “3-12 PAVE” Used in This Study	33
4.1 Distribution of Thickness of AC Using Monte Carlo Simulation for “3-12 PAVE”	38
4.2 Variations in Critical Strains with Thickness of AC Layer for Pavement Section “3-12 PAVE”	40
4.3 Variations in Remaining Lives with Thickness of AC layer for “3-12 PAVE”	41
4.4 Variations in Critical Tensile Strain with Parameters for Pavement “3-12 PAVE”	44
4.5 Variations in Fatigue Remaining Life with Parameters for Pavement “3-12 PAVE”	45
4.6 Variations in Critical Compressive Strain with Parameters for Pavement “3-12 PAVE”	47
4.7 Variations in Rutting Remaining Life with Parameters for Pavement “3-12 PAVE”	48
5.1 Variations in Critical Strains with Parameter k_2 of Base for “3-12 PAVE”	62
5.2 Variations in Remaining Lives with Parameter k_2 of Base.....	63
5.3 Variations in Critical Strains with Parameter k_3 of Base for “3-12 PAVE”	64
5.4 Variations in Remaining Lives with Parameter k_3 of Base for “3-12 PAVE”.....	65
5.5 Variations in Critical Strains with Parameter k_2 of Upper Subgrade for “3-12 PAVE”....	66

5.6	Variations in Remaining Lives with Parameter k_2 of Upper Subgrade for “3-12 PAVE”	67
5.7	Variations in Critical Strains with Parameter k_3 of Upper Subgrade.....	68
5.8	Variations in Remaining Lives with Parameter k_3 of Upper Subgrade	69
6.1	Variations in Critical Strains with Parameter k_2 of Base	81
6.2	Variations in Remaining Lives with Parameter k_2 of Base.....	82
6.3	Variations in Critical Strains with Parameter k_3 of Base	83
6.4	Variations in Remaining Lives with Parameter k_3 of Base.....	84
6.5	Variations in Critical Strains with Parameter k_2 of Upper Subgrade.....	86
6.6	Variations in Remaining Lives with Parameter k_2 of Upper Subgrade	87
6.7	Variations in Critical Strains with Parameter k_3 of Upper Subgrade.....	88
6.8	Variations in Remaining Lives with Parameter k_3 of Upper Subgrade	89
7.1	Typical Half Sine Impulse Assumed in Dynamic Analysis.....	97
7.2	Surface Deflections of Typical Pavement Section Under Linear Dynamic Model	98
7.3	Critical Strains of Typical Pavement Section Under Linear Dynamic Model.....	99
7.4	Surface Deflections of Typical Pavement Section Under Nonlinear Dynamic Model ...	101
7.5	Critical Strains of Typical Pavement Section Under Nonlinear Dynamic Model	101
7.6	Surface Deflections Under Nonlinear Dynamic Model with Different k_2 of Base.....	107
7.7	Surface Deflections Under Nonlinear Dynamic Model with Different k_3 of Base.....	108
7.8	Surface Deflections Under Nonlinear Dynamic Model with Different k_2 of Upper Subgrade	110
7.9	Surface Deflections under Nonlinear Dynamic Model with Different k_3 of Upper Subgrade	111

LIST OF TABLES

Table	Page
3.1 Parameters Affecting Modulus of Granular Bases and Subgrades (after Hardin and Drnevich, 1972).....	20
3.2 Properties of Pavement Section “3-12 PAVE”	34
4.1 Response of Pavement 3-12 PAVE with Different Computer Programs	36
4.2 Levels of Sensitivity Assigned to Each Parameter Based on Sensitivity Index	37
4.3 Variation in Response of Pavement Section “3-12 PAVE” with Depth of Bedrock.....	42
4.4 Levels of Sensitivity of Pavement Parameters with Respect to Critical Tensile Strain and Fatigue Remaining Life for Pavement “3-12 PAVE”	46
4.5 Levels of Sensitivity of Pavement Parameters with Respect to Critical Compressive Strain and Rutting Remaining Life for Pavement “3-12 PAVE”	49
4.6 Sensitivity of Pavement Parameters to Critical Tensile Strain under Linear Elastic Model.....	50
4.7 Sensitivity of Pavement Parameters to Critical Compressive Strain under Linear Elastic Model	51
4.8 Sensitivity of Pavement Parameters to Fatigue Remaining Life under Linear Elastic Model.....	52
4.9 Sensitivity of Pavement Parameters to Rutting Remaining Life under Linear Elastic Model.....	53
5.1 Comparison of Deflections with Different Number of Sublayers in Equivalent-Linear Mode for “3-12 PAVE”	57
5.2 Comparison of Critical Strains and Remaining Lives with Different Number of Sublayers in Equivalent-Linear Model for “3-12 PAVE”	58
5.3 Levels of Sensitivity of Pavement Parameters with Respect to Critical Tensile Strain and Fatigue Remaining Life for “3-12 PAVE”	60
5.4 Levels of Sensitivity of Pavement Parameters with Respect to Critical Compressive Strain and Rutting Remaining Life for “3-12 PAVE”	61
5.5 Response of Typical Pavement Section with Different Depths of Bedrock for “3-12 PAVE”	71
5.6 Sensitivity of Critical Tensile Strain to Pavement Parameters under Equivalent-Linear Model	72

5.7	Sensitivity of Critical Compressive Strain to Pavement Parameters under Equivalent-Linear Model	73
5.8	Sensitivity of Fatigue Remaining Life to Pavement Parameters under Equivalent-Linear Model	74
5.9	Sensitivity of Rutting Remaining Life to Pavement Parameters under Equivalent-Linear Model	75
6.1	Sensitivity of Critical Tensile Strain and Fatigue Remaining Life to Pavement Parameters	79
6.2	Sensitivity of Critical Compressive Strain and Rutting Remaining Life to Pavement Parameters	80
6.3	Sensitivity of Critical Tensile Strain to Pavement Parameters under Nonlinear Model	90
6.4	Sensitivity of Critical Compressive Strain to Pavement Parameters under Nonlinear Model	91
6.5	Sensitivity of Fatigue Remaining Life to Pavement Parameters under Nonlinear Model	92
6.6	Sensitivity of Rutting Remaining Life to Pavement Parameters under Nonlinear Model	93
7.1	Peak Deflections and Critical Strains Under Linear Dynamic Models	100
7.2	Peak Deflections and Critical Strains with Different Damping Coefficients (β) Under Linear Dynamic Model.....	103
7.3	Peak Deflections and Critical Strains with Different Material Densities Under Linear Dynamic Model	104
7.4	Levels of Sensitivity of Nonlinear Parameters	109
7.5	Sensitivity of Nonlinear Parameters in Different Pavements with Respect to Critical Tensile Strain and Fatigue Remaining Life	112
7.6	Sensitivity of Nonlinear Parameters in Different Pavements with Respect to Critical Compressive Strain and Rutting Remaining Life	113
8.1	Pavement Responses Under Linear Static Models in BISAR and ABAQUS for “3-12 PAVE”.....	116
8.2	Pavement Responses Under Different Models for “3-12 PAVE”	118
8.3	Approximate Computation Times of Different Models.....	119
8.4	Summary of Impact of Different Pavement Parameters on Fatigue Cracking Remaining Life of Pavement for Different Analysis Methods (Thin AC Layer)	122
8.5	Summary of Impact of Different Pavement Parameters on Fatigue Cracking Remaining Life of Pavement for Different Analysis Methods (Thick AC Layer).....	123
8.6	Summary of Impact of Different Pavement Parameters on Rutting Remaining Life of Pavement for Different Analysis Methods (Thin AC Layer)	124
8.7	Summary of Impact of Different Pavement Parameters on Rutting Remaining Life of Pavement for Different Analysis Methods (Thick AC Layer)	125

CHAPTER ONE

INTRODUCTION

1.1 PROBLEM STATEMENT

Nondestructive testing techniques are widely used as tools for measuring the stiffness parameters of pavement sections. Moduli of pavement materials obtained in that manner are used to determine the critical strains and, thus, to estimate the remaining lives of pavement systems.

The Falling Weight Deflectometer (FWD) is one of the most popular nondestructive testing devices. The FWD applies an impulse load to the pavement, and seven sensors measure the surface deflections of the pavement. Moduli of pavement layers can be obtained from these deflections by using a backcalculation program. Since the load applied by the FWD to the pavement is similar to that exerted by traffic, the FWD moduli are used in pavement design and analysis without considering the nonlinear behavior of materials. One shortcoming of this method is the nonuniqueness of the backcalculated moduli from the FWD deflections.

Another nondestructive testing device is the Seismic Pavement Analyzer (SPA), whose operating principle is based on generating and detecting stress waves in a layered medium. Based on a dispersion curve, the elastic moduli of different layers can be obtained through an inversion process. Seismic moduli are linear elastic moduli since they correspond to very small external loads. However, the SPA moduli cannot be used in pavement analysis and design without transformation because the traffic load applied to the pavement is much larger than that applied by the SPA. To use seismic moduli, the load-induced nonlinear behavior of pavement materials has to be taken into consideration.

1.2 OBJECTIVE AND APPROACHES

The major objective of Project 0-1780 is to explore the feasibility of incorporating seismic moduli in pavement design and analysis. For this purpose, a constitutive model recommended by a National Cooperative Highway Research Program (NCHRP) project was used. This model relates the nonlinear modulus of a pavement material with its state of stress. Seismic moduli can be combined to determine the nonlinear modulus.

The above constitutive model was implemented into several computer algorithms. The algorithms include equivalent-linear, nonlinear static and nonlinear dynamic. An equivalent-linear algorithm, which is based on static linear elastic layered algorithms, in an approximate fashion, can consider the load-induced nonlinear behavior of pavement. An iterative process is employed to consider the nonlinearity of the pavement materials. The nonlinear static model is carried out by using the comprehensive finite element software ABAQUS. The dynamic nature of load can also be investigated in ABAQUS. The nonlinear dynamic model considers both nonlinear and dynamic behavior of pavement materials.

Four typical pavement sections are assumed. The base and the upper subgrade are considered to exhibit load-induced nonlinear behavior. By comparing the responses of the typical pavement sections under different algorithms, the degrees of influence of material nonlinearity and the dynamic effects on pavement response are investigated.

1.3 ORGANIZATION

Chapter 2 contains a review of relevant literature dealing with data interpretation from the FWD and the SPA devices. The FWD data interpretation requires a backcalculation process to obtain material properties from the deflection basin. An inversion process is involved in the SPA data interpretation. Material characterization and the method of analyzing pavement remaining life are also included in this chapter.

Chapter 3 presents the pavement analysis algorithms. Basically, three algorithms are used in this study: linear elastic, equivalent-linear, and nonlinear. The derivation of the constitutive model and the definition of the typical pavement section are also included in Chapter 3.

The responses of pavement sections typically encountered in Texas under the linear elastic model are discussed in Chapter 4. Pavement responses using BISAR and ABAQUS are compared. The sensitivity of pavement response to variations in relevant pavement parameters is studied.

The nonlinear behavior of pavement materials can be considered in the equivalent-linear model. The pavement responses under this algorithm are discussed and their sensitivity is studied in Chapter 5.

The finite element method can be used to simulate the behavior of pavement under the nonlinear static model, which accounts for material nonlinearity in a comprehensive way. Chapter 6 discusses the sensitivity to that model.

The effects of the dynamic nature of the load can be obtained using the finite element software ABAQUS. This is the topic of Chapter 7. The linear dynamic and nonlinear dynamic models are implemented, and the influences of some parameters are studied.

In this study, the linear models include the linear static and the linear dynamic models. Models that consider material nonlinearity are the equivalent-linear, nonlinear static and nonlinear

dynamic models. Chapter 8 discusses the validity of these models by comparing the response of a typical pavement section.

In Chapter 9, the report is summarized, the relevant conclusions are drawn, and recommendations for improving and expanding this work are presented.

CHAPTER TWO

LITERATURE REVIEW

2.1 GENERAL

Nondestructive testing techniques are widely used to obtain field stiffness parameters of pavement materials. Moduli obtained with the FWD are used with a desired pavement analysis model to determine the remaining life of a pavement system and to estimate overlay thickness.

Several nondestructive testing and evaluation devices are available. Two nondestructive testing (NDT) devices, the Falling Weight Deflectometer (FWD) and the Seismic Pavement Analyzer (SPA), are involved in this study. The FWD applies an impulse load to the pavement, and seven sensors measure the deflection bowl on the pavement. The SPA applies small impulse loads to the pavement so that the elastic moduli of different layers can be determined. Because loads applied by the FWD and the SPA are different in magnitude, variation in pavement material characterization under different magnitudes of loads should be explored. In this chapter, the focus is on data interpretation for the two nondestructive tests.

2.2 FALLING WEIGHT DEFLECTOMETER

The Falling Weight Deflectometer (FWD) is the most popular NDT device. As shown in Figure 2.1, the FWD applies an impulse load to the pavement, and seven sensors measure the deflections of the pavement. The deflections obtained from the seven sensors are analyzed to determine the layer moduli of the pavement. Normally, a backcalculation program is employed to implement this analysis.

The peak magnitude of the FWD load typically ranges from about 5000 lbs (20 kN) to 24000 lbs (100 kN). For this reason, the FWD test is considered to characterize pavements for load levels similar to those applied by truck wheels.

The procedures used to interpret the FWD deflection data fall into three categories: empirical, mechanistic, and analytical (Hicks and Munismith, 1972). In an empirical analysis, the general overall stiffness ratios of pavements relative to one another are estimated. However, material properties, namely pavement layer moduli, are not obtained.

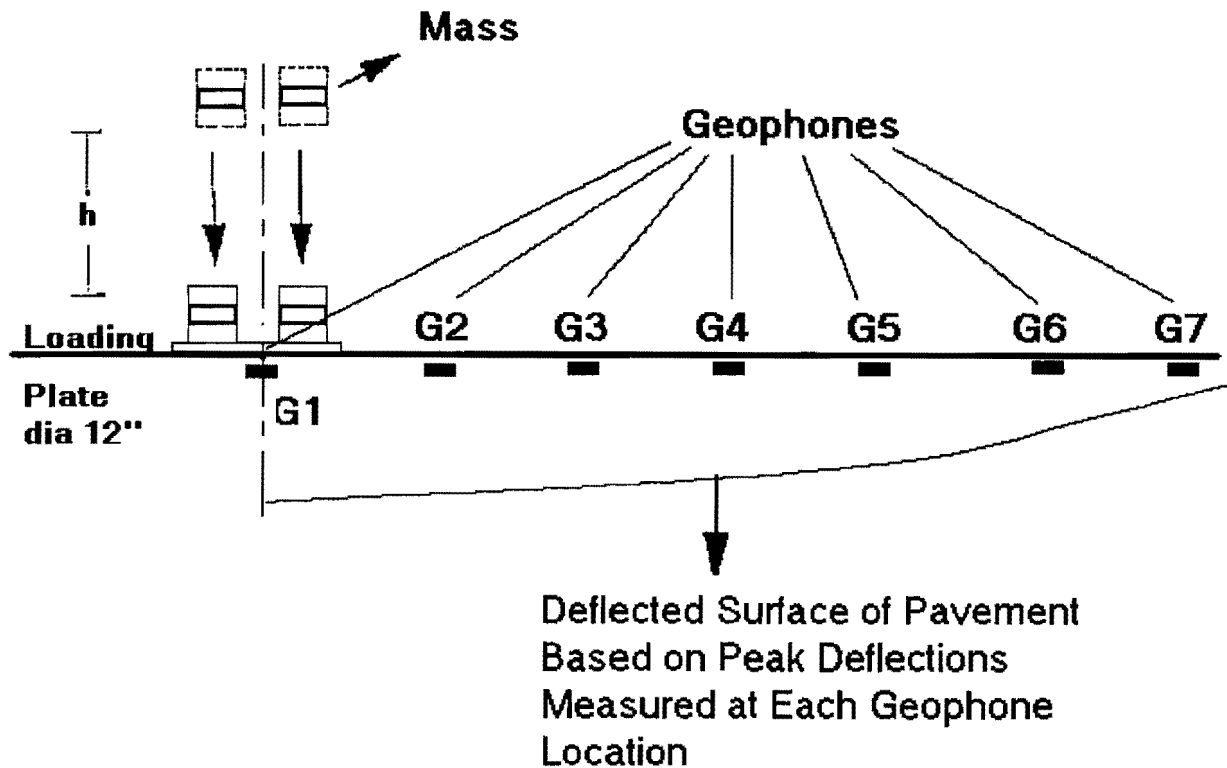


**Figure 2.1 - Geometrical Configuration of Falling Weight Deflectometer Test
(Uddin et al., 1983)**

In the mechanistic methods, deflection data from a pavement section are combined with empirical observations and mathematical equations to develop numerical correlations that quantify the condition of the pavement. These correlations are then used with only a few constraints (Hoffman and Thompson, 1982).

The Boussinesq's solutions are based on the assumption that the medium is a half-space and that the material is linearly elastic. Equations are readily available to calculate stresses, strains, and deflections from these solutions. Foster and Ahlvin (1954) also presented charts for them. To approximate a pavement using the Boussinesq's solutions, it is usually assumed that the pavement region above the subgrade does not contribute to the deflections on the pavement surface. The deflections on the pavement surface are then equal to that on the top of subgrade. Most solutions based on layered theory are also based on the assumption that the materials do behave in a linearly elastic manner. Therefore, the effect of multiple loads can be determined by the principle of superposition. However, closed-form solutions are not available for layered systems. Jones (1962) presented a series of tables for determining stresses in a three-layer system, and Peattie (1962) plotted Jones' tables in graphical forms.

The FWD data processing usually requires a backcalculation algorithm to obtain material properties from the deflection basin. Because of the nonuniqueness of the solutions, some layer properties have to be either determined by other measurements or assumed based on expert judgement.

According to Lytton (1989), the first backcalculation method was a closed-form solution for two layers, developed by Scrivner et al. (1973), using Burmister's equations (1943). Scrivner assumed that the Poisson's ratio of each layer was 0.5.

Swift (1973) developed a graphical method for determining the moduli of a two-layer pavement. With this method, the same basin shape can produce two different values of the modulus. Therefore, some expert knowledge of the expected results is needed in determining which is the correct solution. Swift (1972) also developed an "empirical" equation to measure and calculate basins on a two-layer pavement.

Hou (1977) developed the first closed-form, multi-layer solution for the backcalculation of layer moduli. The central feature of that method was a search algorithm that estimates the set of moduli, which reduced the sum of the squared differences between the calculated and measured deflections to a minimum.

The method of equivalent thickness based on the Odemark's assumption (1949) is sometimes utilized. The Odemark's assumption is that the deflections of multi-layered pavement with moduli, E_i , and layer thickness, h_i , may be represented by a single layer with a thickness, H , and a single modulus, E_0 , if the thickness is chosen to be

$$H = \sum_{i=1}^m h_i \left[\frac{E_i (1 - \nu_0^2)}{E_0 (1 - \nu_i^2)} \right]^{1/3} \quad (2.1)$$

where m is the number of layers, ν is the Poisson's ratio of the i th layer, and ν_0 is the Poisson's ratio of the equivalent single layer.

The determination of pavement moduli using the static layer elastic backcalculation method is, by far, the most widely used procedure (Bush, 1980; Lytton, et al., 1985; Uzan, et al., 1990). The application of layered theory for in-situ material characterization requires the estimation of only one unknown parameter, the Young's modulus, of each layer. The Poisson's ratio can be assumed from the literature. The following assumptions are made in layered theory solutions (Uddin, et al., 1989):

- The material in each layer is linearly elastic, homogeneous, and isotropic.
- The layers overlaying the elastic half space are weightless, finite in thickness, but extended to infinity in the horizontal plane.
- A uniform static load is applied on a circular area of the surface.
- The inertia effect is neglected.

- The normal stress outside the loaded area and the shearing stress at the top of the surface layer are negligible.
- The stresses and displacements approach zero at large depths.

2.3 SEISMIC PAVEMENT ANALYZER

The Seismic Pavement Analyzer (SPA) is a trailer-mounted nondestructive testing device, as shown in Figure 2.2. Its operating principle is based on generating and detecting stress waves in a layered medium. Several seismic testing techniques are combined. A detailed discussion on the background of the device can be found in Nazarian et al. (1995).

The SPA lowers several transducers and sources to the pavement. Surface deformations are recorded digitally. The deformations are induced by a large pneumatic hammer, which generates low-frequency vibrations, and a small pneumatic hammer, which generates high-frequency vibrations.

The SPA is similar in size to the FWD. However, the SPA uses more transducers with higher frequencies and more sophisticated interpretation techniques. The measurement is rapid. A complete testing cycle at one point takes less than one minute (lowering sources and receivers, making measurements, and withdrawing the equipment).

The SPA collects three categories of data - raw data, processed data and interpreted data. Raw data are the waveforms generated by hammer impacts and collected by the transducers. The processed data are pavement layer properties derived from the raw data through established theoretical models. Interpreted data are diagnoses of pavement distress precursors from data processed through models.

Pavement properties estimated by the SPA include: Young's modulus, shear modulus, thickness, and temperature of top pavement layer; Young's modulus and thickness of base layer; and Young's modulus of subgrade.

Five methods are used in SPA tests. In the Impulse Response (IR) tests, the low-frequency source and geophone G1 are used (see Figure 2.2). With this method, the modulus of the subgrade and the damping ratio of the system are extracted from the flexibility spectrum measured in the field (Nazarian and Desai, 1993). Theoretically speaking, the pavement is modeled as a single-degree-of-freedom (SDOF) system. To determine the modal parameters, a curve is fitted to the flexibility spectrum. The shear modulus of the subgrade, G , is calculated from (Dobry and Gazetas, 1986):

$$G = (1 - \nu) / [2LA_0 I_s S_z] \quad (2.2)$$

where ν = Poisson's ratio of subgrade, L = length of slab, and A_0 = static flexibility of slab. The shape factor, S_z , has been developed by Dobry and Gazetas (1986). The value of S_z is equal to 0.80 for a long flexible pavement. Parameter I_s is a parameter that considers the effects of an increase in flexibility near the edges and corners of a slab. Parameter I_s is a function of the length and width of the slab as well as of the coordinates of the impact point relative to one corner. The

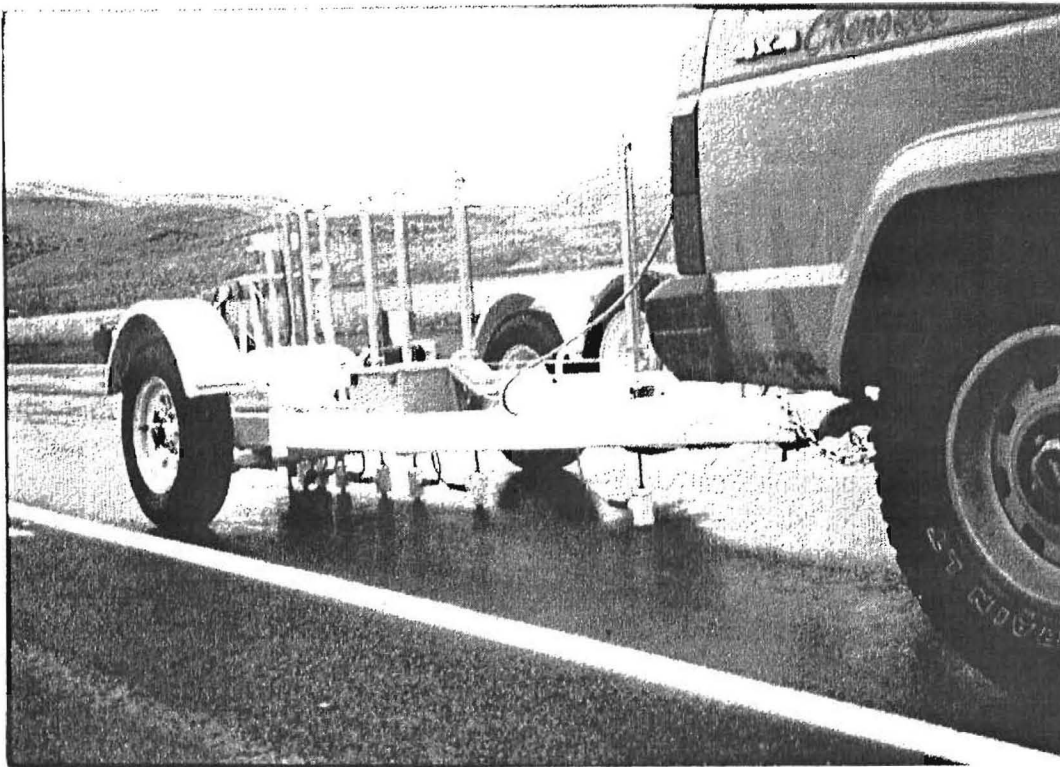
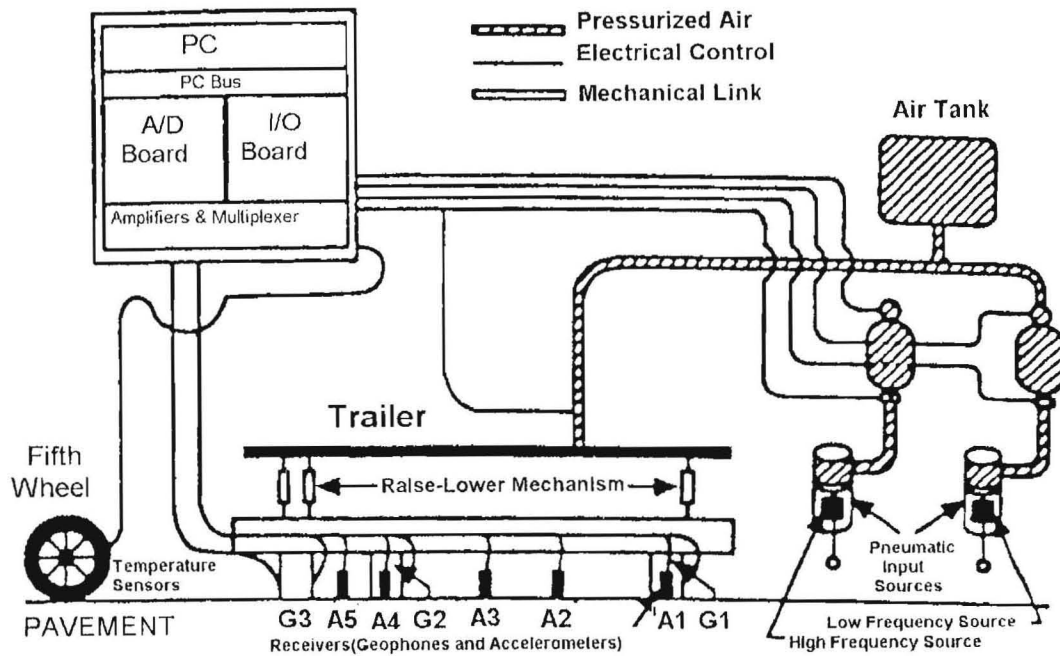


Figure 2.2 - Schematic of Seismic Pavement Analyzer

damping ratio is a qualitative indicator of the slab's resistance to movement. For example, if a slab contains an edge void, it would demonstrate a damping ratio on the order of 10 to 40 percent.

The Spectral-Analysis-of-Surface-Waves (SASW) method is a seismic method that can determine modulus profiles of pavement sections by measuring the dispersive nature of surface waves. All accelerometers and geophones are active in SASW tests. The procedure includes collecting data, determining the experimental dispersion curve, and obtaining the stiffness profile.

In data collection, the transfer function and the coherence function between pairs of receivers are determined. Thus, the phase information of the cross power spectra and the coherence functions are used to determine a representative dispersion curve in an automated fashion (Nazarian and Desai, 1993). Finally, the elastic modulus of different layers can be determined from the dispersion using an automated inversion process (Yuan and Nazarian, 1993).

The Ultrasonic-Surface-Wave (USW) method is similar to the SASW method. The difference is that, in the USW method, the properties of the top pavement layer can be easily and directly determined without a complex inversion algorithm. The high-frequency source and accelerometers A2 and A3 are utilized in this method.

Up to a wavelength approximately equal to the thickness of the uppermost layer, the velocity of propagation is independent of wavelength. Therefore, if high-frequency waves are generated and if it is assumed that the properties of the uppermost layer are uniform, the shear modulus of the top layer, G , can be determined by

$$G = \rho[1.13 - 0.16\nu]V_{ph}^2 \quad (2.3)$$

where V_{ph} = phase velocity of surface waves, ρ = mass density, and ν = Poisson ratio. The shear modulus can be readily converted to Young's modulus using

$$E = 2G(1 + \nu) \quad (2.4)$$

where E is Young's modulus. The thickness of the surface layer can be estimated by determining the wavelength above which the surface velocity is constant.

The setup to measure the compression wave velocity of the upper layer of the pavement is the same as that for the SASW tests. Once the compression wave velocity of a material is known, its Young's modulus can be determined. Miller and Pursey (1955) found that when the surface of a medium is impacted Rayleigh waves propagate with most of the energy. A small portion of the generated stress wave energy propagates with shear and compression wave energy. Compression waves arrive first on seismic records because they travel faster than any other type of seismic waves. An automated technique has been developed to determine the compression wave velocity by measuring the times of the first arrival of compression waves (Willis and Toksoz, 1983).

The impact-echo method is employed to locate defects, voids, cracks and zones of deterioration within concrete. The high-frequency source and accelerometer A1 and, possibly, A2 are used. Once the compression wave velocity of concrete, V_p , is measured, the depth-to-reflector, T , can be determined from (Sansalone and Carino, 1986):

$$T = V_p / (2f) \quad (2.5)$$

where f is the resonant (return) frequency obtained by transforming the deformation record into the frequency domain.

2.4 PAVEMENT MATERIAL CHARACTERIZATION

Moduli of different pavement layers can be determined with either laboratory tests or field tests. Laboratory tests are essential for studying the parameters that affect the properties of materials. However, typically, moduli from laboratory tests significantly differ from those obtained from in-situ tests. The differences are normally attributed to sampling disturbance, differences in the state-of-stress between the specimen and in-situ pavement material, nonrepresentative specimens, long-term time effects, and inherent errors in the field and laboratory test procedures (Anderson and Woods, 1975).

To develop a constitutive model for a pavement material, the resilient modulus tests are useful tools. Since the process of specimen preparation and testing is time-consuming and expensive, these tests are not used as often as they should be. In addition, constructing specimens with the same characteristics as in-situ materials is rather difficult.

Field tests are practical and more desirable because they are quick to perform and because they test a large volume of material in its natural state-of-stress. Since pavement materials normally exhibit a nonlinear stress-strain relationship, moduli measured with different field tests differ. The deflection-based field test methods, such as FWD, impose loads that approximate wheel loads. Seismic tests apply small loads to pavements.

The behavior of most soils and pavement materials under load can be represented by a stress-strain curve similar to the one shown in Figure 2.3 (Nazarian et al., 1998). In this figure, three significant parameters are:

- The initial tangent modulus, or maximum modulus (E_{max}), the slope of the line tangent to the curve passing through the origin.
- The strength of the material (σ_{max}), the horizontal line asymptotic to the curve.
- The secant modulus (E_1 , E_2 , or E_3), the slope of a line connecting the origin to any point on the curve.

The initial tangent modulus is directly affected by the initial state of stress and the density of the material. The secant modulus is strongly affected by the magnitude of strain experienced by the material.

In this report, the FWD modulus refers to the modulus of a pavement material determined from the backcalculation of a deflection basin measured in the field. This modulus normally corresponds to a secant modulus for materials close to the loading pad (i.e., AC layer, base and shallow subgrade) and to an initial tangent modulus for materials far from the impact point (i.e., deeper subgrade materials).

The seismic modulus of a layer is either directly measured or backcalculated using a small seismic impact. Because the seismic impact is small, this modulus always corresponds to the initial tangent modulus.

The resilient modulus of pavement material is determined in the laboratory from a variety of test protocols. This modulus normally corresponds to a secant modulus. Due to limitations with the existing equipment, it may be very difficult to determine the initial tangent modulus with the resilient modulus tests.

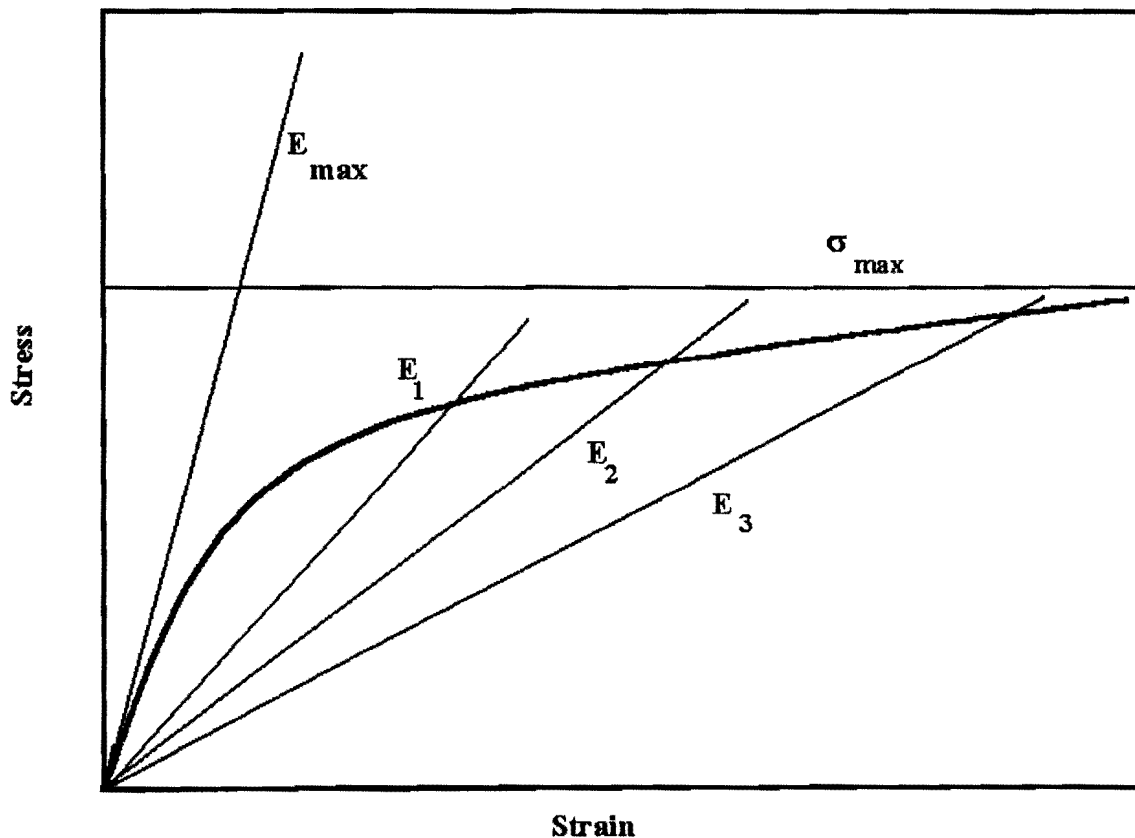


Figure 2.3 - Typical Stress-Strain Curve for a Pavement Material

The basic materials used in flexible pavements are granular bases or subgrades and bituminous materials. Characterizations of these materials are discussed below.

2.4.1 Base and Subgrade Materials

Depending on their gradation and plasticity, the base and subgrade materials can be divided into two groups: fine-grained (cohesive) or coarse-grained (cohesionless or granular).

For granular materials, one conventional constitutive model is expressed as (Huang, 1994):

$$E = K_1 \theta^{K_2} \quad (2.6)$$

in which K_1 and K_2 are experimentally-derived constants, θ is the stress invariant or the bulk stress (the sum of three mutually-perpendicular normal stresses such as σ_x , σ_y , and σ_z), and E is the resilient modulus.

For fine-grained soils, the resilient modulus decreases with an increase in the deviatoric stress. This model can be expressed as a bilinear behavior:

$$\begin{cases} E = K_1 + K_3(K_2 - \sigma_d) & \text{if } \sigma_d < K_2 \\ E = K_1 - K_4(\sigma_d - K_2) & \text{if } \sigma_d \geq K_2 \end{cases} \quad (2.7)$$

in which σ_d is the deviatoric stress and K_1 , K_2 , K_3 and K_4 are material constants.

Barksdale et al. (1994), based on a recent NCHRP project, have endorsed a universal relationship in the form of:

$$E = k_1 \sigma_c^{k_2} \sigma_d^{k_3} \quad (2.8)$$

where σ_c and σ_d are the confining pressure and the deviatoric stress, respectively. Parameters k_1 through k_3 are coefficients statistically determined from the results of the laboratory resilient modulus tests. This constitutive model was adopted in this study for its convenience. The advantage of the model presented in Equation 2.8 is that it is universally applicable to fine-grained and coarse-grained base and subgrade materials. The derivation and application of this model are detailed in Chapter 3.

2.4.2 Bituminous Materials

Several parameters affect the modulus of bituminous materials. The most important parameters to be considered are the rate of loading (i.e., frequency of loading), temperature, and air void content.

The typical frequency at which the AC moduli are measured with seismic methods is about 15 KHz to 25 KHz, whereas the actual traffic load has a dominant frequency of about 10 to 30 Hz. Aouad et al. (1993) clearly demonstrated the importance of considering the rate of loading. As

shown in Figure 2.4, depending on the temperature, the modulus measured with seismic methods should be reduced by a factor of about 3 to 15.

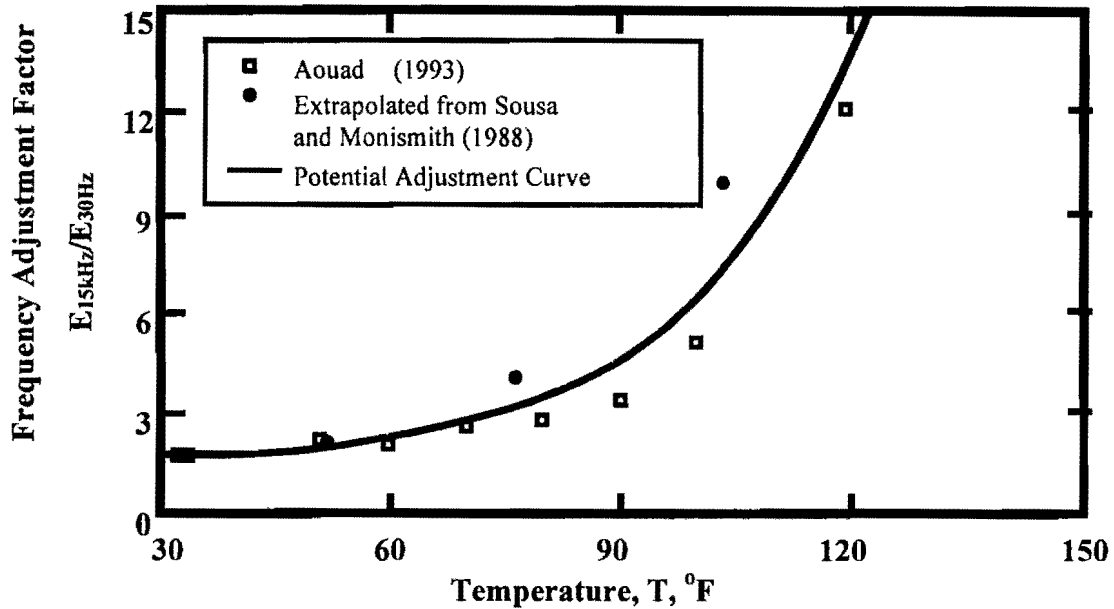


Figure 2.4 – Variation in AC Modulus with Frequency and Temperature (from Aouad et al., 1993)

Daniel and Kim (1998) and Kim and Lee (1995) used the results from several laboratory and field tests (such as FWD, ultrasonic, uniaxial sweep, and creep) to show the frequency-dependency of modulus. The results from Daniel and Kim are shown in Figure 2.5. Again, the frequency-dependency is temperature-related.

The AC modulus is strongly dependent on temperature. Von Quintus and Kilingsworth (1998) demonstrate the importance of temperature correction and the complexity involved in considering the temperature gradient within a pavement section. Aouad et al. (1993), Li and Nazarian (1994) and several other investigators have studied the variation in modulus with temperature for seismic methods. Many relationships exist that recommend a means for temperature adjustment. With the advancement in measuring the modulus of pavements, the methodology for temperature correction should be studied and improved.

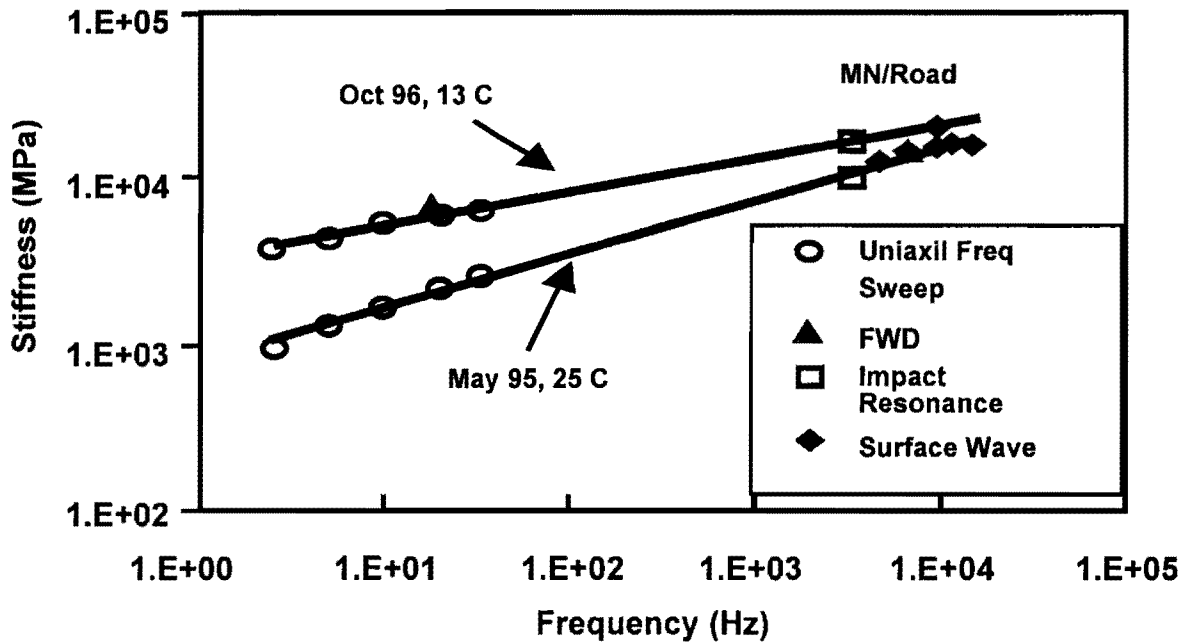


Figure 2.5 – Frequency Dependency of AC Modulus
(from Daniel and Kim, 1998)

Air void content has a significant impact on the modulus of AC as well. Rojas (1999) clearly demonstrated that the modulus of a mix is inversely proportional to the air void content of the mix (See Figure 2.6). He also showed that the aggregate gradation and the asphalt viscosity affect the modulus of the mix.

2.5 PAVEMENT REMAINING LIFE

This study also contains the analysis of pavement remaining life for fatigue cracking and permanent deformation. According to Huang (1994), the failure criterion for fatigue cracking is expressed as:

$$N_f = f_1(\epsilon_t)^{-f_2} (E_1)^{-f_3} \quad (2.9)$$

in which N_f is the allowable number of load repetitions to prevent fatigue cracking, ϵ_t is the tensile strain at the bottom of AC layer, E_1 is the elastic modulus of the AC layer, and f_1 , f_2 and f_3 are constants determined from laboratory fatigue tests with f_1 modified to correlate with field performance observations. The Asphalt Institute recommends 0.0796, 3.291, and 0.854 for f_1 , f_2 and f_3 , respectively.

The failure criterion for permanent deformation is expressed as:

$$N_r = f_4(\epsilon_c)^{-f_5} \quad (2.10)$$

in which N_r is the allowable number of load repetitions to limit permanent deformation, ϵ_c is the compressive strain on the top of subgrade, and f_4 and f_5 are constants determined from road tests or field performance. The Asphalt Institute (1982) suggested that the values of f_4 and f_5 are 1.365×10^{-9} and 4.477, respectively. Therefore, fatigue remaining life, N_f , and rutting remaining life, N_r , can be easily obtained given the two critical strains – tangential tensile strain at the bottom of AC layer and vertical compressive strain at the top of subgrade.

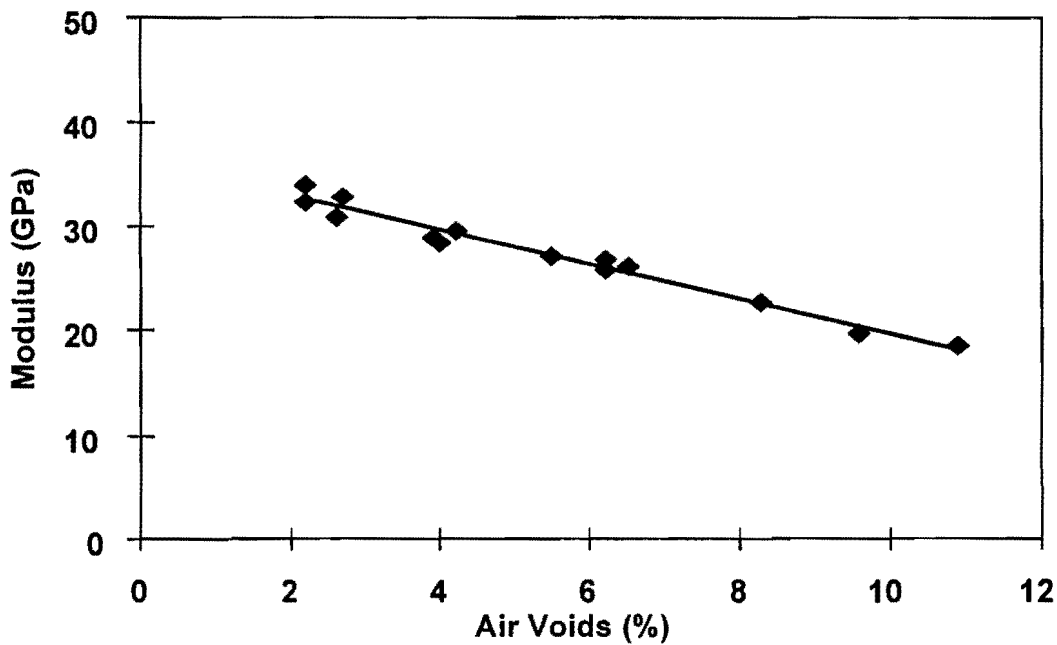


**Figure 2.6 – Impact of Air Void Content on Modulus of AC
(from Rojas, 1999)**

CHAPTER THREE

DESCRIPTION OF PAVEMENT ANALYSIS MODELS

3.1 INTRODUCTION

The response of a pavement system under actual wheel loading has been of interest to pavement engineers for some time. For example, Westergaard (1926) predicted the response of rigid pavements by the principal of continuum mechanics, and Burmister (1943) solved the classical layered, elastic problem.

Linear elastic models are the simplest models used to characterize the behavior of pavement systems. Several computer programs were developed for analyzing the structural response of pavement systems based on linear elastic theory (Uzan et al., 1989). One disadvantage of linear elastic models is that the nonlinear behavior of the pavement materials cannot be considered, even though granular materials may exhibit nonlinear behavior under actual truck traffic. To take the nonlinear behavior of pavement materials into consideration in a simple manner, an equivalent-linear model can be used in conjunction with the layered elastic programs such as BISAR (Nazarian et al., 1998). These models are approximate because they cannot consider the variation in the stiffness of pavement layers in the lateral direction. The finite element method can be employed to overcome this shortcoming at the expense of a more time-consuming and sophisticated analysis (Brown, 1996).

In this chapter, each constitutive model used in this study is discussed. The algorithms to implement these constitutive models are also described. Finally, the typical pavement sections used throughout this study are detailed.

3.2 CONSTITUTIVE MODELS USED

Brown (1996) discusses a spectrum of analytical and numerical models that can be used in conjunction with a variety of constitutive material behaviors in pavement design. With these models, the critical stresses, strains, and deformations within a pavement structure and the remaining lives can be estimated under a number of material behaviors. Many computer programs with different levels of sophistication exist that can incorporate these models. The numerical and constitutive models used in this study are described in this section.

3.2.1 Linear Elastic Model

The simplest models for evaluating the behavior of pavements under load are linear elastic models. The constitutive model for a linear elastic material is rather simple since the modulus is considered as a constant value independent of the state of stress applied to the pavement. Therefore, the modulus of each layer does not change with the variation in other properties. Most algorithms used in pavement analysis and design take advantage of this type of solution. KENLAYER (Huang, 1994), WESLEA (Van Cauwelaert et al., 1989), and BISAR (De Jong et al., 1973) are three of the popular programs in this category. The advantage of these models is that they can rapidly yield results. Their main limitation is that the results are rather approximate if the loads are large enough for the material to exhibit a nonlinear behavior.

3.2.2 Equivalent-Linear Model

An equivalent-linear model is a model that in an approximate fashion can consider the load-induced nonlinear behavior based on the static linear elastic layered theory. An iterative process is employed to consider the nonlinearity of the pavement materials. The constitutive model adopted in the equivalent linear model, as discussed in Chapter 2, is

$$E = k_1 \sigma_c^{k_2} \sigma_d^{k_3} \quad (3.1)$$

In this equation, k_1 , k_2 and k_3 are statistically-determined coefficients. In Equation 3.1, the modulus at a given point within the pavement structure is related to the state of stress. Since the state of stress can be known only if the material properties, including modulus, are known, an iterative process has to be used to implement this stress-modulus relationship.

The advantage of the model presented in Equation 3.1 is that it is universally applicable to fine-grained and coarse-grained base and subgrade materials. The accuracy and reasonableness of this model are extremely important because they are the keys to successfully combining laboratory and field results.

In Equation 3.1, the term $k_1 \sigma_c^{k_2}$ corresponds to the initial tangent modulus, E_{\max} , which is related to the confining pressure. Normally parameter k_2 is positive. Therefore, the initial tangent modulus increases as the confining pressure increases. Parameter k_3 suggests that the modulus changes as the deviatoric stress changes. Because k_3 is usually negative, the modulus decreases with an increase in the deviatoric stress.

Hardin and Drnevich (1972), based on many laboratory tests, accumulated a list of parameters that affect the moduli of both fine-grained and coarse-grained soils. These parameters and their significance are summarized in Table 3.1. The state of stress, void ratio, and strain amplitude are the main parameters that affect the modulus of a material. For fine-grained soils, the degree of saturation is also important.

The impact of these parameters on the three k parameters is also added to Table 3.1. Most parameters that were suggested by Hardin and Drnevich affect k_1 . Most of these parameters cannot be reproduced in a laboratory specimen, which may be the reason for a lack of similarity

between the field moduli and those obtained from laboratory testing. However, k_2 and k_3 are affected by a few parameters. Therefore, determining k_2 and k_3 in the laboratory is relatively easy, whereas measuring k_1 in the laboratory is rather difficult.

One of the major purposes of this study is to relate the seismic modulus with the load-induced nonlinear modulus. For this reason, parameter k_1 in Equation 3.1 will be replaced by a term that is a function of the seismic modulus and the stresses under seismic test.

Two different states of stress are considered: under seismic loads and under external loads, such as those imparted by a FWD or an actual truck. Figure 3.1a shows stresses for an infinitesimal material element during seismic tests. Only a very small external load is applied to generate various waves. Therefore, only stresses generated by geostatic pressure should be considered. If it is assumed that there are n layers of materials above the element shown in Figure 3.1a, each with a unit weight of γ_i and a thickness of h_i , then:

$$\sigma_v = \sum_{i=1}^n \gamma_i h_i \quad (3.2)$$

where σ_v is the vertical stress. Similarly, σ_h , the horizontal stress on the element, is related to σ_v by

$$\sigma_h = k_0 \sigma_v \quad (3.3)$$

where k_0 is the coefficient of lateral earth pressure at rest.

As shown in Figure 3.2a, additional stresses, σ_x , σ_y and σ_z , are induced under the application of an external load. A multi-layer elastic program can conveniently compute these additional stresses.

To implement the equivalent linear model, it is essential that these stresses be reformulated in terms of confining pressure and deviatoric stress. Figure 3.1b shows the transformed state of stress, which includes the initial confining pressure, σ_{c_init} , and the initial deviatoric stress, σ_{d_init} .

The initial confining pressure is the arithmetic mean value of the three original principal stresses. Since the two horizontal stresses can be considered equal:

$$\sigma_{c_init} = \frac{1 + 2k_0}{3} \sigma_v \quad (3.4)$$

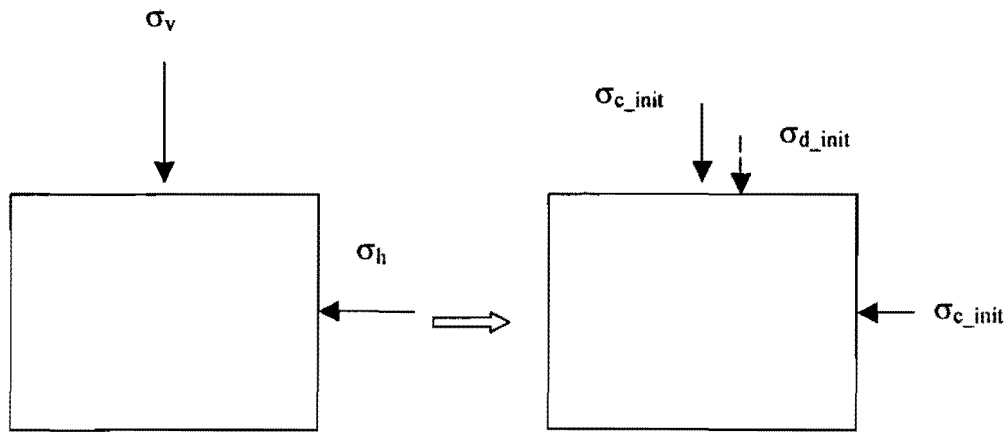
The initial deviatoric stress, which is the difference between σ_v and σ_{c_init} , can be written as

$$\sigma_{d_init} = \frac{2 - 2k_0}{3} \sigma_v \quad (3.5)$$

**Table 3.1 - Parameters Affecting Modulus of Granular Bases and Subgrades
(after Hardin and Drnevich, 1972)**

Parameter	Importance*		Parameter Affected in Equation 3.1		
	Coarse-Grained Materials	Fine-Grained Materials	k_1	k_2	k_3
Strain Amplitude	V	V			√
Effective Mean Principal Stress (Confining pressure)	V	V		√	√
Void Ratio	V	V	√		
Degree of Saturation	R	V	√	√	
Overconsolidation Ratio	R	V	√		
Effective Stress Envelop	R	L	√		
Octahedral Shear Stress	L	L	√		
Frequency of Loading	L	L	√		
Long-Term Time Effects (Thixotropy)	R	R	√		
Grain Characteristics	R	L	√		√
Soil Structures	R	R	√		√
Volume Change Due to Shear Strain	V	R	√		

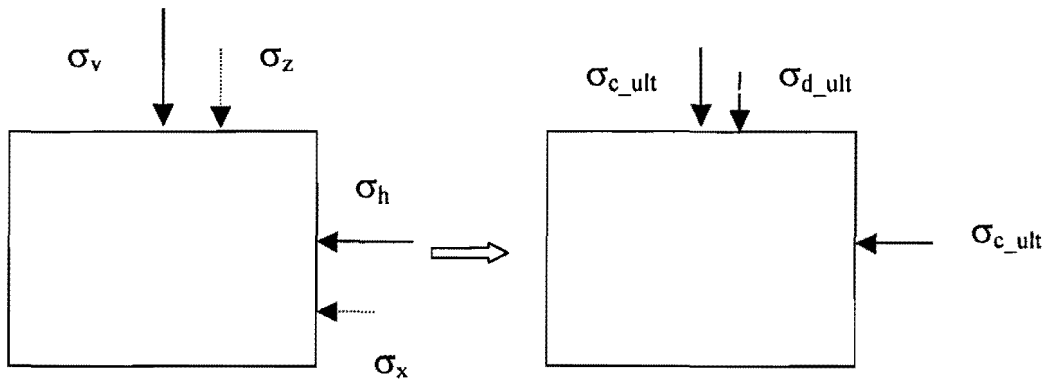
- V means important, L means less important, R means relatively unimportant.



(a) Actual state of stress

(b) Transformed state of stress

Figure 3.1 – State of Stress under Seismic Test



(a) Actual state of stress

(b) Transformed state of stress

Figure 3.2 – State of Stress under FWD Test

Figure 3.2b shows the transformed state of stress under load, such as those applied by an FWD. The state of stress consists of an ultimate confining pressure, σ_{c_ult} , and an ultimate deviatoric stress, σ_{d_ult} . The ultimate confining pressure contains two components, σ_{c_init} and $\Delta\sigma_c$. Parameter $\Delta\sigma_c$ is the arithmetic mean value of the three principal stresses σ_x , σ_y , and σ_z :

$$\Delta\sigma_c = \frac{\sigma_x + \sigma_y + \sigma_z}{3} \quad (3.6)$$

Thus, the ultimate confining pressure is

$$\sigma_{c_ult} = \sigma_{c_init} + \Delta\sigma_c \quad (3.7)$$

or

$$\sigma_{c_ult} = \frac{1 + 2k_0}{3} \sigma_v + \frac{\sigma_x + \sigma_y + \sigma_z}{3} \quad (3.8)$$

The ultimate deviatoric stress also includes two parts, σ_{d_init} and $\Delta\sigma_d$. The parameter $\Delta\sigma_d$ is the difference between σ_z and $\Delta\sigma_c$:

$$\Delta\sigma_d = \sigma_z - \Delta\sigma_c \quad (3.9)$$

$$\Delta\sigma_d = \frac{2\sigma_z - \sigma_x - \sigma_y}{3} \quad (3.10)$$

Thus, the ultimate deviatoric stress is

$$\sigma_{d_ult} = \sigma_{d_init} + \Delta\sigma_d \quad (3.11)$$

or

$$\sigma_{d_ult} = \frac{2 - 2k_0}{3} \sigma_v + \frac{2\sigma_z - \sigma_x - \sigma_y}{3} \quad (3.12)$$

As indicated before, to obtain the seismic modulus, E_{seis} , very small external loads are applied. Therefore, the corresponding confining pressure and deviatoric stress are σ_{c_init} and σ_{d_init} , respectively. Therefore, Equation 3.1 can be changed to

$$E_{seis} = k_1 \sigma_{c_init}^{k_2} \sigma_{d_init}^{k_3} \quad (3.13)$$

Thus,

$$k_1 = \frac{E_{seis}}{\sigma_{c_init}^{k_2} \sigma_{d_init}^{k_3}} \quad (3.14)$$

In FWD tests or under actual truckloads, the modulus can become nonlinear depending on the amplitude of confining pressure σ_{c_ult} and deviatoric stress of σ_{d_ult} . In that case:

$$E = k_1 \sigma_{c_ult}^{k_2} \sigma_{d_ult}^{k_3} \quad (3.15)$$

Therefore, when combined with Equation 3.14, the nonlinear modulus can be related to the seismic modulus through

$$E = E_{seis} \left(\frac{\sigma_{c_ult}}{\sigma_{c_init}} \right)^{k_2} \left(\frac{\sigma_{d_ult}}{\sigma_{d_init}} \right)^{k_3} \quad (3.16)$$

Compared to Equation 3.1, parameter k_1 is eliminated when the seismic modulus is considered as input. As indicated before, a large number of parameters impact the determination of k_1 in the laboratory. Therefore, replacing k_1 with a parameter measured in the field may reduce some of the uncertainties associated with the laboratory tests. Equation 3.16 can be used in an equivalent-linear model to obtain the modulus of a nonlinear material in this study.

One of the limitations of Equation 3.1 is that at very small or very large deviatoric stresses the modulus tends to be infinity and zero, respectively. Many years of research (see Kramer, 1996) have shown that below a certain strain level (or deviatoric stress) the modulus is constant and equal to the small-strain linear-elastic modulus of the material. Conversely, at higher strain levels (or higher deviatoric stresses), the modulus becomes more or less constant as well. Therefore, if the vertical strain is less than 0.01%, the modulus corresponding to a strain of 0.01% will be adopted. On the other hand, if the vertical strain is greater than 1%, the modulus corresponding to a strain of 1% will be adopted. The relationship among the modulus, stress, and strain is:

$$E = \frac{\sigma_{d_ult}}{\varepsilon} \quad (3.17)$$

Thus

$$\sigma_{d_ult} = E\varepsilon \quad (3.18)$$

Substituting the above equation in Equation 3.15

$$E = k_1 \sigma_{c_ult}^{k_2} (E\varepsilon)^{k_3} \quad (3.19)$$

or

$$E = k_1^{1/(1-k_3)} \sigma_{c_ult}^{k_2/(1-k_3)} \varepsilon^{k_3/(1-k_3)} \quad (3.20)$$

With respect to a strain of 1%, the lower bound of the modulus is:

$$E_{low} = k_1^{1/(1-k_3)} \sigma_{c_ult}^{k_2/(1-k_3)} (0.01)^{k_3/(1-k_3)} \quad (3.21)$$

With respect to a strain of 0.01%, the upper bound of the modulus is:

$$E_{up} = k_1^{1/(1-k_3)} \sigma_{c_ult}^{k_2/(1-k_3)} (0.0001)^{k_3/(1-k_3)} \quad (3.22)$$

Since k_3 is normally a negative value, the upper bound, E_{up} , is larger than the lower bound, E_{low} . The two bounds shown in Equations 3.21 and 3.22 are checked after each iteration in the equivalent-linear model.

3.2.3 Nonlinear Models

The all-purpose finite element software packages, such as ABAQUS, can be used for nonlinear models. These programs allow a user to model the behavior of a pavement in the most comprehensive manner and to select the most sophisticated constitutive models for each layer of pavement. The dynamic nature of the loading can also be considered.

The constitutive model adopted in nonlinear models is the same as that in the equivalent-linear model, as described in Equation 3.16. In nonlinear analysis using ABAQUS, this constitutive model was implemented in a user subroutine. Whenever an element in a nonlinear layer is involved, that subroutine is called to compute the nonlinear modulus related to its existing state of stress.

The analytical solutions are highly efficient and are quite advanced. However, expertise is needed to review the input and output to ensure that all aspects of modeling are considered.

3.3 DESCRIPTION OF ALGORITHMS

The following three algorithms were used in this study:

- a multi-layer linear system,
- a multi-layer equivalent-linear system, and
- a finite element code for a comprehensive nonlinear dynamic system.

In this section, these three algorithms are discussed.

3.3.1 Multi-Layer Linear System

Flexible pavements are layered systems with stiffer materials on top. Burmister (1943) first developed solutions for a two-layer system and then extended them to a three-layer system (Burmister, 1945). With the advent of computers, the theory can be applied to a multi-layer system with any number of layers (Uzan, 1994). A typical n-layer system subjected to a circular load is shown in Figure 3.3.

The basic assumptions to be satisfied are:

- Each layer is homogeneous, isotropic, and linear elastic.
- The material is weightless and extended to infinity in horizontal directions.
- Each layer has a finite thickness, except the bottom layer, which is extended to infinity.
- A uniform pressure is applied to the pavement surface over a circular area.

Continuity conditions at the layer interfaces, as indicated by the same vertical stress, shear stress, vertical displacement, and radial displacement, are satisfied. For a frictionless interface, the continuity of shear stress and radial displacement is replaced by zero shear stress at each side of the interface.

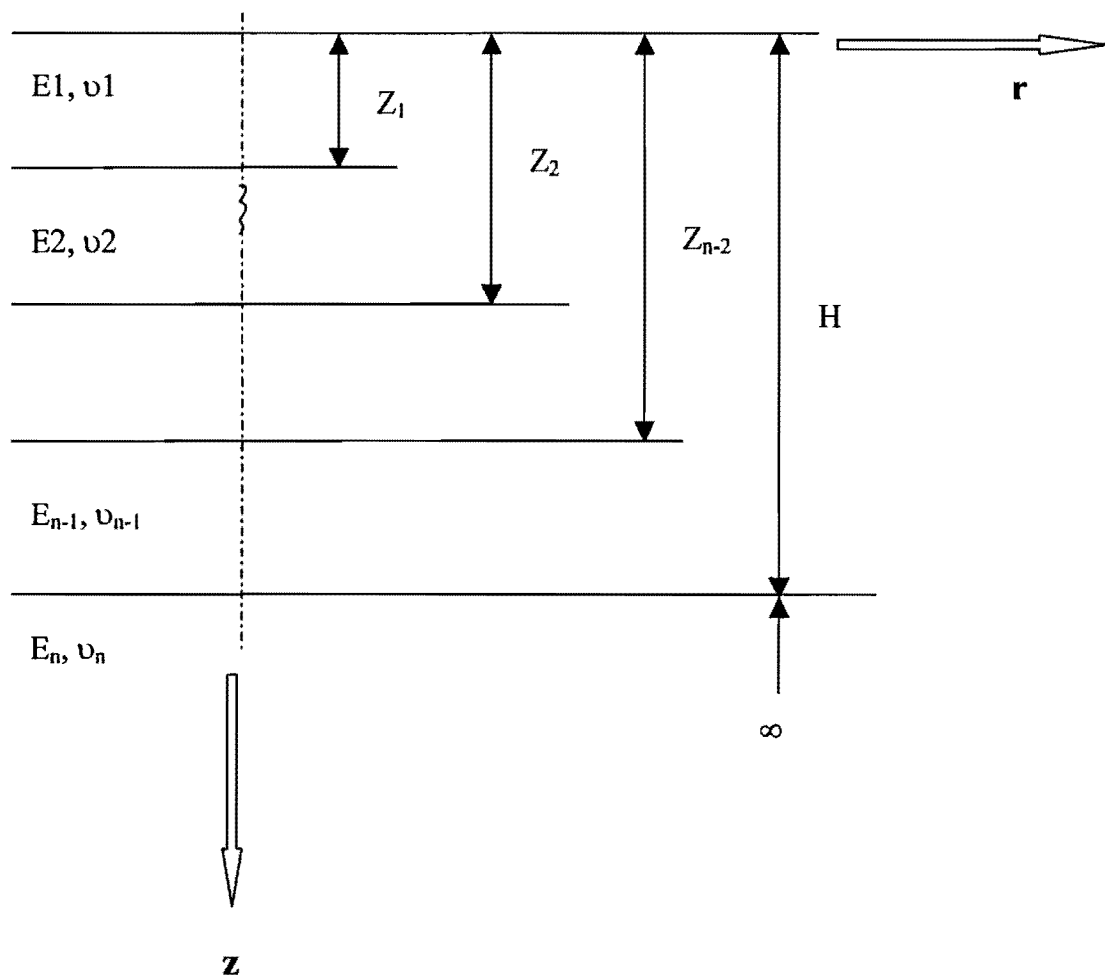


Figure 3.3 – A Typical n-layer System

As in the classical theory of elasticity, a stress function ϕ that satisfies the governing differential equation

$$\nabla^4 \phi = 0 \quad (3.23)$$

is assumed for each layer. As shown in Figure 3.3, the system has an axially symmetrical stress distribution, thus

$$\nabla^4 = \left(\frac{\partial^2}{\partial^2 r} + \frac{1}{r} \frac{\partial}{\partial r} + \frac{\partial^2}{\partial^2 z} \right) \left(\frac{\partial^2}{\partial^2 r} + \frac{1}{r} \frac{\partial}{\partial r} + \frac{\partial^2}{\partial^2 z} \right) \quad (3.24)$$

After solving the stress function ϕ from the above fourth-order differential equation and applying boundary and continuity conditions, the layered system problem can be solved. After the stress function is found, the stresses can be determined by

$$\sigma_{rz} = \frac{\partial}{\partial z} \left(\nu \nabla^2 \phi - \frac{1}{r} \frac{\partial \phi}{\partial r} \right) \quad (3.25)$$

$$\sigma_r = \frac{\partial}{\partial z} \left(\nu \nabla^2 \phi - \frac{\partial^2 \phi}{\partial r^2} \right) \quad (3.26)$$

$$\sigma_{zz} = \frac{\partial}{\partial z} \left(\nu \nabla^2 \phi - \frac{1}{r} \frac{\partial \phi}{\partial r} \right) \quad (3.27)$$

Many computer programs, such as BISAR, WESLEA and KENLAYER, are available to obtain stresses and strains for linear elastic problems utilizing the solution of the multi-layered system. Throughout this study, the well-established computer program BISAR was used.

3.3.2 Multi-Layer Equivalent-Linear System

As indicated before, the equivalent-linear model is based on the static linear elastic layered theory. The constitutive model described in Equation 3.16 is adopted. An iterative process is employed to consider the nonlinear behavior of the pavement materials in an approximate fashion.

The implemented process is summarized in Figure 3.4. The nonlinear layers are divided into several sub-layers. The number of sub-layers depends on the accuracy required and the number of layers allowed by the program. One stress point is chosen for each nonlinear sub-layer. An initial modulus is assigned to each stress point. Basically, the seismic modulus is assigned to be the initial value since it will not have any effect on the final results. The stresses and strains are calculated for all stress points using a multi-layer elastic computer program. The confining pressure and deviatoric stress can then be calculated for each stress point using Equations 3.2 through 3.12. From Equation 3.16, a new modulus can be obtained. The assumed modulus and the newly calculated modulus at each stress point are compared. If the difference is larger than a pre-assigned tolerance, the process will be repeated using updated assumed moduli. To

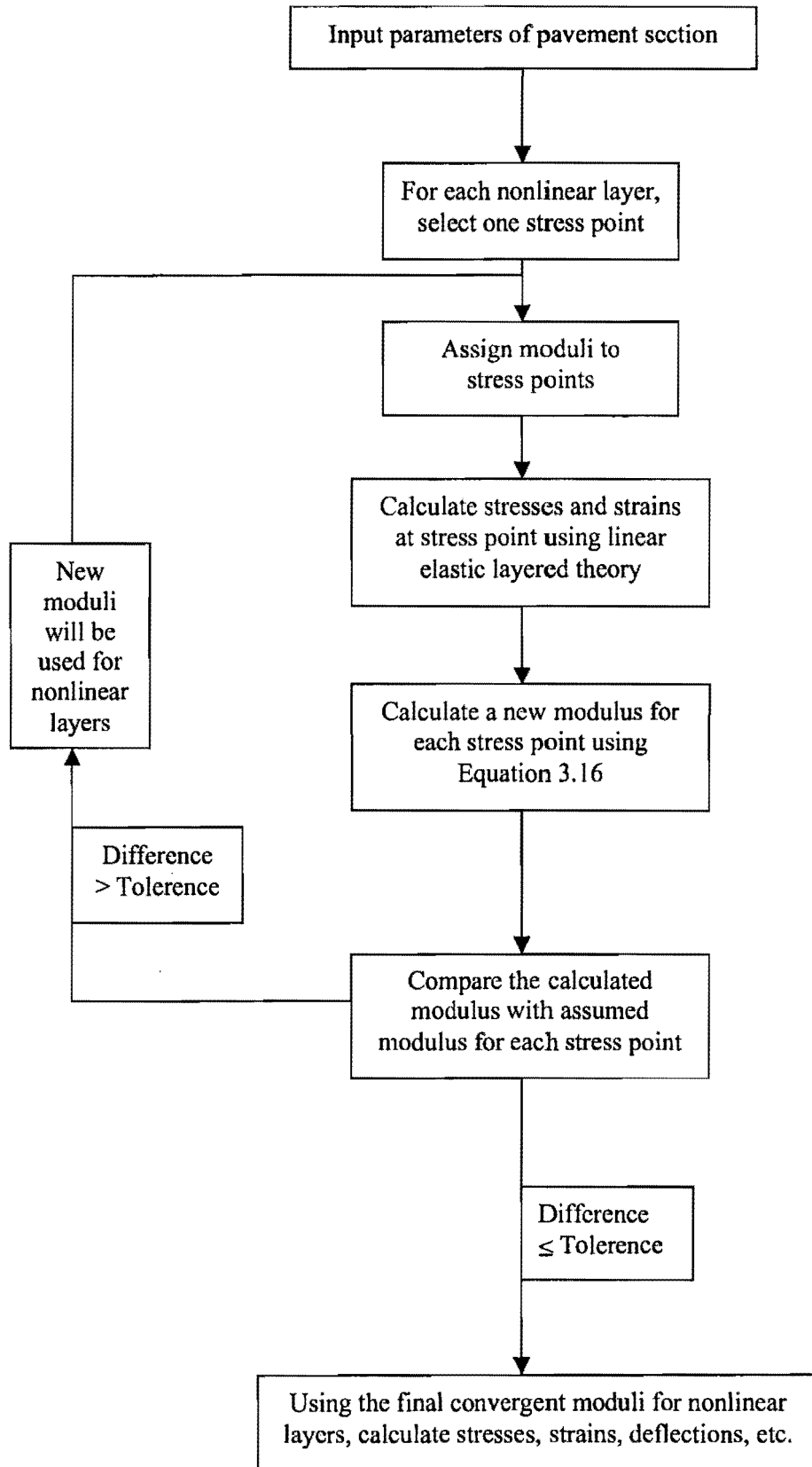


Figure 3.4 – Flow Chart of Implementation of Equivalent-Linear Model

accelerate convergence, the updated assumed modulus for each nonlinear sub-layer equal to the average of the assumed and calculated moduli is used. The above procedure is repeated until the modulus difference is within the tolerance and, thus, convergence is reached. Finally, the required stresses and strains are computed using final moduli for all nonlinear sub-layers.

This method is relatively rapid; however, the results are approximate. In a linear-elastic layered solution, the lateral variation of modulus within a layer cannot be considered. To compensate to a certain extent for this disadvantage, a set of stress points at different radial distances are considered. The source code of a program capable of this feature was not readily available. Program BISAR was modified to carry out this algorithm.

3.3.3 Finite Element Analysis

Finite element analysis is the most comprehensive approach to study pavement response. The method has been used by a number of researchers to analyze pavement response (Raad and Figueroa, 1980; Hoffman and Thompson, 1982).

Finite element programs allow users to select the most sophisticated constitutive models for the materials. Nonlinear behavior of pavement materials can be fully taken into consideration by permitting each element to have different characteristics. Furthermore, inertia effects can be considered in finite element analysis. Therefore, dynamic analysis can be implemented. Program ABAQUS, developed by Habbit, Karlsson & Sorensen, Inc., was used in this study.

Input files for ABAQUS contain model data and history data. The model data defines a finite element model (i.e., the elements, nodes, element properties, and material definitions). The history data defines what happens to the model (i.e., the sequence of events or loading for which the model's response is sought). In ABAQUS, the user divides this history into a sequence of steps. For each step, the user chooses an analysis procedure (static stress analysis, dynamic stress analysis, etc). Any combination of these procedures can be used from step to step. Each step may be divided into several increments.

For a linear static analysis, only a linear perturbation analysis step is needed. A linear perturbation analysis gives the linear response of the system. For nonlinear static analysis, a sequence of events is defined. These events follow one another; the state of the model at the end of the last nonlinear step provides the initial conditions for the start of the next step. In this study, a user-defined subroutine that contains Equation 3.16 was integrated with the input file. The subroutine defines the updated modulus for each element. The updated modulus is a solution-dependent variable, in that its value is decided by the state of stress of the corresponding element. Steps can be further divided into increments. In each increment, the user-defined subroutine is called once for each element. Thus, the modulus of one element is the result of the state of stress of the previous step. The number of increments has an effect on the accuracy of the analysis. To keep the accuracy acceptable, the automatic incrementation scheme is preferred in most cases. The automatic incrementation scheme can adjust increment sizes based on computational efficiency. In this study, the nonlinear problem was solved by dividing it into two steps. The first step was for obtaining initial moduli of nonlinear elements. The second step was further divided into increments so that the nonlinear solution path can be followed. At each

increment the load condition was the same. However, the moduli computed in the current increment were used in the next increment.

In a dynamic analysis, the inertia effects are considered. The input file should include information about material density and damping ratio. For linear dynamic analysis, a sequence of loads is provided with progress of time, and no user subroutine is needed. For nonlinear dynamic analysis, the same user subroutine as the one in nonlinear static analysis is needed to account for material nonlinearity.

The characteristics of the finite element mesh (i.e., locations of the vertical and horizontal boundaries, the element size and shape, and the distribution of elements) affect the accuracy of the calculated stresses, strains and deflections. ABAQUS has provided extensive options of element types for solving different problems. Both the pavement section and the applied load are axisymmetric; therefore, axisymmetric solid elements are the most appropriate element type. The adoption of axisymmetric solid elements dramatically simplifies the problem, reduces the number of elements and, thus, has more computational efficiency.

To ensure that the mesh generated simulates the layered theory, a “mesh optimization” approach was utilized. The mesh optimization follows a trial and error procedure. Several meshes were generated and analyzed. The surface deflections from the analysis were then compared to those obtained from well-established linear elastic layered computer programs, such as BISAR. If a large variation was found in the comparison, the mesh would be refined and analyzed. This process was repeated until ABAQUS yielded reasonable results.

The optimized mesh is shown in Figure 3.5. Most elements are of the type CAX4 (Figure 3.6a). The CAX4 element is a 4-node bilinear axisymmetric continuum element. For progressive transition of the CAX4 elements with different sizes, element type CAX3 was used (Figure 3.6b), which is a 3-node, bilinear, axisymmetric, continuum element.

For the mesh shown in Figure 3.5, the discretization was applied to an area that was extended to 480 in. (6 m) laterally and 300 in. (7.5 m) vertically. Elements along the left side of the mesh, which was located on an axis of symmetry, were restrained from radial movement. To simplify the mesh, the elements located at the bottom and right-hand side of the mesh were restricted from radial and vertical movements.

3.4 TYPICAL PAVEMENT SECTIONS

To observe the differences among models and to determine the sensitivity of the models to the change in parameters, four hypothetical pavement sections were considered. Each pavement section is assumed to have four layers, an asphalt concrete layer over a granular base over a subgrade over bedrock. For all four pavement sections, the moduli and Poisson’s ratios were assumed to be the same. The thickness of the AC and base layers was varied. The pavement sections are named “3-6 PAVE,” “3-12 PAVE,” “5-6 PAVE,” and “5-12 PAVE,” where the first number represents the thickness of the AC layer and the second number represents the thickness of the base layer. The profile of the pavement section “3-12 PAVE” is shown in Figure 3.7.

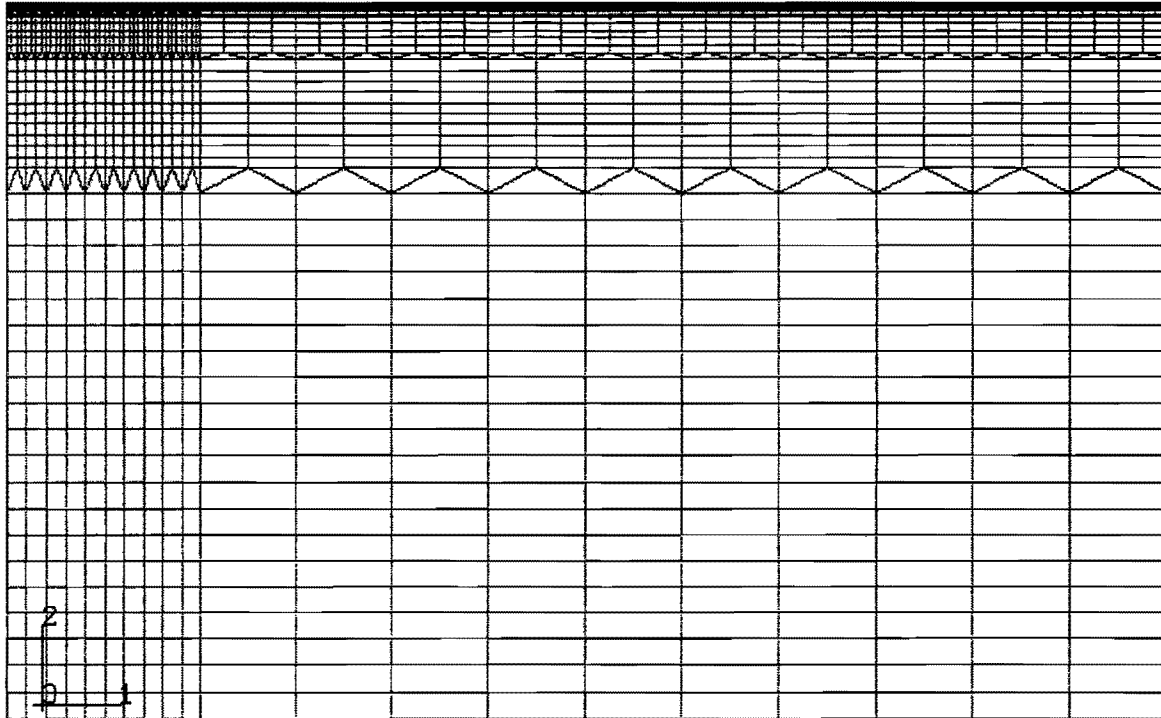
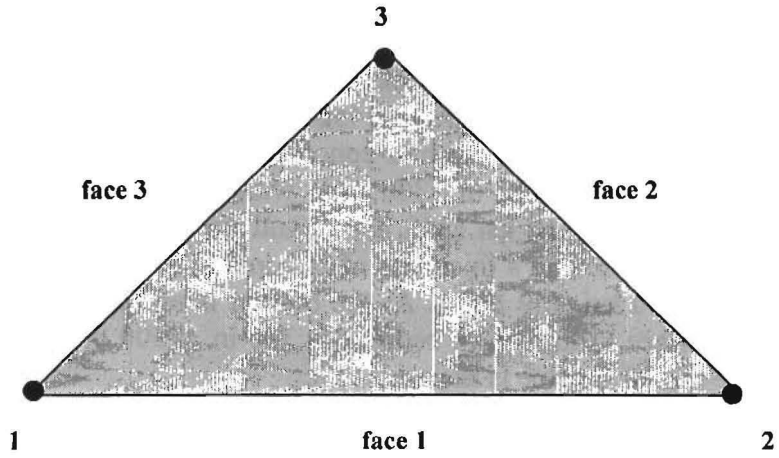
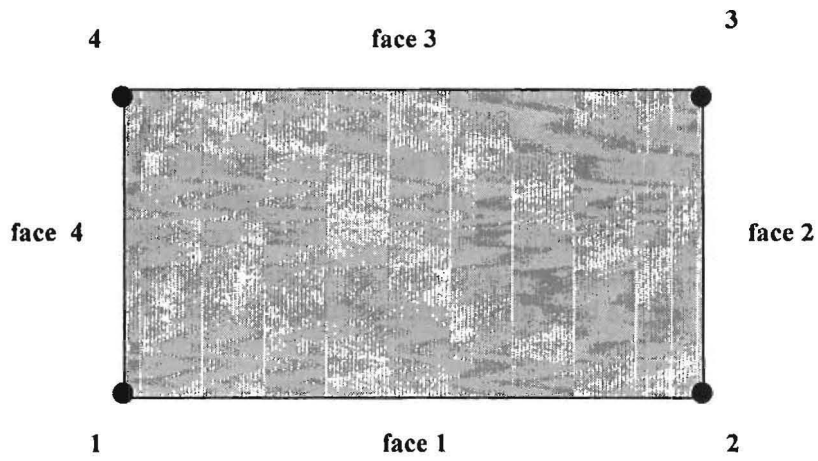


Figure 3.5 - Optimal Mesh Used to Analyze Typical Pavement in ABAQUS



(a) CAX3 ELEMENT



(b) CAX4 ELEMENT

Figure 3.6 – Two Types of Elements Used in Finite Element Analysis

The properties of the typical pavement section “3-12 PAVE” are summarized in Table 3.2. The top layer is an asphalt-concrete pavement with a thickness of 3 in. (75 mm). Its Poisson’s ratio is assumed to be 0.35 and its seismic modulus 500 ksi (3450 MPa). The unit weight of this asphalt concrete is 140 pcf (22 kN/m³). Under the asphalt concrete layer lies the granular base. The thickness of this layer is assumed to be 12 in. (300 mm) with a Poisson’s ratio of 0.35. The seismic modulus of the base layer is 50 ksi (345 MPa), and its unit weight is 120 pcf (18.8 kN/m³). The third layer is subgrade with a thickness of 285 in. (7125 mm), a Poisson’s ratio of 0.4 and a seismic modulus of 10 ksi (69 MPa). At the bottom is an infinite layer of bedrock. The depth from pavement surface to the top of bedrock is 300 in. (7500 mm). To simulate the stiffness of bedrock, a large modulus value is assigned to it.

In static analyses, a 9000-lb (40-kN) load was applied to a circular area on top of the AC layer. The radius of the loaded area was 6 in. (150 mm). In dynamic analyses, the magnitude of the load changes with time. The FWD impulse loading was simulated as a haversine. The duration of the loading was typically 30 msec with a peak load of 9000 lb (40 kN).

As indicated before, in the equivalent linear model or nonlinear model, the constitutive model presented in Equation 3.16 is adopted. In those models, the base and the subgrade were considered nonlinear. Parameters k_2 and k_3 need to be provided for this reason. Considering the fact that the subgrade is deep and the nonlinear behavior decreases rapidly with depth, only the top 18 in. (450 mm) of the subgrade is considered to exhibit nonlinear behavior. As seen in Figure 3.7, the top 18 in. (450 mm) of subgrade is defined as upper subgrade and the rest is lower subgrade. According to laboratory tests (Shahriyar, 1991), the range of parameter k_2 for aggregates was from 0.3 to 0.5 and the range of parameter k_2 for clays was from 0.15 to 0.3. Therefore, in the typical pavement sections in this study, it is assumed that parameter k_2 is 0.4 and 0.2 for the base and the upper subgrade, respectively. Based on experience (Nazarian et. al., 1998), typical values of k_3 for the pavement materials in Texas are from 0 to -0.5. Parameter k_3 is assumed to be -0.3 and -0.2 for the base and the upper subgrade, respectively.

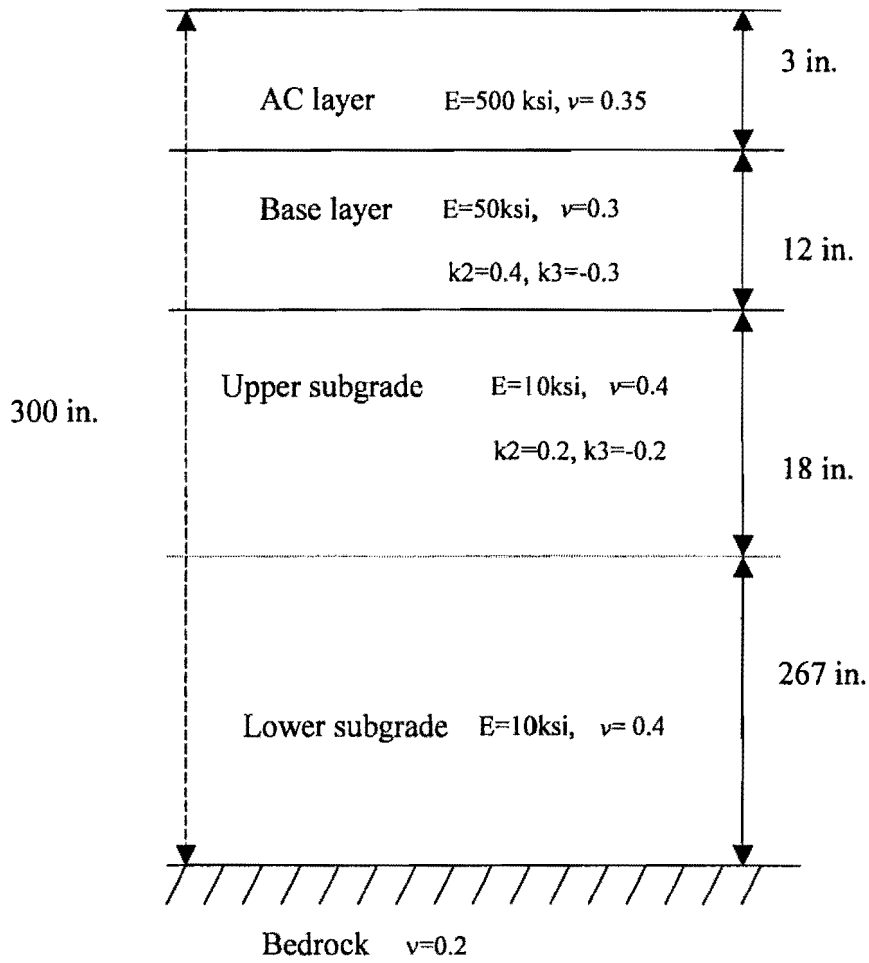


Figure 3.7 – Profile of Pavement Section “3-12 PAVE” Used in This Study

Table 3.2 - Properties of Pavement Section "3-12 PAVE"

No.	Layer	Modulus		Poisson Ratio	Thickness		Nonlinear Parameters		Unit Weight	
		(ksi)	(MPa)		(inch)	(mm)	k ₂	k ₃	(pcf)	(kN/m ³)
1	AC	500	3450	0.35	3	75	--	--	140	22.0
2	Base	50	345	0.35	12	300	0.4	-0.3	120	18.8
3	Upper Subgrade	10	69	0.4	18	450	0.2	-0.2	110	17.2
	Lower Subgrade	10	69	0.4	267	6675	--	--	110	17.2
4	Bedrock	1000	6900	0.2	Infinity	Infinity	--	--		

CHAPTER FOUR

PAVEMENT RESPONSE UNDER LINEAR ELASTIC MODEL

4.1 INTRODUCTION

In this chapter, the pavement response with an assumed linear elastic model is studied. The sensitivity of critical strains and remaining lives of the four typical pavements to the variation in pavement parameters is studied. Based on the sensitivity study, the degrees of significance of different parameters are determined.

Two computer programs were considered. Program BISAR, an example of a multi-layer linear elastic algorithm, as well as ABAQUS, an example of a finite element analysis algorithm, were used.

As indicated before, a 9000-lb (40 kN) load is assumed to be uniformly distributed over a circular area. The magnitude of the load does not affect the generality of the study since this problem is assumed to be linear and elastic in nature.

The surface deflections of the 3-12 PAVE section (3 in. of AC over 12 in. of base) determined from BISAR are reported in Table 4.1. Also included in the table are the deflections from ABAQUS after the mesh was optimized. The two programs yield similar deflections, indicating that they can be used interchangeably. Since the pre-processing of the input file for ABAQUS is time-consuming, it was not used in the sensitivity study in this chapter.

In the remainder of this chapter, the results from the pavement section 3-12 PAVE will be comprehensively discussed as an illustrative example. The results from the four pavement sections will then be used to draw appropriate conclusions.

4.2 SENSITIVITY STUDY OF “3-12 PAVE”

The variations of the two critical strains (tensile strain at the bottom of the AC layer and compressive strain at the top of the subgrade) and fatigue and rutting remaining lives due to

variation in pavement parameters for each layer are studied in this section. The variables studied included the thickness, modulus and Poisson's ratio of the AC layer; the thickness, modulus and Poisson's ratio of the base layer; the modulus and Poisson's ratio of the subgrade; and the depth to bedrock.

Table 4.1 - Response of Pavement 3-12 PAVE with Different Computer Programs

Item		Surface deflections (mils)						
		1	2	3	4	5	6	7
Sensor No.		1	2	3	4	5	6	7
Radial Distance (in.)		0	12	24	36	48	60	72
Programs	BISAR	21.1	13.2	8.5	5.9	4.2	3.1	2.3
	ABAQUS	21.3	13.1	8.4	5.8	4.1	3.0	2.3

In each case, a particular parameter was allowed to vary by 25 percent above and below the assigned value. Five hundred sets of input data were generated using a Monte Carlo simulation (Ang and Tang, 1984a, 1984b). The values were uniformly distributed within the minimum and maximum values assigned to a parameter. The program BISAR was then executed to obtain the two critical strains and the two remaining lives (fatigue and rutting).

In this study, the sensitivity index is used to measure the level of sensitivity of a parameter. The sensitivity index is defined as the ratio of the percentage change in the target parameter (the output of BISAR) to the percentage change in the perturbed input parameter. Mathematically,

$$\text{Sensitivity Index} = \frac{\text{Percentage Change in Target Parameter}}{\text{Percentage Change in Perturbed Input Parameter}} \quad (4.1)$$

The percentage change is defined as

$$\text{Percentage Change} = \frac{|\text{Calculated or Used Quantity} - \text{Original Quantity}|}{\text{Original Quantity}} \times 100 \quad (4.2)$$

Therefore, the larger the sensitivity index is, the more sensitive the target parameter will be to the varied parameter. Based on the sensitivity indices of critical strains and remaining lives, the factors that significantly affect the pavement response were identified. A set of arbitrary limits was used to define the significance of a given parameter. These levels are defined in Table 4.2 and were used throughout this study.

Table 4.2 – Levels of Sensitivity Assigned to Each Parameter Based on Sensitivity Index

Level Of Sensitivity	Sensitivity Index ^[1]		Significance to Pavement Design
	Critical strains	Remaining Lives	
Not Sensitive (NS)	<0.1	<0.25	Can be probably estimated with small error in final results
Moderately Sensitive (MS)	≥0.1 and < 0.2	≥0.25 and < 0.5	Must be measured to limit errors in design
Sensitive (S)	≥0.2 and <0.4	≥0.5 and <1.0	Must be measured with reasonable accuracy for satisfactory design
Very Sensitive (VS)	≥0.4	≥1.0	Must be measured very accurately or design may not be considered appropriate

[1]: Sensitivity index is defined in equation 4.1.

4.2.1 Thickness of AC Layer

The original thickness of the AC layer in pavement “3-12 PAVE” is 3 in. (75 mm). Five hundred sets of data were generated wherein the thickness of the AC layer varied between 2.25 in. (56 mm) to 3.75 in. (94 mm) with a uniform distribution. The other parameters were maintained at their default values defined in Chapter 3. The distribution of the thickness of the AC for the five hundred cases is shown in Figure 4.1. The distribution is fairly uniform.

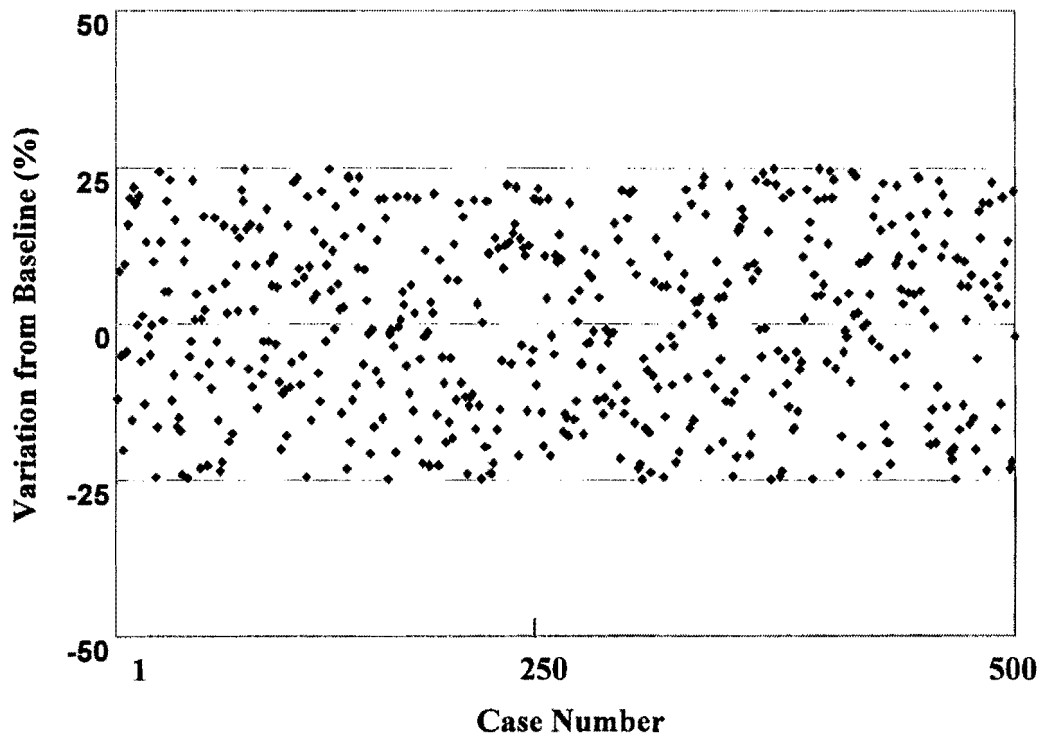


Figure 4.1 – Distribution of Thickness of AC Using Monte Carlo Simulation for “3-12 PAVE”

Variations in the two critical strains with the thickness of the AC layer, t_{AC} , are shown in Figure 4.2. Similarly, Figure 4.3 depicts the variation in the two remaining lives with t_{AC} . From Figure 4.2a, the tangential tensile strain at the bottom of the AC layer, ϵ_t , decreases when t_{AC} increases from 3 in. (75 mm) to 3.75 in. (94 mm). For AC thickness less than 3 in. (75 mm), ϵ_t decreases with a decrease in t_{AC} . Since thin AC layers provide little rigidity, the base layer provides a relatively strong support and carries most of the applied load. For a thin AC layer that was investigated here, ϵ_t decreases by about 5 percent when the thickness increases by 25 percent. Therefore, in this case, the thickness of the AC does not appreciably impact the tensile strain at the bottom of the AC. Correspondingly, the fatigue remaining life of the pavement in this case varied by about 18 percent for a 25 percent variation of t_{AC} . With a sensitivity index of 0.75 with respect to fatigue remaining life, one can consider this parameter to be sensitive in this case.

The variation in the vertical compressive strain at the top of the subgrade, ϵ_c , with thickness of the AC layer is shown in Figure 4.2b. As the AC layer becomes thicker, the vertical strain on top of the subgrade becomes smaller. Parameter ϵ_c decreases by about 15 percent when t_{AC} increases by 25 percent, from 3 in. (75mm) to 3.75 in. (94mm).

Similarly, ϵ_c increases by about 13 percent when t_{AC} decreases by 25 percent, from 3 in. (75mm) to 2.25 in. (56mm). Correspondingly, the remaining life due to rutting of the pavement increases by about 89 percent with a 25 percent increase in t_{AC} . In this case, since the sensitivity index is about 0.6 and 3.6 with respect to critical compressive strain and rutting remaining life, respectively, it can be concluded that the compressive strain on top of the subgrade is very sensitive to the thickness of the AC layer.

4.2.2 Depth to Bedrock

The original depth to bedrock in pavement section “3-12 PAVE” is 300 in. (7.5 m). Again, five hundred sets of data were generated wherein the depth to bedrock varied between 225 in. (5.6 m) and 375 in. (9.4 m) with a uniform distribution. In this case, the sensitivity indices were all very small, indicating that the pavement response is not sensitive to the variation in depth to bedrock in this case.

Boddapati (1992) indicated that the depth to bedrock plays an important role in properly predicting the remaining lives of pavements. Many investigators reported that a critical depth exists below which the impact of the bedrock on the predicted parameters is negligible (see Boddapati, 1992 for an overview). For the typical pavement section shown in Figure 3.7, the bedrock was intentionally placed at a depth that would not significantly impact the results. In order to quantify the influence of bedrock, another study was carried out in which its depth was varied from 75 in. (1.9 m) to 450 in. (11.3 m). The results are shown in Table 4.3.

As the depth to bedrock is reduced from 300 in. (7.5 m) to 75 in. (1.9 m), the deflection of the first sensor decreases from about 21 mils (525 microns) to about 18 mils (450 microns). At the same time, the deflection of the last sensor decreases by a factor of about 10, from about 2.3 mils

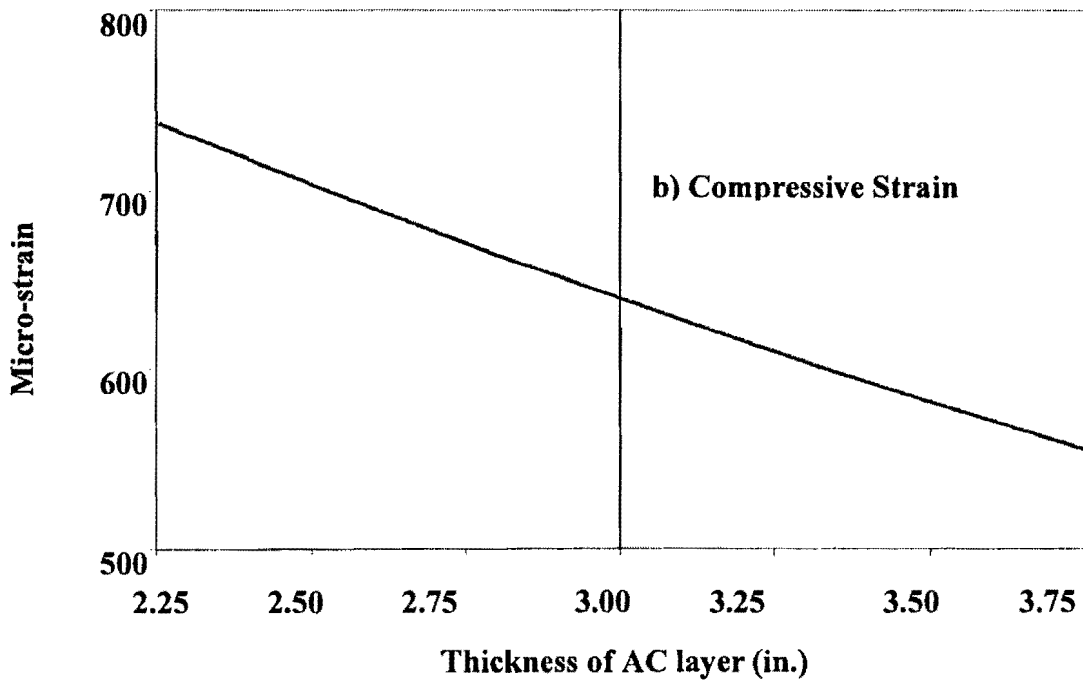
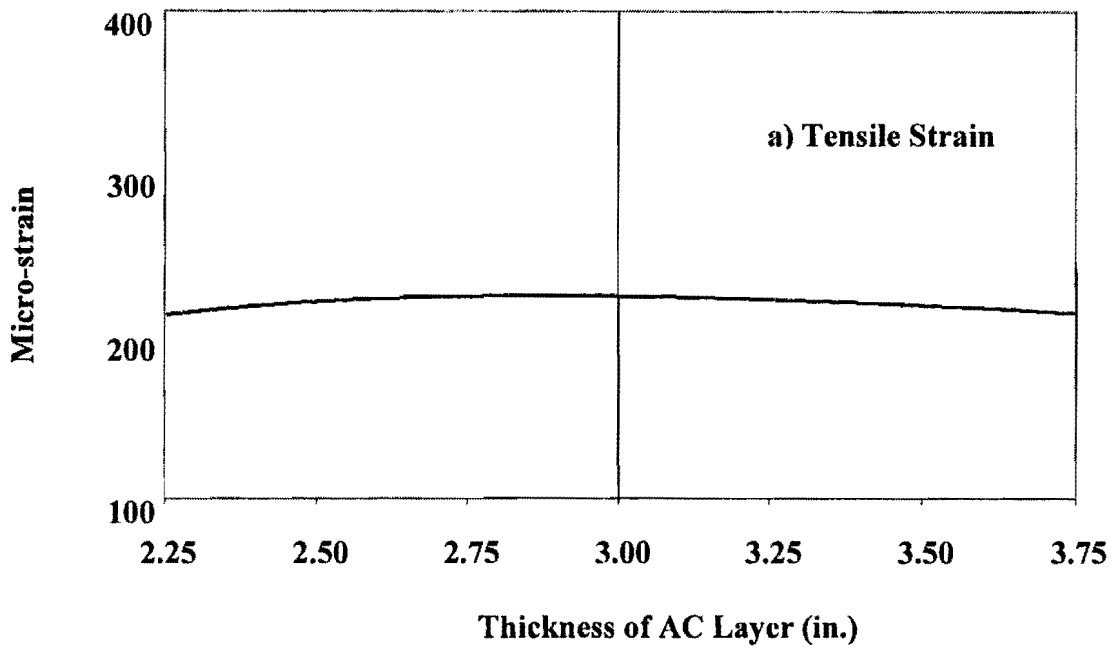


Figure 4.2—Variations in Critical Strains with Thickness of AC Layer for Pavement Section “3-12 PAVE”

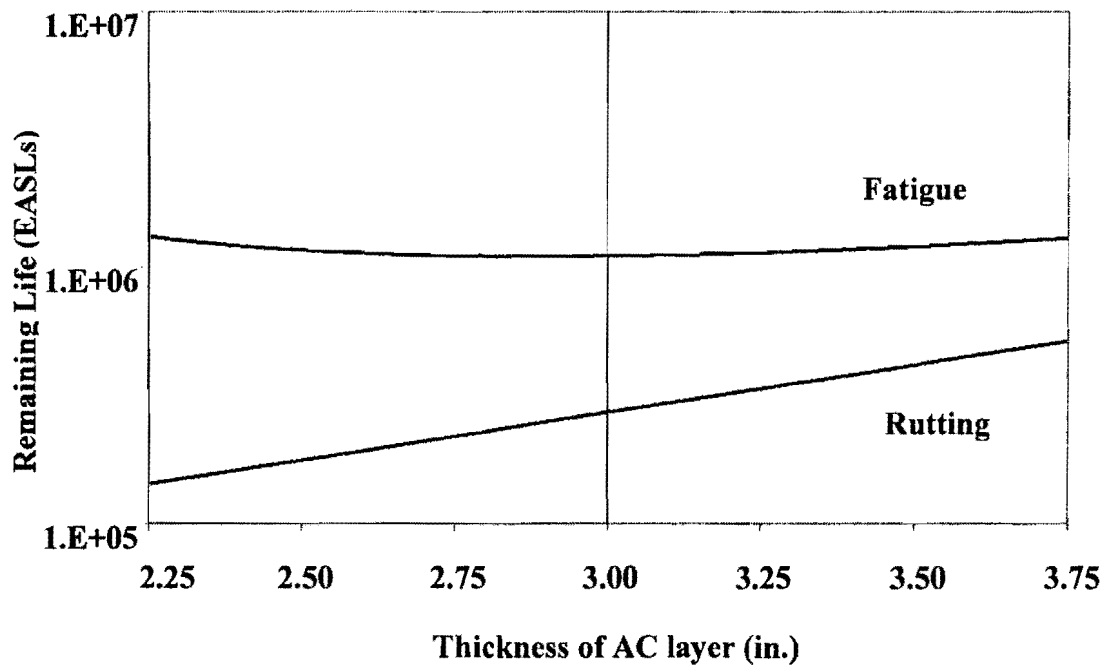


Figure 4.3 – Variations in Remaining Lives with Thickness of AC Layer for “3-12 PAVE”

(57.5 microns) to almost 0.2 mils (5 microns). However, the two critical strains reported in Table 4.3 do not vary at all when the depth to bedrock is varied between 75 in. (1.9 m) and 450 in. (11.3 m). As a result, the depth to bedrock does not impact the remaining lives. These results should be interpreted with caution. If the depth to bedrock is known and if the backcalculation can be done properly, one can accurately determine the remaining life of the pavement. However, if the depth to bedrock is misjudged and the bedrock is shallow, the remaining lives will be significantly misjudged.

4.2.3 Other Properties

A similar procedure was followed for every other parameter. The results are presented in Appendix A in a comprehensive manner and are summarized in Tables 4.4 and 4.5. The results in these two tables are elaborated below.

The results from the Monte Carlo simulations for different parameters are summarized in Figures 4.4 through 4.7. In each graph, the y-axis corresponds to the difference between the parameter calculated from the perturbed model and that calculated from the baseline model (values from Figure 3.7) normalized by the parameter calculated from the baseline model. The larger the range that the parameter covers along the y-axis, the more sensitive a critical strain or remaining life will be to the variation of the corresponding parameter.

Table 4.3 – Variation in Response of Pavement Section “3-12 PAVE” with Depth of Bedrock

Depth to Bedrock		$\epsilon_t^{[1]}$	$\epsilon_c^{[2]}$	$N_f^{[3]}$	$N_r^{[4]}$	$d_1^{[5]}$	d_2	d_3	d_4	d_5	d_6	d_7
(inch)	(m)	(micro-strain)		(1000 EASLs)		(milli-in.)						
75	1.9	227	641	1069	269	17.8 (-15.6) ^[6]	9.9 (-25.0)	5.3 (-37.6)	2.9 (-50.8)	1.5 (-64.3)	0.7 (-77.4)	0.2 (-91.3)
150	3.8	225	640	1094	272	20 (-5.2)	12 (-9.1)	7.3 (-14.1)	4.8 (-18.6)	3.1 (26.2)	2.1 (-32.3)	1.4 (-39.1)
225	5.6	225	640	1102	272	20.7 (-1.9)	12.8 (-3.0)	8.1 (-4.7)	5.5 (-6.8)	3.8 (-9.5)	2.7 (-12.9)	2 (-13.0)
300	7.5	224	640	1105	273	21.1	13.2	8.5	5.9	4.2	3.1	2.3
375	9.4	224	639	1105	273	21.4 (1.4)	13.4 (1.5)	8.7 (2.4)	6.1 (3.4)	4.4 (4.8)	3.3 (6.5)	2.5 (8.7)
450	11.3	224	639	1103	273	21.5 (1.9)	13.6 (3.0)	8.8 (3.5)	6.2 (5.1)	4.6 (9.5)	3.5 (12.9)	2.7 (17.4)

[1]: Tensile strain at the bottom of AC layer;

[2]: Compressive strain at the top the subgrade;

[3]: Pavement remaining life due to fatigue cracking;

[4]: Pavement remaining life due to rutting;

[5]: d_1 to d_7 are surface deflections at radial distances of 0, 12, 24, 36, 48, 60 and 72 in., respectively. 1 milli-inch = 0.025 mm;

[6]: Value in parenthesis is percent difference between this quantity and the similar quantity with depth to bedrock of 300 in.

The sensitivity of tensile strain at the bottom of AC (ϵ_t) and the remaining life due to fatigue cracking (N_f) to different pavement parameters are summarized in Figures 4.4 and 4.5 and Table 4.4. For the thin pavement studied here, ϵ_t and N_f are very sensitive to the modulus of the base layer. Parameters ϵ_t and N_f are also sensitive to the thickness of the AC layer, the thickness of the base layer, the modulus of the AC layer, and the Poisson's ratio of the base layer. On the contrary, ϵ_t and N_f are not very sensitive to the Poisson's ratio of the AC layer or subgrade or the modulus of subgrade.

The impact of the pavement parameters on the compressive strain on top of the subgrade (ϵ_c) and the remaining life due to rutting (N_r) is illustrated in Figures 4.6 and 4.7 and Table 4.5. Parameters ϵ_c and N_r are very sensitive to the thickness of the base layer, the thickness of the AC layer, the modulus of the base layer, the modulus of the subgrade, and the Poisson's ratio of the subgrade. On the other hand, ϵ_c and N_r are only slightly sensitive to the Poisson's ratio of the AC layer and the Poisson's ratio of the base.

From the above analysis, for a pavement with thin AC layer, only the Poisson's ratio of the AC layer has little effect on the pavement critical strains and remaining lives. All the other parameters except the depth to bedrock are significant either to ϵ_t , to ϵ_c , or to both, and, therefore, are significant to the remaining life of the pavement. As analyzed before, the depth to bedrock is not directly significant to the pavement remaining lives. However, it has large influence on surface deflections and, thus, it significantly affects the backcalculated set of moduli in FWD test.

4.3 SUMMARY OF THE SENSITIVITY STUDY FOR THE LINEAR ELASTIC MODELS

The other three typical pavement sections, PAVE 3-6, PAVE 5-6 and PAVE 5-12, are also analyzed for sensitivity of critical strains and remaining lives. Thickness, modulus and the Poisson's ratio of the AC and base layers as well as the modulus and Poisson's ratio of the subgrade are studied. The results are presented in Tables 4.6 through 4.9.

The sensitivity indexes and levels are somewhat different for different pavements. This fact indicates that the thickness of the AC layer or the base impacts the characteristics of the pavement response. For example, when the thickness of the AC layer is 3 in. (75 mm) (i.e., 3-6 PAVE and 3-12 PAVE), the critical tensile strain is sensitive to the modulus of the AC layer. However, if the thickness of the AC layer is increased to 5 in. (125 mm) (5-6 PAVE and 5-12 PAVE), the critical tensile strain is more sensitive to the modulus of the AC layer. However, in some cases, this impact is not large enough to change the sensitivity level although the sensitivity index exhibits some difference.

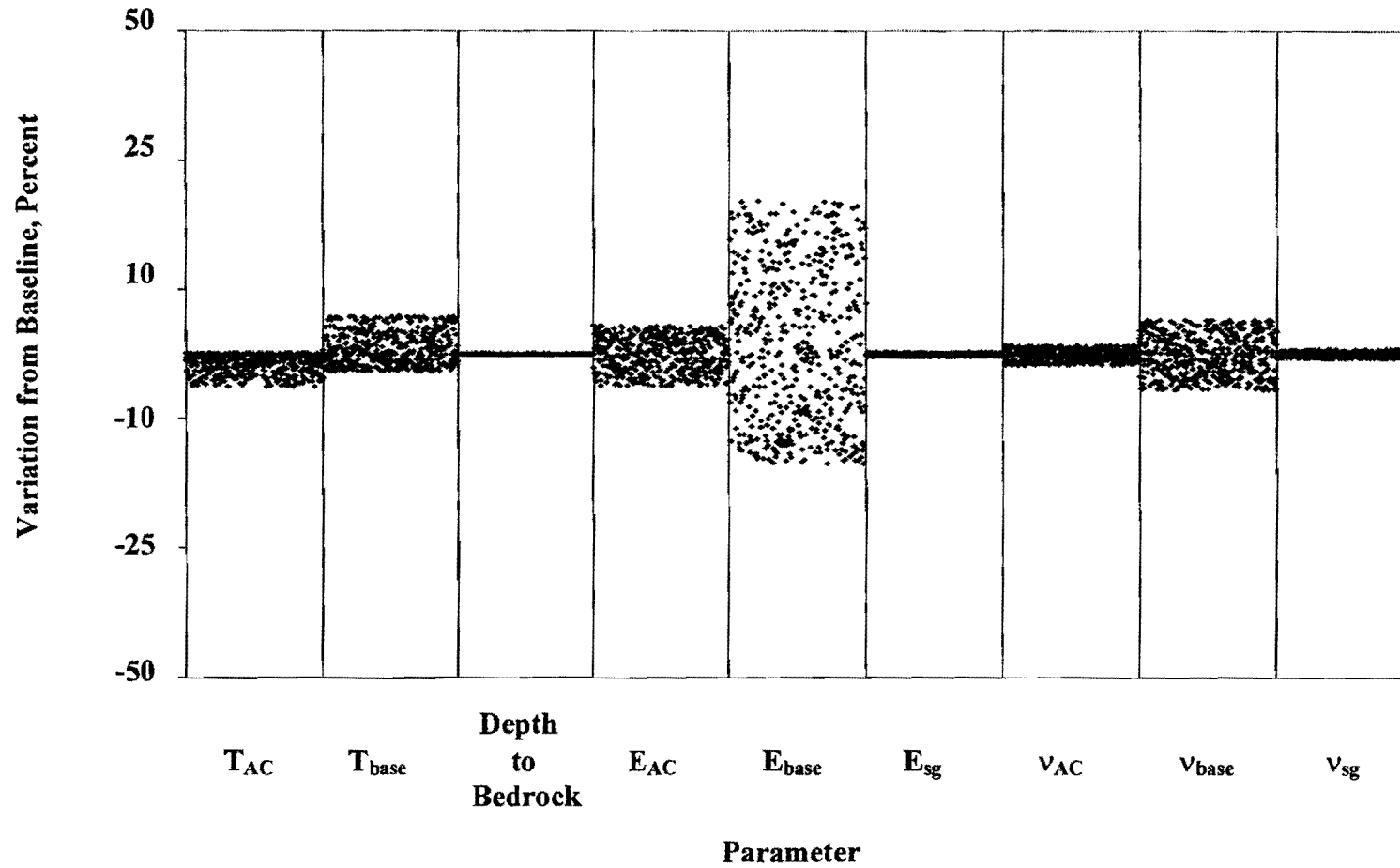


Figure 4.4 – Variations in Critical Tensile Strain with Parameters for Pavement “3-12 PAVE”

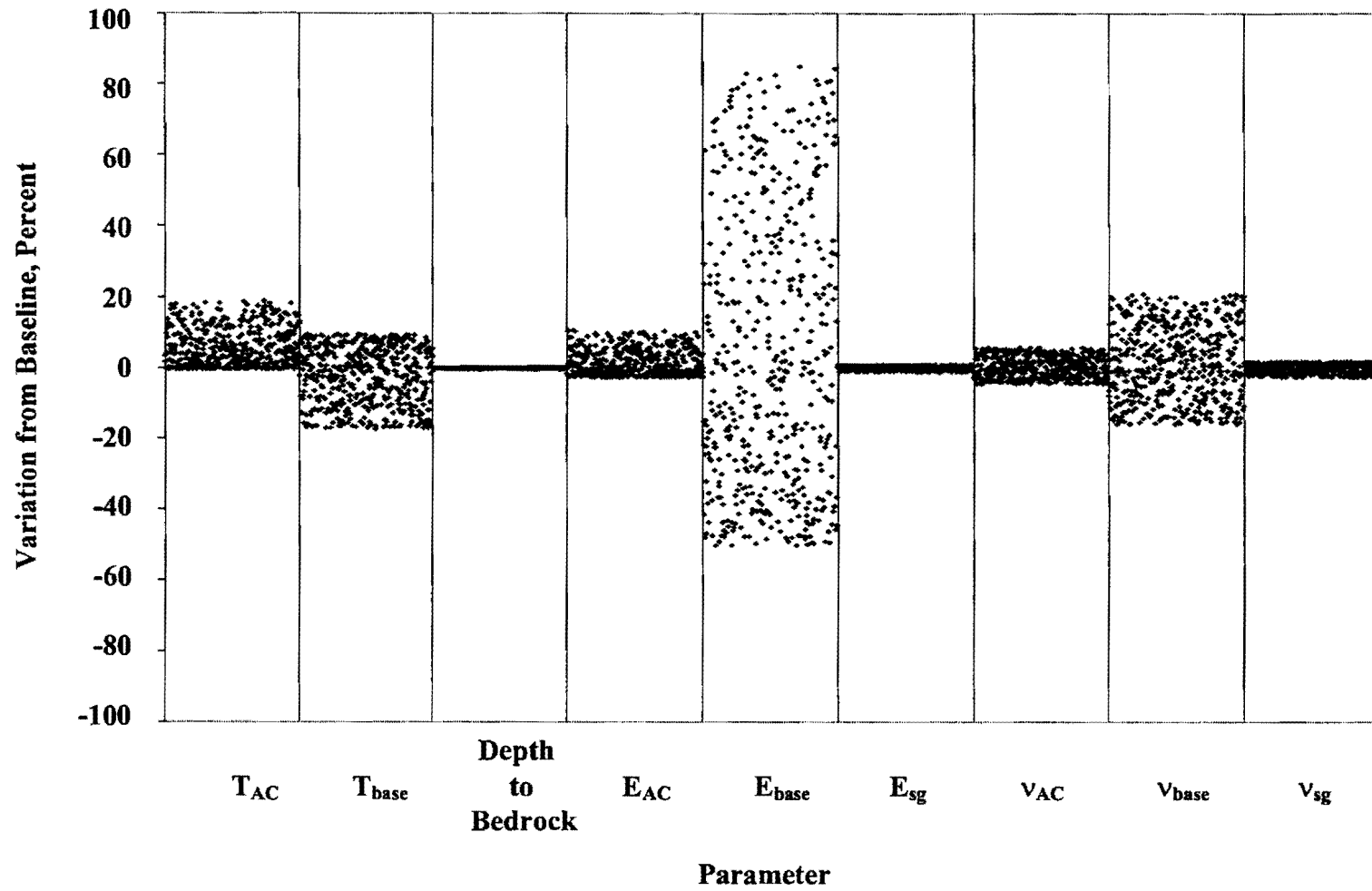


Figure 4.5 – Variations in Fatigue Remaining Life with Parameters for Pavement “3-12 PAVE”

Table 4.4 – Levels of Sensitivity of Pavement Parameters with Respect to Critical Tensile Strain and Fatigue Remaining Life for Pavement “3-12 PAVE”

Layer		AC			Base			Subgrade		Depth to Bedrock
Parameters		Thickness	Modulus	Poisson's Ratio	Thickness	Modulus	Poisson's Ratio	Modulus	Poisson's Ratio	
$\epsilon_t^{[1]}$	Sensitivity Index	0.20	0.20	0.07	0.24	0.95	0.22	0.01	0.03	0.01
	Level of Sensitivity	S ^[3]	S	NS	S	VS	S	NS	NS	NS
$N_f^{[2]}$	Sensitivity Index	0.75	0.42	0.23	0.69	3.4	0.84	0.04	0.11	0.04
	Level of Sensitivity	S	S	NS	S	VS	S	NS	NS	NS

[1] ϵ_t : Critical Tensile Strain;

[2] N_f : Fatigue Remaining Life;

[3] VS: Very Sensitive; S: Sensitive; MS: Moderately Sensitive; NS: Not Sensitive.

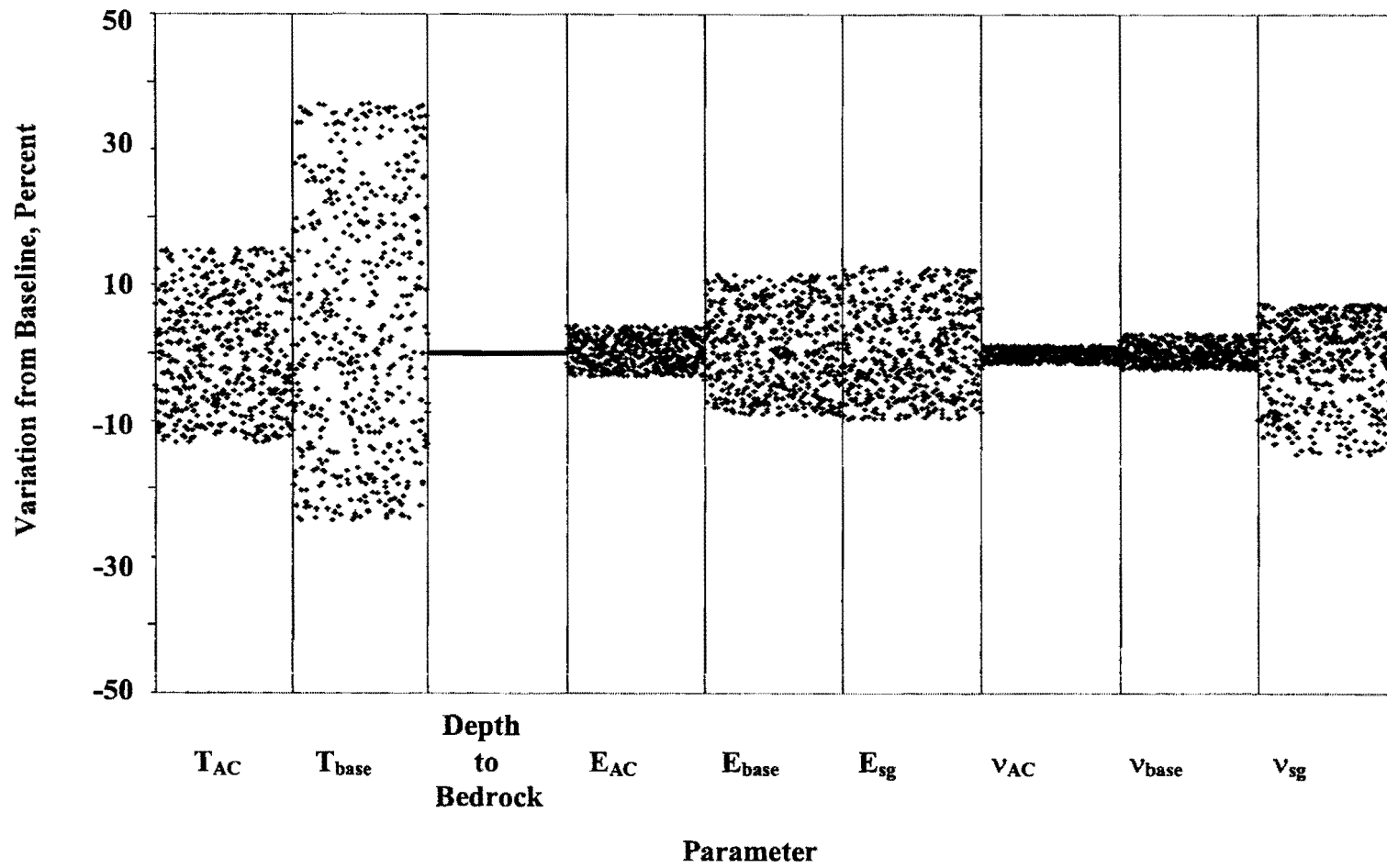


Figure 4.6 – Variations in Critical Compressive Strain with Parameters for Pavement “3-12 PAVE”

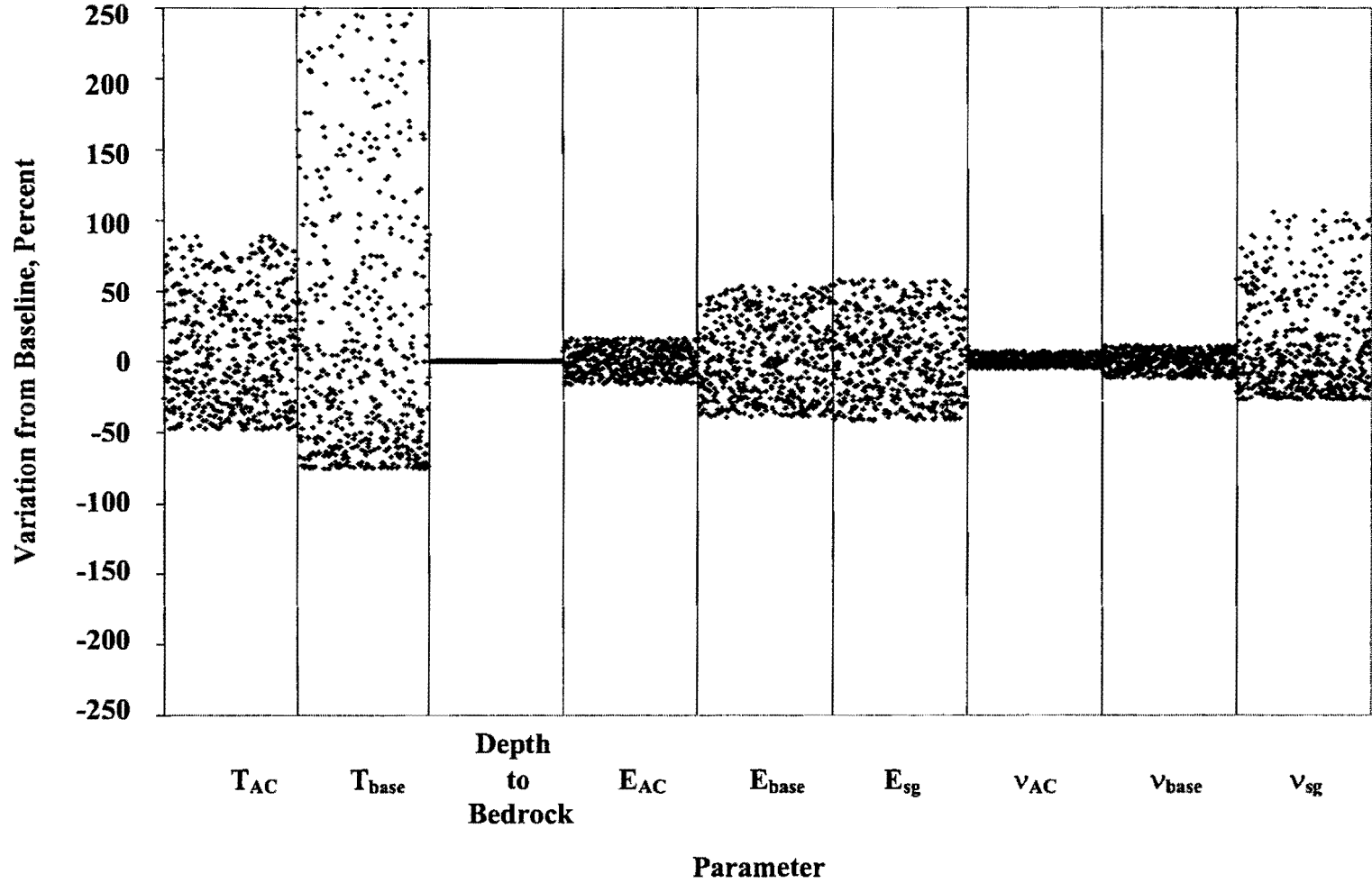


Figure 4.7 – Variations in Rutting Remaining Life with Parameters for Pavement “3-12 PAVE”

Table 4.5 – Levels of Sensitivity of Pavement Parameters with Respect to Critical Compressive Strain and Rutting Remaining Life for Pavement “3-12 PAVE”

Layer		AC			Base			Subgrade		Depth to Bedrock
Parameters		Thickness	Modulus	Poisson's Ratio	Thickness	Modulus	Poisson's Ratio	Modulus	Poisson's Ratio	
$\epsilon_c^{[1]}$	Sensitivity Index	0.62	0.17	0.06	1.48	0.46	0.12	0.51	0.61	0.004
	Level of Sensitivity	VS ^[3]	MS	NS	VS	VS	MS	VS	VS	NS
$N_r^{[2]}$	Sensitivity Index	3.56	0.67	0.29	10.1	2.17	0.49	2.32	4.32	0.02
	Level of Sensitivity	VS	S	MS	VS	S	MS	VS	VS	NS

[1] ϵ_c : Critical Compressive Strain;

[2] N_r : Rutting Remaining Life;

[3] VS: Very Sensitive; S: Sensitive; MS: Moderately Sensitive; NS: Not Sensitive.

**Table 4.6 – Sensitivity of Pavement Parameters to
Critical Tensile Strain under Linear Elastic Model**

Layer	Parameter	Sensitivity	Thin AC (3 in.)		Thick AC (5 in.)	
			Thin Base (6 in.)	Thick Base (12 in.)	Thin Base (6 in.)	Thick Base (18 in.)
AC	Thickness	Index	0.23	0.20	0.73	0.68
		Level	S	S	VS	VS
	Modulus	Index	0.26	0.20	0.47	0.46
		Level	S	S	VS	VS
	Poisson's Ratio	Index	0.04	0.07	0.08	0.05
		Level	NS	NS	NS	NS
Base	Thickness	Index	0.47	0.24	0.31	0.23
		Level	VS	S	S	S
	Modulus	Index	0.79	0.95	0.48	0.62
		Level	VS	VS	VS	VS
	Poisson's Ratio	Index	0.17	0.22	0.10	0.16
		Level	MS	S	MS	MS
Subgrade	Modulus	Index	0.15	0.01	0.17	0.06
		Level	MS	NS	MS	NS
	Poisson's Ratio	Index	0.07	0.03	0.06	0.04
		Level	NS	NS	NS	NS

[1] VS: Very Sensitive; S: Sensitive; MS: Moderately Sensitive; NS: Not Sensitive.

Table 4.7 – Sensitivity of Pavement Parameters to Critical Compressive Strain under Linear Elastic Model

Layer	Parameter	Sensitivity	Thin AC (3 in.)		Thick AC (5 in.)	
			Thin Base (6 in.)	Thick Base (12 in.)	Thin Base (6 in.)	Thick Base (18 in.)
AC	Thickness	Index	0.94	0.62	1.42	1.01
		Level	VS	VS	VS	VS
	Modulus	Index	0.19	0.17	0.42	0.28
		Level	MS	MS	VS	S
	Poisson's Ratio	Index	0.08	0.06	0.11	0.09
		Level	NS	NS	MS	NS
Base	Thickness	Index	0.81	1.48	0.61	1.15
		Level	VS	VS	VS	VS
	Modulus	Index	0.30	0.46	0.18	0.33
		Level	S	VS	MS	S
	Poisson's Ratio	Index	0.03	0.12	0.04	0.06
		Level	NS	MS	NS	NS
Subgrade	Modulus	Index	0.57	0.51	0.54	0.52
		Level	VS	VS	VS	VS
	Poisson's Ratio	Index	0.71	0.61	0.71	0.63
		Level	VS	VS	VS	VS

[1] VS: Very Sensitive; S: Sensitive; MS: Moderately Sensitive; NS: Not Sensitive.

**Table 4.8 – Sensitivity of Pavement Parameters to Fatigue Remaining Life
under Linear Elastic Model**

Layer	Parameter	Sensitivity	Thin AC (3 in.)		Thick AC (5 in.)	
			Thin Base (6 in.)	Thick Base (12 in.)	Thin Base (6 in.)	Thick Base (18 in.)
AC	Thickness	Index	0.85	0.75	3.40	3.08
		Level	S	S	VS	VS
	Modulus	Index	1.11	0.42	0.60	0.54
		Level	VS	MS	S	S
	Poisson's Ratio	Index	0.12	0.23	0.27	0.17
		Level	NS	NS	MS	NS
Base	Thickness	Index	1.21	0.69	0.87	.68
		Level	VS	S	S	S
	Modulus	Index	2.83	3.40	1.61	2.09
		Level	VS	VS	VS	VS
	Poisson's Ratio	Index	0.63	0.84	0.35	0.53
		Level	S	S	MS	S
Subgrade	Modulus	Index	0.47	0.04	0.52	0.20
		Level	MS	NS	S	NS
	Poisson's Ratio	Index	0.22	0.11	0.20	0.13
		Level	NS	NS	NS	NS

[1] VS: Very Sensitive; S: Sensitive; MS: Moderately Sensitive; NS: Not Sensitive.

Table 4.9 – Sensitivity of Pavement Parameters to Rutting Remaining Life under Linear Elastic Model

Layer	Parameter	Sensitivity	Thin AC (3 in.)		Thick AC (5 in.)	
			Thin Base (6 in.)	Thick Base (12 in.)	Thin Base (6 in.)	Thick Base (18 in.)
AC	Thickness	Index	5.80	3.56	9.24	6.13
		Level	VS	VS	VS	VS
	Modulus	Index	0.48	0.67	1.81	1.15
		Level	MS	S	VS	VS
	Poisson's Ratio	Index	0.37	0.29	0.53	0.40
		Level	MS	MS	S	MS
Base	Thickness	Index	4.91	10.10	3.46	7.28
		Level	VS	VS	VS	VS
	Modulus	Index	1.46	2.17	0.91	1.61
		Level	VS	VS	S	VS
	Poisson's Ratio	Index	0.11	0.49	0.18	0.25
		Level	NS	MS	NS	MS
Subgrade	Modulus	Index	2.56	2.32	2.41	2.34
		Level	VS	VS	VS	VS
	Poisson's Ratio	Index	5.54	4.32	5.61	4.56
		Level	VS	VS	VS	VS

[1] VS: Very Sensitive; S: Sensitive; MS: Moderately Sensitive; NS: Not Sensitive.

CHAPTER FIVE

PAVEMENT RESPONSE UNDER EQUIVALENT-LINEAR MODEL

5.1 INTRODUCTION

As indicated in Chapter 3, the material nonlinearity can be taken into consideration in an approximate fashion using an equivalent-linear model. An iterative process, based on the linear static layered-system program BISAR, is employed to implement the equivalent-linear model.

In this chapter, the validity of the equivalent-linear model is studied. The effect of different numbers of sublayers on the response from the equivalent-linear model is analyzed. The sensitivity of the pavement response to the variations in pavement parameters is studied. In this case, the Monte Carlo simulation was not used in the sensitivity study because it is more time-consuming to execute the equivalent-linear model. Since the relation between each parameter and pavement response is unique, the results were valid as long as enough cases were generated for each parameter.

5.2 EFFECTS OF NUMBER OF SUBLAYERS ON RESPONSE FROM EQUIVALENT-LINEAR MODEL

To verify the robustness of the equivalent-linear algorithm and to determine the optimum number of sublayers to be used, a sample problem was solved, and its results were analyzed. This problem is based on the typical pavement section shown in Figure 3.7. First, only the base was considered nonlinear. The base layer was assumed to have a seismic modulus of 50 ksi (345 MPa), a thickness of 12 in. (300 mm), and a Poisson's ratio of 0.35. Its nonlinear parameters k_2 and k_3 were considered as 0.4 and -0.3 , respectively.

Seven cases, with different numbers of base sublayers, were analyzed. The base was subdivided into 1, 2, 3, 4, 5, 6 and 12 layers (see Tables 5.1 and 5.2). The seven surface deflections, the

tangential tensile strain at the bottom of the AC layer, the vertical compressive strain at the top of the subgrade, and the two remaining lives of the pavement using the Asphalt Institute equation were calculated for each case.

As shown in Table 5.1, the surface deflections at radial distances in excess of 24 in. (600 mm) hardly vary with the change in the number of sublayers. This is expected for two reasons. First, the additional stresses induced by the external loads are relatively small for large radial distances. Second, the surface deflections at large radial distances are mainly determined by material behavior at large depths. Therefore, the nonlinearity of the base layer has little effect on surface deflections at large radial distances.

The surface deflections at radial distances of 0 in. (0 mm) and 12 in. (300 mm) vary with the number of sublayers (see Table 5.1). For fewer than three sublayers, the deflections increase as the number of sublayers increases. For three or more sublayers, the deflections remain more or less constant.

The variations in the two critical strains and the two remaining lives with the number of sublayers are shown in Table 5.2. When only one sublayer is used, the remaining life may vary by more than 30%. However, for three or more sublayers, the differences in remaining lives are reasonably small.

As shown in Table 5.1, the number of iterations significantly increases with the number of sublayers. The conclusion of this study is that, typically, 3 to 5 sublayers are adequate for use with an equivalent-linear model. Since the stresses and strains are much smaller for the subgrade, it is anticipated that the same number of sublayers should be adequate. The issue of the level of approximation introduced by using an equivalent-linear model, as opposed to a “true” nonlinear model, is discussed in Chapter 8.

5.3 SENSITIVITY STUDY FOR “3-12 PAVE”

In this section, the sensitivity of the two critical strains and fatigue and rutting remaining lives to variations in parameters of pavement layers is studied. Since the load-induced nonlinearity is not significant at large depths, only the upper 18 inches (450 mm) of the subgrade is considered nonlinear (see Figure 3.7). The variables to be analyzed in this sensitivity study are:

- a. Thickness, modulus and Poisson’s Ratio of the AC layer;
- b. Thickness, seismic modulus, Poisson’s Ratio and nonlinear parameters k_2 and k_3 of the base layer;
- c. Seismic modulus, Poisson’s Ratio and nonlinear parameters k_2 and k_3 of the upper subgrade;
- d. Depth to bedrock.

Table 5.1 - Comparison of Deflections with Different Number of Sublayers in Equivalent-Linear Model for "3-12 PAVE"

Number of Sublayers	Total Thickness	Thickness of each Sublayer	Number of Iterations	Radial distance (in.)						
				0	12	24	36	48	60	72
	(inch)	(inch)	Deflection (mils)							
1	12	12.0	47	23.5	14.3	11.1	8.8	5.8	4.1	3.0
2	12	6.0	142	24.6	14.8	11.2	8.8	5.8	4.1	3.0
3	12	4.0	264	24.9	14.9	11.2	8.8	5.8	4.1	3.0
4	12	3.0	428	25.0	14.9	11.2	8.8	5.8	4.1	3.0
5	12	2.4	575	25.1	14.9	11.2	8.8	5.8	4.1	3.0
6	12	2.0	732	25.2	14.9	11.2	8.8	5.8	4.1	3.0
12	12	1.0	1692	25.2	14.9	11.2	8.8	5.8	4.1	3.0

Table 5.2 - Comparison of Critical Strains and Remaining Lives with Different Number of Sublayers in Equivalent-Linear Model for "3-12 PAVE"

Number of Sublayers	Total Thickness (inch)	Thickness of Each Sublayer (inch)	Tensile Strain at Bottom of AC		Comp. Strain at Top of Subgrade		Remaining Lives			
			Micro-strain	Diff. (%)	Micro-strain	Diff. (%)	Fatigue		Rutting	
							10 ⁵ EASLs	Diff. (%)	10 ⁵ EASLs	Diff. (%)
1	12	12.0	275	2.0	710	-5.7	5.7	-6.5	1.7	29.8
2	12	6.0	269	-0.2	740	-1.6	6.1	0.5	1.4	7.8
3	12	4.0	269	-0.3	746	-0.7	6.1	0.8	1.3	3.3
4	12	3.0	269	-0.2	749	-0.4	6.1	0.6	1.3	1.8
5	12	2.4	269	-0.1	751	-0.2	6.1	0.4	1.3	1.1
6	12	2.0	269	-0.1	751	-0.1	6.1	0.3	1.3	0.7
12	12	1.0	269	0.0	752	0.0	6.1	0.0	1.3	0.0

- Difference is defined as percent difference between the calculated quantity and the similar quantity calculated with 12 sublayers.

For each parameter, several different reasonable values were adopted. For each case, the equivalent-linear program was executed to obtain the two critical strains and, thus, the fatigue and rutting remaining lives.

5.3.1 AC Layer

The AC layer is considered linear. Therefore, the properties to be studied are thickness, modulus and Poisson's ratio. The results, in a detailed manner, are included in Appendix B and are summarized in Tables 5.3 and 5.4.

The critical strains and remaining lives, as reflected in Table 5.3 and 5.4, are very sensitive to the variation in the thickness of the AC layer. A 25 percent variation in the thickness of the AC layer can result in a variation of 24 percent in critical tensile strain and 16 percent in critical compressive strain and, thus, a variation of 355 percent in both remaining lives. The modulus of the AC layer is of secondary importance. However, the response is not sensitive to the variation in the Poisson's ratio of the AC layer.

5.3.2 Base Layer

The base layer is considered to behave nonlinearly. Therefore, the variables to be considered also include nonlinear parameters k_2 and k_3 , as well as the thickness, seismic modulus and Poisson's Ratio. Appendix B shows the trends of the variations in critical strains and remaining lives with these variables.

The sensitivity study of parameters k_2 and k_3 is especially important since the purpose of the equivalent-linear model is to take the nonlinear behavior of pavement materials into consideration.

Figures 5.1 and 5.2 show the impact of the values of k_2 on the two critical strains and remaining lives. In the constitutive model, the larger k_2 is, the more rapidly the base becomes stiffer as a result of an increase in confining pressure. This is consistent with the trends shown in Figures 5.1 and 5.2. With an increase in k_2 , both critical tensile strain and critical compressive strain decrease and, thus, the remaining lives increase.

The impacts of the parameter k_3 on strains and remaining lives are shown in Figures 5.3 and 5.4. In contrast to k_2 , the larger the absolute value of k_3 , the more rapidly the base softens as deviatoric stress increases. This trend can also be observed in these two figures.

The levels of sensitivity of different parameters with respect to the critical tensile strain, ϵ_t , and the remaining life due to fatigue cracking, N_f , are summarized in Table 5.3. The ϵ_t and the N_f are very sensitive to the variation in the thickness, seismic modulus, and nonlinear parameters k_2 and k_3 of the base layer. On the other hand, the Poisson's ratio of the base does not seem to impact the fatigue remaining life.

Table 5.3 – Levels of Sensitivity of Pavement Parameters with Respect to Critical Tensile Strain and Fatigue Remaining Life for “3-12 PAVE”

Layer Parameters		AC			Base					Upper Subgrade				Depth To Bedrock
		Thickness	Modulus	Poisson's Ratio	Thickness	Seismic Modulus	Poisson's Ratio	k_2	k_3	Seismic Modulus	Poisson's Ratio	k_2	k_3	
$\epsilon_t^{[1]}$	Sensitivity Index	0.34	0.53	0.05	0.59	0.55	0.01	0.59	0.67	0.39	0.07	0.06	0.11	0.01
	Level of Sensitivity	S ^[3]	VS	NS	VS	VS	NS	VS	VS	S	NS	NS	MS	NS
$N_f^{[2]}$	Sensitivity Index	1.35	0.64	0.16	1.57	1.50	0.04	1.59	3.61	1.05	0.23	0.19	0.39	0.02
	Level of Sensitivity	VS	S	NS	VS	VS	NS	VS	VS	VS	NS	NS	MS	NS

[1] ϵ_t : Critical Tensile Strain;

[2] N_f : Fatigue Remaining Life;

[3] VS: Very Sensitive; S: Sensitive; MS: Moderately Sensitive; NS: Not Sensitive.

Table 5.4 – Levels of Sensitivity of Pavement Parameters with Respect to Critical Compressive Strain and Rutting Remaining Life for “3-12 PAVE”

Layer Parameters		AC			Base					Upper Subgrade				Depth To Bedrock
		Thickness	Modulus	Poisson's Ratio	Thickness	Seismic Modulus	Poisson's Ratio	k ₂	k ₃	Seismic Modulus	Poisson's Ratio	k ₂	k ₃	
$\epsilon_c^{[1]}$	Sensitivity Index	0.64	0.45	0.06	1.49	0.18	0.02	0.16	0.20	0.83	0.61	0.16	0.28	0.002
	Level of Sensitivity	VS ^[3]	VS	NS	VS	MS	NS	MS	S	VS	VS	MS	S	NS
$N_r^{[2]}$	Sensitivity Index	4.03	1.94	0.26	10.94	0.72	0.09	0.62	1.02	3.66	4.37	0.81	2.27	0.01
	Level of Sensitivity	VS	VS	MS	VS	S	NS	S	VS	VS	VS	S	VS	NS

[1] ϵ_c : Critical Compressive Strain;

[2] N_r : Rutting Remaining Life;

[3] VS : Very Sensitive; S: Sensitive; MS: Moderately Sensitive; NS: Not Sensitive.

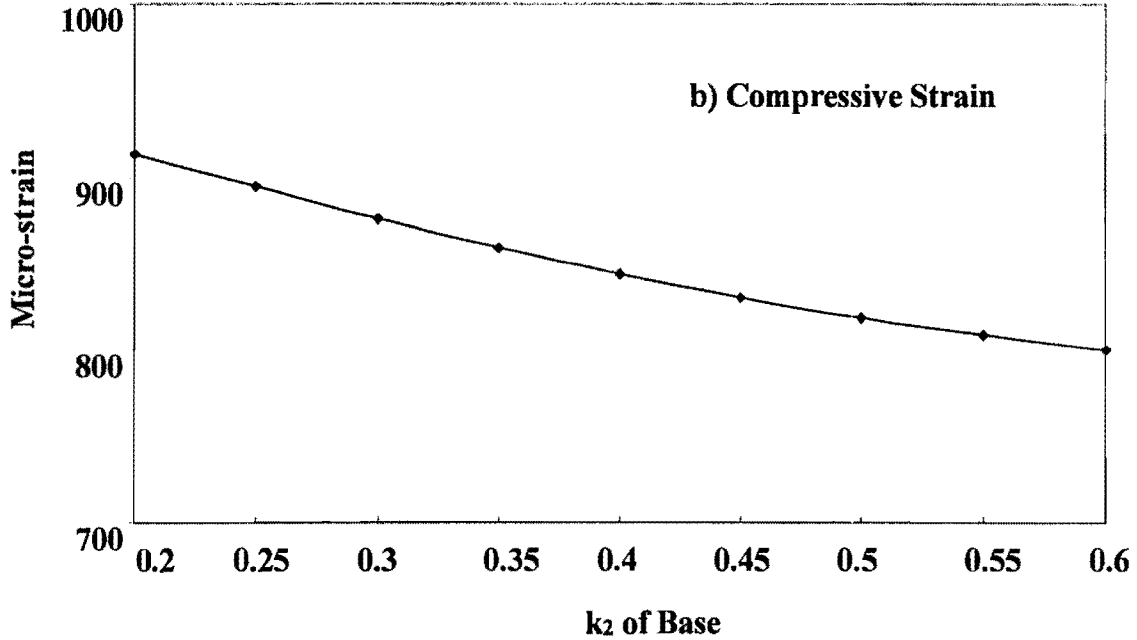
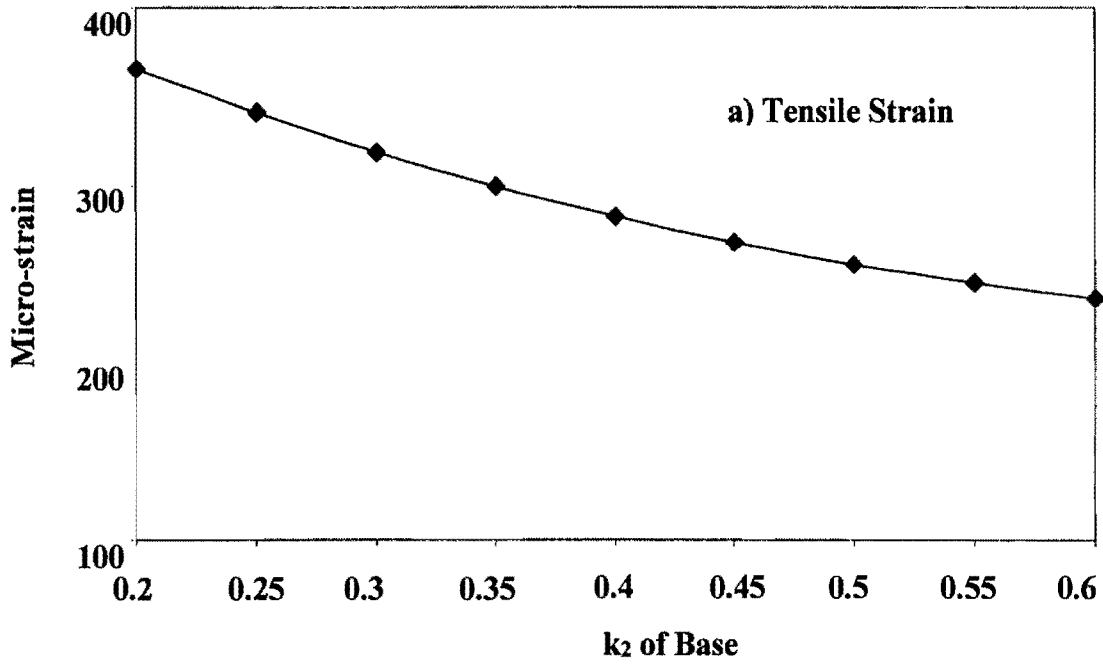


Figure 5.1 –Variations in Critical Strains with Parameter k₂ of Base for “3-12 PAVE”

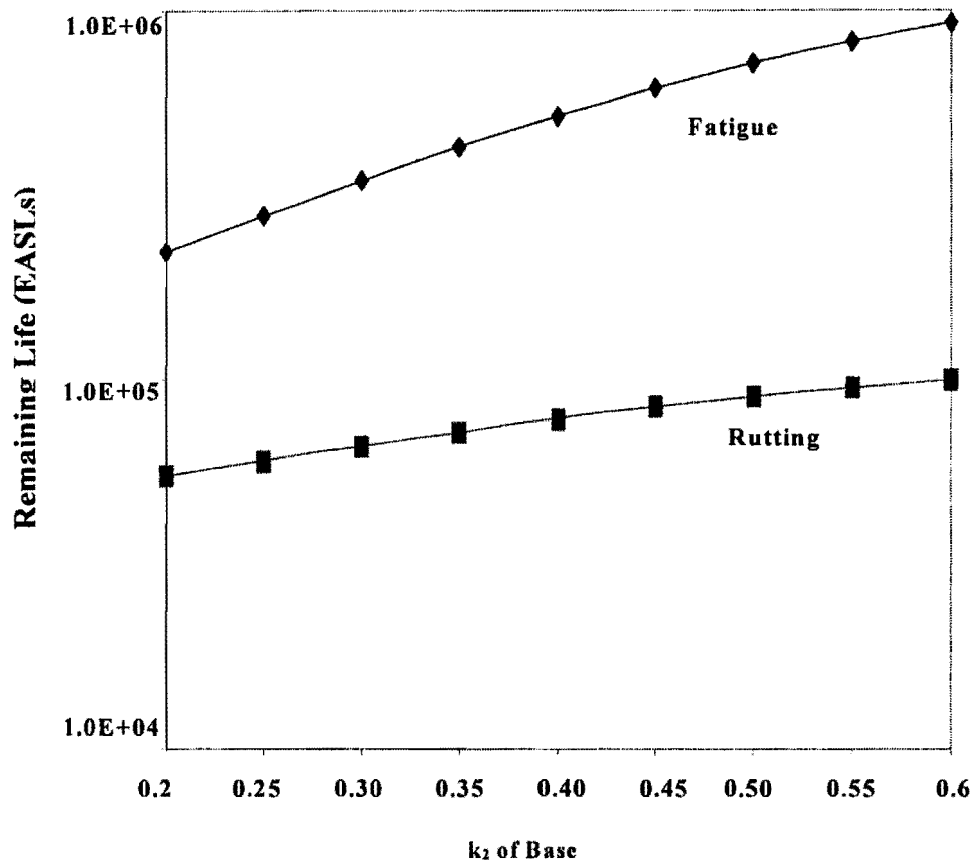


Figure 5.2 - Variations in Remaining Lives with Parameter k_2 of Base

In addition, the levels of sensitivity of different parameters with respect to the critical compressive strain ϵ_c and the remaining life due to rutting, N_r , are summarized in Table 5.4. The ϵ_c and the N_r are very sensitive to the variations in the thickness and the parameter k_3 of the base layer. On the other hand, the Poisson's ratio of the base does not seem to impact the fatigue remaining life. The seismic modulus and parameter k_2 of the base are of secondary importance.

5.3.3 Upper Subgrade

The upper subgrade is considered to behave nonlinearly. Thus, the variables include nonlinear parameters k_2 and k_3 as well as the seismic modulus and Poisson's Ratio. Appendix B contains the detailed results.

Again, the sensitivity study of parameters k_2 and k_3 is especially important since the purpose of the equivalent-linear model is to take the nonlinear behavior of pavement materials into consideration.

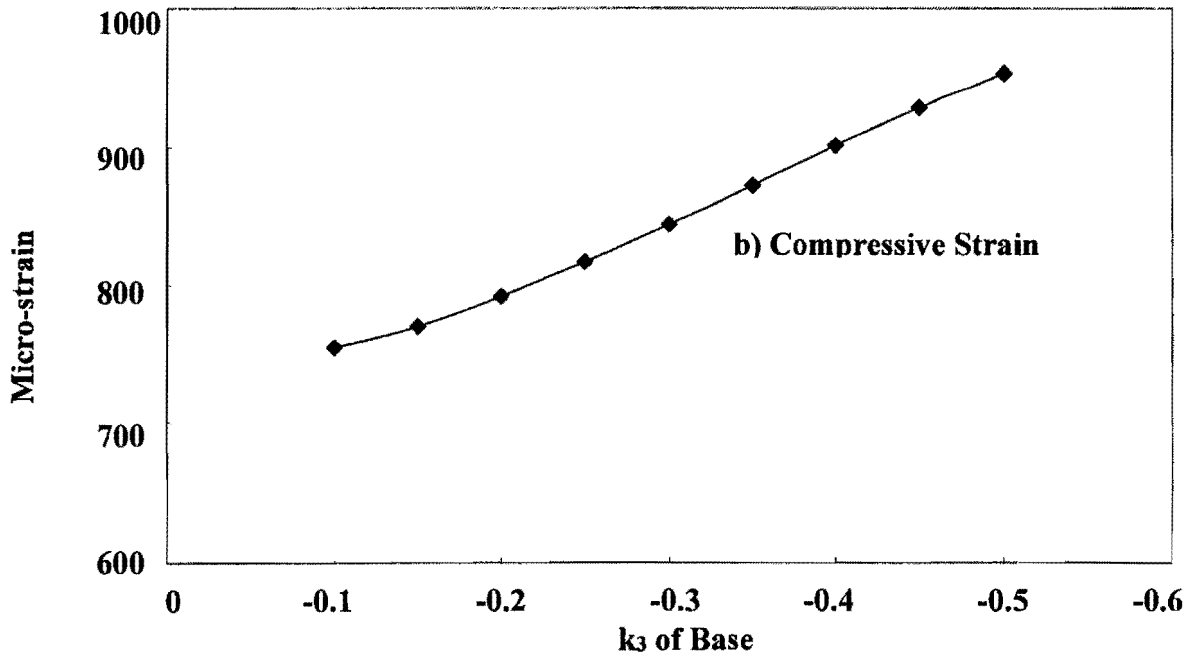
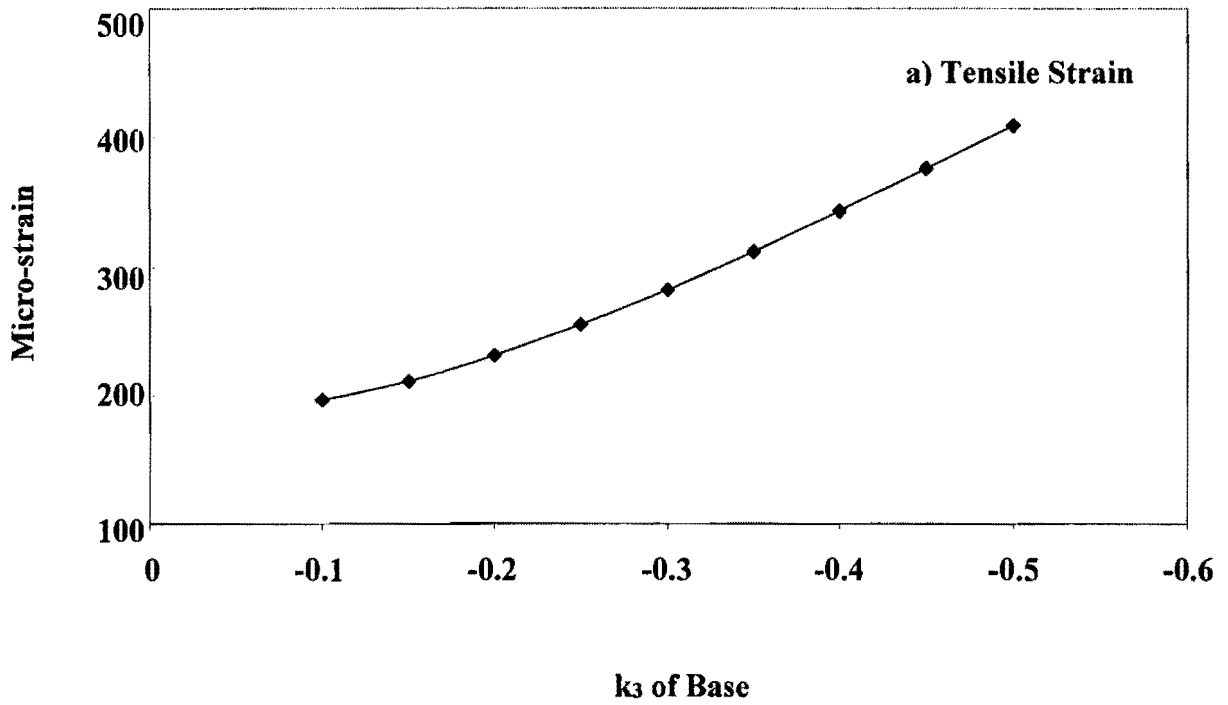


Figure 5.3 - Variations in Critical Strains with Parameter k_3 of Base for “3-12 PAVE”

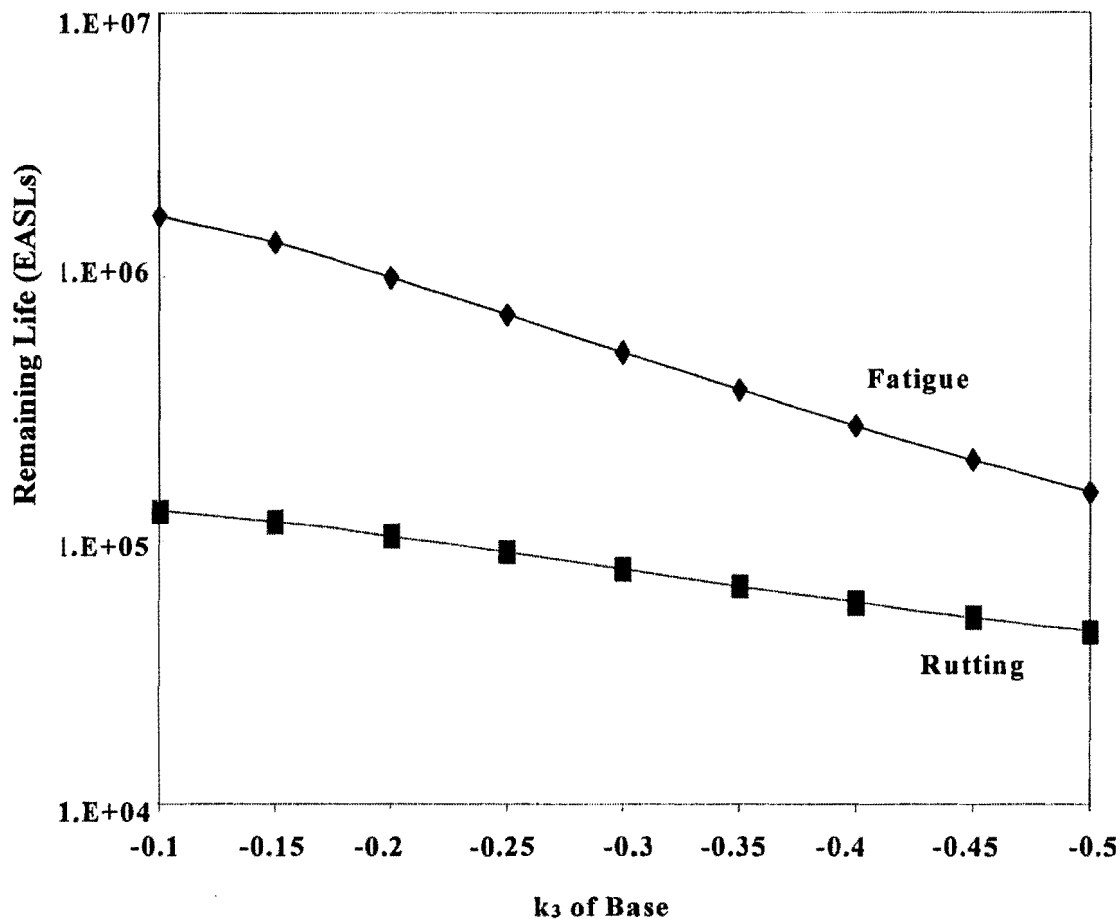


Figure 5.4 -Variations in Remaining Lives with Parameter k_3 of Base for “3-12 PAVE”

The impact of the values of k_2 on the critical strains and remaining lives is shown in Figures 5.5 and 5.6. In the constitutive model, the larger k_2 is, the more rapidly the upper subgrade becomes stiff as a result of an increase in confining pressure. Therefore, as reflected in Figures 5.5 and 5.6, with an increase in k_2 , both critical strain and critical compressive strain decrease and, thus, the remaining lives increase.

The impacts of parameter k_3 on critical strains and remaining lives are shown in Figures 5.7 and 5.8. In contrast to k_2 , the larger the absolute value of k_3 , the more rapidly the upper subgrade becomes soft as deviatoric stress increases. From these two figures, with an increase in k_3 (absolute value), critical strains increase and, as a result, remaining lives decrease.

The levels of sensitivity of different parameters with respect to the critical tensile strain, ϵ_t , and the remaining life due to fatigue cracking, N_f , are summarized in Table 5.3. The ϵ_t and the N_f are very sensitive to the variation in the seismic modulus of the upper subgrade. On the other hand, the Poisson’s ratio of the subgrade, as well as parameter k_2 of subgrade, does not seem to impact the fatigue remaining life. The parameter k_3 of subgrade is of secondary importance.

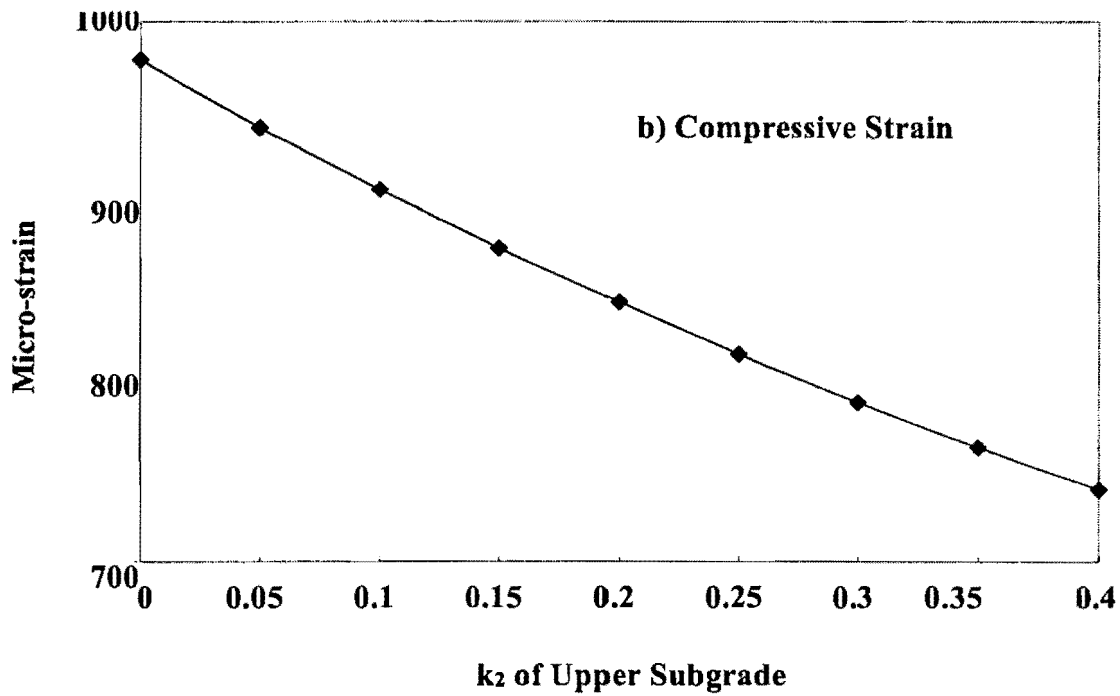
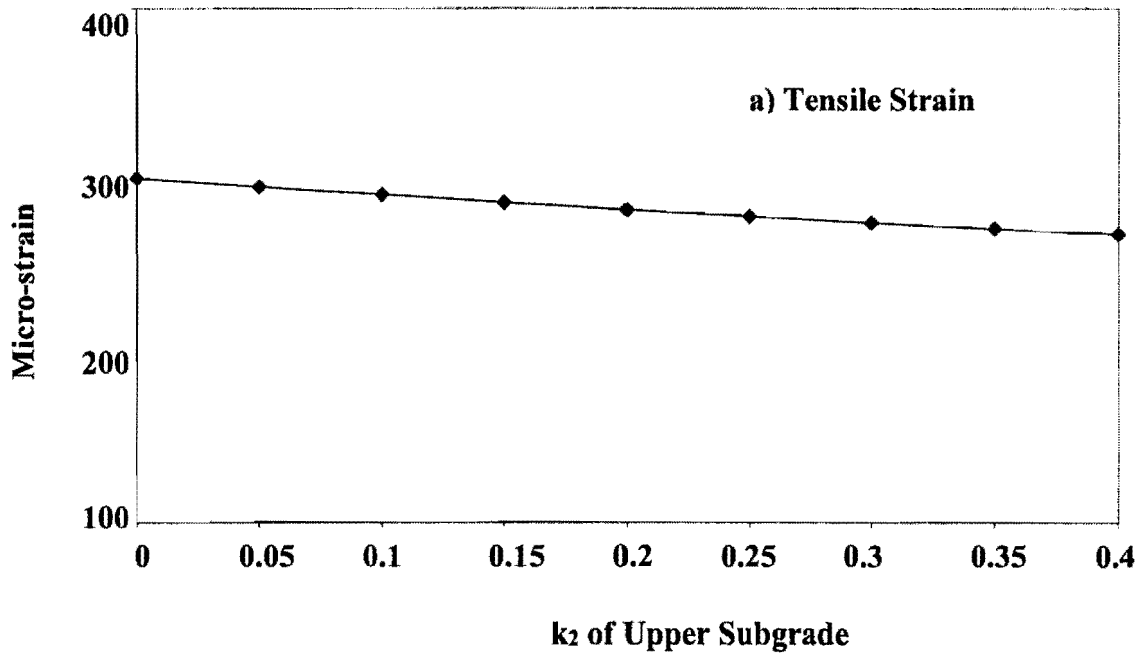


Figure 5.5 - Variations in Critical Strains with Parameter k₂ of Upper Subgrade for “3-12 PAVE”

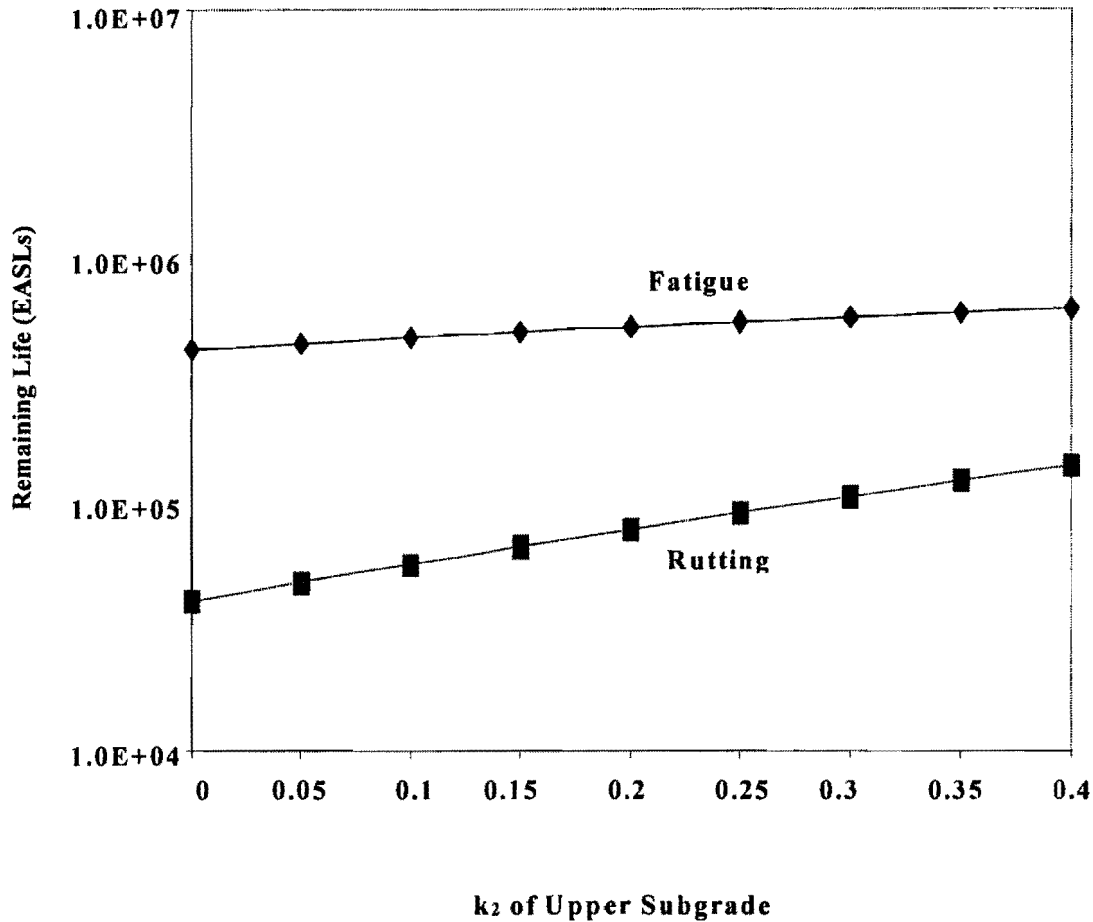


Figure 5.6 – Variations in Remaining Lives with Parameter k_2 of Upper Subgrade for “3-12 PAVE”

The levels of sensitivity of different parameters with respect to the critical compressive strain, ϵ_c , and the remaining life due to rutting, N_r , are shown in Table 5.4. The ϵ_c and the N_r are very sensitive to seismic modulus, Poisson’s ratio and parameter k_3 of subgrade. Parameter k_2 of subgrade is of secondary importance.

5.3.4 Depth to Bedrock

As indicated before, the depth to bedrock plays an important role in properly predicting the remaining lives of pavements, and a critical depth exists below which the impact of the bedrock on predicted parameters is negligible (Boddapati, 1992). For the typical pavement section shown in Figure 3.7, the bedrock was intentionally placed at a depth that would not significantly impact the results. In order to quantify the influence of bedrock, another study was carried out in which the depth was varied from 75 in. (1.9 m) to 450 in. (11.3 m). The results are shown in Table 5.5.

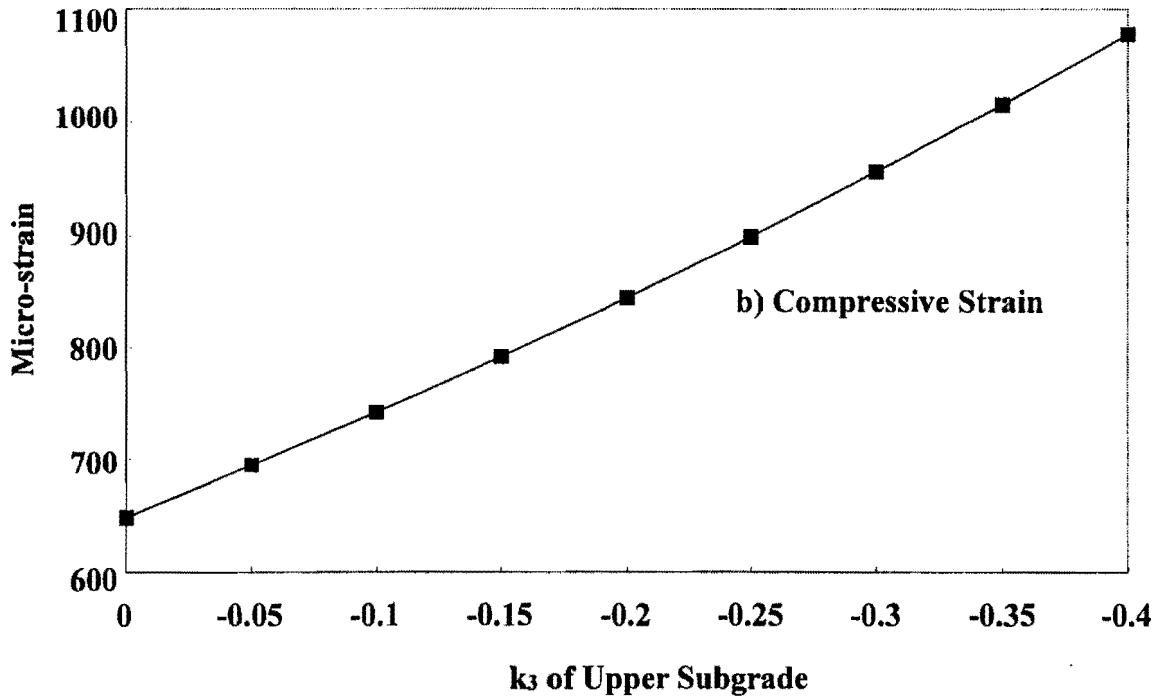
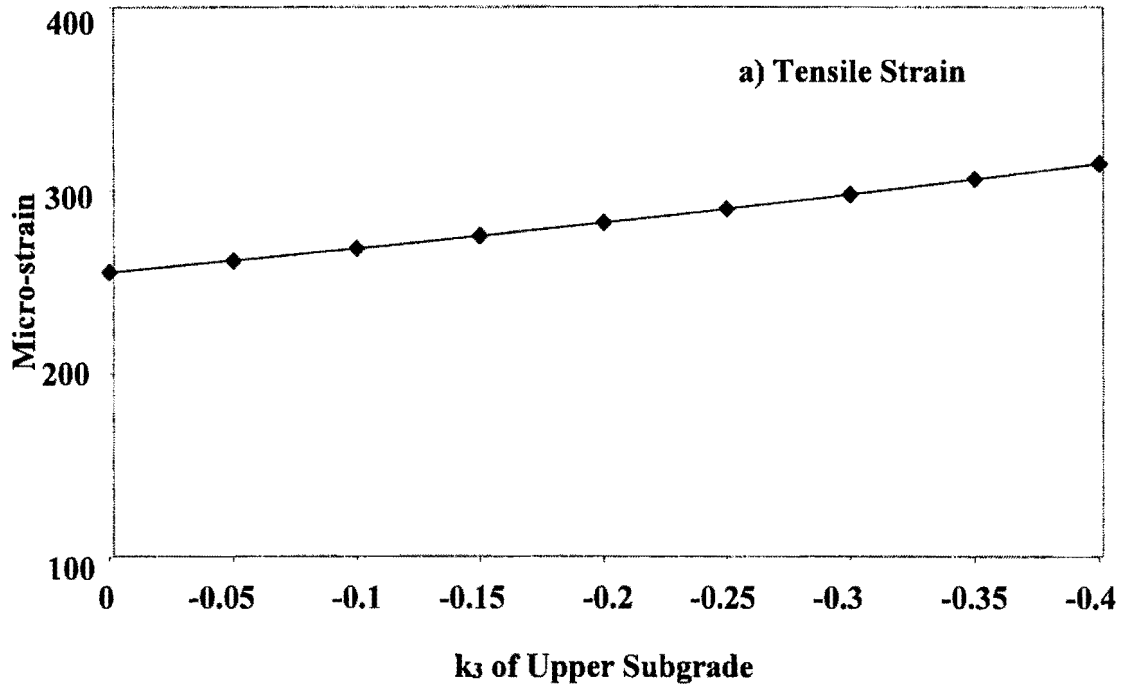


Figure 5.7 –Variations in Critical Strains with Parameter k_3 of Upper Subgrade

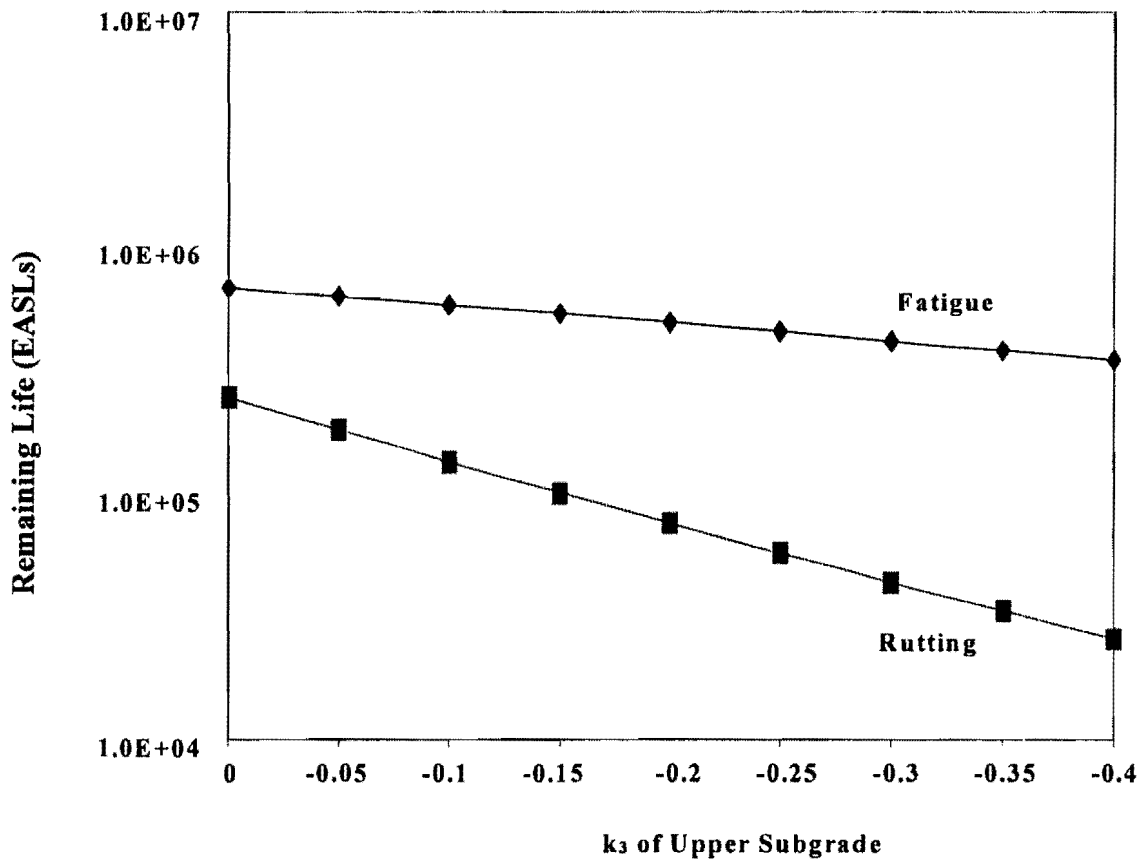


Figure 5.8 – Variations in Remaining Lives with Parameter k_3 of Upper Subgrade

As the depth to bedrock is reduced from 300 in. (7.5 m) to 75 in. (1.9 m), the deflection of the first sensor decreases from about 26.5 mils (662.5 microns) to about 23 mils (575 microns). At the same time, the deflection of the last sensor decreases by a factor of about 10, from about 2.3 mils (57.5 microns) to almost 0.2 mils (5 microns). However, the two critical strains reported in Table 5.5 do not vary at all when the depth to bedrock is varied between 75 in. (1.9 m) and 450 in. (11.3 m). As a result, the depth to bedrock does not impact the remaining lives. Therefore, if the depth to bedrock is known and if the backcalculation can be done properly, one can accurately determine the remaining life of the pavement. However, if the depth to bedrock is misestimated and the bedrock is shallow, the remaining lives will be significantly misjudged.

5.3.5 Summary

Based on the above sensitivity study, the following conclusions can be drawn:

- a. Both critical strains and remaining lives are very sensitive to the thickness of the AC and base layers.

- b. The critical tensile strain and fatigue remaining life are very sensitive to the moduli of the base and subgrade, but they are not very sensitive to the modulus of the AC layer. The critical compressive strain and rutting remaining life are very sensitive to the modulus of the subgrade, but they are less sensitive to the moduli of the AC and base layers.
- c. Nonlinear parameters k_2 and k_3 of the base greatly influence the critical tensile strain and fatigue remaining life, but their influence on the critical compressive strain and rutting remaining life is less pronounced.
- d. Nonlinear parameters k_2 and k_3 of the subgrade have little impact on the critical tensile strain and fatigue remaining life, but they affect the critical compressive strain and rutting remaining life to a greater degree.
- e. The Poisson's ratios of the AC and base layers have little influence on the critical strains and remaining lives. However, the critical compressive strain and rutting remaining life are sensitive to Poisson's ratio of the subgrade.
- f. The depth to bedrock is not directly significant to the pavement remaining lives. However, it has a large influence on surface deflections and, thus, significantly affects the backcalculated set of moduli in FWD test. In this sense, the depth to bedrock is significant in assessing pavements as long as the bedrock is not deep.

5.4 SENSITIVITY STUDY RESULTS FOR THE FOUR PAVEMENTS

The other three typical pavement sections, PAVE 3-6, PAVE 5-6 and PAVE 5-12, are also analyzed for sensitivity of critical strains and remaining lives. The thickness, modulus and Poisson's ratio of the AC; the thickness, modulus, Poisson's ratio and nonlinear parameters of the base layer; and the modulus, Poisson's ratio and nonlinear parameters of the subgrade are studied. The results are presented in Tables 5-6 through 5-9.

With the change of the thickness of the AC layer or the base layer, the sensitivities of critical strains and remaining lives also change. For example, when the thickness of the AC layer increases, the critical strains and remaining lives are less sensitive to the nonlinear parameters of the base and the upper subgrade, while they are more sensitive to the modulus of the AC layer.

Table 5.5 – Response of Typical Pavement Section with Different Depths of Bedrock for “3-12 PAVE”

Depth to Bedrock		$\epsilon_t^{[1]}$	$\epsilon_c^{[2]}$	$N_f^{[3]}$	$N_r^{[4]}$	$d_1^{[5]}$	d_2	d_3	d_4	d_5	d_6	d_7
(inch)	(m)	(micro-strain)		(EASLs)		(milli-in.)						
75	1.9	282.7	842.4	515800	79340	23.0 (-13) ^[6]	12.2 (-22)	5.7 (-36)	2.9 (-51)	1.4 (-66)	0.6 (-81)	0.2 (-93)
150	3.8	283.0	845.1	513100	78240	25.3 (-4)	14.4 (-7)	7.8 (-13)	4.7 (-19)	3.0 (-26)	2.0 (-34)	1.3 (-43)
225	5.6	282.7	844.5	516000	78470	26.1 (-1)	15.2 (-2)	8.5 (-4)	5.5 (-7)	3.7 (-9)	2.6 (-12)	1.9 (-16)
300	7.5	282.4	844.4	517900	78540	26.5	15.6	8.9	5.8	4.1	3.0	2.3
375	9.4	282.4	844.3	517800	78550	26.7 (0.9)	15.8 (1)	9.1 (3)	6.1 (4)	4.3 (6)	3.2 (7)	2.5 (10)
450	11.3	282.3	844.1	518600	78650	26.9 (1.4)	16.0 (2)	9.3 (4)	6.2 (7)	4.5 (9)	3.4 (12)	2.6 (16)

[1]: Tensile strain at the bottom of AC layer;

[2]: Compressive strain at the top the subgrade;

[3]: Pavement remaining life due to fatigue cracking;

[4]: Pavement remaining life due to rutting;

[5]: d_1 to d_7 are surface deflections at radial distances of 0, 12, 24, 36, 48, 60 and 72 in., respectively. 1 milli-inch = 0.025 mm;

[6]: Value in parenthesis is percent difference between this quantity and the similar quantity with depth to bedrock of 300 in.

Table 5.6 – Sensitivity of Critical Tensile Strain to Pavement Parameters under Equivalent-Linear Model

Layer	Parameter	Sensitivity	Thin AC (3 in.)		Thick AC (5 in.)		
			Thin Base (6 in.)	Thick Base (12 in.)	Thin Base (6 in.)	Thick Base (18 in.)	
AC	Thickness	Index	0.41	0.34	1.00	0.76	
		Level	VS	S	VS	VS	
	Modulus	Index	0.94	0.53	1.60	1.35	
		Level	VS	VS	VS	VS	
	Poisson's Ratio	Index	0.05	0.05	0.14	0.09	
		Level	NS	NS	MS	NS	
Base	Thickness	Index	0.44	0.59	0.21	0.36	
		Level	VS	VS	S	S	
	Modulus	Index	0.22	0.55	0.11	0.29	
		Level	S	VS	MS	S	
	Poisson's Ratio	Index	0.01	0.01	0.01	0.02	
		Level	NS	NS	NS	NS	
	k ₂	Index	0.25	0.59	0.07	0.19	
		Level	S	VS	NS	MS	
	k ₃	Index	0.32	0.67	0.13	0.27	
		Level	S	VS	MS	S	
	Subgrade	Modulus	Index	0.55	0.39	0.32	0.26
			Level	VS	S	S	S
Poisson's Ratio		Index	0.10	0.07	0.04	0.07	
		Level	MS	NS	NS	NS	
k ₂		Index	0.17	0.06	0.07	0.03	
		Level	MS	NS	NS	NS	
k ₃		Index	0.25	0.11	0.11	0.06	
		Level	S	MS	MS	NS	

[1] VS: Very Sensitive; S: Sensitive; MS: Moderately Sensitive; NS: Not Sensitive.

**Table 5.7 – Sensitivity of Critical Compressive Strain to Pavement Parameters
under Equivalent-Linear Model**

Layer	Parameter	Sensitivity	Thin AC (3 in.)		Thick AC (5 in.)	
			Thin Base (6 in.)	Thick Base (12 in.)	Thin Base (6 in.)	Thick Base (18 in.)
AC	Thickness	Index	1.23	0.64	1.69	1.17
		Level	VS	VS	VS	VS
	Modulus	Index	0.88	0.45	1.24	0.83
		Level	VS	VS	VS	VS
	Poisson's Ratio	Index	0.12	0.06	0.14	0.10
		Level	MS	NS	MS	MS
Base	Thickness	Index	0.70	1.49	0.46	1.06
		Level	VS	VS	VS	VS
	Modulus	Index	0.14	0.18	0.01	0.09
		Level	MS	MS	NS	NS
	Poisson's Ratio	Index	0.04	0.02	0.02	0.01
		Level	NS	NS	NS	NS
	k ₂	Index	0.12	0.16	0.01	0.05
		Level	MS	MS	NS	NS
	k ₃	Index	0.09	0.20	0.01	0.09
		Level	NS	S	NS	NS
Subgrade	Modulus	Index	0.81	0.83	0.66	0.75
		Level	VS	VS	VS	VS
	Poisson's Ratio	Index	0.74	0.61	0.81	0.65
		Level	VS	VS	VS	VS
	k ₂	Index	0.29	0.16	0.18	0.11
		Level	S	MS	MS	MS
	k ₃	Index	0.41	0.28	0.26	0.20
		Level	VS	S	S	S

[1] VS: Very Sensitive; S: Sensitive; MS: Moderately Sensitive; NS: Not Sensitive.

**Table 5.8 – Sensitivity of Fatigue Remaining Life to Pavement Parameters
under Equivalent-Linear Model**

Layer	Parameter	Sensitivity	Thin AC (3 in.)		Thick AC (5 in.)		
			Thin Base (6 in.)	Thick Base (12 in.)	Thin Base (6 in.)	Thick Base (18 in.)	
AC	Thickness	Index	1.63	1.35	4.49	3.51	
		Level	VS	VS	VS	VS	
	Modulus	Index	0.70	0.64	2.72	1.97	
		Level	S	S	VS	VS	
	Poisson's Ratio	Index	0.16	0.16	0.51	0.32	
		Level	NS	NS	S	MS	
Base	Thickness	Index	1.41	1.57	0.72	1.05	
		Level	VS	VS	S	VS	
	Modulus	Index	0.64	1.50	0.35	0.83	
		Level	S	VS	MS	S	
	Poisson's Ratio	Index	0.02	0.04	0.02	0.07	
		Level	NS	NS	NS	NS	
	k ₂	Index	0.64	1.59	0.21	0.52	
		Level	S	VS	NS	S	
	k ₃	Index	0.79	3.61	0.36	0.99	
		Level	S	VS	MS	S	
	Subgrade	Modulus	Index	1.51	1.05	0.90	0.76
			Level	VS	VS	S	S
Poisson's Ratio		Index	0.21	0.23	0.14	0.18	
		Level	NS	NS	NS	NS	
k ₂		Index	0.57	0.19	0.23	0.10	
		Level	S	NS	NS	NS	
k ₃		Index	1.13	0.39	0.46	0.22	
		Level	VS	MS	MS	NS	

[1] VS: Very Sensitive; S: Sensitive; MS: Moderately Sensitive; NS: Not Sensitive.

**Table 5.9 – Sensitivity of Rutting Remaining Life to Pavement Parameters
under Equivalent-Linear Model**

Layer	Parameter	Sensitivity	Thin AC (3 in.)		Thick AC (5 in.)	
			Thin Base (6 in.)	Thick Base (12 in.)	Thin Base (6 in.)	Thick Base (18 in.)
AC	Thickness	Index	7.38	4.03	11.65	7.76
		Level	VS	VS	VS	VS
	Modulus	Index	3.53	1.94	5.09	3.50
		Level	VS	VS	VS	VS
	Poisson's Ratio	Index	0.44	0.26	0.67	0.46
		Level	MS	MS	S	MS
Base	Thickness	Index	4.24	10.94	2.67	7.19
		Level	VS	VS	VS	VS
	Modulus	Index	0.20	0.72	0.01	0.39
		Level	NS	S	NS	MS
	Poisson's Ratio	Index	0.10	0.09	0.11	0.04
		Level	NS	NS	NS	NS
	k ₂	Index	0.18	0.62	0.02	0.19
		Level	NS	S	NS	NS
	k ₃	Index	0.26	1.02	0.06	0.40
		Level	MS	VS	NS	MS
Subgrade	Modulus	Index	3.55	3.66	2.91	3.29
		Level	VS	VS	VS	VS
	Poisson's Ratio	Index	5.91	4.37	6.95	4.86
		Level	VS	VS	VS	VS
	k ₂	Index	1.78	0.81	0.98	0.54
		Level	VS	S	S	S
	k ₃	Index	4.55	2.27	2.29	1.47
		Level	VS	VS	VS	VS

[1] VS: Very Sensitive; S: Sensitive; MS: Moderately Sensitive; NS: Not Sensitive.

CHAPTER SIX

PAVEMENT RESPONSE UNDER NONLINEAR STATIC MODEL

6.1 INTRODUCTION

In this chapter, pavement response using a nonlinear algorithm is studied. The comprehensive finite element analysis software package ABAQUS was used to carry out this study. The sensitivities of the critical strains and remaining lives of the typical pavements, defined in Chapter 3, to the variations in pavement parameters are studied.

6.2 SENSITIVITY STUDY FOR TYPICAL SECTION

The sensitivity of the two critical strains and remaining lives to the variations in the parameters of different layers are included in this section. As shown in Figure 3.7, the base layer and the upper 18 inches (450 mm) of the subgrade were considered nonlinear. The variables included in the sensitivity study are:

- a. Thickness, modulus and Poisson's ratio of the AC layer;
- b. Thickness, seismic modulus, Poisson's ratio, and nonlinear parameters k_2 and k_3 of the base layer;
- c. Seismic modulus, Poisson's ratio and nonlinear parameters k_2 and k_3 of the upper subgrade.

The process of the sensitivity study is identical to that of Chapter 5 for consistency.

6.2.1 AC Layer

The AC layer is considered linear. Therefore, the parameters to be considered are thickness, modulus and Poisson's ratio. Detailed results are included in Appendix C for completeness. Sensitivity levels are summarized in Tables 6.1 and 6.2.

The critical strains and remaining lives, as shown in Tables 6.1 and 6.2, are very sensitive to the thickness and modulus of the AC layer, but not to the Poisson's ratio of the AC layer.

6.2.2 Base Layer

The variables considered in the sensitivity study of the base include the nonlinear parameters k_2 and k_3 , as well as the thickness, seismic modulus and Poisson's ratio. The detailed results are also included in Appendix C.

The sensitivity levels with respect to the critical tensile strain, ε_t , and the remaining life due to fatigue cracking, N_f , are summarized in Table 6.1. The ε_t and N_f are very sensitive to the variation in thickness, seismic modulus and nonlinear parameters k_2 and k_3 of the base layer. However, its Poisson's ratio has only a small impact on ε_t and N_f .

Table 6.2 contains the sensitivity levels with respect to the critical compressive strain, ε_c , and the remaining life due to rutting, N_r . The ε_c and N_r are very sensitive to the variations in the thickness of the base layer, the seismic modulus, and nonlinear parameter k_3 . They are also sensitive to the nonlinear parameter k_2 , to a lesser degree. Again, the Poisson's ratio of the base has little impact on ε_c and N_r .

The impact of k_2 on the critical strains and remaining lives is shown in Figures 6.1 and 6.2. With the increase in k_2 , the two critical strains decrease and the remaining lives increase. Again, the larger the k_2 is, the more rapidly the base stiffens with an increase in confining pressure. In contrast to the k_2 , the larger the absolute value of k_3 , the more rapidly the base becomes soft with an increase in deviatoric stress and, thus, the larger the developed strains and the smaller the remaining lives will be (Figures 6.3 and 6.4). Upon comparison with the critical tensile strain and fatigue remaining life, the critical compressive strain and rutting remaining life are generally less influenced by nonlinear parameters k_2 and k_3 of the base.

6.2.3 Upper Subgrade

In a similar manner to that used for the base layer, the variables studied were the seismic modulus, Poisson's ratio and nonlinear parameters k_2 and k_3 . Refer to Appendix C for detailed results.

The levels of sensitivity with respect to critical strains and remaining lives are summarized in Tables 6.1 and 6.2. The seismic modulus of the subgrade significantly affects the critical tensile strain and fatigue remaining life, while the nonlinear parameters k_2 and k_3 , as well as the Poisson's ratio, have little influence on them. The critical compressive strain and rutting remaining life, on the other hand, are sensitive not only to the seismic modulus and Poisson's ratio of the subgrade but also to the nonlinear parameters, especially k_3 , of the subgrade.

Table 6.1 - Sensitivity of Critical Tensile Strain and Fatigue Remaining Life to Pavement Parameters

Layer Parameters		AC			Base					Upper Subgrade			
		Thickness	Modulus	Poisson's Ratio	Thickness	Seismic Modulus	Poisson's Ratio	k_2	k_3	Seismic Modulus	Poisson's Ratio	k_2	k_3
$\epsilon_t^{[1]}$	Sensitivity Index	0.86	0.18	0.07	0.76	0.62	0.14	0.65	0.66	0.47	0.12	0.10	0.15
	Level of Sensitivity	VS ^[3]	MS	NS	VS	VS	MS	VS	VS	VS	MS	MS	MS
$N_f^{[2]}$	Sensitivity Index	23.10	1.42	0.24	1.94	2.34	0.41	3.79	3.63	1.28	0.39	0.29	0.43
	Level of Sensitivity	VS	VS	NS	VS	VS	MS	VS	VS	VS	MS	MS	MS

[1] ϵ_t : Critical Tensile Strain;

[2] N_f : Fatigue Remaining Life;

[3] VS: Very Sensitive; S: Sensitive; MS: Moderately Sensitive; NS: Not Sensitive.

Table 6.2 –Sensitivity of Critical Compressive Strain and Rutting Remaining Life to Pavement Parameters

Layer Parameters		AC			Base					Upper Subgrade			
		Thickness	Modulus	Poisson's Ratio	Thickness	Seismic Modulus	Poisson's Ratio	k_2	k_3	Seismic Modulus	Poisson's Ratio	k_2	k_3
$\epsilon_c^{[1]}$	Sensitivity Index	0.45	0.28	0.16	2.05	0.32	0.07	0.20	0.20	0.85	0.72	0.14	0.25
	Level of Sensitivity	VS ^[3]	S	MS	VS	S	NS	S	S	VS	VS	MS	S
$N_r^{[2]}$	Sensitivity Index	5.94	1.48	0.88	25.25	1.74	0.33	0.69	1.31	4.15	5.71	0.77	2.48
	Level of Sensitivity	VS	VS	S	VS	VS	MS	S	VS	VS	VS	S	VS

[1] ϵ_c : Critical Compressive Strain;

[2] N_r : Rutting Remaining Life;

[3] VS: Very Sensitive; S: Sensitive; MS: Moderately Sensitive; NS: Not Sensitive.

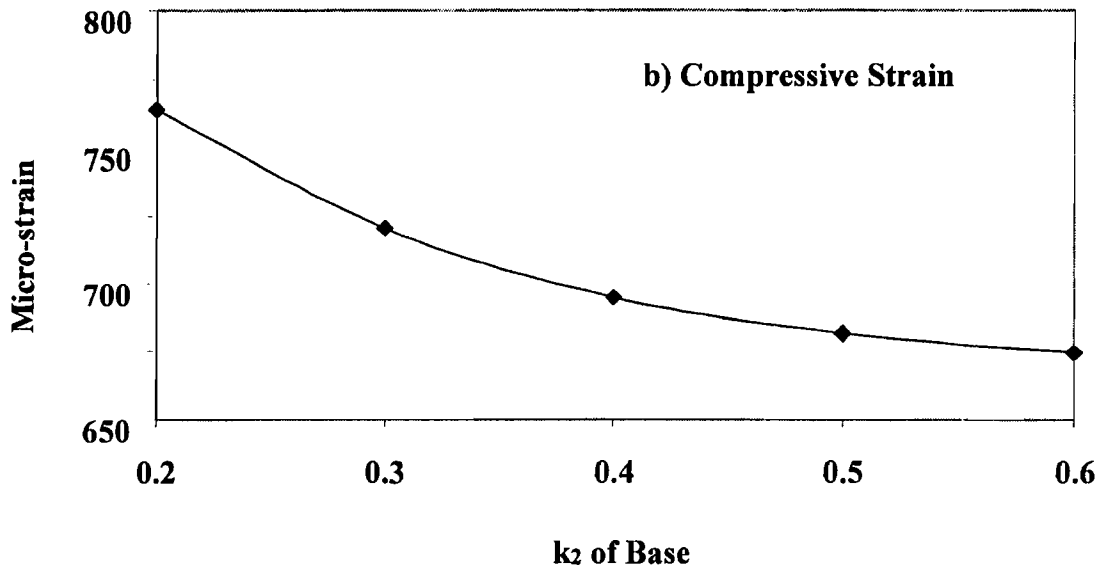
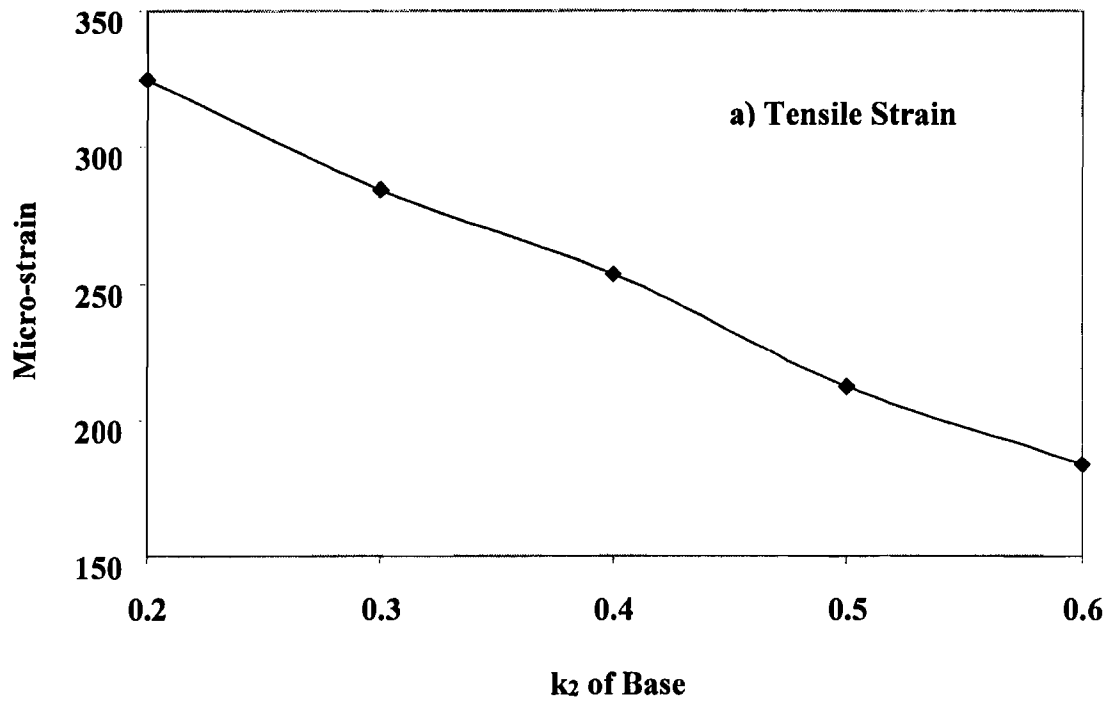


Figure 6.1 - Variations in Critical Strains with Parameter k_2 of Base

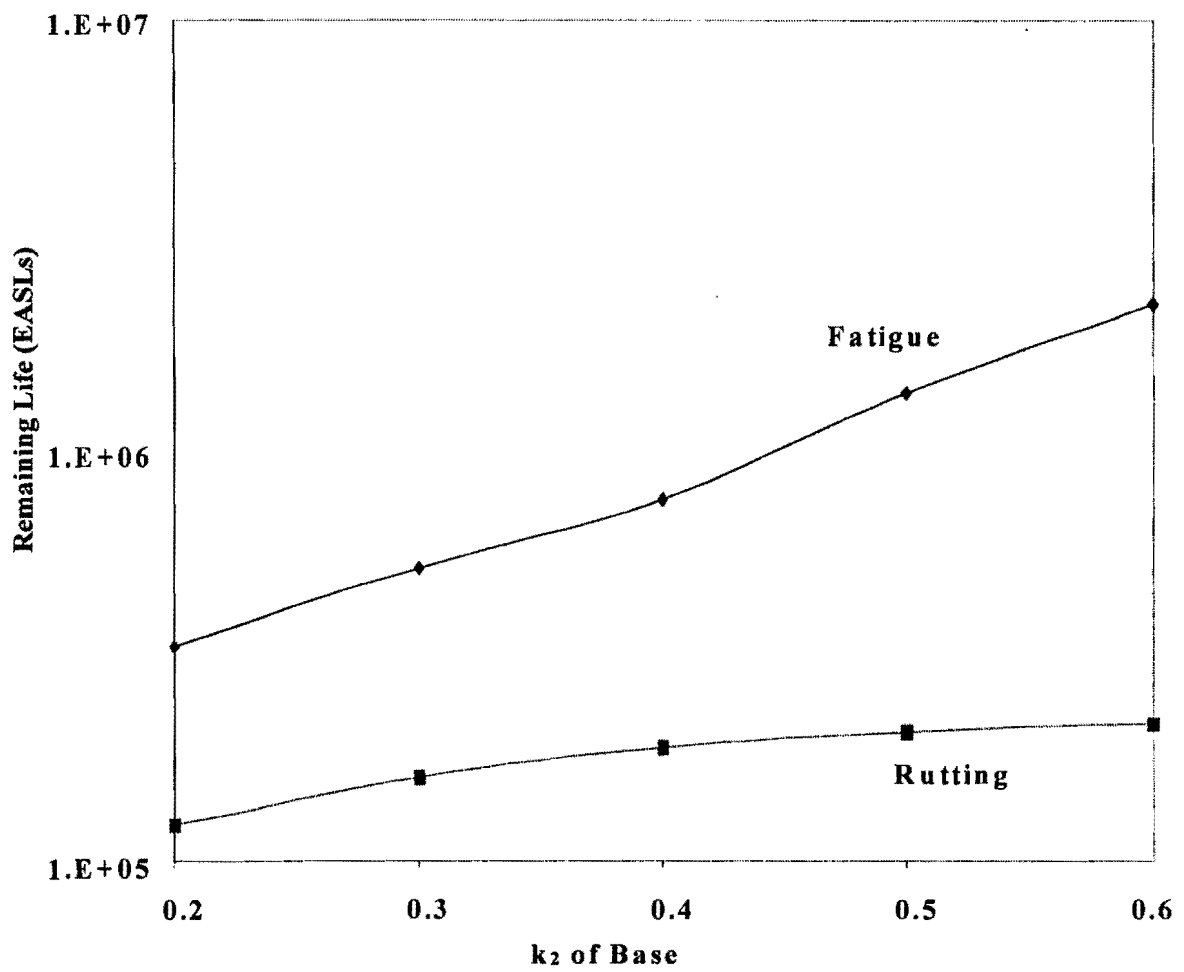


Figure 6.2 - Variations in Remaining Lives with Parameter k_2 of Base

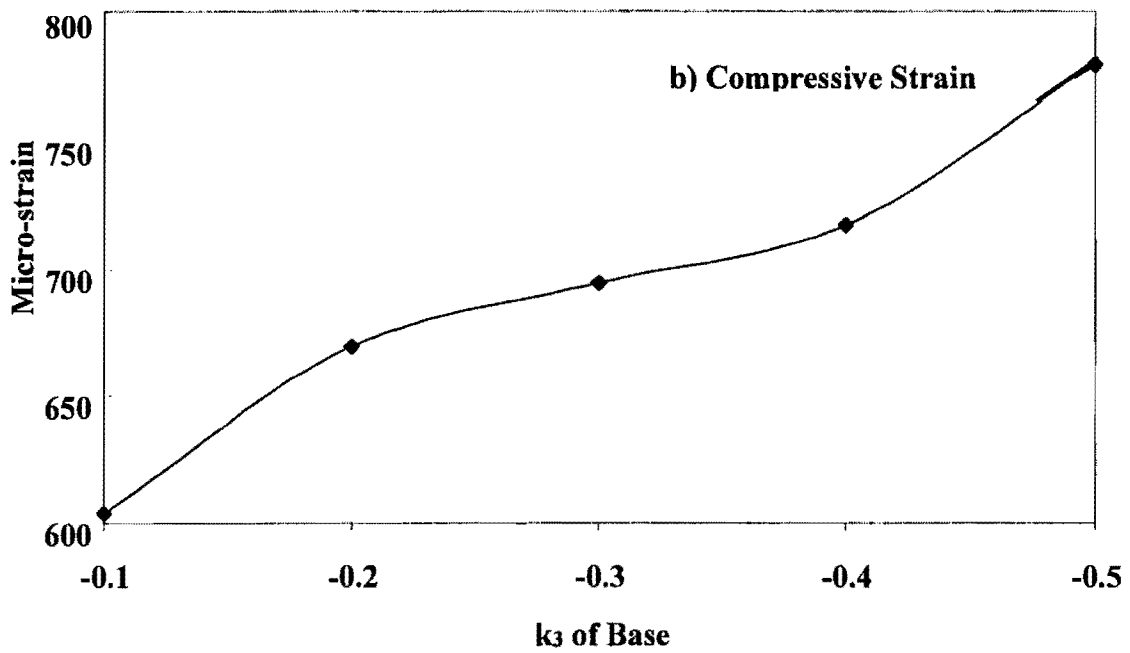
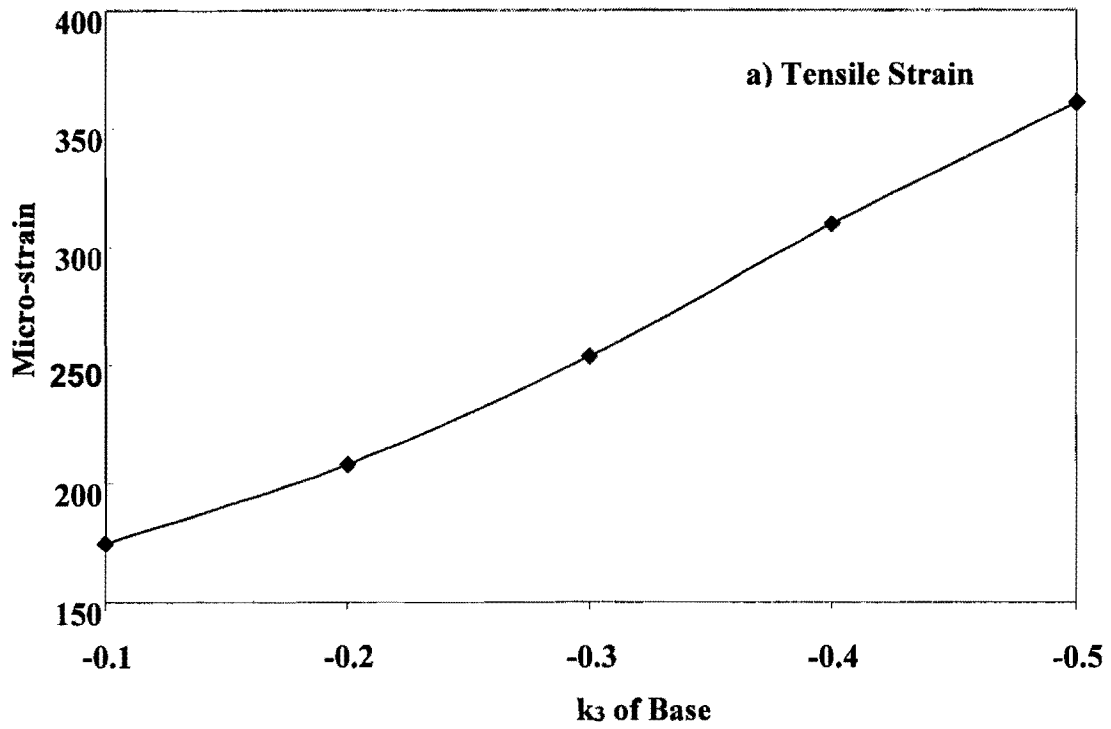


Figure 6.3 – Variations in Critical Strains with Parameter k_3 of Base

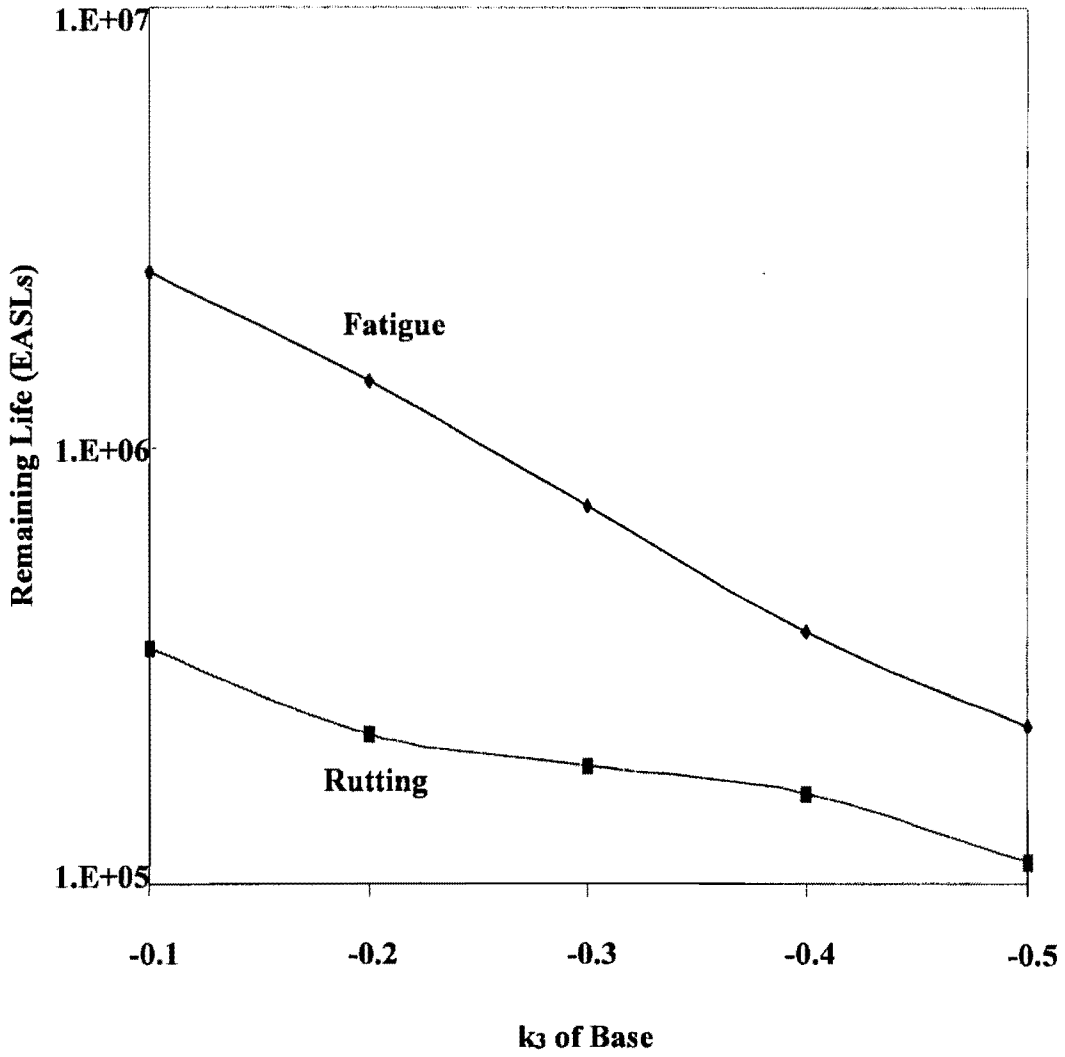


Figure 6.4 - Variations in Remaining Lives with Parameter k_3 of Base

The impact of parameters k_2 and k_3 of the upper subgrade on the critical strains and remaining lives is shown in Figures 6.5 through 6.8. The trends are similar to those of the base layer. With the increase in k_2 , the critical strains decrease and the remaining lives increase. In contrast to k_2 , with a larger absolute value of k_3 , the critical strains are larger and the remaining lives are smaller. However, the responses are much less sensitive to parameters k_2 and k_3 , when compared with those in the case of the base layer.

6.2.4 Conclusions of Sensitivity Study

The following conclusions can be drawn from this sensitivity study:

- a. The thicknesses of the AC and base layers significantly influence the critical strains and remaining lives.
- b. The critical strains and remaining lives are very sensitive to variations in the moduli of the base and subgrade and, to a lesser extent, to the variation in the modulus of AC.
- c. The Poisson's ratios of all layers have little effect on the critical tensile strain and fatigue remaining life. On the other hand, the Poisson's ratios of the AC and base layers have moderate effects on the critical compressive strain and rutting remaining life, and the Poisson's ratio of the subgrade is one of the factors that have a significant effect on the critical compressive strain and rutting remaining life.
- d. The nonlinear parameters k_2 and k_3 of the base greatly influence the critical tensile strain and fatigue remaining life, but their influence on the critical compressive strain and rutting remaining life is less pronounced.
- e. The nonlinear parameters k_2 and k_3 of the subgrade have little influence on the critical tensile strain and fatigue remaining life, but they, especially k_3 , significantly impact the critical compressive strain and rutting remaining life.

6.3 SENSITIVITY STUDY RESULTS FOR THE FOUR PAVEMENTS

The other three typical pavement sections, PAVE 3-6, PAVE 5-6 and PAVE 5-12, are also analyzed for sensitivity of critical strains and remaining lives. The thickness, modulus and Poisson's ratio of the AC, the thickness, modulus, Poisson's ratio and nonlinear parameters of the base layer, and the modulus, Poisson's ratio and nonlinear parameters of the subgrade are studied. The results are presented in Tables 6.3 through 6.6. The sensitivity of critical strains and remaining lives vary with the change of the thickness of the AC layer or the base layer. However, the sensitivity levels are unchanged in many cases since the variation of the sensitivity indexes is not large enough.

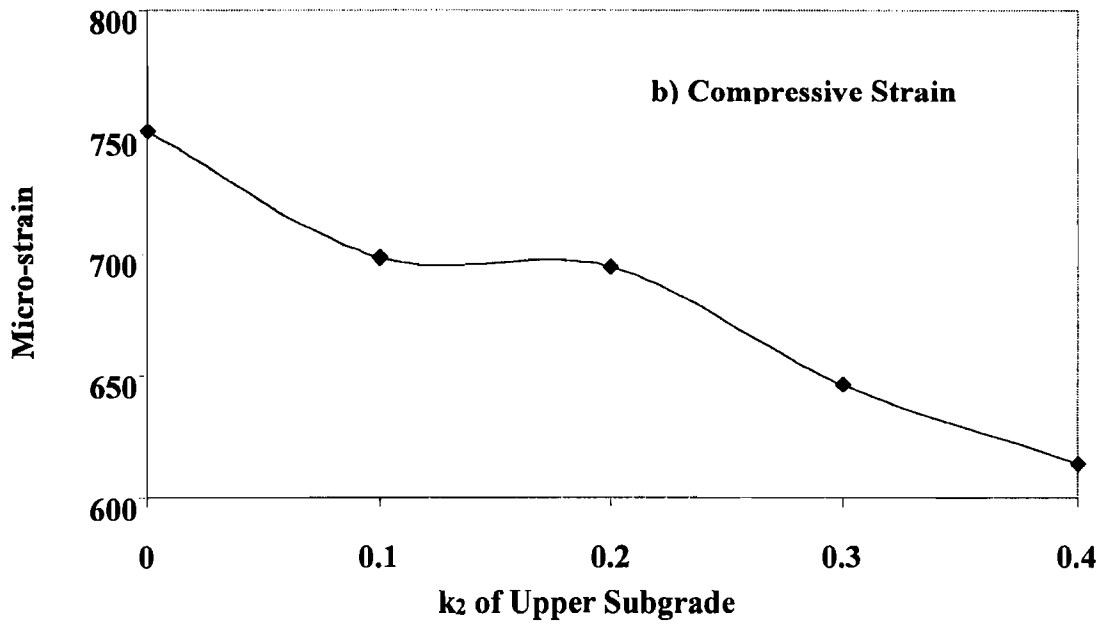
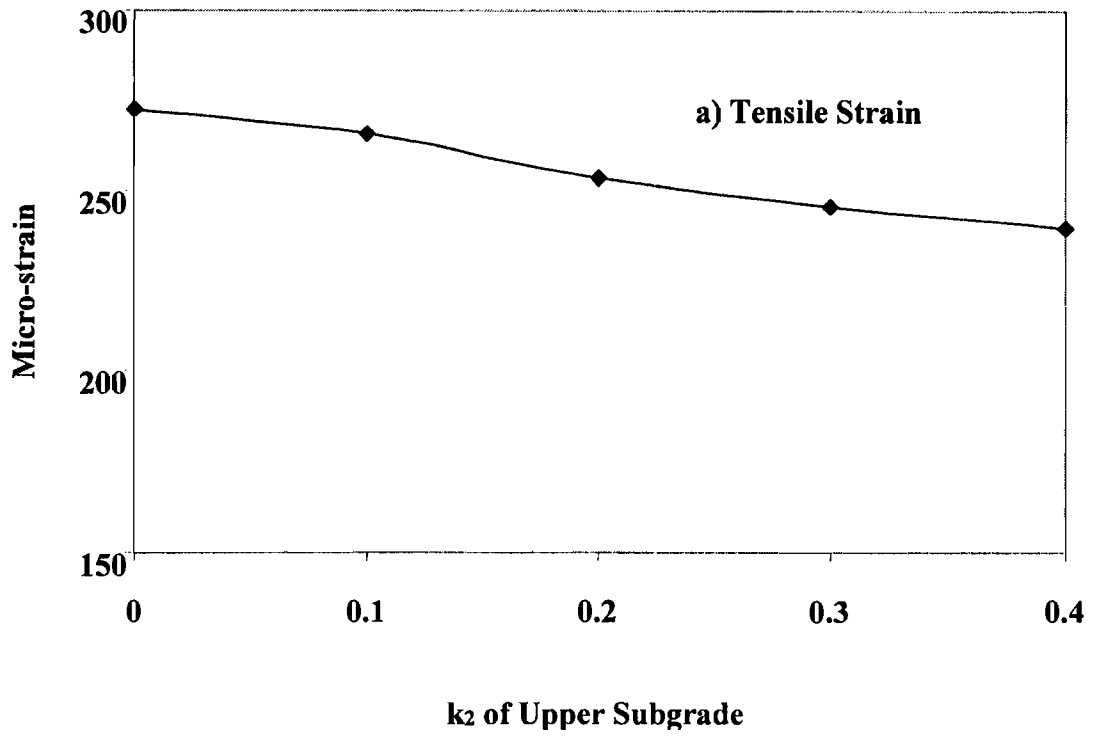


Figure 6.5 – Variations in Critical Strains with Parameter k_2 of Upper Subgrade

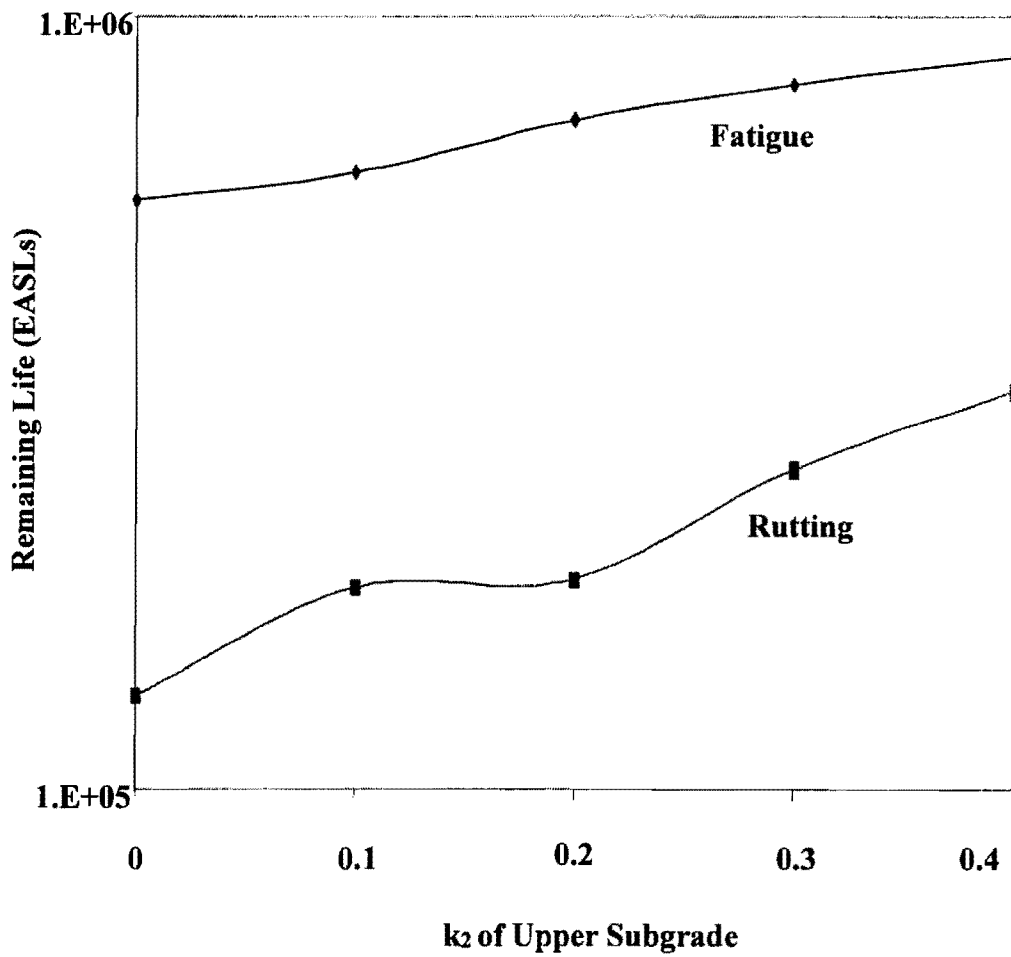


Figure 6.6 - Variations in Remaining Lives with Parameter k_2 of Upper Subgrade

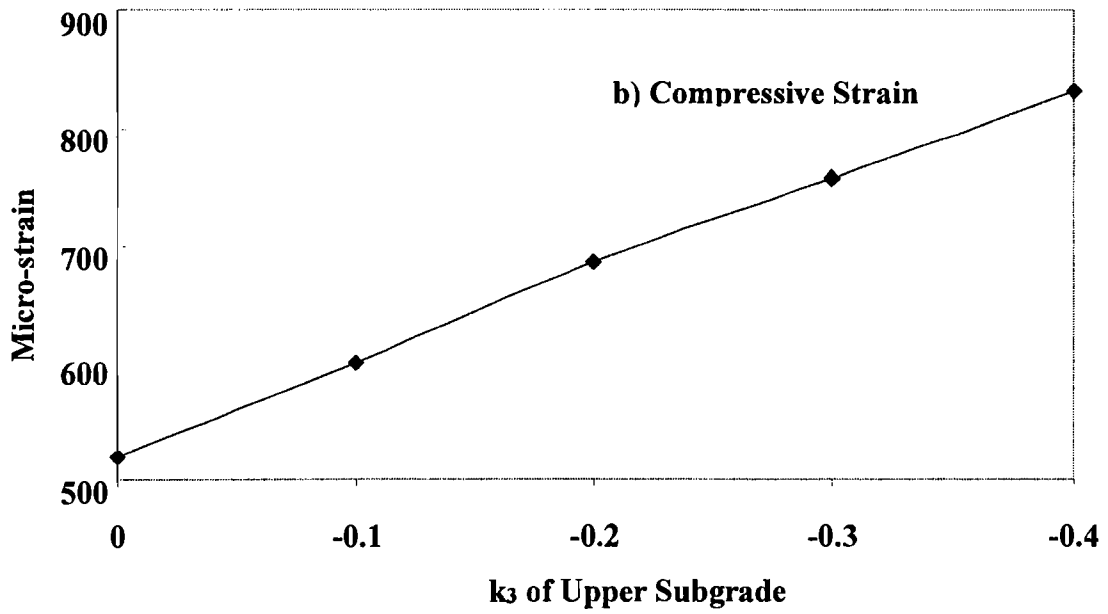
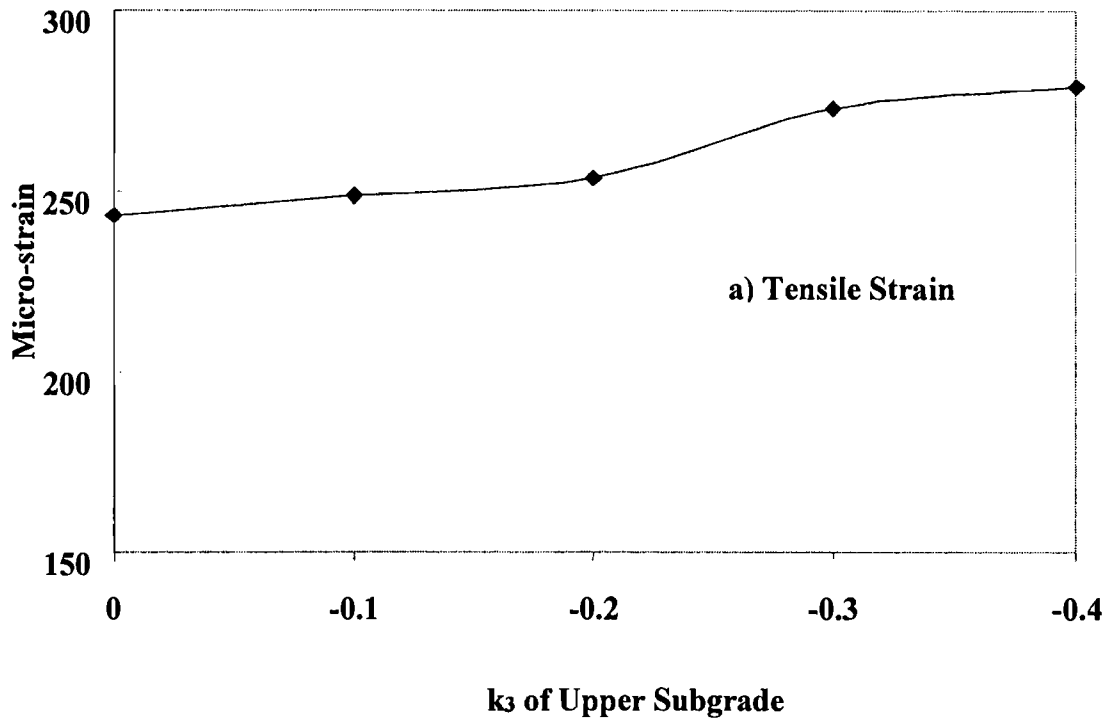


Figure 6.7 – Variations in Critical Strains with Parameter k_3 of Upper Subgrade

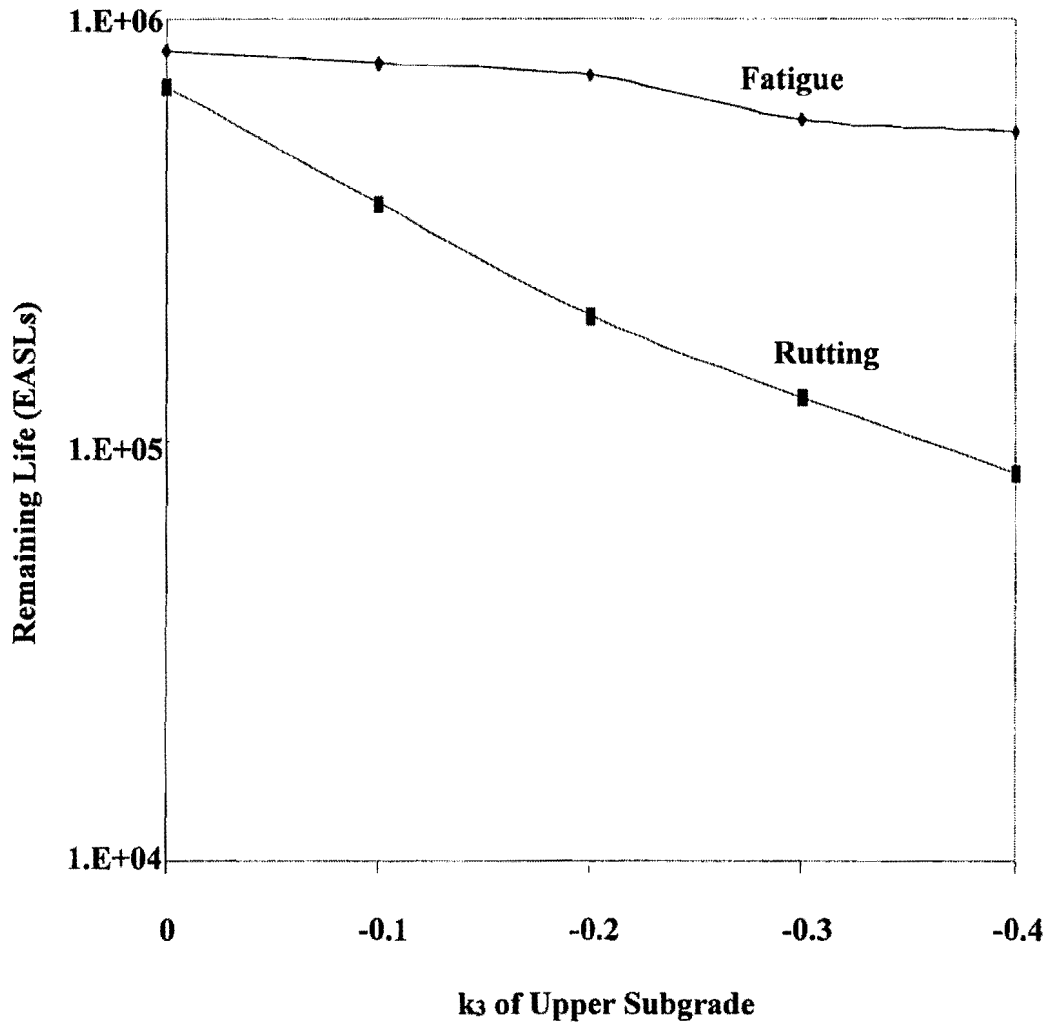


Figure 6.8 - Variations in Remaining Lives with Parameter k_3 of Upper Subgrade

**Table 6.3 – Sensitivity of Critical Tensile Strain to Pavement Parameters
under Nonlinear Model**

Layer	Parameter	Sensitivity	Thin AC (3 in.)		Thick AC (5 in.)		
			Thin Base (6 in.)	Thick Base (12 in.)	Thin Base (6 in.)	Thick Base (18 in.)	
AC	Thickness	Index	1.14	0.86	2.03	2.00	
		Level	VS	VS	VS	VS	
	Modulus	Index	0.30	0.18	0.79	0.63	
		Level	S	MS	VS	VS	
	Poisson's Ratio	Index	0.50	0.07	0.15	0.11	
		Level	VS	NS	MS	MS	
Base	Thickness	Index	0.27	0.76	0.18	0.44	
		Level	S	VS	MS	VS	
	Modulus	Index	0.50	0.62	0.59	0.24	
		Level	VS	VS	VS	S	
	Poisson's Ratio	Index	0.17	0.14	0.27	0.05	
		Level	MS	MS	S	NS	
	k ₂	Index	0.48	0.65	0.51	0.35	
		Level	VS	VS	VS	S	
	k ₃	Index	0.50	0.66	0.46	0.22	
		Level	VS	VS	VS	S	
	Subgrade	Modulus	Index	0.39	0.47	0.38	0.32
			Level	S	VS	S	S
Poisson's Ratio		Index	0.05	0.12	0.08	0.07	
		Level	NS	MS	NS	NS	
k ₂		Index	0.09	0.10	0.11	0.03	
		Level	NS	MS	MS	NS	
k ₃		Index	0.13	0.15	0.10	0.06	
		Level	MS	MS	MS	NS	

[1] VS: Very Sensitive; S: Sensitive; MS: Moderately Sensitive; NS: Not Sensitive.

Table 6.4 – Sensitivity of Critical Compressive Strain to Pavement Parameters under Nonlinear Model

Layer	Parameter	Sensitivity	Thin AC (3 in.)		Thick AC (5 in.)		
			Thin Base (6 in.)	Thick Base (12 in.)	Thin Base (6 in.)	Thick Base (18 in.)	
AC	Thickness	Index	1.00	0.45	2.00	1.19	
		Level	VS	VS	VS	VS	
	Modulus	Index	0.31	0.28	0.53	0.32	
		Level	S	S	VS	S	
	Poisson's Ratio	Index	0.42	0.16	0.14	0.09	
		Level	VS	MS	MS	NS	
Base	Thickness	Index	0.64	2.05	0.61	1.23	
		Level	VS	VS	VS	VS	
	Modulus	Index	0.25	0.32	0.10	0.23	
		Level	S	S	MS	S	
	Poisson's Ratio	Index	0.06	0.07	0.06	0.17	
		Level	NS	NS	NS	MS	
	k ₂	Index	0.13	0.20	0.08	0.15	
		Level	MS	S	NS	MS	
	k ₃	Index	0.15	0.20	0.06	0.12	
		Level	MS	S	NS	MS	
	Subgrade	Modulus	Index	0.84	0.85	0.83	0.97
			Level	VS	VS	VS	VS
Poisson's Ratio		Index	0.67	0.72	0.79	0.56	
		Level	VS	VS	VS	VS	
k ₂		Index	0.23	0.14	0.19	0.12	
		Level	S	MS	MS	MS	
k ₃		Index	0.23	0.14	0.19	0.12	
		Level	S	S	S	S	

[1] VS: Very Sensitive; S: Sensitive; MS: Moderately Sensitive; NS: Not Sensitive.

**Table 6.5 – Sensitivity of Fatigue Remaining Life to Pavement Parameters
under Nonlinear Model**

Layer	Parameter	Sensitivity	Thin AC (3 in.)		Thick AC (5 in.)	
			Thin Base (6 in.)	Thick Base (12 in.)	Thin Base (6 in.)	Thick Base (18 in.)
AC	Thickness	Index	161.07	23.10	619.10	506.90
		Level	VS	VS	VS	VS
	Modulus	Index	0.20	1.42	1.28	0.91
		Level	NS	VS	VS	S
	Poisson's Ratio	Index	1.43	0.24	0.59	0.40
		Level	VS	NS	S	MS
Base	Thickness	Index	1.76	1.94	0.91	1.58
		Level	VS	VS	S	VS
	Modulus	Index	1.34	2.34	2.54	0.67
		Level	VS	VS	VS	S
	Poisson's Ratio	Index	0.49	0.41	0.97	0.18
		Level	MS	MS	S	NS
	k ₂	Index	2.11	3.79	2.28	1.78
		Level	VS	VS	VS	VS
	k ₃	Index	2.48	3.63	2.20	1.00
		Level	VS	VS	VS	VS
Subgrade	Modulus	Index	0.94	1.28	1.47	1.22
		Level	S	VS	VS	VS
	Poisson's Ratio	Index	0.17	0.39	0.29	0.24
		Level	NS	MS	MS	NS
	k ₂	Index	0.27	0.29	0.41	0.10
		Level	MS	MS	MS	NS
	k ₃	Index	0.61	0.43	0.44	0.23
		Level	S	MS	MS	NS

[1] VS: Very Sensitive; S: Sensitive; MS: Moderately Sensitive; NS: Not Sensitive.

**Table 6.6 – Sensitivity of Rutting Remaining Life to Pavement Parameters
under Nonlinear Model**

Layer	Parameter	Sensitivity	Thin AC (3 in.)		Thick AC (5 in.)		
			Thin Base (6 in.)	Thick Base (12 in.)	Thin Base (6 in.)	Thick Base (18 in.)	
AC	Thickness	Index	19.31	5.94	15.54	12.38	
		Level	VS	VS	VS	VS	
	Modulus	Index	1.25	1.48	2.34	1.57	
		Level	VS	VS	VS	VS	
	Poisson's Ratio	Index	2.25	0.88	0.72	0.44	
		Level	VS	S	S	MS	
Base	Thickness	Index	19.89	25.25	7.59	13.58	
		Level	VS	VS	VS	VS	
	Modulus	Index	1.31	1.74	0.41	0.82	
		Level	VS	VS	MS	S	
	Poisson's Ratio	Index	0.27	0.33	0.27	0.80	
		Level	MS	MS	MS	S	
	k ₂	Index	0.63	0.69	0.34	0.62	
		Level	S	S	MS	S	
	k ₃	Index	0.78	1.31	0.24	0.43	
		Level	S	VS	NS	MS	
	Subgrade	Modulus	Index	5.63	4.15	3.15	4.53
			Level	VS	VS	VS	VS
Poisson's Ratio		Index	5.06	5.71	6.75	3.87	
		Level	VS	VS	VS	VS	
k ₂		Index	1.47	0.77	0.91	0.62	
		Level	VS	S	S	S	
k ₃		Index	3.51	2.48	1.99	1.51	
		Level	VS	VS	VS	VS	

[1] VS: Very Sensitive; S: Sensitive; MS: Moderately Sensitive; NS: Not Sensitive.

CHAPTER SEVEN

DYNAMIC RESPONSES OF PAVEMENT

7.1 INTRODUCTION

In the previous three chapters, the applied load was assumed to be static. Since the FWD and SPA apply impulse loads to the pavement and since the actual traffic loads are also dynamic in nature, it is essential to study the responses of the pavement systems considering the dynamic effects.

Basically, the dynamic responses under two conditions were considered. In the first condition, the materials were assumed to behave linearly, while in the second condition, the material nonlinearity was considered. For the linear dynamic condition, the influences of material damping and material density on pavement responses were explored by comparing the surface deflections, the critical strains, and the remaining lives of the pavement. For the nonlinear dynamic condition, the impact of parameters k_2 and k_3 of the base and upper subgrade (see Figure 3.17) on the response of the pavement was also studied.

7.2 APPROACHES TO MODELING OF DYNAMIC EFFECTS

As indicated before, the software package ABAQUS was used to analyze the dynamic response of the pavements. The user-defined nonlinear model used in Chapter 6 was also utilized here.

The dynamic loading was simulated as a haversine as illustrated in Figure 7.1. The duration of the simulated impulse loading was 30 msec with the peak load at 15 msec. The peak load of 9000 lbs (40kN), which was the same as the load magnitude in static models, was considered. However, the response of the pavement was observed for a longer period. This would ensure that delays in peak deflections due to damping or other dynamic effects of the pavement are accommodated.

ABAQUS offers several options for dynamic analyses. In this study, the direct integration of dynamic response was used for both linear dynamic analysis and nonlinear dynamic analysis. ABAQUS also offers different approaches for direct integration. The standard method provided in the program uses an implicit time integration operator. This integration method is a slight modification of the trapezoidal rule and is called Hilber-Hughes-Taylor operator.

A major advantage of the implicit method is that it is normally stable. In other methods, the stability limit, the longest time increment that can be taken without generating large, rapidly growing errors, is related to the smallest element dimension in the mesh. Therefore, the time increment has to be very short if the mesh contains small elements or if the modulus of the material is very high. Since the optimized mesh selected for this analysis contains materials with high modulus and different sizes of elements, implicit time integration was found to be economical.

Material damping should be considered in any dynamic analysis. The so-called Rayleigh damping was introduced into the system. This method gives the damping matrix as

$$[C] = \alpha[M] + \beta[K] \quad (7.1)$$

where,

- [C] = Rayleigh damping matrix;
- [M] = Mass matrix;
- [K] = Stiffness matrix;
- α = mass proportional coefficient;
- β = Stiffness proportional coefficient.

The material damping ratio (ζ) in this study was assumed to be 5%, a value commonly used in pavement analysis. The relationship between α , β and the fraction of critical damping ζ , at the frequency ω , is given by

$$\zeta = (\alpha / \omega + \beta \omega) / 2 \quad (7.2)$$

In this study, the mass proportional coefficient is set to zero. When α is zero, undesirable high frequency components of the response will be filtered out (Siddarthan et al., 1991). Equation 7.2 then changes to be

$$\beta = \frac{2\zeta}{\omega} \quad (7.3)$$

where ω is the natural angular frequency ($=2\pi f$), and f is the fundamental frequency of the pavement in Hertz. Assuming a fundamental frequency of 15Hz, the resulting value of β is 0.00114.

The dynamic nonlinear model is implemented, in a manner similar to that of the static nonlinear model, by adding a user subroutine into the input file and defining the moduli of nonlinear elements as solution-dependent. During each time increment, the nonlinear moduli of elements obtained from the last time increment are used to provide pavement response. In the meantime, for each element, the user subroutine is called to calculate the nonlinear modulus for the next time increment. As long as the time increment and the increase of load between neighboring increments is small, this approach can be accurate enough to obtain nonlinear dynamic response of pavement.

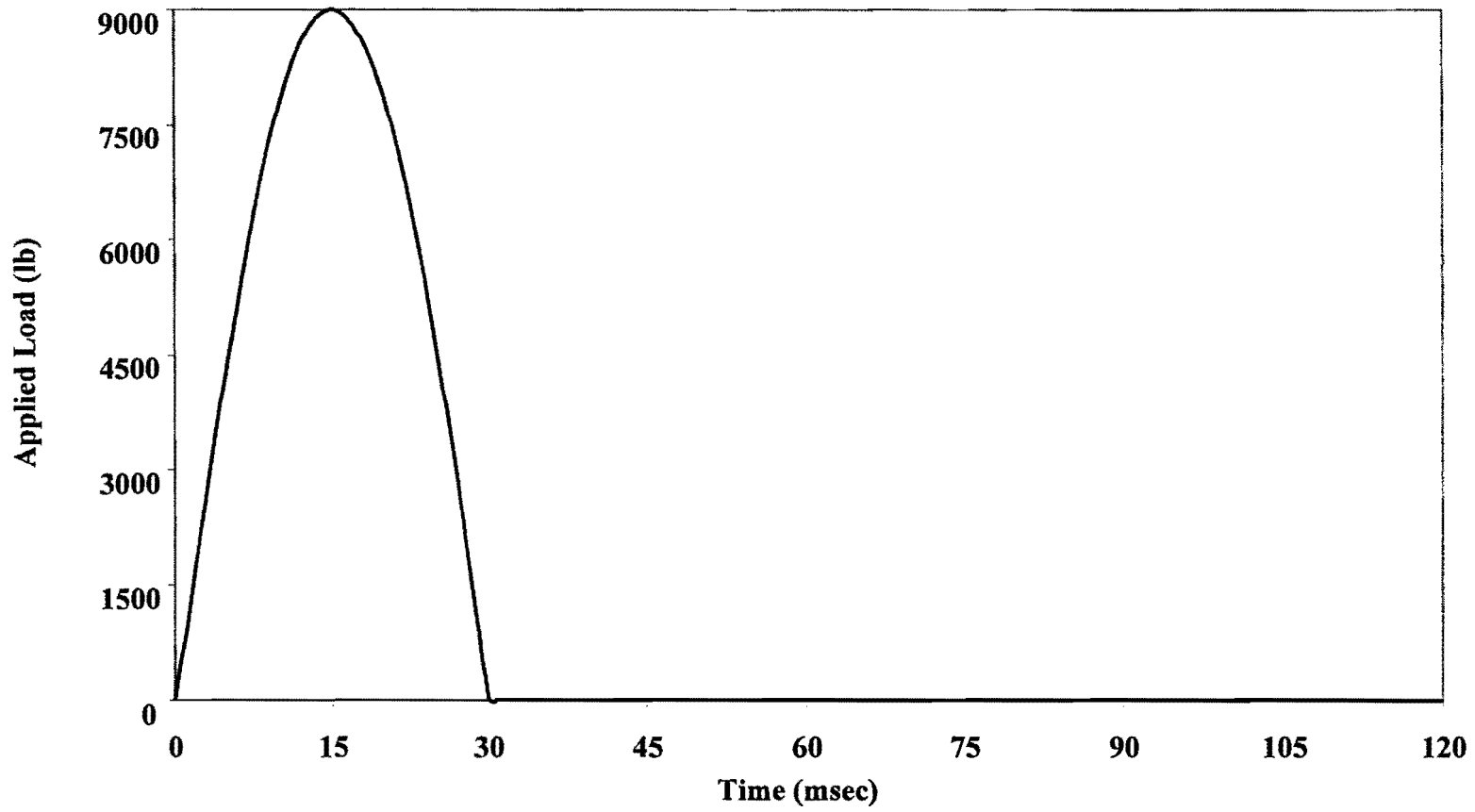


Figure 7.1 – Typical Half Sine Impulse Assumed in Dynamic Analysis

7.3 DYNAMIC RESPONSES OF ONE TYPICAL PAVEMENT SECTION

In this section, the dynamic responses of the typical pavement section “3-12 PAVE” under both linear dynamic and nonlinear dynamic models are discussed. As shown in Figure 3.7, the typical pavement section has four physical layers: the AC layer, the base layer, the subgrade and the bedrock. A dynamic load, shown in Figure 7.1, is applied to the surface layer on a circular area with a radius of 6 inches (150 mm). As discussed in the previous section, the damping coefficient α was assumed to be zero and the damping coefficient β was 0.00114. In the linear dynamic model, the materials of the four layers were considered linear. In the nonlinear dynamic model, the base layer and the upper 18 inches (450 mm) of the subgrade were considered nonlinear with a constitutive model, as shown in Equation 3.16. As shown in Table 3.2, parameters k_2 and k_3 of the base layer were assumed as 0.4 and -0.3, respectively, and parameters k_2 and k_3 of the upper subgrade as 0.2 and -0.2, respectively.

7.3.1 Response Under Linear Dynamic Model

Time histories of the seven surface deflections at different radial distances are shown in Figure 7.2. Each deflection increases with time, reaches its peak, and then decreases with time. However, the seven deflections reach their peak values at different times, as reflected in Table 7.1. The peak deflection under the load occurs first at a time of 19 msec, 4 msec after the peak of the external dynamic load. With the increase in the radial distance, the peak deflection occurs at a longer time. The deflection at the radial distance of 72 inches (1.8 m) reaches its peak at a time of 33 msec, 3 msec after the external load is released from the pavement.

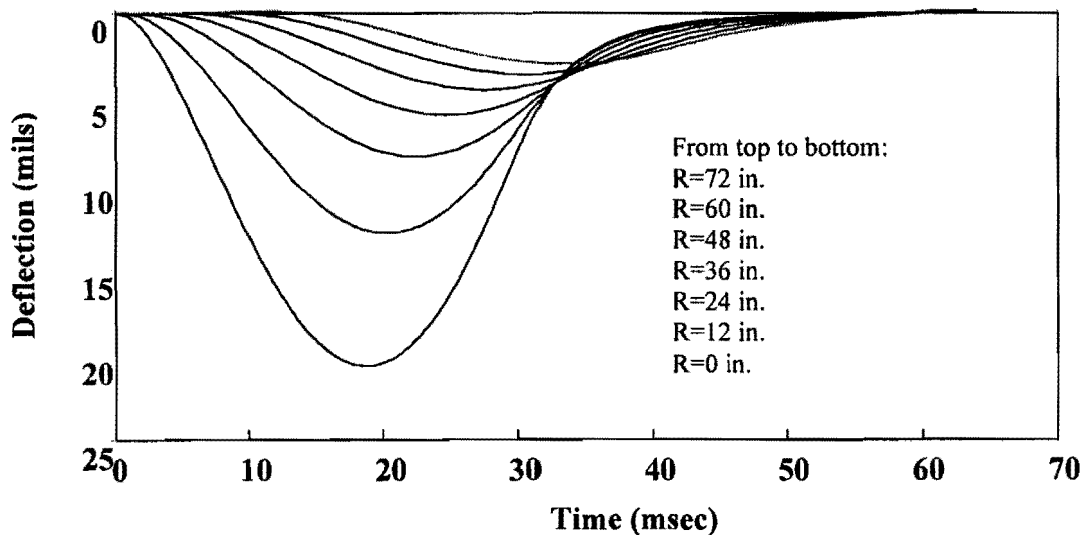


Figure 7.2 – Surface Deflections of Typical Pavement Section Under Linear Dynamic Model

The two critical strains, contrary to the central deflection, achieve their maximum values almost concurrently with the peak load, as shown in Figure 7.3 and Table 7.1. When the pavement is experiencing its peak surface deflection directly under the load, the critical strains decrease at a rapid rate.

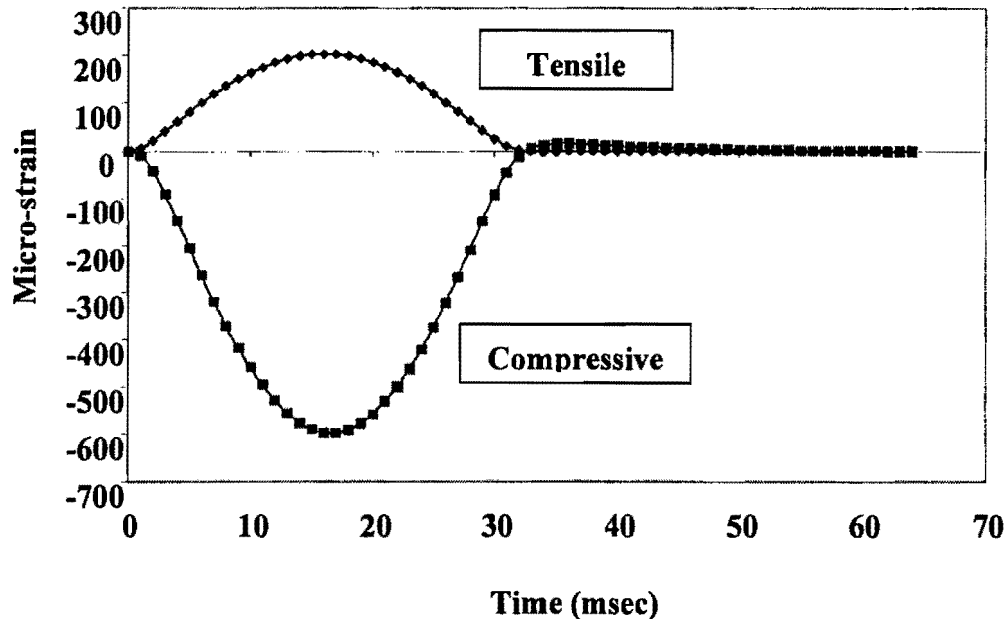


Figure 7.3 - Critical Strains of Typical Pavement Section Under Linear Dynamic Model

7.3.2 Response Under Nonlinear Dynamic Model

Time histories of the surface deflections and critical strains for the typical 3-12 PAVE pavement section under the nonlinear dynamic model are shown in Figures 7.4 and 7.5. The deflection time histories exhibit similar behavior to those of the linear dynamic model. The times at which the surface deflections reach their peak values are almost the same in the nonlinear dynamic model as in the linear dynamic model (Table 7.1). However, the nonlinear dynamic responses exhibit two different characteristics. First, the surface deflections near the load and the critical strains are significantly larger. The first surface deflection is about 25 percent larger for the nonlinear dynamic model than for the linear dynamic one. This is a direct result of considering the nonlinear behavior of pavement materials. Second, the critical strain time histories are not as smooth as the linear dynamic response. The reason for this is that the level of nonlinearity induced is not exactly proportional to the instant magnitude of the applied load.

7.4 SENSITIVITY STUDY FOR “3-12 PAVE”

7.4.1 Linear Dynamic Model

Two variables are studied in the sensitivity analysis of the linear dynamic model: system damping and density of the materials.

Table 7.1 - Peak Deflections and Critical Strains Under Dynamic Models

Model	Radial Distance (inch)	0	12	24	36	48	60	72
Linear Dynamic	Peak Deflections (mils)	20.6	12.9	8.4	6.0	4.5	3.6	3.0
	Occurrence Time (msec)	9	20	22	25	27	30	33
	Peak Critical Tensile strain (micro-strain)	203						
	Occurrence Time (msec)	16						
	Peak Critical Compressive Strain (micro-strain)	596						
	Occurrence Time (msec)	17						
	Nonlinear Dynamic	Peak Deflections (mils)	24.9	15.2	9.3	6.3	4.6	3.7
Occurrence Time (msec)		19	20	22	25	28	31	34
Peak Critical Tensile strain (micro-strain)		251						
Occurrence Time (msec)		17						
Peak Critical Compressive Strain (micro-strain)		642						
Occurrence Time (msec)		14						

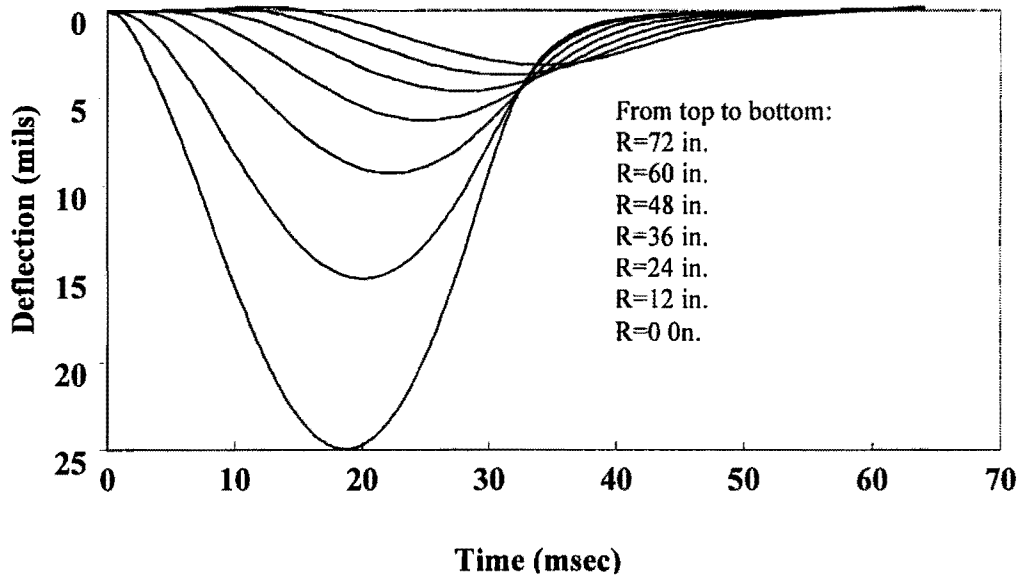


Figure 7.4 - Surface Deflections of Typical Pavement Section Under Nonlinear Dynamic Model

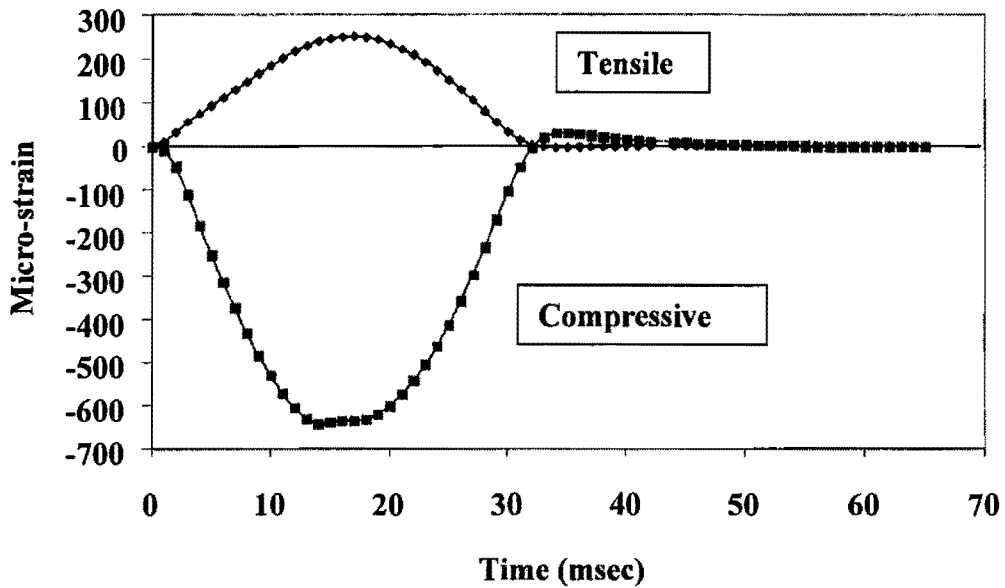


Figure 7.5 - Critical Strains of Typical Pavement Section Under Nonlinear Dynamic Model

As shown in Equations 7.2 and 7.3, with the assumption that the mass proportional coefficient, α , is zero, the only variable related to system damping is the stiffness proportional coefficient, β . Three values of β were considered: 0, 0.00114 and 0.00228. Time histories of the deflections and the critical strains of these three cases are shown in Appendix D.

When the system damping increases, the delays of the peak deflection and the peak critical strains relative to the peak load increase. In addition, the peak values of these variables become smaller (see Table 7.2). With a larger system damping, the power can be absorbed faster, and the dynamic effects are overcome more efficiently.

As a comparison, when coefficient β decreases from 0.00114 to 0, the deflection at $R=0$ increases by about 2 percent, and the two critical strains increase by about 1 percent. In the meantime, when coefficient β increases from 0.00114 to 0.00228, the deflection at $R=0$ decreases about 3 percent, and the two critical strains decrease about 2 percent. Thus, the effects of the system damping ratio on the pavement critical strains are not pronounced. However, coefficient β has more influence on surface deflections at the outer sensors. For example, the surface deflection of the last sensor increases by 10 percent when β decreases from 0.00114 to 0 and decreases by 10 percent when β increases from 0.00114 to 0.00228. This phenomenon has a large impact on the backcalculated moduli. Since the backcalculated moduli are used to calculate critical strains and remaining lives, in actual design cases, the strains may be significantly misestimated.

The assumed standard densities for all layers were increased and decreased by 25 percent. Time histories of the deflections and critical strains for these three cases are presented in Appendix D.

When the densities of the materials increase, the inertia effects become more pronounced. Therefore, as seen in Table 7.3, the deflections and critical strains reach their peaks at slightly later times at the higher densities. The magnitudes of these peaks are also smaller.

A 25 percent variation in densities results in only a 1.5 percent change in deflections. The two critical strains are even less impacted. Therefore, the effects of the densities of the materials on the dynamic response of pavements are insignificant.

7.4.2 Nonlinear Dynamic Model

In this section, the sensitivities of the responses of the typical pavement to variations of nonlinear parameters are studied. Time histories of the responses are included in Appendix E.

The times at which surface deflections and critical strains reach their peaks do not change with the variation of nonlinear parameters. Therefore, only the peak values of deflections are discussed in this section.

**Table 7.2 – Peak Deflections and Critical Strains with Different Damping Coefficients (β)
Under Linear Dynamic Model**

Case	Radial Distance (inch)	0	12	24	36	48	60	72
$\beta = 0$	Peak Deflections (mills)	21.0 (18)*	13.2 (19)	8.7 (21)	6.3 (24)	4.8 (27)	3.9 (30)	3.3 (33)
	Peak Critical Tensile Strain (micro-strain)	204 (15)						
	Peak Critical Compressive Strain (micro-strain)	605 (16)						
$\beta = 0.00114$	Peak Deflections (mils)	20.6 (19)	12.9 (20)	8.4 (22)	6.0 (25)	4.5 (27)	3.6 (30)	3.0 (33)
	Peak Critical Tensile Strain (micro-strain)	203 (16)						
	Peak Critical Compressive Strain (micro-strain)	596 (17)						
$\beta = 0.00228$	Peak Deflections (mils)	20.1 (20)	12.4 (21)	8.1 (23)	5.7 (25)	4.2 (28)	3.3 (31)	2.7 (34)
	Peak Critical Tensile Strain (micro-strain)	199 (17)						
	Peak Critical Compressive Strain (micro-strain)	582 (18)						

* Values in parenthesis are time in msec when the corresponding peak occurs.

**Table 7.3 - Peak Deflections and Critical Strains with Different Material Densities
Under Linear Dynamic Model**

Case	Radial Distance (inch)	0	12	24	36	48	60	72
75% of Standard Densities	Peak Deflections (mils)	20.9 (18)	13.1 (20)	8.6 (22)	6.1 (24)	4.6 (26)	3.7 (29)	3.0 (31)
	Peak Critical Tensile Strain (micro-strain)	203 (16)						
	Peak Critical Compressive Strain (micro-strain)	594 (16)						
Standard Densities	Peak Deflections (mils)	20.6 (19)	12.9 (20)	8.4 (22)	6.0 (25)	4.5 (27)	3.6 (30)	3.0 (33)
	Peak Critical Tensile strain (micro-strain)	203 (16)						
	Peak Critical Compressive Strain (micro-strain)	596 (17)						
125% of Standard Densities	Peak Deflections (mils)	20.4 (19)	12.6 (21)	8.2 (23)	5.8 (26)	4.4 (29)	3.5 (32)	2.9 (35)
	Peak Critical Tensile strain (micro-strain)	204 (16)						
	Peak Critical Compressive Strain (micro-strain)	598 (17)						

* Values in parenthesis are time in msec when the corresponding peak occurs.

7.4.2.1 Nonlinear Parameters of Base Layer

To determine the impacts of k_2 of the base layer, five cases were studied. Parameter k_2 of 0.2, 0.3, 0.4, 0.5 and 0.6 was considered. In the constitutive model shown in Equation 3.16, the larger the k_2 is, the more rapidly the base stiffens with an increase in the confining pressure. Therefore, with the increase of k_2 , the surface deflections and the two critical strains decrease and, thus, the remaining lives increase.

The seven surface deflections calculated with different values of parameter k_2 of the base are shown in Figure 7.6. The deflections of the outer sensors hardly vary with k_2 . Far from the impact, the materials experience very little nonlinearity. In addition, the surface deflections of the outer sensors are mainly determined by the properties of deep materials. The largest variation in deflections occurs immediately under the load. The surface deflection under the load increases by 10 percent when k_2 changes from 0.4 to 0.2 and decreases by 5 percent when k_2 changes from 0.4 to 0.6.

Similarly, parameter k_3 of the base layer was assumed to be 0.0, -0.1, -0.2, -0.3 and -0.4. In contrast to k_2 , the larger the absolute value of k_3 , the more rapidly the base becomes soft, with an increase in the deviatoric stress. Therefore, with an increase of the absolute value of k_3 , the surface deflections and the two critical strains increase and, thus, the remaining lives decrease.

Figure 7.7 shows the impact of the variation in k_3 on surface deflections. Again, a change in k_3 mainly affects the surface deflections close to the load application. The first surface deflection increases by 18 percent when k_3 varies from -0.3 to -0.5. In the opposite direction, the first surface deflection decreases by approximately 13 percent when k_3 is increased from -0.3 to -0.1.

The levels of sensitivity of critical strains and remaining lives to variations in nonlinear parameters are summarized in Table 7.4. The critical strains and remaining lives are very sensitive to variations in k_2 and k_3 of the base layer.

7.4.2.2 Nonlinear Parameters of Upper Subgrade

As before, the upper 18 inches (450 mm) of the subgrade (upper subgrade) was considered to exhibit nonlinear behavior. The original parameters k_2 and k_3 for the upper subgrade are 0.2 and -0.2, respectively.

Similar to the k_2 of the base layer, with an increase of k_2 , the surface deflections decrease. Figure 7.8 shows the impact of the change in value of k_2 on the surface deflections. However, the impacts of the variations in k_2 of the upper subgrade on the pavement response are less significant as compared with those in the case of the base layer. The first deflection increases approximately 5 percent when k_2 varies from 0.2 to 0.0 and decreases by 4 percent when k_2 varies from 0.2 to 0.4.

The impacts of variation in k_3 of the upper subgrade are shown in Figure 7.9. Again, the trends of variation in pavement responses are similar to those of the base. With the increase of the absolute value of k_3 , the surface deflections increase. However, the surface deflections are less sensitive

to the variation in k_3 of the upper subgrade than to that of the base. The first deflection increases approximately 7 percent when k_3 varies from -0.2 to -0.4 and decreases by only about 7 percent when k_3 varies from -0.2 to 0.0.

The levels of sensitivity of critical strains and remaining lives to the variations in nonlinear parameters are summarized in Table 7.4. Parameter k_3 of the upper subgrade has a small impact on critical tensile strain and fatigue remaining life, while k_2 does not impact them at all. However, the critical compressive strain and rutting remaining life are sensitive to k_3 , though they are less sensitive to k_2 .

7.4.3 Conclusions of Sensitivity Study for “3-12 PAVE”

The conclusions of the sensitivity study from this chapter are summarized as follows:

- a. In the linear dynamic model, the surface deflections at the outer sensors change significantly with the variation in damping coefficient β . However, the damping coefficient β has little effect on the critical strains and the surface deflections at the first two sensors.
- b. In the linear dynamic model, the densities of the materials have very little influence on the pavement response.
- c. In the nonlinear dynamic model, the increase of parameter k_2 for either the base or the subgrade reduces the first two surface deflections, but it has little effect on the other surface deflections. The increase of the absolute value of parameter k_3 increases the first two deflections. The influences of these parameters of the base are larger than those of the subgrade.

In the nonlinear dynamic model, the critical strains and remaining lives are sensitive to the variations of nonlinear parameters of the base. However, they are less sensitive to the variations in the nonlinear parameters of the subgrade.

7.5 SENSITIVITY STUDY RESULTS FOR THE FOUR PAVEMENTS

The other three typical pavement sections, PAVE 3-6, PAVE 5-6 and PAVE 5-12, are also analyzed for sensitivity of critical strains and remaining lives. Nonlinear parameters k_2 and k_3 of the base layer and the upper subgrade are studied. The results are presented in Tables 7.5 and 7.6.

With the change of the thickness of the AC layer or the base layer, the sensitivity of critical strains and remaining lives varies. With the increase of the thickness of the AC layer, the critical strains and remaining lives become less sensitive to the nonlinear parameters of both the base and the subgrade. However, with the increase of the thickness of the base layer, the critical tensile strain and fatigue remaining life are more sensitive to the nonlinear parameters of the base layer but less sensitive to those of the subgrade. Also, the critical compressive strain and rutting remaining life are less sensitive to the nonlinear parameters of both layers.

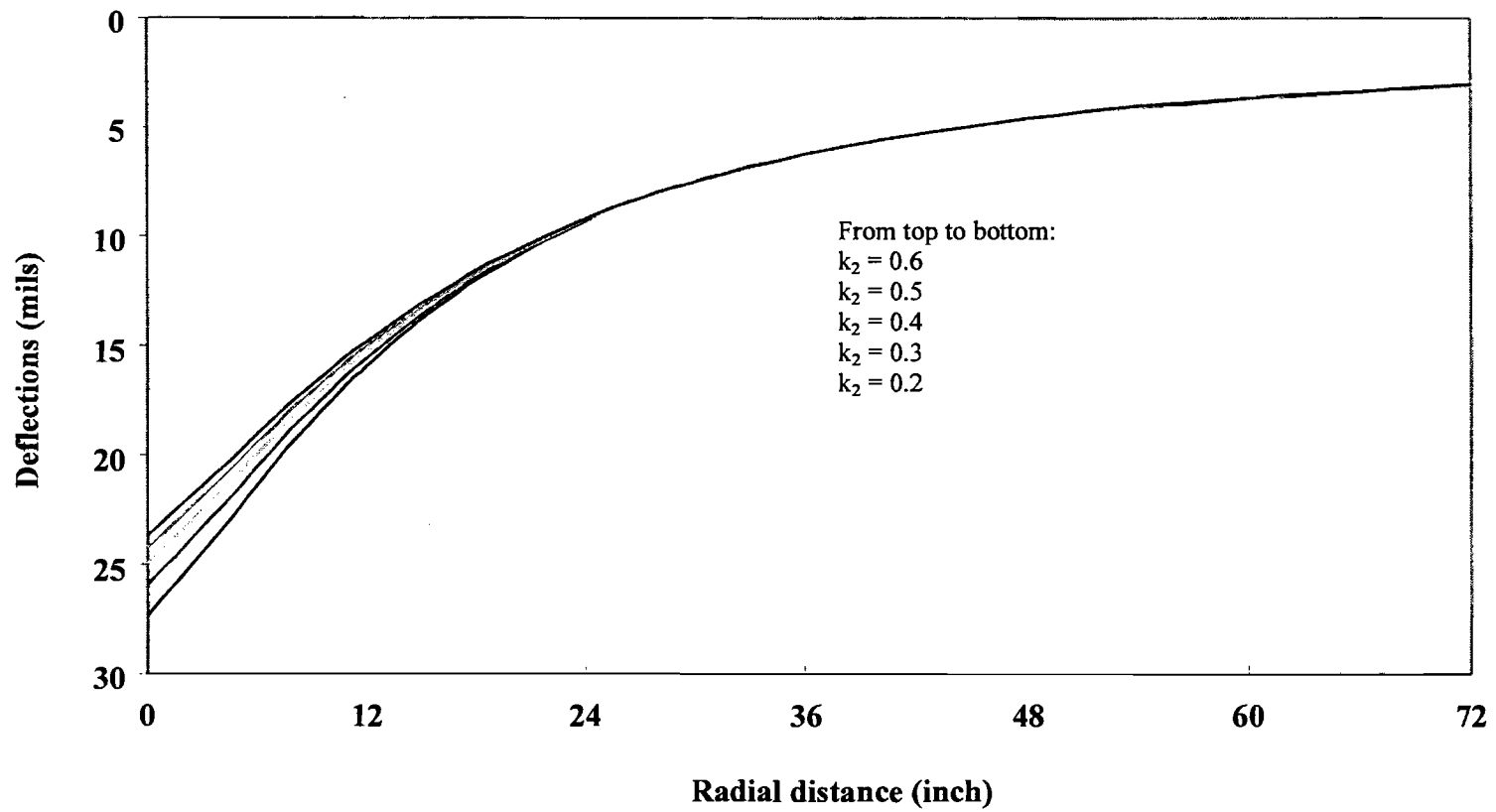


Figure 7.6 - Surface Deflections Under Nonlinear Dynamic Model with Different k_2 of Base

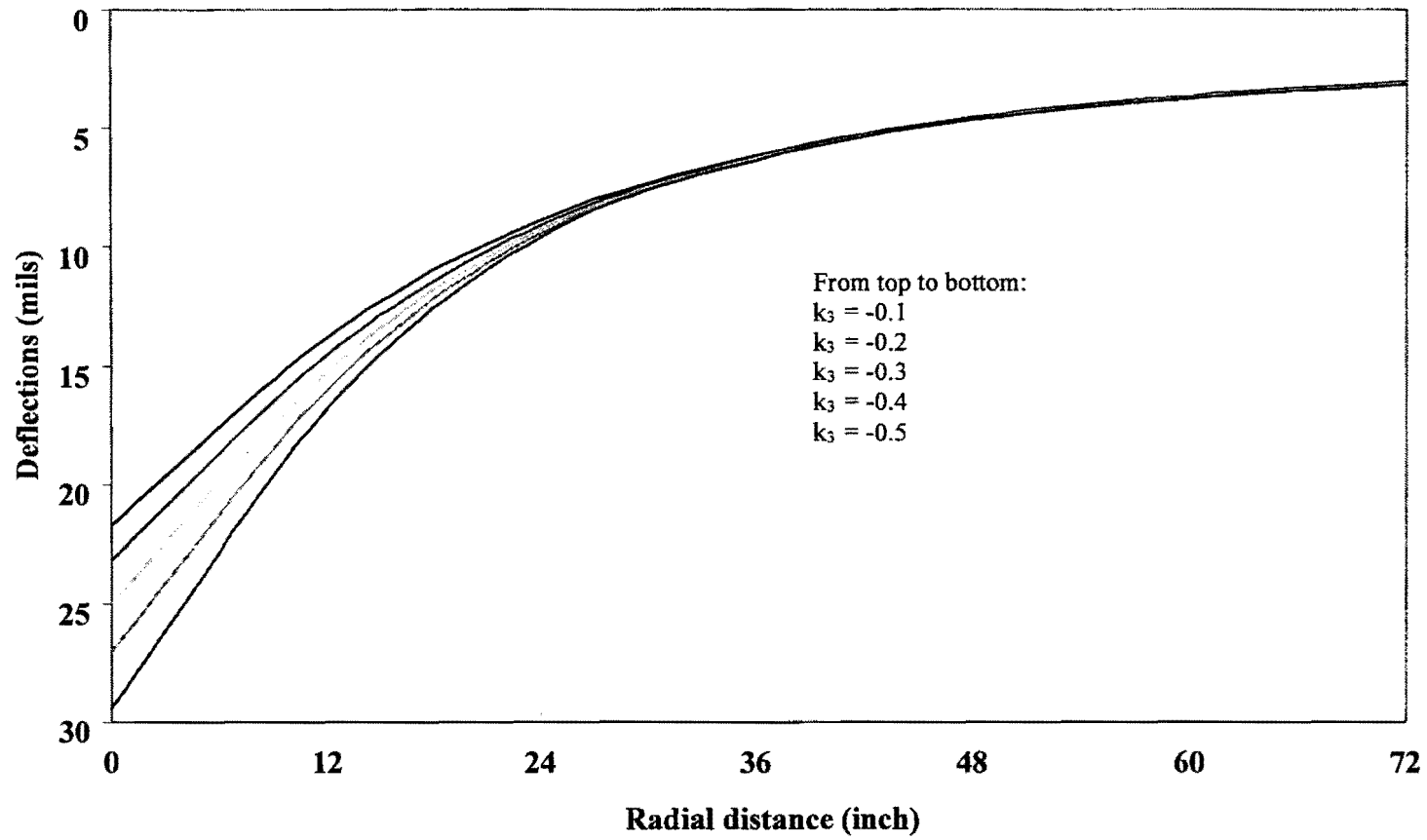


Figure 7.7 - Surface Deflections Under Nonlinear Dynamic Model with Different k_3 of base

Table 7.4 – Levels of Sensitivity of Nonlinear Parameters

Target variable		Base		Upper Subgrade	
		k ₂	k ₃	k ₂	k ₃
Critical Tensile Strain (ϵ_t)	Sensitivity Index	0.58	0.66	0.05	0.10
	Level of Sensitivity	VS*	VS	NS	MS
Fatigue Remaining Life (N_f)	Sensitivity Index	1.26	1.70	0.17	0.34
	Level of Sensitivity	VS	VS	NS	MS
Critical Compressive Strain (ϵ_c)	Sensitivity Index	0.55	0.56	0.10	0.22
	Level of Sensitivity	VS	VS	MS	S
Rutting Remaining Life (N_r)	Sensitivity Index	1.78	1.99	0.36	0.70
	Level of Sensitivity	VS	VS	MS	S

* VS: Very Sensitive; S: Sensitive; MS: Moderately Sensitive; NS: Not Sensitive.

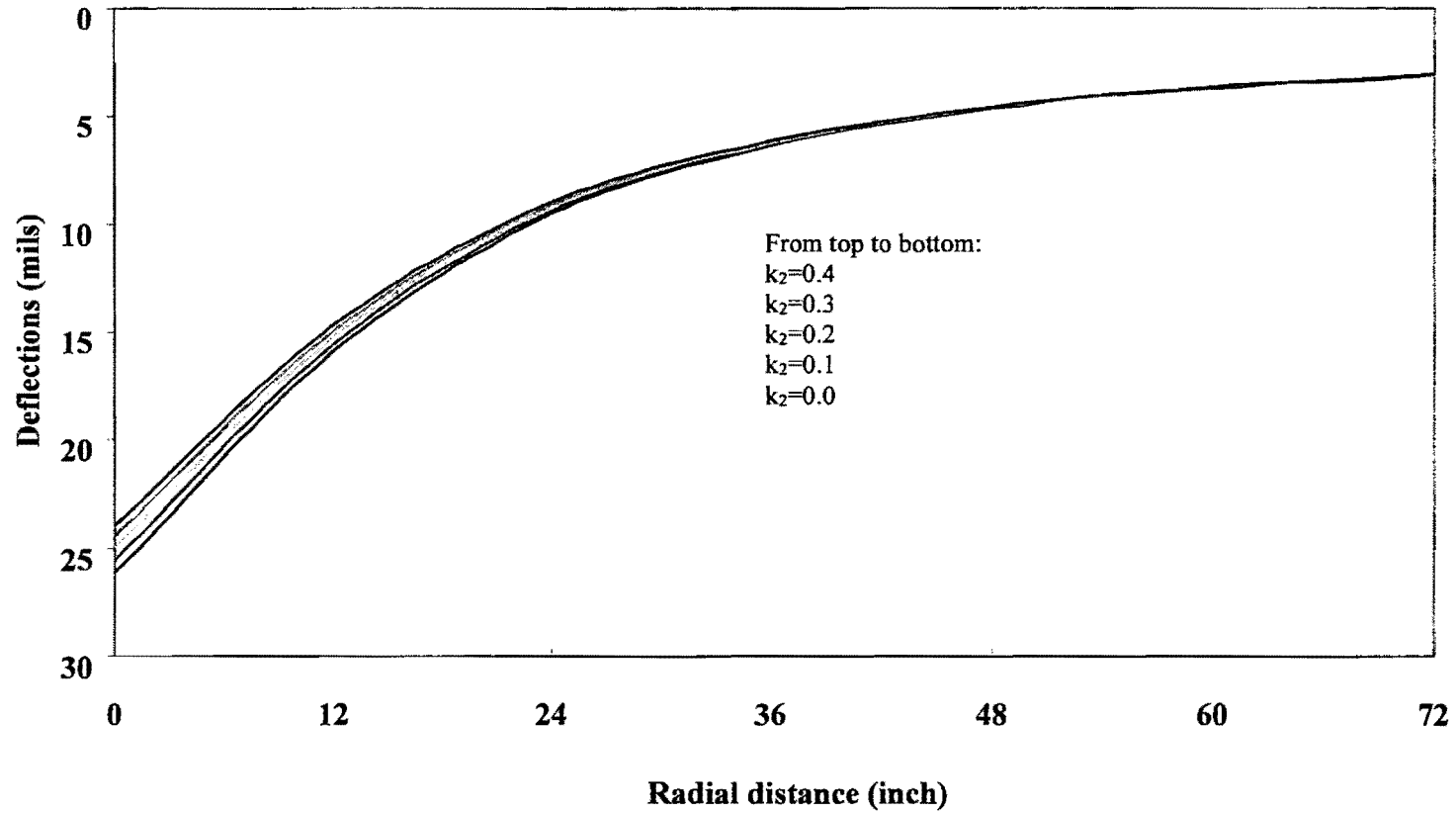


Figure 7.8 - Surface Deflections Under Nonlinear Dynamic Model with Different k_2 of Upper Subgrade

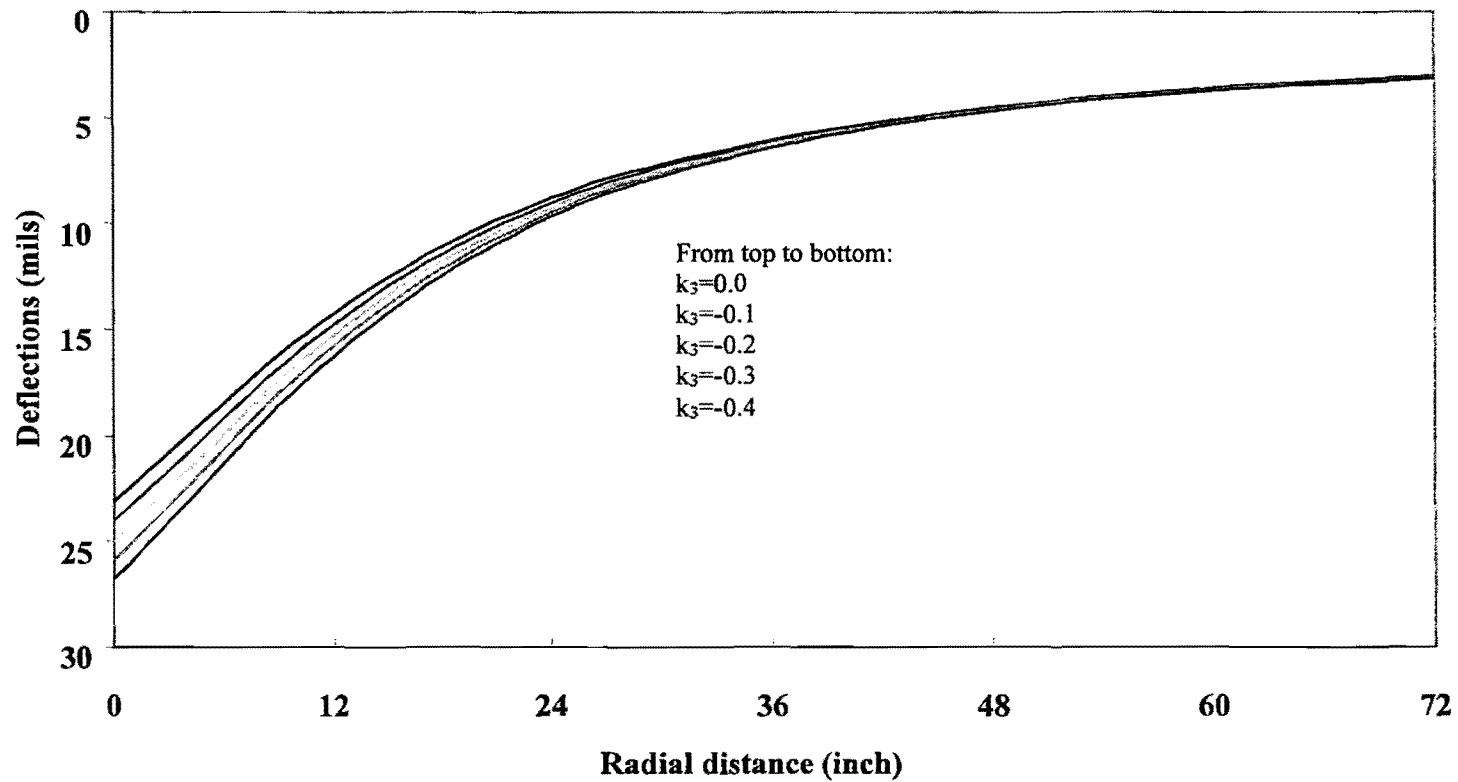


Figure 7.9 - Surface Deflections Under Nonlinear Dynamic Model with Different k_3 of Upper Subgrade

Table 7.5 – Sensitivity of Nonlinear Parameters in Different Pavements with Respect to Critical Tensile Strain and Fatigue Remaining Life

Target variable	Parameter	Sensitivity	Thin AC (3 in.)		Thick AC (5 in.)	
			Thin Base (6 in.)	Thick Base (12 in.)	Thin Base (6 in.)	Thick Base (18 in.)
Critical Tensile Strain	k ₂ of Base	Index	0.36	0.58	0.05	0.17
		Level	S	VS	NS	MS
	k ₃ of Base	Index	0.31	0.66	0.13	0.26
		Level	S	VS	MS	S
	k ₂ of Subgrade	Index	0.16	0.05	0.07	0.03
		Level	MS	NS	NS	NS
	k ₃ of Subgrade	Index	0.23	0.10	0.13	0.05
		Level	S	MS	MS	NS
Fatigue Remaining Life	k ₂ of Base	Index	0.85	0.26	0.18	0.46
		Level	VS	VS	NS	MS
	k ₃ of Base	Index	1.73	1.70	0.51	0.69
		Level	VS	VS	S	S
	k ₂ of Subgrade	Index	0.58	0.17	0.28	0.09
		Level	S	NS	MS	NS
	k ₃ of Subgrade	Index	1.09	0.34	0.49	0.18
		Level	VS	MS	MS	NS

Table 7.6 – Sensitivity of Nonlinear Parameters in Different Pavements with Respect to Critical Compressive Strain and Rutting Remaining Life

Target variable	Parameter	Sensitivity	Thin AC (3 in.)		Thick AC (5 in.)	
			Thin Base (6 in.)	Thick Base (12 in.)	Thin Base (6 in.)	Thick Base (18 in.)
Critical Comp. Strain	k ₂ of Base	Index	0.59	0.55	0.27	0.28
		Level	VS	VS	S	S
	k ₃ of Base	Index	0.51	0.56	0.26	0.25
		Level	VS	VS	S	S
	k ₂ of Subgrade	Index	0.27	0.10	0.13	0.06
		Level	S	MS	MS	NS
	k ₃ of Subgrade	Index	0.39	0.22	0.21	0.13
		Level	S	S	S	MS
Rutting Remaining Life	k ₂ of Base	Index	1.84	1.78	1.02	1.66
		Level	VS	VS	VS	VS
	k ₃ of Base	Index	1.52	1.99	0.93	1.42
		Level	VS	VS	S	VS
	k ₂ of Subgrade	Index	0.66	0.36	0.44	0.30
		Level	S	MS	MS	MS
	k ₃ of Subgrade	Index	1.47	0.70	1.07	0.90
		Level	VS	S	VS	S

CHAPTER EIGHT

ANALYSIS OF RESULTS

8.1 INTRODUCTION

In the previous chapters, the responses of four typical pavement sections under different loading conditions and material characteristics were obtained and analyzed. The impact of a number of pavement parameters on the critical strains and remaining lives of typical pavements was also studied. In this chapter, the responses obtained from different conditions are compared in an effort to explore the interrelation of these models, the impacts of material nonlinearity, and the dynamic nature of loading.

The multi-layer program BISAR and the finite element software ABAQUS were employed to simulate different conditions. These two programs should result in a similar response under the simplest model – static linear model. Therefore, the responses from BISAR and ABAQUS under the static linear model were compared and analyzed for the 3-12 PAVE model.

The nonlinear behavior of pavement materials is considered in two different algorithms: an equivalent-linear algorithm and a nonlinear algorithm. The constitutive relationships of these two models are the same, while the implementation methods are different. The dynamic responses can be obtained only from ABAQUS. By comparing the pavement responses from these algorithms, the levels of approximation associated with them and the importance of considering the dynamic nature of the load and material nonlinearity can be appreciated.

8.2 LINEAR STATIC MODELS

The responses of the typical pavement section under the linear static model from BISAR and ABAQUS should be close to one another. Since BISAR was used to implement the equivalent-linear model and ABAQUS was used to implement the nonlinear model, it is especially important that their corresponding linear static models be comparable.

The surface deflections at seven typical radial distances, as well as the critical strains and the remaining lives, calculated from BISAR and ABAQUS under the linear static model for the pavement section 3-12 PAVE, are compared in Table 8.1. The difference between the two deflections at each sensor is less than 3.2%; thus, they are compatible.

Table 8.1 - Pavement Responses Under Linear Static Models in BISAR and ABAQUS for “3-12 PAVE”

Program	Surface Deflections (mils)							Critical Strains (micro-strain)		Remaining Life (10 ³ EASLs)	
	Radial Distance(inch)							Tensile ^[1]	Compressive ^[2]	Fatigue	Rutting
	0	12	24	36	48	60	72				
BISAR	21.1	13.2	8.5	5.9	4.2	3.1	2.3	224	640	1105	273
ABAQUS	21.3	13.1	8.4	5.8	4.1	3.0	2.3	204	587	1505	401
Difference (%) ^[3]	0.9	-0.8	-0.9	-1.7	-2.4	-3.2	0.0	-9.0	-8.3	36	47

[1]: The tangential tensile strain at the bottom of the AC layer.

[2]: The vertical compressive strain at the top of the subgrade.

[3]: Percent difference between the calculated quantities from BISAR and ABAQUS.

The two critical strains from ABAQUS are about 10% less than those from BISAR. One reason for this discrepancy may be that the boundary at the top of the bedrock is fixed in both vertical and radial directions in the ABAQUS mesh, but in BISAR, the bedrock is simulated as a material with a high modulus (1000 ksi). Also, the size and the shape of the elements affect the strains from ABAQUS. The magnitude of the nodal strain is extrapolated from the element strain at its integration point. The implication of such differences in critical strains is that a more refined mesh is required, even though more than 2500 elements are used in this study. Comparable deflections between a finite element solution and a closed-form (or more robust) numerical algorithm do not guarantee similar strains. The fatigue remaining life from ABAQUS is 36 percent larger than from BISAR, and the rutting remaining life is 47 percent larger. In this study, since the major concern is to explore the sensitivities of the pavement responses to the variations of properties of pavement materials, this level of difference is still considered to be acceptable.

8.3 APPROXIMATION IN MODELS

As indicated before, the nonlinear effects of pavement responses can be taken into consideration in two different manners using either an equivalent-linear model or a nonlinear model. However, the implementation methods are different, as detailed in Chapter 3. The equivalent-linear model is unable to consider the nonlinear behavior of materials in the radial direction. The nonlinear model in ABAQUS, on the other hand, can consider not only the nonlinearity in vertical direction but also the nonlinearity in the radial direction. Dynamic effects of pavement responses can be considered only in the finite element software ABAQUS. In this study, two models take dynamic effects into consideration: linear dynamic model and nonlinear dynamic model. By comparing the responses of the typical pavement sections under these models, the levels of computation-related approximation included can be determined.

The surface deflections, critical strains, and remaining lives of the typical pavement section 3-12 PAVE from all models are presented in Table 8.2. Assuming the results from the nonlinear dynamic model are the most accurate ones, the differences in the results of the other models from those of the nonlinear dynamic model are also given in Table 8.2. The approximate computation times of the models are shown in Table 8.3. In terms of adapting a computational model for mechanistic pavement design, one should carefully study Tables 8.2 and 8.3 to balance the model sophistication with the time required for one pavement analysis.

8.3.1 Linear Static Model

In the linear static model, neither the material nonlinearity nor the dynamic effects are considered. The surface deflections are about 8 to 29 percent less than those from the nonlinear dynamic model. For the first three sensors, most of the differences in deflections are from the material nonlinearity. For the other sensors, on the other hand, the differences are mainly from the dynamic effects.

As compared with the nonlinear dynamic model, the critical tensile strain is about 33 percent smaller, and the critical compressive strain is about 21 percent smaller. Correspondingly, the fatigue remaining life and the rutting remaining life are overestimated by 271 percent and 185 percent, respectively.

Table 8.2 - Pavement Responses Under Different Models for “3-12 PAVE”

Model	Surface Deflections (mils)							Critical Strains (micro-strain)		Remaining Lives (10 ³ EASLs)	
	Radial Distance (in.)							Tensile ^[1]	Compressive ^[2]	Fatigue	Rutting
	0	12	24	36	48	60	72				
Linear Static	21.3 (-15) ^[3]	13.1 (-14)	8.4 (-10)	5.8 (-8)	4.1 (-11)	3.0 (-19)	2.3 (-29)	204 (-33)	587 (-21)	1505 (271)	401 (185)
Linear Dynamic	20.6 (-17)	12.9 (-15)	8.4 (-10)	6.0 (-5)	4.5 (-2)	3.6 (-3)	3.0 (-3)	203 (-33)	596 (-20)	1532 (278)	373 (165)
Equivalent – Linear	26.5 (6)	15.6 (2)	8.9 (-4)	5.8 (-7)	4.1 (-11)	3.0 (-20)	2.3 (-27)	282 (-7)	844 (14)	518 (28)	79 (-44)
Nonlinear Static	25.1 (1)	15.1 (-1)	9.0 (-3)	5.9 (-6)	4.1 (-11)	2.9 (-22)	2.2 (-29)	307 (1)	702 (-5)	392 (-3)	120 (28)
Nonlinear Dynamic	24.9	15.2	9.3	6.3	4.6	3.7	3.1	304	764	406	141

[1]: The tangential tensile strain at the bottom of the AC layer.

[2]: The vertical compressive strain at the top of the subgrade.

[3]: Values in the parentheses are percent difference between this quantity and the quantity from nonlinear dynamic model.

Table 8.3 – Approximate Computation Times of Different Models

Models	Computation Time, sec
Linear Elastic (BISAR)	2
Linear Elastic (ABAQUS)	30
Linear Dynamic	600
Equivalent-Linear	120
Nonlinear Static	1500
Nonlinear Dynamic	2400

The computation of the linear static model is very rapid (see Table 8.3). However, without considering material nonlinearity and dynamic effects, the results are far from satisfactory.

8.3.2 Linear Dynamic Model

In the linear dynamic model, the dynamic effects are considered, but the material nonlinearity is not considered. Since the material nonlinearity affects the surface deflections near the load application and the dynamic effects mainly affect the surface deflections at the outer sensors, the last four surface deflections are very close to those from the nonlinear dynamic model. However, the first three surface deflections are 10 to 17 percent less than those from the nonlinear dynamic model.

As compared with the nonlinear dynamic model, the critical tensile strain is 33 percent smaller and the critical compressive strain is 20 percent smaller. Correspondingly, the fatigue remaining life and the rutting remaining life are overestimated by 278 percent and 165 percent, respectively.

The computation of the linear dynamic model is relatively rapid (see Table 8.3). However, the levels of approximation in the critical strains and remaining lives are similar to those in the linear static model, and the results are not satisfactory.

8.3.3 Equivalent-Linear Model

In the equivalent-linear model, the material nonlinearity is taken into consideration in an approximate fashion, while the dynamic effects are not considered. The largest differences in deflections occur at the three outer sensors, 11 to 27 percent smaller than those from the nonlinear dynamic model. The differences in the surface deflections at the first four sensors are small.

The critical tensile strain is 7 percent smaller and the critical compressive strain is 14 percent larger than the results from the nonlinear dynamic model. Part of these differences is attributed to the difference between the programs ABAQUS and BISAR. From Table 8.1, even in the linear static model, the two critical strains from ABAQUS are 9 and 8 percent smaller than those from BISAR. Correspondingly, in the equivalent-linear model, the fatigue remaining life and the rutting remaining life are underestimated by 28 percent and 44 percent, respectively.

The computation of the equivalent-linear model is rapid (see Table 8.3). The levels of approximation in the critical strains and remaining lives are relatively large but, given the state of practice, perhaps acceptable.

8.3.4 Nonlinear Static Model

In the nonlinear static model, the material nonlinearity is taken into consideration, but the dynamic effects are not considered. The largest differences in deflections occur at the three outer sensors, 11 to 29 percent smaller than those from the nonlinear dynamic model. These differences are similar in magnitude to those of the equivalent-linear model.

The critical tensile strain is 1 percent larger, and the critical compressive strain is 5 percent smaller, than the results from the nonlinear dynamic model. Correspondingly, the fatigue remaining life is underestimated by 3 percent, and the rutting remaining life is overestimated by 28 percent.

The results from the nonlinear static model are close to those from the nonlinear dynamic model, in this case, except for the three surface deflections at the outer sensors. However, the computation time of the nonlinear static model shows only a small difference from that of the nonlinear dynamic model (see Table 8.3).

8.3.5 Summary

The following conclusions can be drawn from the results presented in this chapter for the typical pavement sections:

- a. For the linear static algorithms, the surface deflections from ABAQUS and BISAR are close. However, the critical strains and remaining lives from these two programs exhibit some differences.

- b. Without considering the material nonlinearity and the dynamic effects, the results from the linear static model are much different from those for the nonlinear dynamic model.
- c. In the linear dynamic model, the surface deflections at the outer sensors are very close to those for the nonlinear dynamic model. However, the critical strains and remaining lives exhibit significant differences without considering material nonlinearity.
- d. By taking material nonlinearity into consideration with an equivalent-linear model, the critical strains and remaining lives resemble those for the nonlinear dynamic model, given the computation time involved.
- e. The critical strains and remaining lives from the nonlinear static model are very close to those from the nonlinear dynamic model. However, the computation times for both are rather long.

8.4 PARAMETERS TO BE CONSIDERED

In the previous section, the consequences of selecting different models on the accuracy of the estimated deflections, strains and remaining lives were studied. In that section, it was also demonstrated that a balance between the acceptable level of model sophistication and the computational time should be struck. In this section, the results from Chapters 3 through 7 are summarized to develop a matrix of parameters that should be considered for each model. For example, for a linear-elastic static analysis of a thin pavement section, the accurate determination of the thickness of the top layer may not be as critical as it is when a nonlinear static analysis is carried out. The discussion in this section will allow the user to balance the level of sophistication in the model with the field and laboratory effort necessary for an accurate pavement analysis.

The sensitivity of different pavement parameters to the final remaining life due to fatigue cracking is summarized in Tables 8.4 and 8.5 for the thin (3 in.) and thick (5 in.) AC layers, respectively. Depending on the thickness of the AC and base layers as well as the analysis model, more or fewer parameters should be considered. For example, for a linear elastic analysis, the accurate determination of the modulus of the subgrade is not as essential as when the nonlinear analysis is carried out. The reason for this matter is rather obvious. In the nonlinear analysis, the state of the stress of the base is significantly dependent on the modulus of the base and subgrade. The softer the subgrade, the more nonlinearity is experienced by the subgrade.

Similarly, the degree of significance of different parameters as related to rutting is included in Tables 8.6 and 8.7 for thin and thick AC, respectively. Again, these tables are very convenient for determining the level of field and laboratory efforts needed for each analysis method.

In summary, for a realistic analysis, one should very carefully balance the computational time, as shown in Table 8.3, with the field and laboratory efforts needed to obtain the parameters that are sensitive to design with the analysis sophistication of the design software.

Table 8.4 – Summary of Impact of Different Pavement Parameters on Fatigue Cracking Remaining Life of Pavement for Different Analysis Methods (Thin AC Layer)

Model Parameter		Linear Elastic		Equivalent Linear		Non –Linear Static		Non-Linear Dynamic	
		Thin Base (6 in.)	Thick Base (12 in.)	Thin Base (6 in.)	Thick Base (12 in.)	Thin Base (6 in.)	Thick Base (12 in.)	Thin Base (6 in.)	Thick Base (12 in.)
AC	Thickness	S	S	VS	VS	VS	VS		
	Modulus	VS	MS	S	S	NS	VS		
	Poisson's Ratio	NS	NS	NS	NS	VS	NS		
Base	Thickness	VS	S	VS	VS	VS	VS		
	Modulus	VS	VS	S	VS	VS	VS		
	Poisson's Ratio	S	S	NS	NS	MS	MS		
	k_2			S	VS	VS	VS	VS	VS
	k_3			S	VS	VS	VS	VS	VS
Subgrade	Modulus	MS	NS	VS	VS	S	VS		
	Poisson's Ratio	NS	NS	NS	NS	NS	MS		
	k_2			S	NS	MS	MS	S	NS
	k_3			VS	MS	S	MS	VS	MS

Table 8.5 – Summary of Impact of Different Pavement Parameters on Fatigue Cracking Remaining Life of Pavement for Different Analysis Methods (Thick AC Layer)

Model Parameter		Linear Elastic		Equivalent Linear		Non –Linear Static		Non-Linear Dynamic	
		Thin Base (6 in.)	Thick Base (12 in.)	Thin Base (6 in.)	Thick Base (12 in.)	Thin Base (6 in.)	Thick Base (12 in.)	Thin Base (6 in.)	Thick Base (12 in.)
AC	Thickness	VS	VS	VS	VS	VS	VS		
	Modulus	MS	S	VS	VS	VS	VS		
	Poisson's Ratio	MS	MS	MS	MS	VS	S		
Base	Thickness	VS	VS	VS	VS	VS	VS		
	Modulus	VS	VS	NS	S	VS	VS		
	Poisson's Ratio	NS	MS	NS	NS	MS	MS		
	k ₂			NS	S	S	S	VS	VS
	k ₃			MS	VS	S	VS	VS	VS
Subgrade	Modulus	VS	VS	VS	VS	VS	VS		
	Poisson's Ratio	VS	VS	VS	VS	VS	VS		
	k ₂			VS	S	VS	S	S	MS
	k ₃			VS	VS	VS	VS	VS	S

Table 8.6 – Summary of Impact of Different Pavement Parameters on Rutting Remaining Life of Pavement for Different Analysis Methods (Thin AC Layer)

Model Parameter		Linear Elastic		Equivalent Linear		Non-Linear Static		Non-Linear Dynamic	
		Thin Base (6 in.)	Thick Base (12 in.)	Thin Base (6 in.)	Thick Base (12 in.)	Thin Base (6 in.)	Thick Base (12 in.)	Thin Base (6 in.)	Thick Base (12 in.)
AC	Thickness	VS	VS	VS	VS	VS	VS		
	Modulus	S	S	VS	VS	VS	S		
	Poisson's Ratio	MS	NS	S	MS	S	MS		
Base	Thickness	S	S	S	VS	S	VS		
	Modulus	VS	VS	MS	S	VS	S		
	Poisson's Ratio	MS	S	NS	NS	S	NS		
	k_2			NS	S	VS	VS	NS	MS
	k_3			MS	S	VS	VS	S	S
Subgrade	Modulus	S	NS	S	S	VS	VS		
	Poisson's Ratio	NS	NS	NS	NS	MS	NS		
	k_2			NS	NS	MS	NS	MS	NS
	k_3			MS	NS	MS	NS	MS	NS

Table 8.7 – Summary of Impact of Different Pavement Parameters on Rutting Remaining Life of Pavement for Different Analysis Methods (Thick AC Layer)

Model Parameter		Linear Elastic		Equivalent Linear		Non –Linear Static		Non-Linear Dynamic	
		Thin Base (6 in.)	Thick Base (12 in.)	Thin Base (6 in.)	Thick Base (12 in.)	Thin Base (6 in.)	Thick Base (12 in.)	Thin Base (6 in.)	Thick Base (12 in.)
AC	Thickness	VS	VS	VS	VS	VS	VS		
	Modulus	VS	VS	VS	VS	VS	VS		
	Poisson's Ratio	S	MS	S	MS	S	MS		
Base	Thickness	VS	VS	VS	VS	VS	VS		
	Modulus	S	VS	NS	MS	MS	S		
	Poisson's Ratio	NS	MS	NS	NS	MS	S		
	k ₂			NS	NS	MS	S	VS	VS
	k ₃			NS	MS	NS	MS	S	VS
Subgrade	Modulus	VS	VS	VS	VS	VS	VS		
	Poisson's Ratio	VS	VS	VS	VS	VS	VS		
	k ₂			S	S	S	S	MS	MS
	k ₃			VS	VS	VS	VS	VS	S

CHAPTER NINE

SUMMARY, CONCLUSIONS AND RECOMMENDATIONS

9.1 SUMMARY

Nondestructive testing techniques are widely used as tools for measuring the stiffness parameters of pavement sections. The moduli of pavement materials obtained in that manner are used to determine the critical strains and, thus, to estimate the remaining lives of pavement systems.

Two nondestructive testing devices, the Falling Weight Deflectometer (FWD) and the Seismic Pavement Analyzer (SPA), are considered. The FWD applies an impulse load to the pavement, and seven sensors measure the surface deflections of the pavement. The moduli of pavement layers can be obtained from these deflections using a backcalculation program. Since the load applied by the FWD to the pavement is similar to that exerted by traffic, the FWD moduli can be used in pavement design and analysis without considering the nonlinear behavior of materials. The operating principle of the SPA is based on generating and detecting stress waves in a layered medium. Elastic moduli of different layers can be obtained through an inversion process from the SPA. Seismic moduli from the SPA are similar to the linear elastic ones since they correspond to very small external loads. It is essential to have a constitutive model that considers nonlinear behavior of pavement materials and, thus, relates the FWD modulus with the SPA modulus.

In this study, a constitutive model that relates the nonlinear modulus of a pavement material with its state of stress was used. The seismic moduli can be input into this model to calculate nonlinear moduli under any other loading regime.

Several computation algorithms were used to implement the constitutive model. These algorithms are based on an equivalent-linear static model, a nonlinear static model, and a nonlinear dynamic model. An equivalent-linear model is a model that, in an approximate fashion, can consider the load-induced nonlinear behavior based on the static linear elastic layered theory. An iterative process is employed to consider the nonlinearity of the pavement materials. The nonlinear static model is carried out by the comprehensive finite element software ABAQUS. In the nonlinear static model, the nonlinearity of each element is considered

separately. The dynamic effects can also be investigated in ABAQUS. The nonlinear dynamic model considers both the nonlinear and the dynamic behavior of pavement materials.

Four typical pavement sections were assumed in this study. The pavement response under a linear elastic model was studied first. The impact of various pavement parameters on the critical strains and on the remaining lives were explored.

In the equivalent-linear and nonlinear algorithms, the pavement responses were investigated by assuming the base and the upper part of the subgrade exhibited load-induced nonlinear behavior. The sensitivity study of the pavement response to the variations of the nonlinear parameters was conducted. By comparing the responses of the four pavement sections under different algorithms, the impact of material nonlinearity was investigated.

The impact of the dynamic nature of the imparted load on pavement response is another concern. By assuming the external load has the shape of a haversine, the pavement response under a linear dynamic model and a nonlinear dynamic model was studied. The influences of the system damping and the material densities on the degree of dynamic effects were also studied. Finally, the levels of approximation in the responses of typical pavement sections associated with different models are compared.

9.2 CONCLUSIONS

Five sets of conclusions can be drawn.

- (1) From the linear elastic models:
 - (a) The surface deflections from the programs BISAR and ABAQUS are similar. However, the critical strains and remaining lives from these two programs are not as close.
 - (b) The sensitivity of the critical strains and remaining lives changes with the thickness of the AC layer or the base. However, this impact is relatively small since in many cases the sensitivity level keeps unchanged.
 - (c) The modulus of the base significantly impacts the magnitudes of the critical tensile strain and fatigue remaining life, which are also sensitive to the variations in the thickness and modulus of the AC and thickness of the base. However, the strength parameters of the subgrade are insignificant to the critical tensile strain and fatigue remaining life.
 - (d) The compressive strain and rutting remaining life are very sensitive to the thickness of the AC, the thickness and modulus of the base, and the modulus and Poisson's ratio of the subgrade. The modulus of the AC is of secondary importance. The Poisson's ratios of the AC and base do not impact the compressive strain and rutting remaining life.
 - (e) The depth to bedrock does not have a direct impact on the critical strains and remaining lives, but it has significant impact on surface deflections if the bedrock is not very deep. If the depth to bedrock is not considered in a backcalculation process, the critical strains and remaining lives may be considerably wrong.

(2) From the equivalent-linear model:

- (a) To adequately model nonlinear behavior of base, three to five sublayers in the typical pavement sections are adequate.
- (b) The sensitivity of the critical strains and remaining lives to nonlinear parameters changes with the thickness of the AC layer or the base.
- (c) The thickness of the AC; the thickness, modulus and nonlinear parameters k_2 and k_3 of the base; and the modulus of the subgrade are significant to the critical tensile strain and fatigue remaining life. The modulus of the AC and the nonlinear parameter k_3 of the upper subgrade are of less importance. However, the Poisson's ratios of all layers and the nonlinear parameter k_2 of the subgrade are insignificant to the critical tensile strain and fatigue remaining life.
- (d) The compressive strain and rutting remaining life are very sensitive to variations in the thickness of the AC, the thickness and k_3 of the base, and the modulus, Poisson's ratio and parameter k_3 of the subgrade. The modulus of the AC and the modulus and parameter k_2 of the base are of secondary importance. The Poisson's ratios of the AC and base are insignificant to the compressive strain and rutting remaining life.
- (e) The depth to bedrock does not have a direct impact on the critical strains and remaining lives, but it has significant impact on surface deflections if the bedrock is not very deep.

(3) From the nonlinear static model:

- (a) The thickness of the AC or base layer has a relatively large impact on the sensitivity of the critical strains and remaining lives to the variation of nonlinear parameters of the base and subgrade.
- (b) The thickness of the AC; the thickness, modulus and nonlinear parameters k_2 and k_3 of the base; and the modulus of the subgrade are significant to the critical tensile strain and fatigue remaining life. The modulus of the AC, the Poisson's ratio of the base, and the Poisson's ratio and nonlinear parameters k_2 and k_3 of the upper subgrade are of less importance. However, the Poisson's ratio of the AC is insignificant to the critical tensile strain and fatigue remaining life.
- (c) The compressive strain and rutting remaining life are very sensitive to variations in the thickness and modulus of the AC, the thickness, modulus and k_3 of the base, and the modulus, Poisson's ratio and parameter k_3 of the subgrade. The Poisson's ratio of the AC, the parameter k_2 of the base, and the parameter k_2 of the upper subgrade are of secondary importance. The Poisson's ratio of the base is insignificant to the compressive strain and rutting remaining life.

(4) From the dynamic models:

- (a) The damping characteristics of a pavement system have little influence on critical strains and pavement remaining lives. However, they have some influence on the surface deflections at the outer sensors. Therefore, if a dynamic algorithm is used for backcalculation, special attention should be paid when selecting the damping parameters.

- (b) The densities of pavement layers have little impact on the pavement responses.
 - (c) The dynamic nature of the load impacts more significantly when the FWD sensors are farther away from the impact.
 - (d) In the nonlinear dynamic model, parameters k_2 and k_3 of the base are significant in the critical strains and remaining lives. Parameters k_2 and k_3 have some influence on the critical compressive strain and the rutting remaining life, but they have little impact on the critical tensile strain and the fatigue remaining life.
- (5) The following conclusions can be drawn from the comparison among all models:
- (a) In the linear static models, the surface deflections of a typical pavement section obtained from ABAQUS and BISAR are close. However, the critical strains and remaining lives from these two programs exhibit some differences.
 - (b) Without considering material nonlinearity and dynamic effects, the results for the linear static model are much different from those for the nonlinear dynamic model.
 - (c) In the linear dynamic model, the surface deflections at the outer sensors are very close to those for the nonlinear dynamic model. However, without considering material nonlinearity, the critical strains and remaining lives are overestimated.
 - (d) By taking material nonlinearity into consideration in the equivalent-linear model, the critical strains and remaining lives are somewhat close to those from the nonlinear dynamic model. The computation time associated with the equivalent-linear algorithm is much shorter when compared to that for the nonlinear algorithms.
 - (e) The critical strains and remaining lives for the nonlinear static model are very close to those for the nonlinear dynamic model. However, the computation times of both of them are rather long.

9.3 RECOMMENDATIONS

Project 0-1780 is an initial step toward relating the seismic moduli with moduli that can be used in pavement design and analysis. The recommendations for future work are:

- (1) The variation in the modulus of the AC layer is not considered in this research. The impacts of temperature and load frequency on the modulus of the AC layer need to be incorporated into the models.
- (2) In the dynamic models, the load is assumed to have a halfsine distribution and a duration of 30 msec. The investigation of different load time histories and load durations can help one to understand, more completely, the impact of the dynamic nature of the applied load on the pavement response.
- (3) The feasibility of relating seismic moduli with the FWD moduli and the various models should be validated with field data.
- (4) The constitutive model presented in Equation 3.16 is adopted. Other constitutive models considering material nonlinearity should be considered in order to compare effects of different constitutive models.

REFERENCES

1. Asphalt Institute (1982), Research and Development of The Asphalt Institute's Thickness Design Manual (MS-1), 9th ed., Research Report 82-2, Asphalt Institute.
2. Anderson, D. G., and Woods, R. D. (1975), "Comparison of Field and Laboratory Shear Modulus," proceedings, In Situ Measurement of Soil Properties, ASCE, Vol I, Rayleigh, NC, pp. 218-232.
3. Ang, A. H-S, and Tang, W. H. (1984a), Probability Concepts in Engineering Planning and Design, Vol. I – Basic Principles, Wiley and Sons Inc., New York.
4. Ang, A. H-S, and Tang, W. H. (1984b), Probability Concepts in Engineering Planning and Design, Vol. II – Decision, Risk, and Reliability, Wiley and Sons Inc., New York.
5. Aouad, M. F. (1993), "Evaluation of Flexible Pavements and Subgrades Using the Spectral-Analysis-of-Surface-Waves (SASW) Method," Ph.D. Dissertation, The University of Texas at Austin.
6. Aouad, M. F., Stokoe, K. H., and Briggs, R. C. (1993), "Stiffness of Asphalt Concrete Surface Layer from Stress Wave Measurements," Transportation Research Record 1384, Washington, D.C., pp. 29-35.
7. Barksdale, R. D., Alba, J., Khosla, P. N., Kim, R., Lambe, P. C. and Rahman, M. S. (1994), "Laboratory Determination of Resilient Modulus for Flexible Pavement Design," Interim Report Project 1-28, Federal Highway Administration, Washington, D.C.
8. Boussinesq, J. (1885), Application des Potentiels a l'Etude de l'Equilibre et du Mouvement des Solids Elastiques, Gauthier-Villars, Paris.
9. Brown, S. F. (1996), "Soil Mechanics in Pavement Engineering," Geotechnique, Vol 46., No. 3, pp. 383-426.
10. Burmister, D. M. (1943), "The Theory of Stresses and Displacements in Layered Systems and Applications to the Design of Airport Runways," Highway Research Board, Vol. 23.
11. Burmister, D. M. (1945), "The General Theory of Stresses and Displacements in Layered Soil Systems," Journal of Applied Physics, Vol. 16, pp. 84-94, 126-127, 296-302.
12. Bush, A. J. (1980), "Development of the Nondestructive Testing for Light Aircraft Pavements," Phase I, Evaluation of NDT Device Report No. FAA-RD-80-9, Washington, D.C.
13. Daniel, J. S. and Kim, Y. R. (1998), "Relationships Among Rate-Dependent Stiffnesses of Asphalt Concrete Using Laboratory and Field Test Methods," Transportation Research Record, Washington D.C.

14. De Jong, D. L., Peatz, M. G. F., and Korswagen, A. R. (1973), "Computer Program Bisar Layered Systems Under Normal and Tangential Loads," Konin Klijke Shell-Laboratorium, External Report AMSR.0006.73, Amsterdam.
15. Dempsey, B. J. (1982), "Laboratory and Field Studies of Channeling and Pumping," Transportation Research Record 849, TRB, Washington D. C., pp 1-12.
16. Dobry, R., and Gazetas, G. (1986), "Dynamic Response of Arbitrary Shaped Foundations," Journal of Geotechnical Engineering, ASCE, Vol. 112, No. 2, New York, NY, pp. 109-35.
17. Foster, C. R., and Ahlvin, R. G. (1954), "Stresses and Deflections Induced by a Uniform Circular Load," Proceedings, Highway Research Board, Vol. 33, pp. 467-470.
18. Hardin, B. O. and Drnevich, V. P. (1972), "Shear Modulus and Damping in Soils: Design Equations and Curves," Journal of Soil Mechanics and Foundations Division, ASCE, Vol. 98, No. SM7, New York, NY, pp. 667-692.
19. Hicks, R. G., and Monismith, C. L. (1972), "Prediction of Resilient Response of Pavements Containing Granular Layers Using Nonlinear Elastic Theory," Proceedings, The Third International Conference on the Structure Design of Asphalt Pavement, London, England.
20. Hoffman, M. S., and Thompson, M. R. (1982), "Comparative Study of Selected Nondestructive Testing Devices," Transportation Research Record 852, Washington D.C., pp. 32-41.
21. Hou, Y. (1977), "Evaluation of Layered Material Properties from Measured Surface Deflections," Ph.D. Dissertation, University of Utah.
22. Huang, Y. H. (1994), Pavement Analysis and Design, Prentice Hall, Inc., Englewood Cliffs, NJ, 805p.
23. Ioannides, A. M. (1990), "Dimensional Analysis in NDT Rigid Pavement Evaluation," Journal of Transportation Engineering, ASCE, Vol. 116, No. 1, New York, NY, pp. 23-36.
24. Jones, A. (1962), "Tables of Stresses in Three-Layer Elastic Systems," Highway Research Board 342, pp. 176-214.
25. Kim, Y. R. and Lee, Y. C. (1995), "Interrelationships among Stiffnesses of Asphalt Aggregate Mixtures," Journal of Association of Asphalt Paving Technologists, Vol. 64, pp. 575-609.
26. Kramer, S. L. (1996), Geotechnical Earthquake Engineering, Prentice Hall, Inc., Upper Saddle River, California, pp. 232-240.
27. Li, Y. and Nazarian, S. (1994), "Evaluation of Aging of Hot-Mix Asphalt Using Wave Propagation Techniques," Proceedings, Engineering Properties of Asphalt Mixtures And the Relationship to Their Performance, ASTM STP 1265, Philadelphia, PA, pp.166-179.
28. Lytton, R. L., Roberts, R. L., and Stoffels, S. (1985), "Determination of Asphaltic Concrete Pavement Structural Properties by Nondestructive Testing," NCHRP Report No. 10-27, Texas A & M University, College Station, Texas.
29. Lytton, R. L., and Michalak, C. H. (1979), "Flexible Pavement Deflection Evaluation Using Elastic Moduli and Field Measurements," Research Report 207-7F, Texas Transportation Institute, Texas A & M University, College Station, Texas.
30. Lytton, R. (1989), "Backcalculation of Pavement Layer Properties," Proceedings, Nondestructive Testing of Pavements and Backcalculation of Moduli, ASTM, STP 1026, Philadelphia.

31. Miller, G. F., and Pursey, H. (1955), "On the Partition of Energy Between Elastic Waves in a Semi-Infinite Solid," Proceeding, International Conference on Microzonation for Safer Construction: Research and Application, Society of Exploration Geophysicists, Seattle, WA, Vol. 2, pp. 545-558.
32. Nazarian, S. and Desai, M. R. (1993), "Automated Surface Wave Method: Field Testing," Journal of the Geotechnical Engineering Division, ASCE, Vol. 119, No. GT7, New York, NY, pp. 1094-1111.
33. Nazarian, S., Yuan D. and Baker M. R. (1995), "Rapid Determination of Pavement Moduli with Spectral-Analysis-of-Surface-Waves Method," Research Report 1243-1F, Center for Geotechnical and Highway Materials Research, The Univ. of Texas at El Paso, El Paso, TX, 76 p.
34. Nazarian, S., Abdallah, I., Yuan, D., and Ke, L. (1998), "Design Modulus Values Using Seismic Data Collection," Research Report 1780-1, the Center for Highway Materials Research, the University of Texas at El Paso, 17 p., 31 p., pp. 42-53.
35. Odemark, N. (1949), Investigation as to the Elastic Properties of Soil Design of Pavements According to the Theory of Elasticity, Statens Valginstut, Stockholm, Sweden.
36. Peattie, K. R. (1962), "Stress and Strain Factors for Three-Layer Elastic System," Bulletin 342, Highway Research Board, pp. 215-253.
37. Raad, L., and Figueroa, J.L. (1980), "Load Response of Transportation Support Systems," Journal of Transportation Engineering, ASCE, Vol. 106, No. TE1, New York, NY, pp. 111-128.
38. Richardson, M.H, and Formenti, D. L. (1982), "Parameter Estimation from Frequency Response Measurements Using Rational Fraction Polynomials." Proceedings, First International Model Analysis Conference, Society for Experimental Mechanics, Orlando, FL, pp. 167-181.
39. Rojas, J. (1999), "Quality Management of Asphalt Concrete Layers Using Wave Propagation Techniques," MS Thesis, The University of Texas at El Paso, 54 p.
40. Sansalone, M., and N. J. Carino (1986). "Impact-Echo: A Method for Flaw Detection in Concrete Using Transient Stress Waves." Report NBSIR 86-3452. National Bureau of Standards, Gaithersburg, MD.
41. Scrivner, F.H., Michalak, C.H., and Moore, W.H. (1973), "Calculation of Elastic Moduli of a Two-Layered Pavement System from Measured Surface Deflections," Highway Research Record No. 431, Highway Research Board, Washington, D.C., pp. 54.
42. Shahriyar, B. (1991), "Evaluation of Piezo-Ceramic Bender Elements for Measuring Low-amplitude Shear Modulus of Various Soils," MS Thesis, The University of Texas at El Paso, pp. 75-162.
43. Siddharthan, R., Norries, G. M., and Epps, J. A. (1991), "Use of FWD Data for Pavement Material Characterization and Performance," Journal of Transportation Engineering, ASCE, Vol. 117, No. 6, New York, NY, pp. 660-678.
44. Sousa, J. B. and Monismith, C. L. (1988), "Dynamic Response of Paving Materials," Transportation Research Record 1136, TRB, Washington, D.C., pp. 57-68.
45. Swift, G. (1973), "Graphical Technique for Determining Elastic Moduli of Two Layered Structure from Measured Surface Deflections," Highway Research Record 432, Washington D.C.

46. Swift, G. (1972), "An Empirical Equation for Calculating Deflections on the Surface of Two-Layer Elastic Pavement System," Texas Transportation Institute Report 136-4, Texas A & M University, College Station, TX.
47. Uddin, W., Meyer, A. H., and Hudson, W. R. (1983), "Rigid Bottom Considerations for Nondestructive Evaluation of Pavement," Transportation Research Record 1007, Washington, D.C.
48. Uddin, W., and McCullough, B. F. (1989), "In Situ Material Properties from Dynamic Deflection Equipment," Nondestructive Testing of Pavements and Backcalculation of Moduli, ASTM, STP 1026, Philadelphia.
49. Ullidtz, P. (1987), Pavement Analysis, Elsevier, Amsterdam.
50. Ullidtz, P., and Peattie, K. R. (1980), "Pavement Analysis by Programmable Calculators," Journal of Transportation Engineering, ASCE, Vol. 106, No. TE5, New York, NY, pp. 581-598.
51. Uzan, J., R. L. Lytton, and Germann, F. P. (1989), "General Procedure for Backcalculating Layer Moduli," STP 1026, ASTM, Philadelphia, PA, pp. 217-228.
52. Uzan, J., and Lytton, R. L. (1990), "Analysis of Pressure Distribution Under Falling Weight Deflectometer Loading," Journal of Transportation Engineering, ASCE, Vol. 116, No. 2, New York, NY, pp. 246-251.
53. Uzan, J. (1994), "Advanced Backcalculation Techniques," ASTM, STP 1198, Philadelphia, PA, pp. 3-37.
54. Van Cauwelaert, F. J., Alexander, D. R., White, T. D., and Baker, W. R. (1989). "Multilayer Elastic Program for Backcalculating Layer Moduli in Pavement Evaluation," ASTM, STP 1026, Philadelphia, PA, pp.171-188.
55. Von Quintus H. L. and Kilingsworth, B. M. (1998), "Comparison of Laboratory and Insitu Determined Elastic Layer Moduli," presented in 77th Annual TRB Meeting, Washington, D.C.
56. Yuan, D. and Nazarian, S. (1993), "Automated Surface Wave Testing: Inversion Technique," Journal of Geotechnical Engineering, ASCE, Vol. 119, No. GT7, New York, NY, pp. 1112-1126.
57. Westergaard, H. M. (1926), "Stresses in Concrete Pavements Computed by Theoretical Analysis," Public Roads, Vol. 7, pp. 25-35.
58. Willis, M. E. and Toksoz, M. N. (1983), "Automatic P and S Velocity Determination from Full Wave Form Digital Acoustic Logs," Geophysics, Vol. 48, No. 12, pp. 1631-44.

APPENDIX A
RESULTS OF SENSITIVITY STUDY
UNDER LINEAR STATIC MODEL

1) Thickness of the AC layer

Original value: 3 in. (75mm)

Variation range: 2.25 in. (56mm) to 3.75 in. (94 mm)

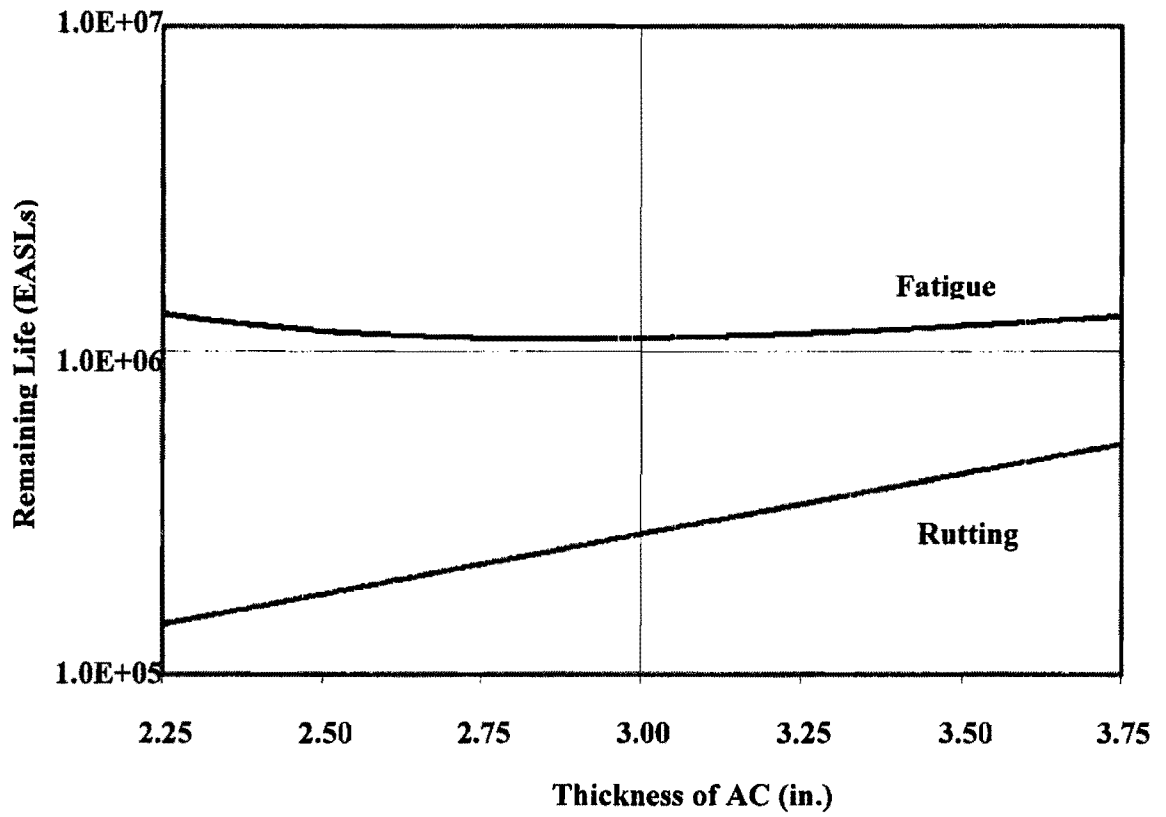


Figure A.1.1 – Variations in Remaining Lives

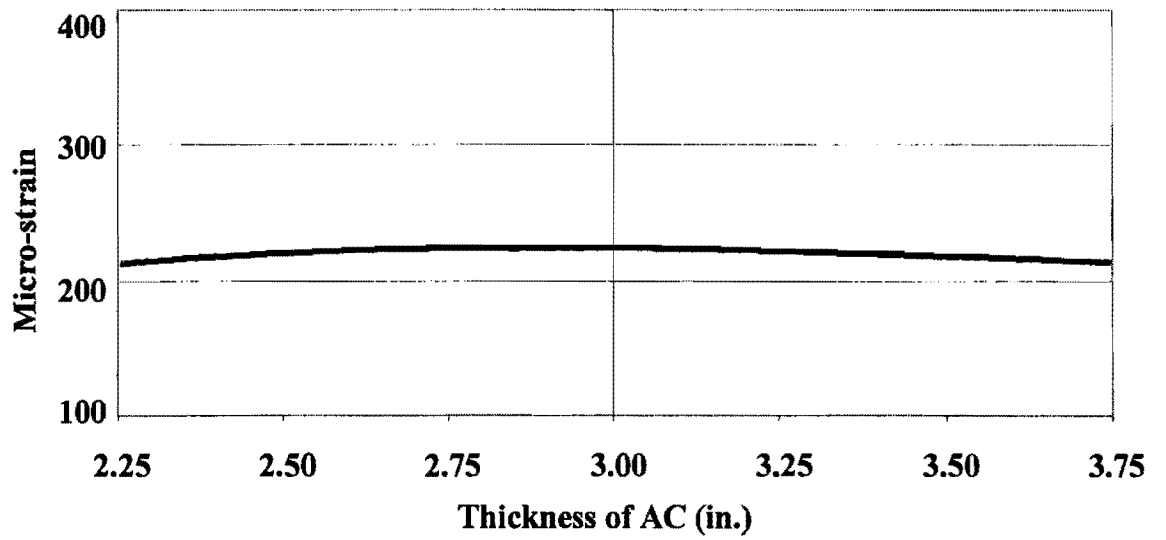


Figure A.1.2 – Variation in Critical Tensile Strain

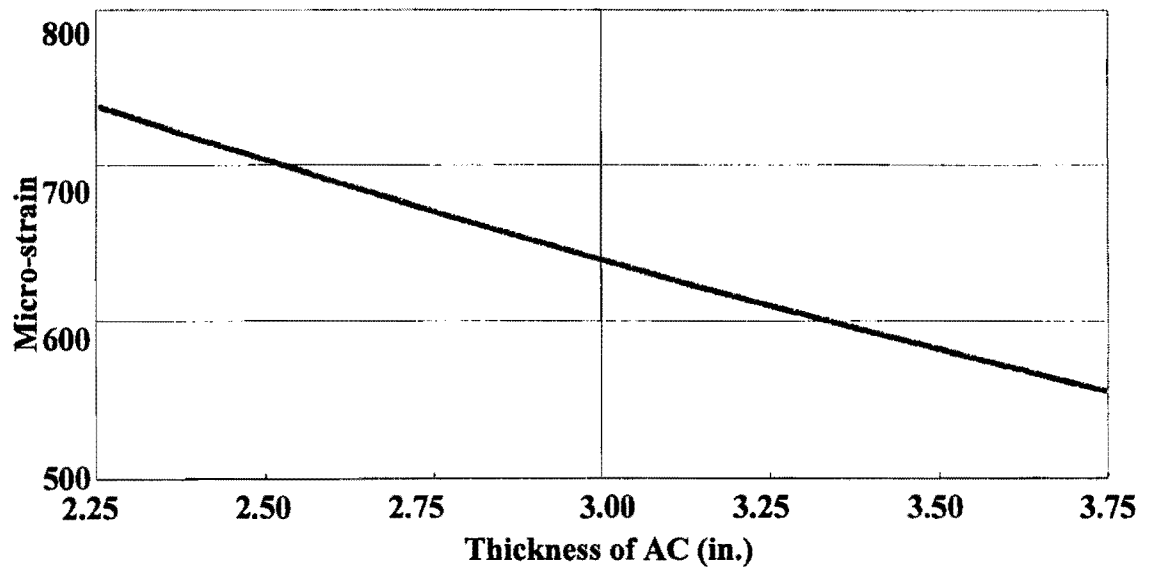


Figure A.1.3 – Variation in Critical Compressive Strain

2) Modulus of AC

Original value: 500 ksi (3450 MPa)

Variation range: 375 ksi (2590MPa) to 625 ksi (4310 MPa)

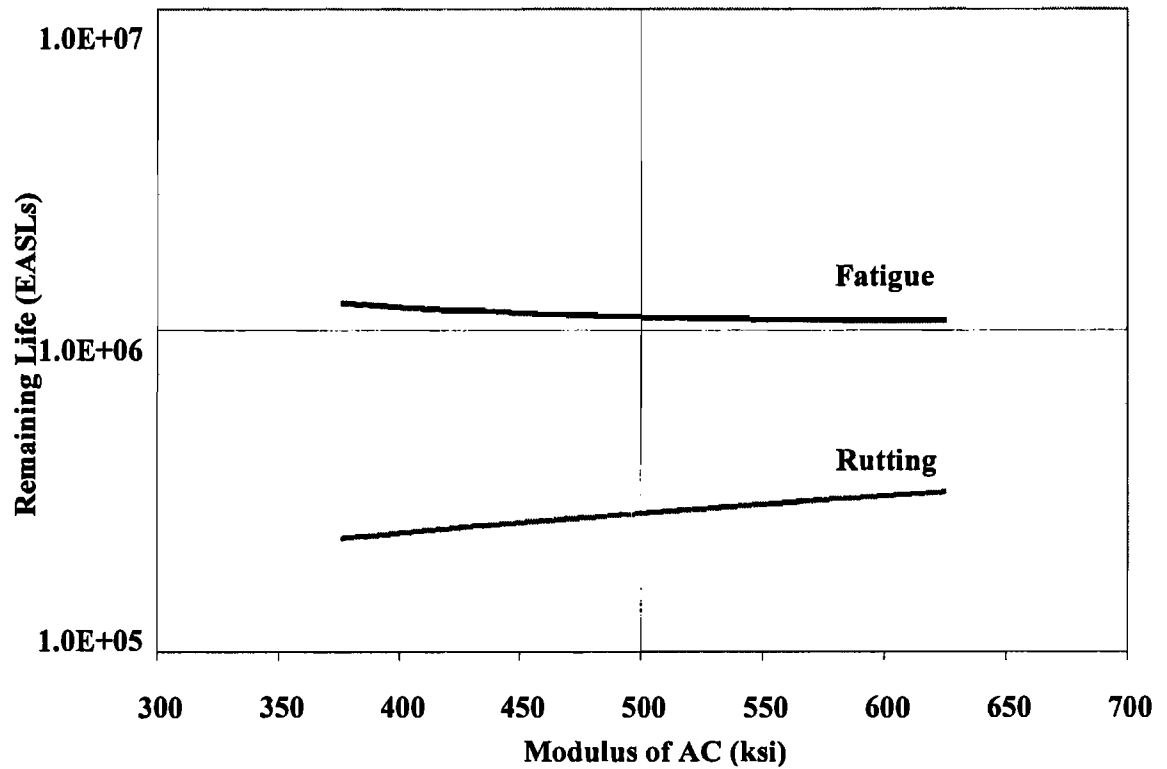


Figure A.2.1 – Variations in Remaining Lives

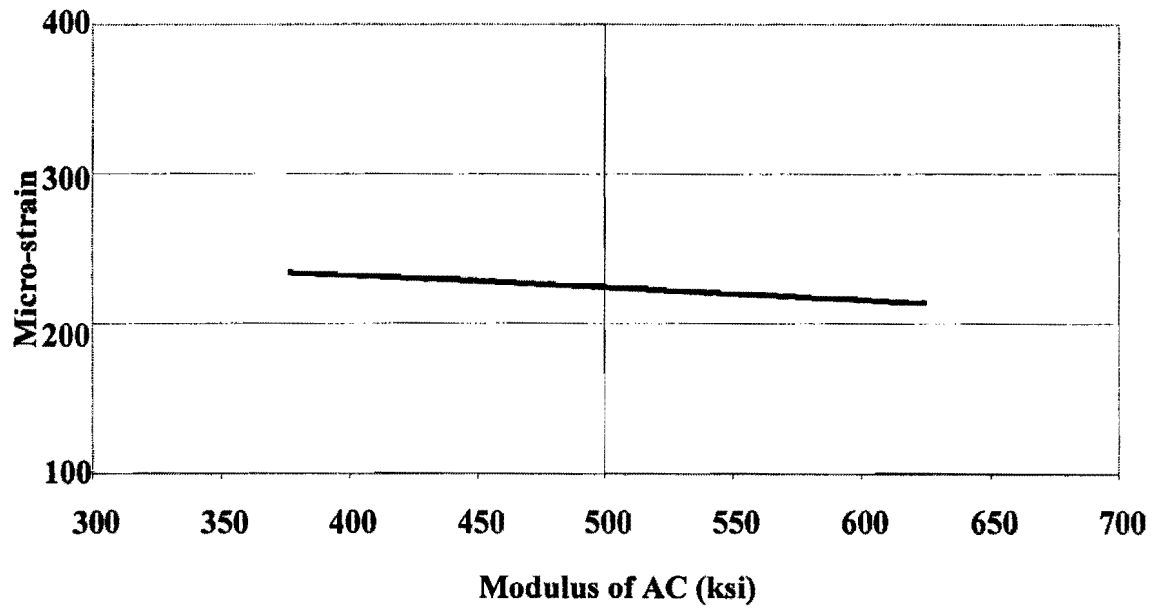


Figure A.2.2 – Variation in Critical Tensile Strain

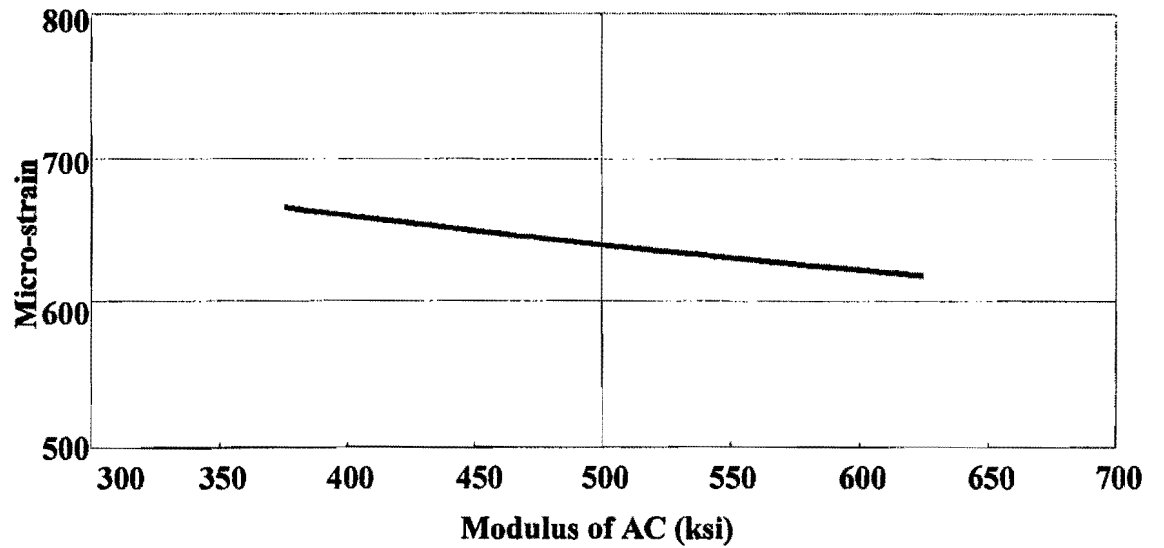


Figure A.2.3 – Variation in Critical Compressive Strain

3) Poisson's ratio of the AC layer

Original value: 0.35

Variation range: 0.2625 to 0.4375

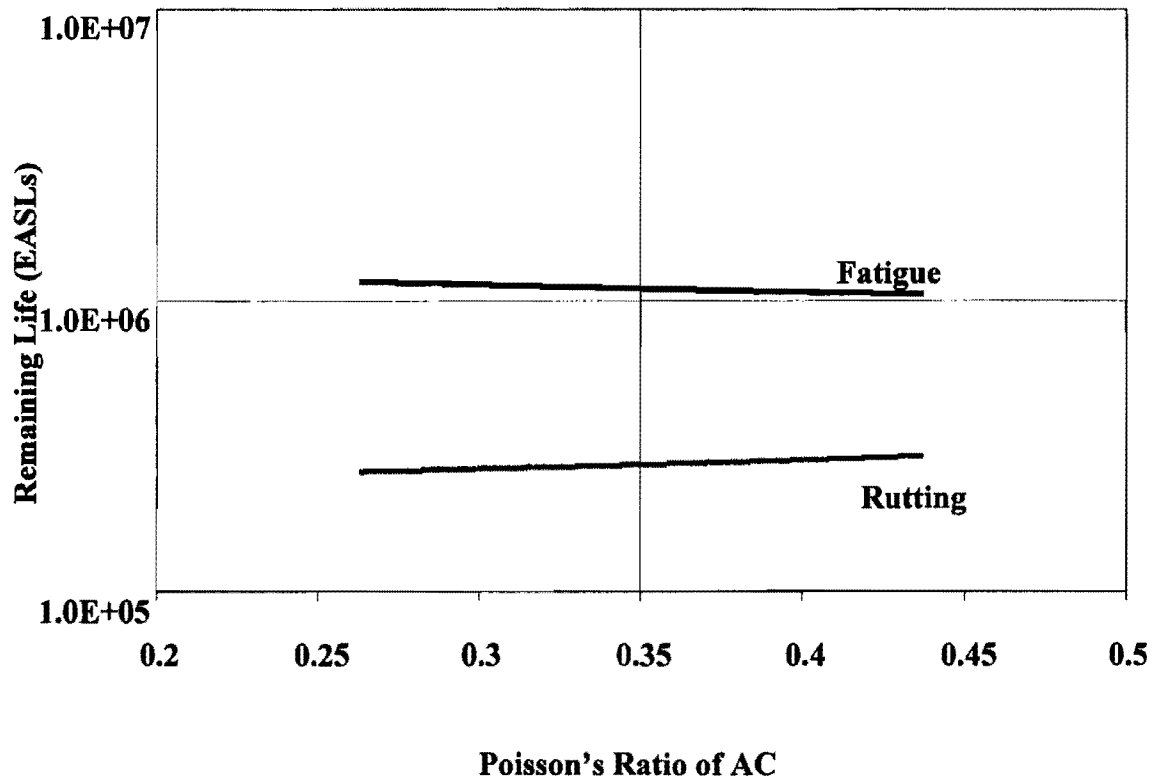


Figure A.3.1 – Variations in Remaining Lives

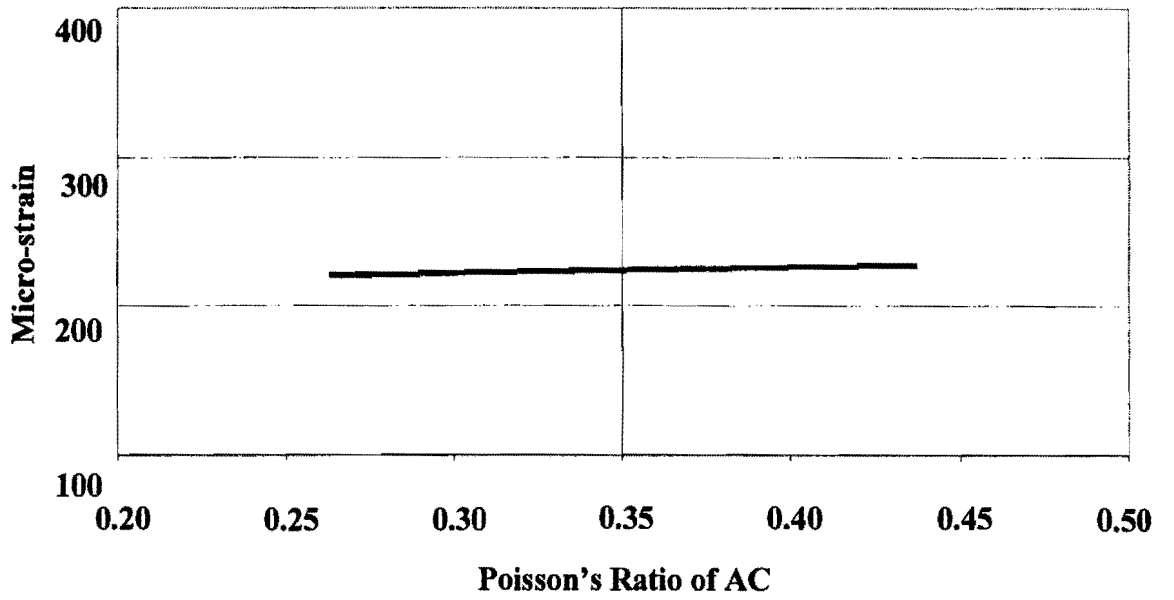


Figure A.3.2 – Variation in Critical Tensile Strain

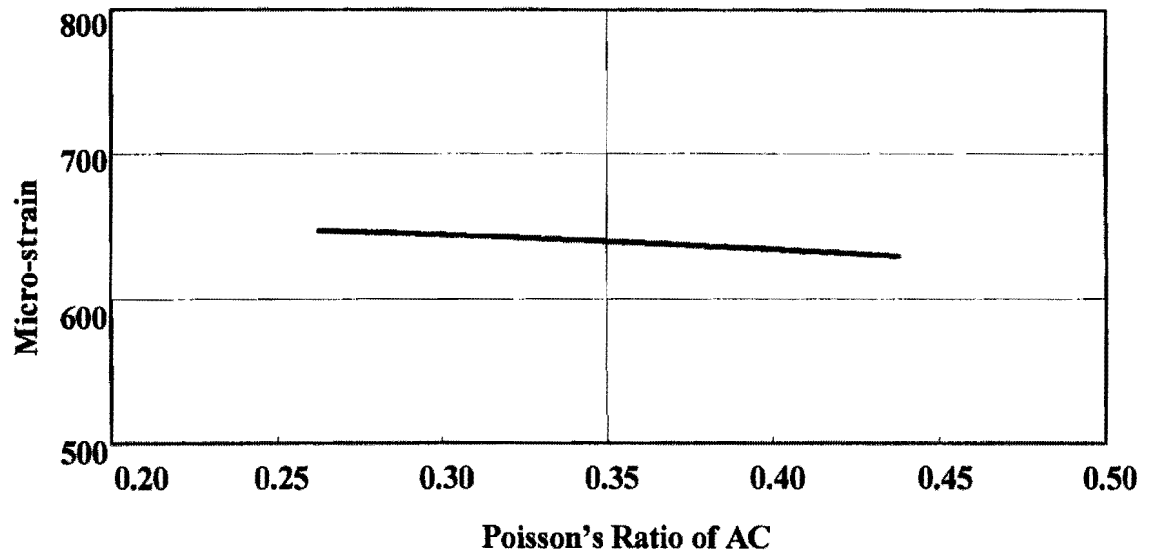


Figure A.3.3 – Variation in Critical Compressive Strain

4) Thickness of the base

Original value: 12 in. (300mm)

Variation range: 9 in. (225mm) to 15 in. (375mm)

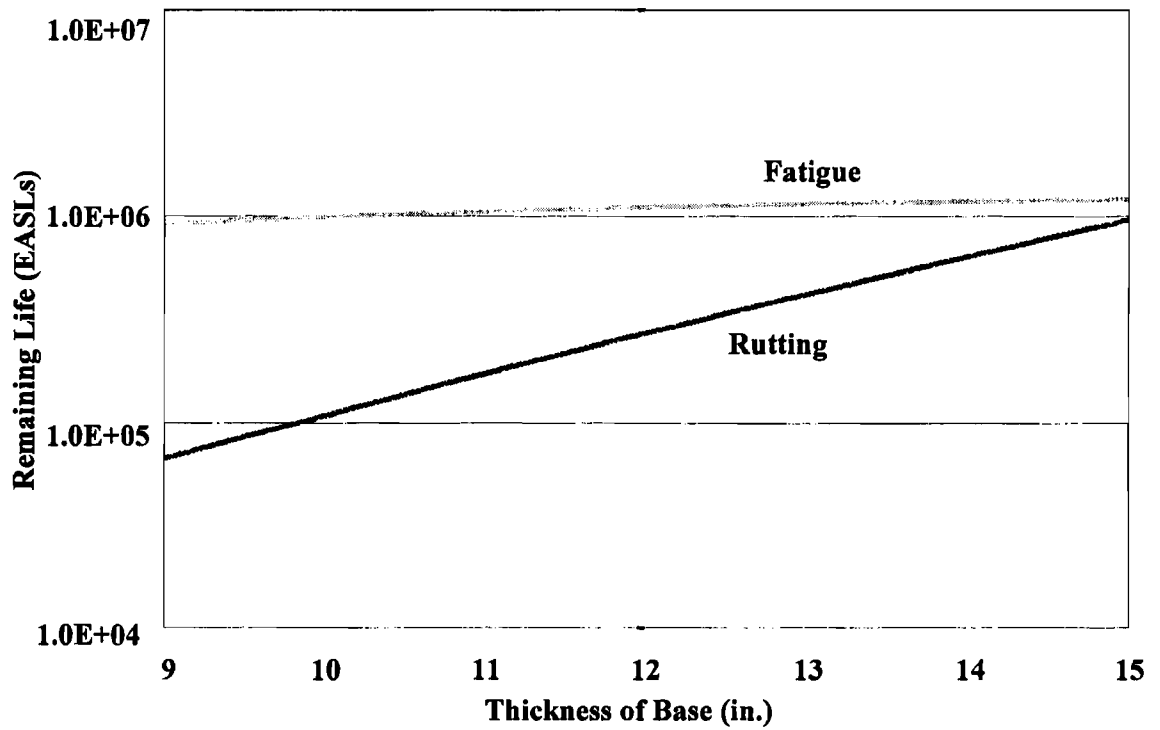


Figure A.4.1 – Variations in Remaining Lives

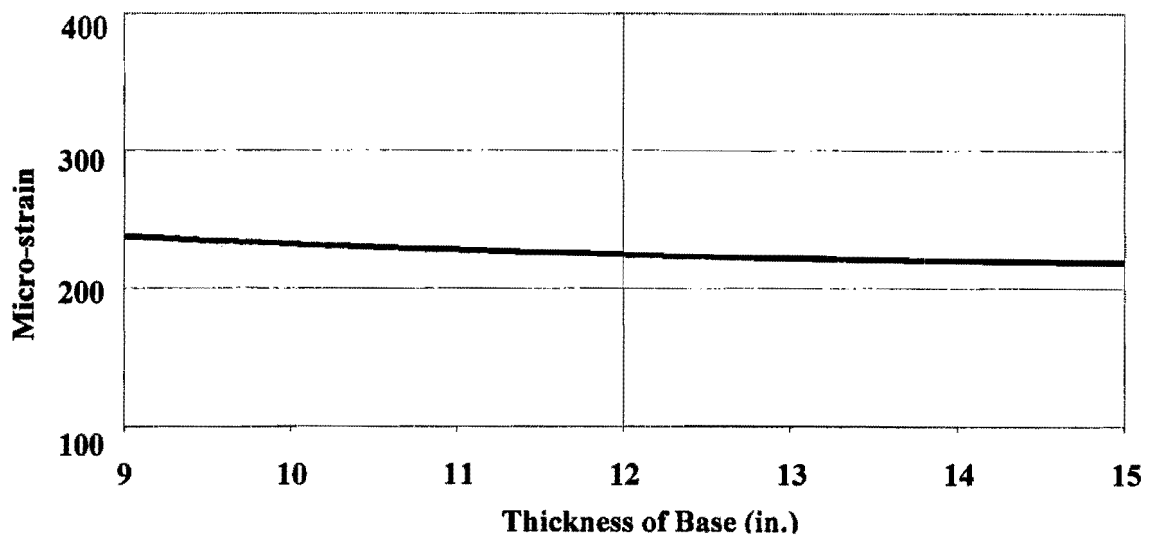


Figure A.4.2 – Variation in Critical Tensile Strain

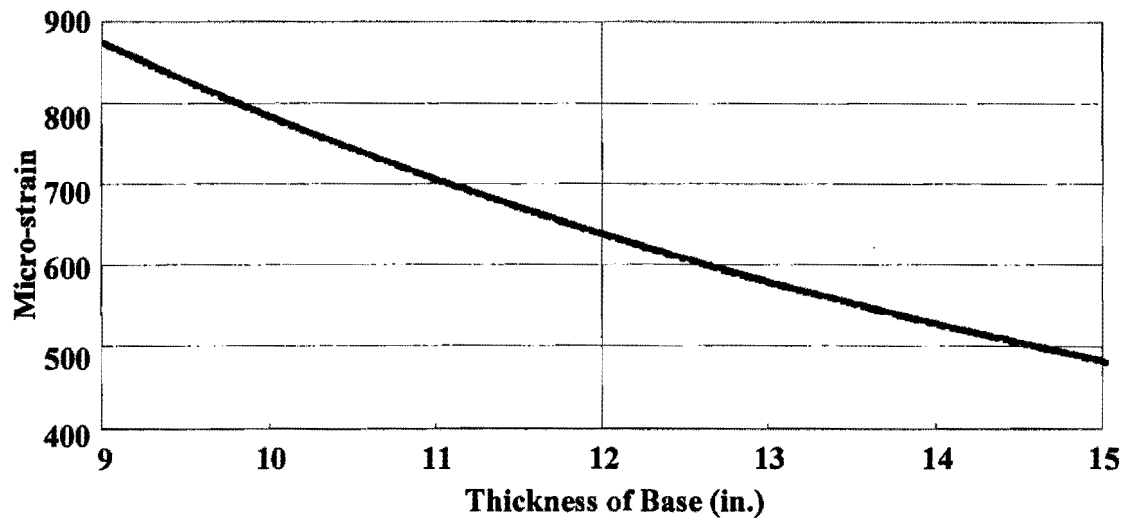


Figure A.4.3 – Variation in Critical Compressive Strain

5) Modulus of Base

Original value: 50 ksi (345MPa)

Variation range: 37.5 ksi (260MPa) to 62.5 ksi (430 MPa)

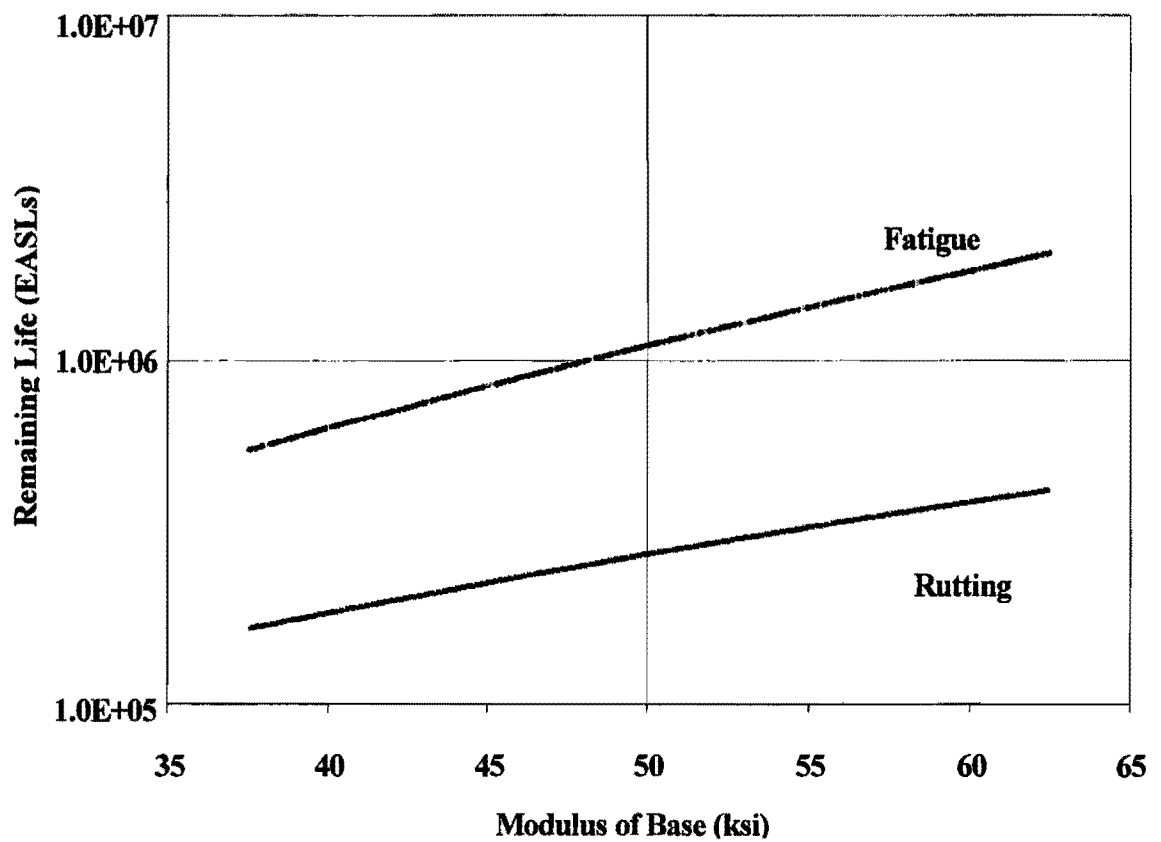


Figure A.5.1 – Variations in Remaining Lives

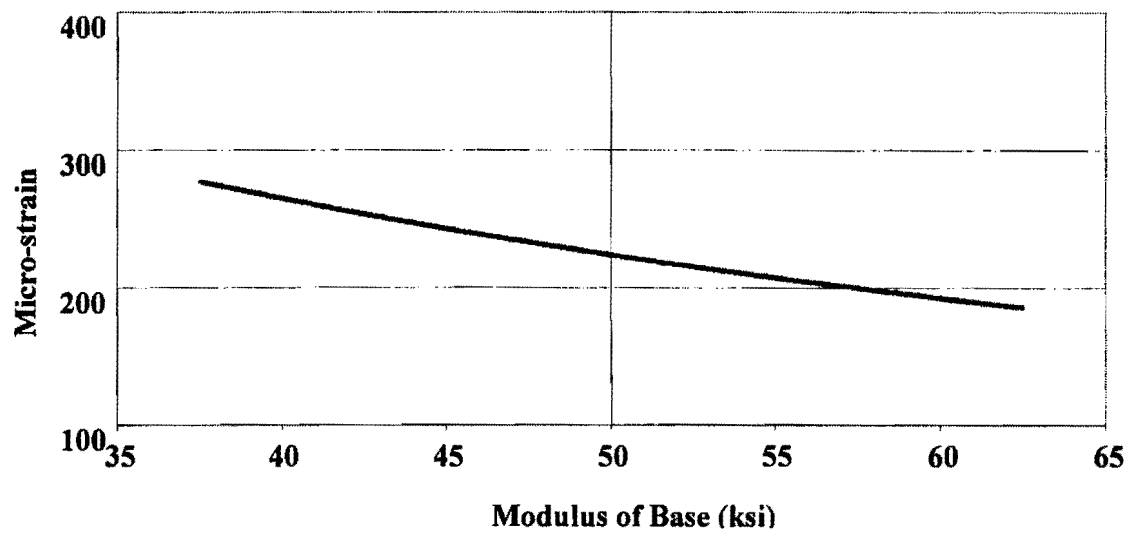


Figure A.5.2 – Variation in Critical Tensile Strain

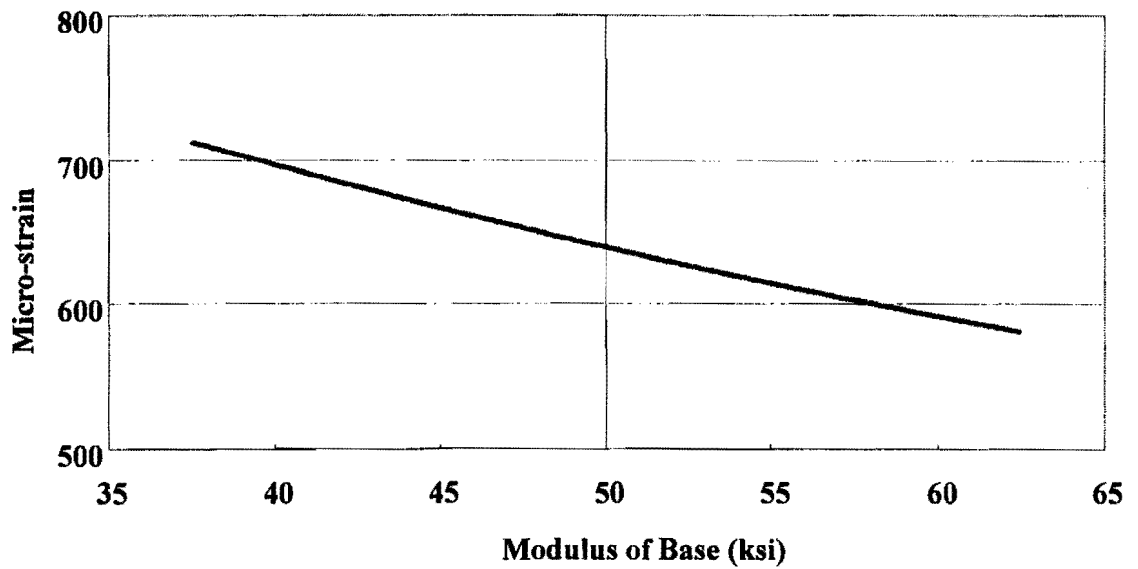


Figure A.5.3 – Variation in Critical Compressive Strain

6) Poisson's Ratio of Base

Original value: 0.35

Variation range: 0.2625 to 0.4375

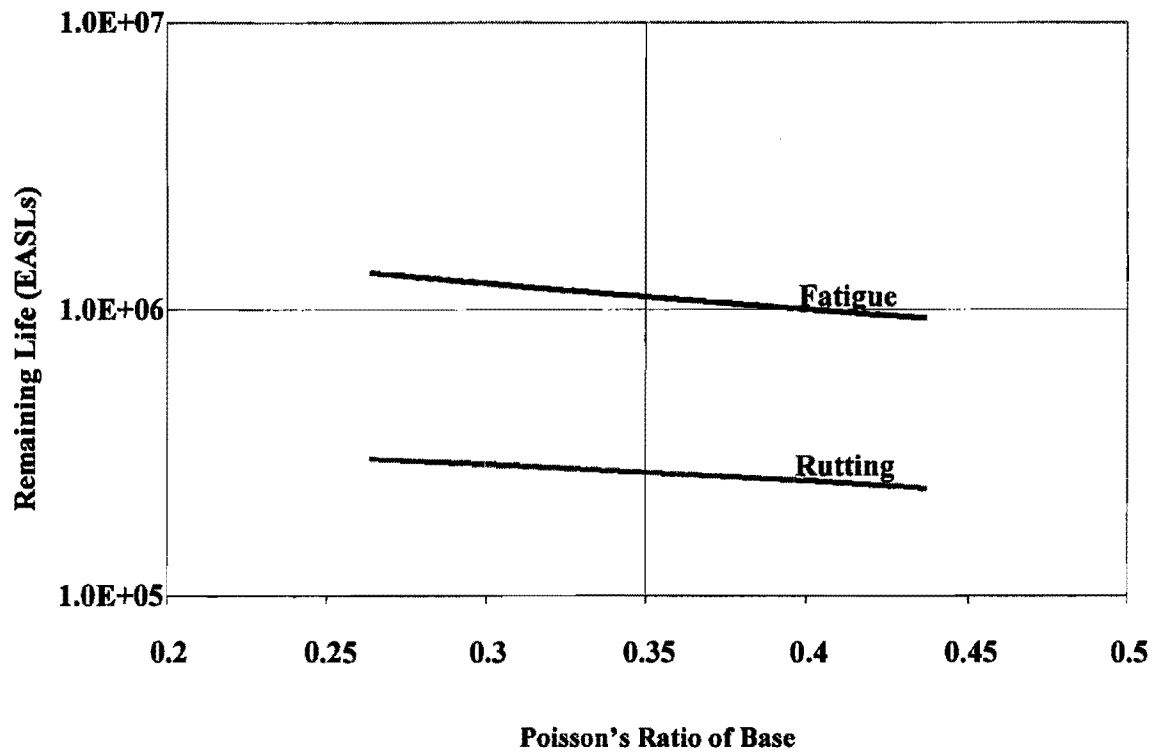


Figure A.6.1 – Variations in Remaining Lives

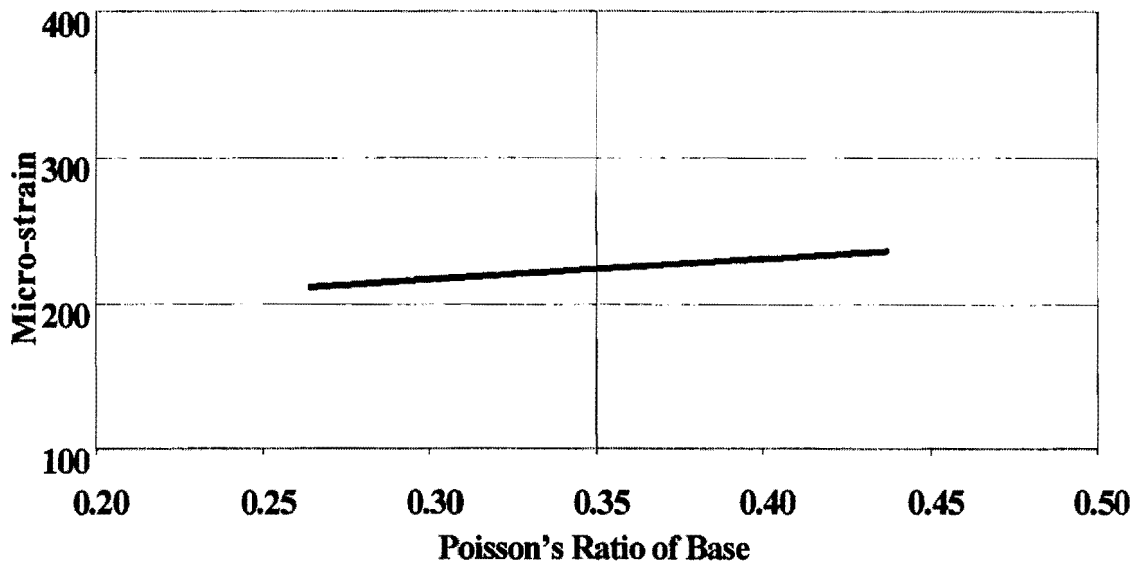


Figure A.6.2 – Variation in Critical Tensile Strain

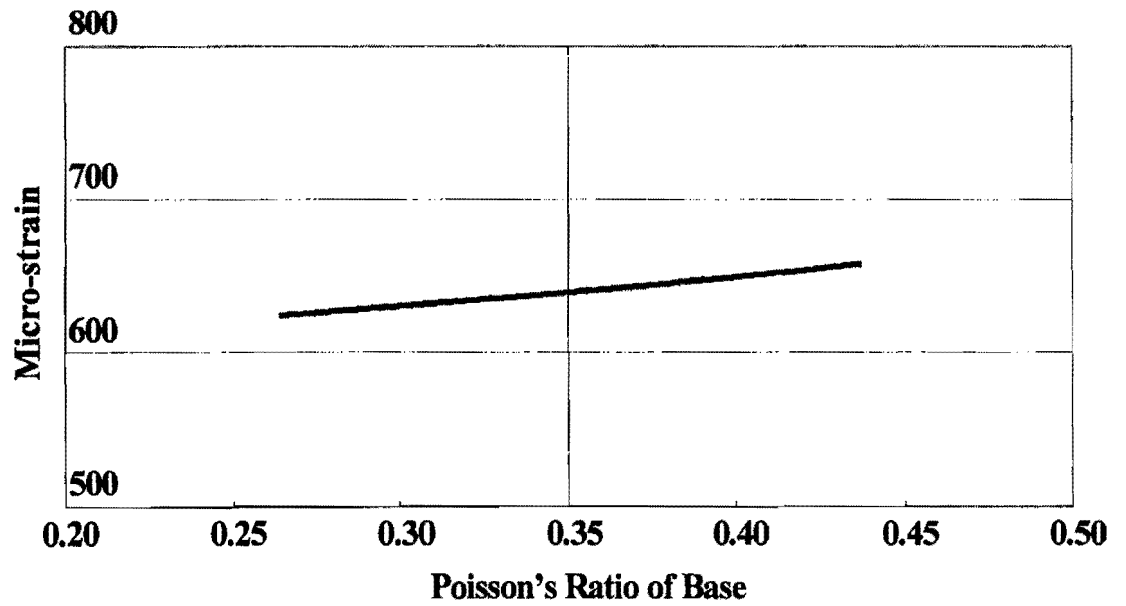


Figure A.6.3 – Variation in Critical Compressive Strain

7) Depth to bedrock

Original value: 300 in. (7.5m)

Variation range: 225 in. (5.6m) to 375 in. (9.4m)

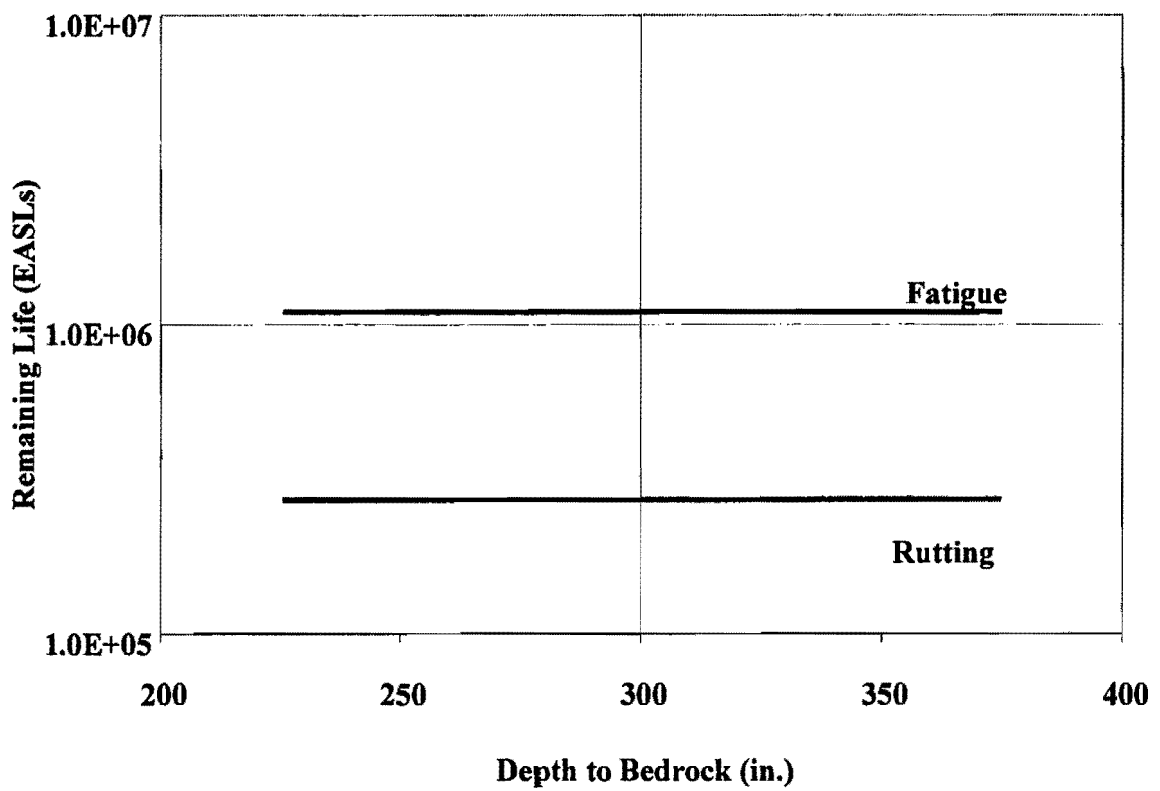


Figure A.7.1 – Variations in Remaining Lives

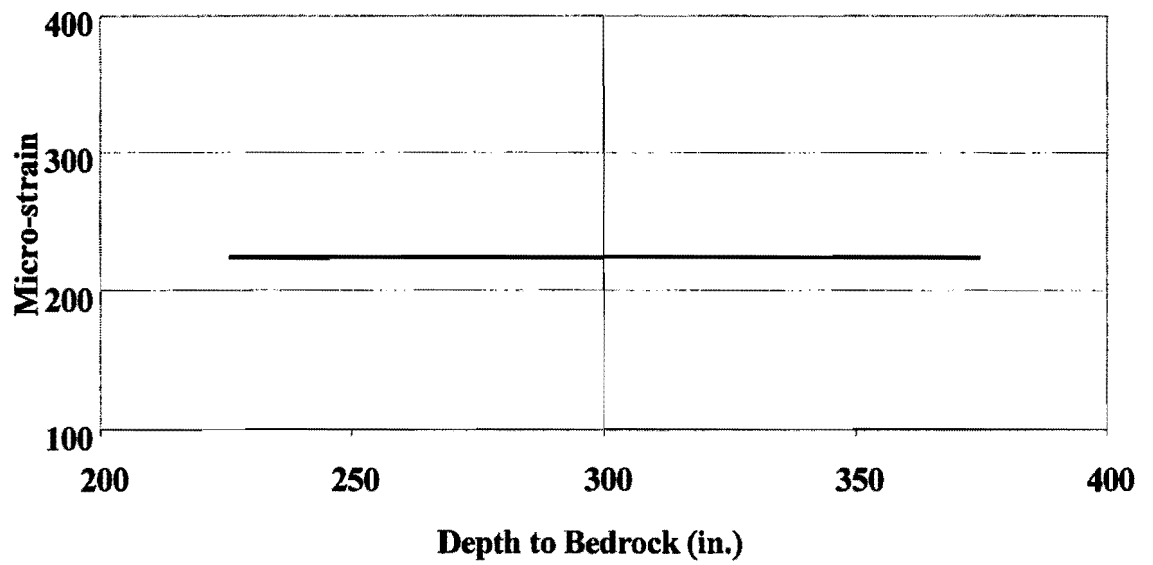


Figure A.7.2 – Variation in Critical Tensile Strain

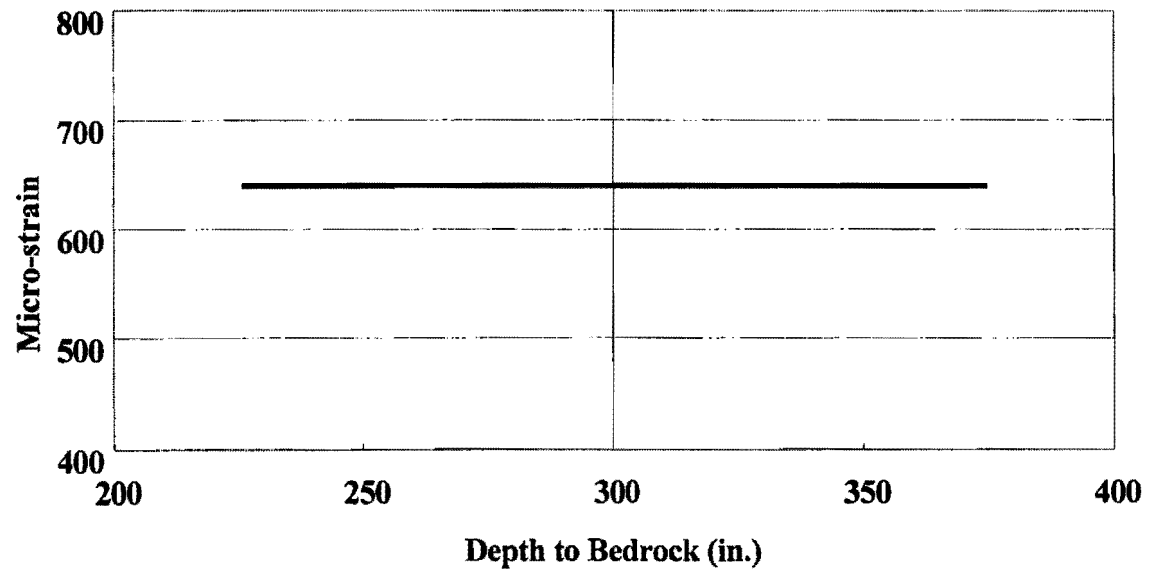


Figure A.7.3 – Variation in Critical Compressive Strain

8) Modulus of Subgrade

Original value: 10 ksi (69 MPa)

Variation range: 7.5 ksi (52 MPa) to 12.5 ksi (86 MPa)

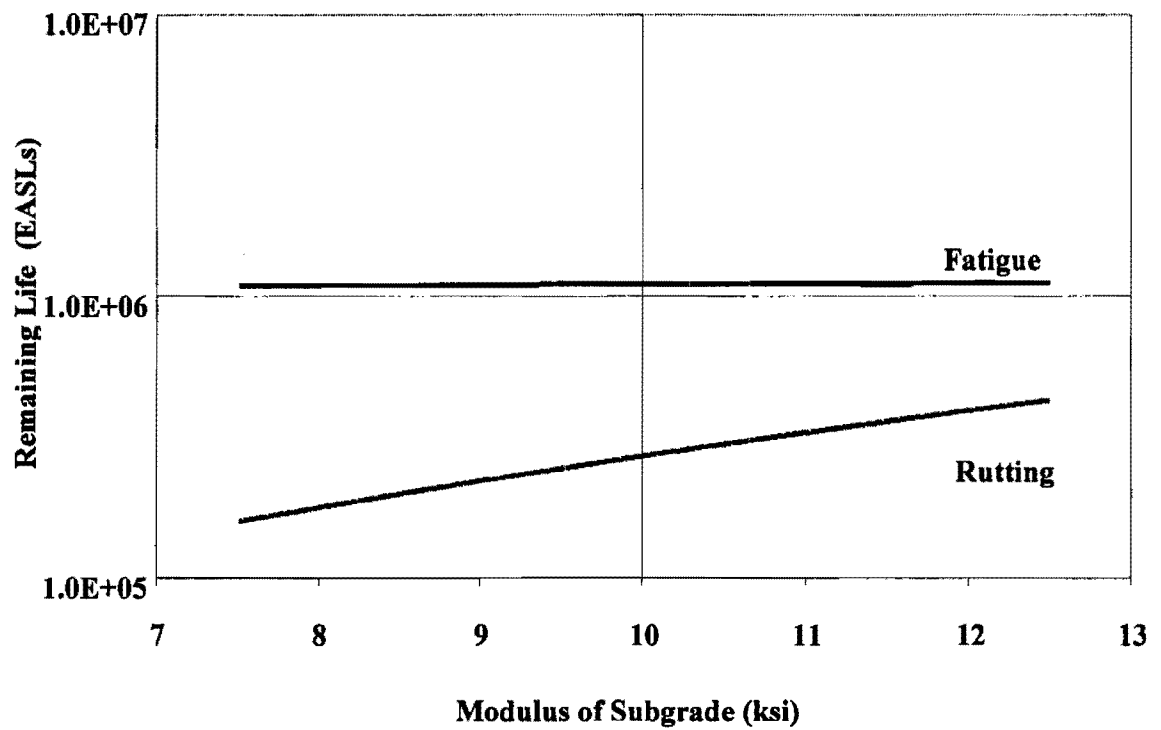


Figure A.8.1 – Variations in Remaining Lives

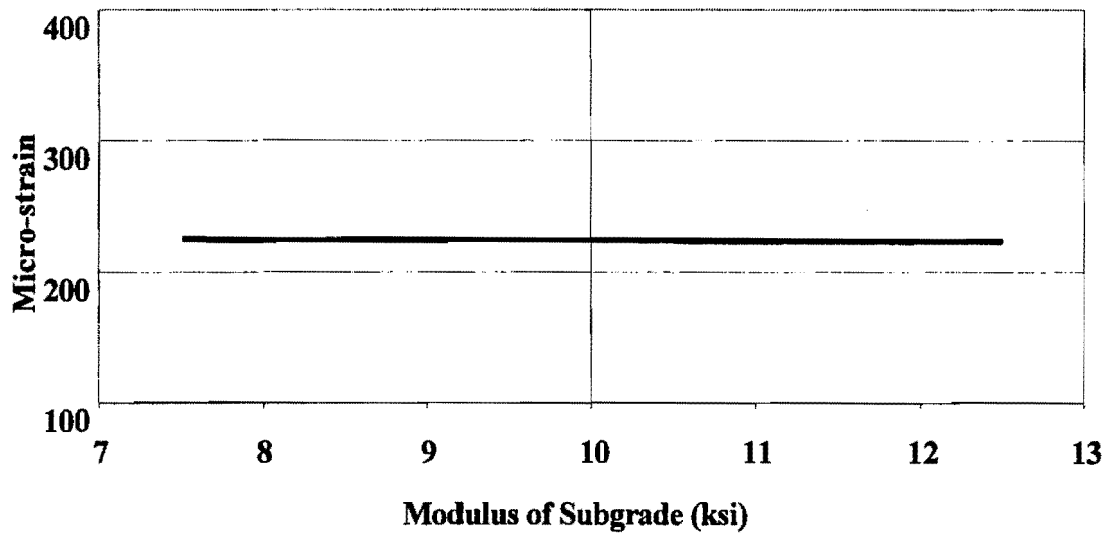


Figure A.8.2 – Variation in Critical Tensile Strain

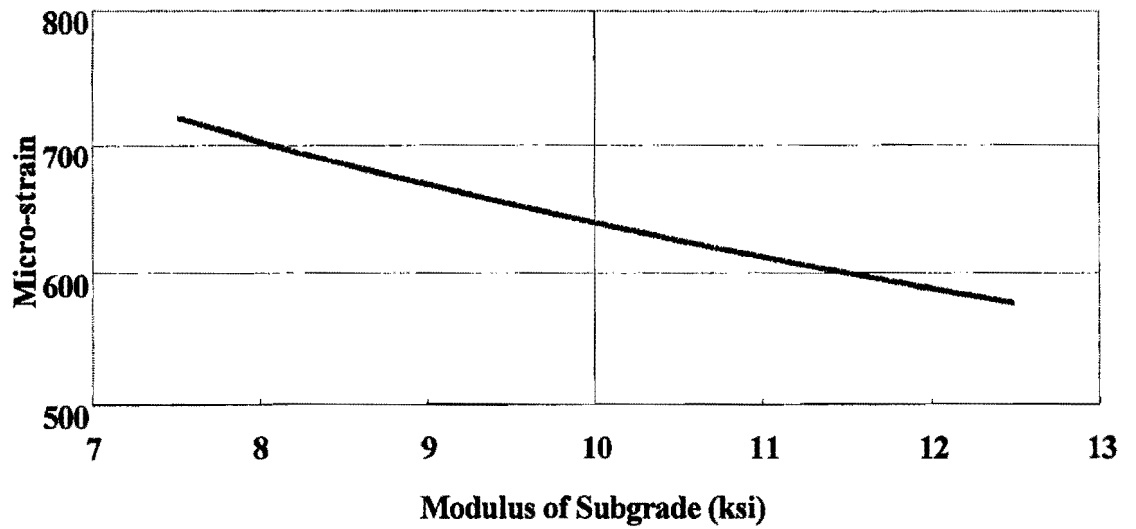


Figure A.8.3 – Variation in Critical Compressive Strain

9) Poisson's Ratio of Subgrade

Original value: 0.4

Variation range: 0.3 to 0.5

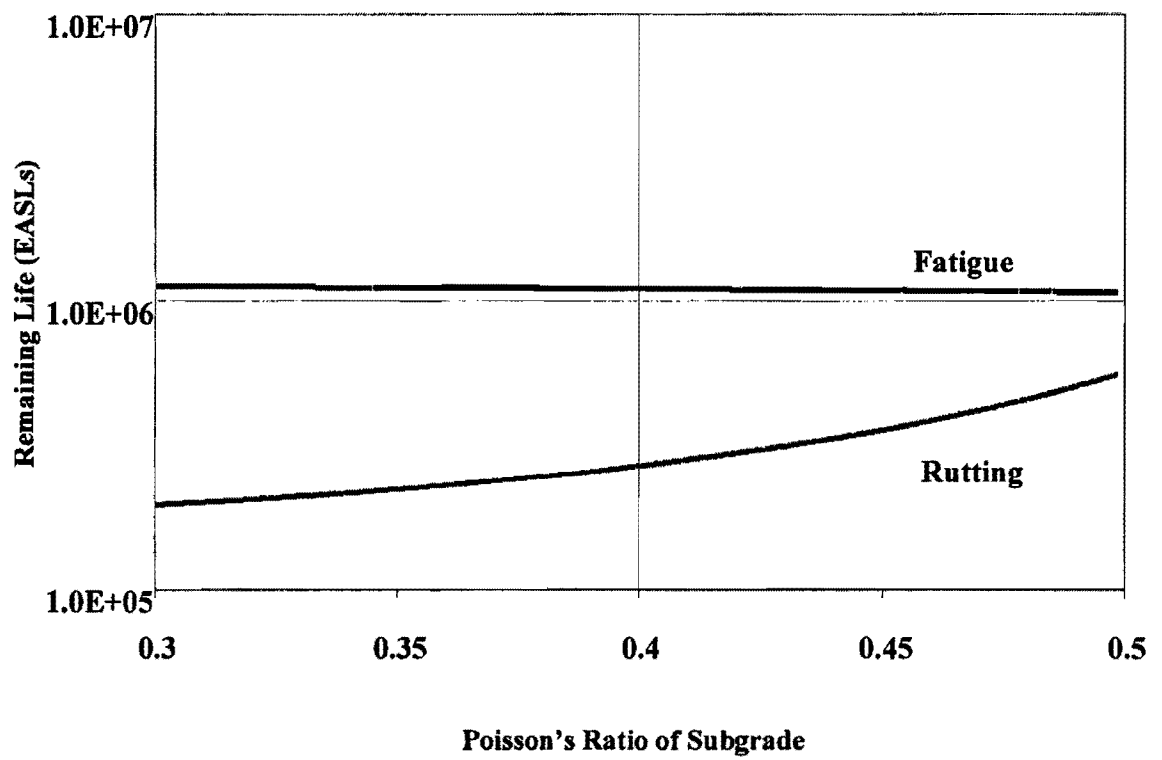


Figure A.9.1 – Variations in Remaining Lives

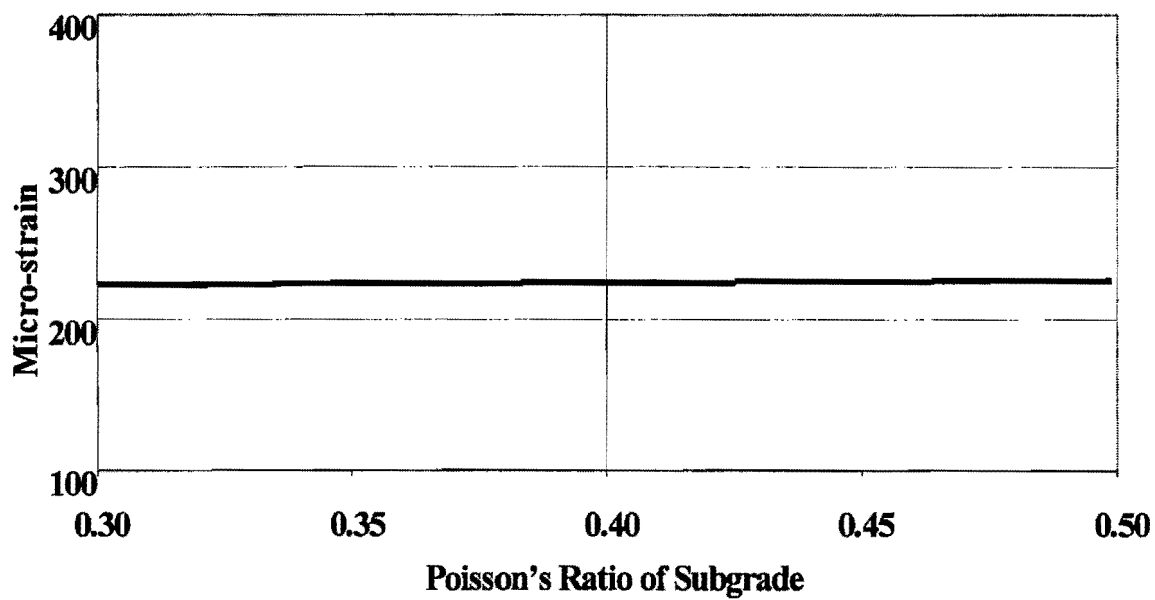


Figure A.9.2 – Variation in Critical Tensile Strain

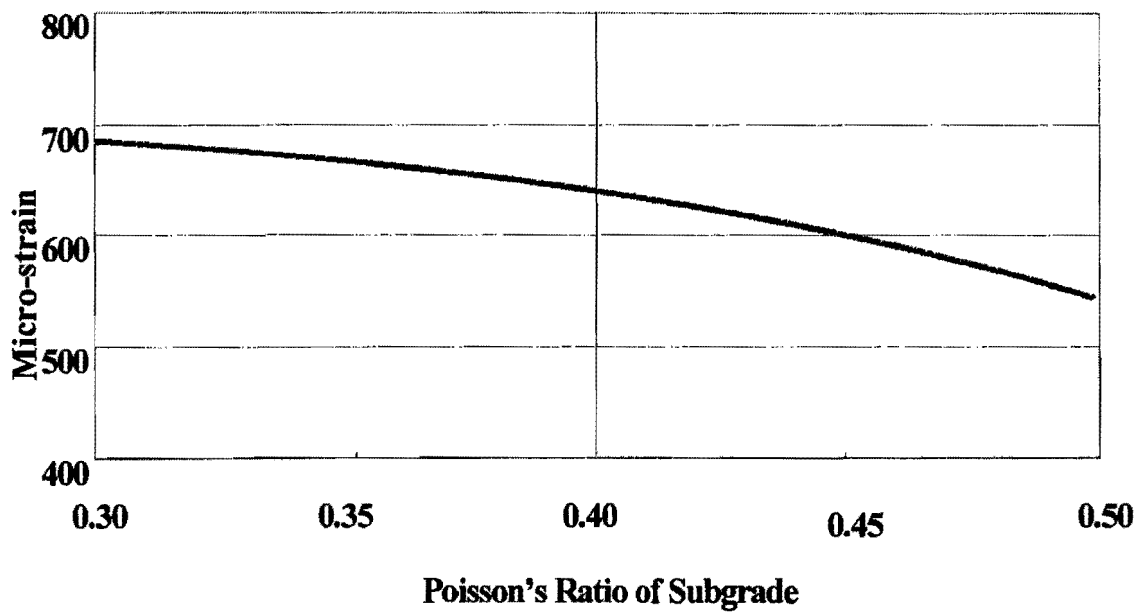


Figure A.9.3 – Variation in Critical Compressive Strain

APPENDIX B

**RESULTS OF SENSITIVITY STUDY
UNDER EQUIVALENT-LINEAR MODEL**

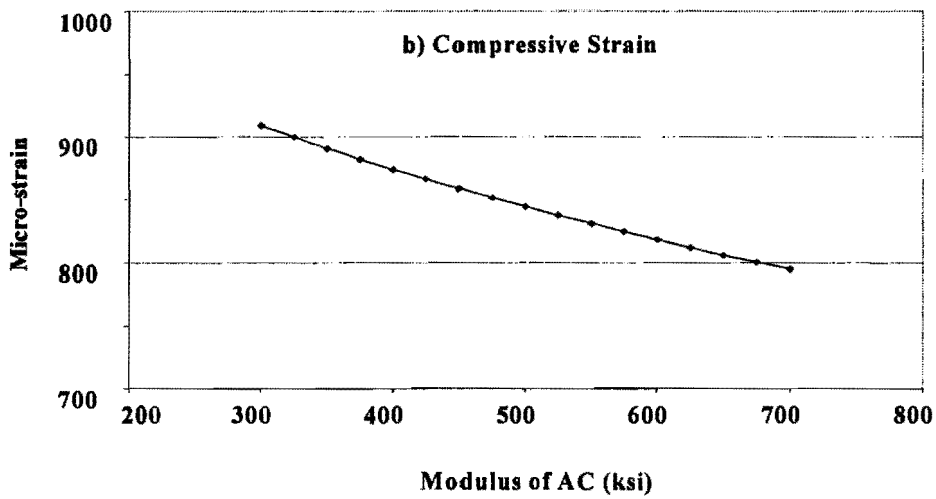
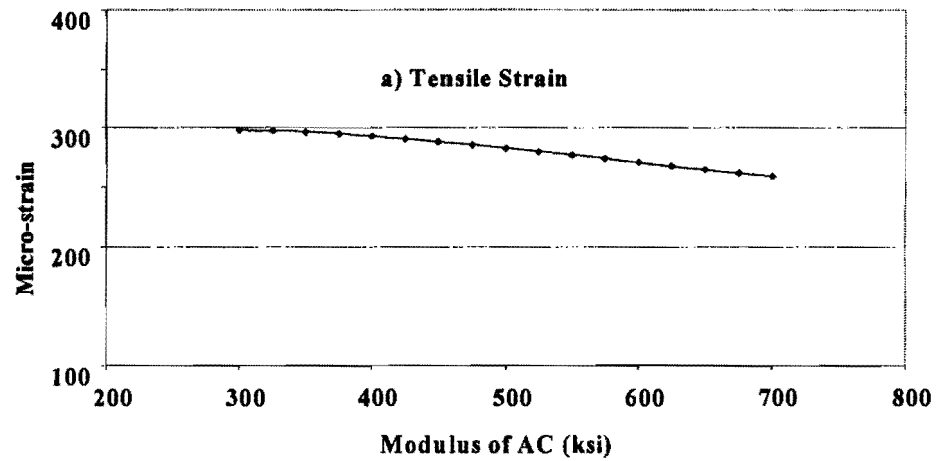


Figure B.1 - Variations in Critical Strains with Modulus of AC

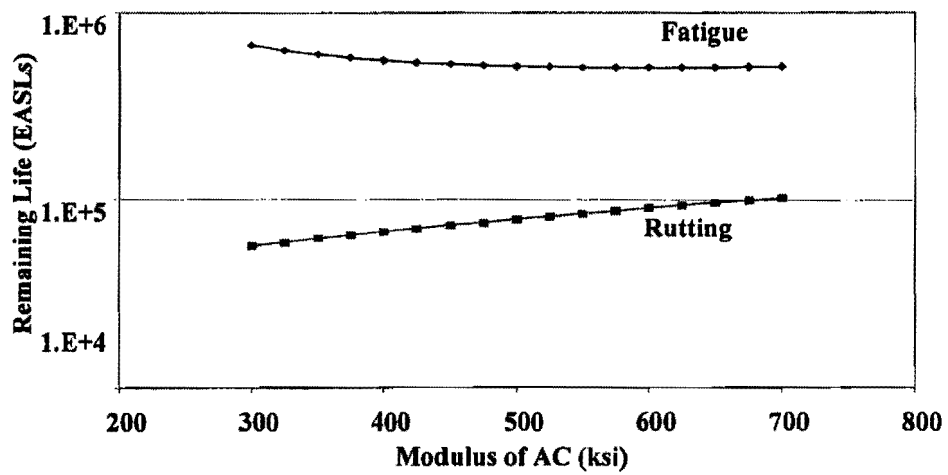


Figure B.2 - Variations in Remaining Lives with Modulus of AC

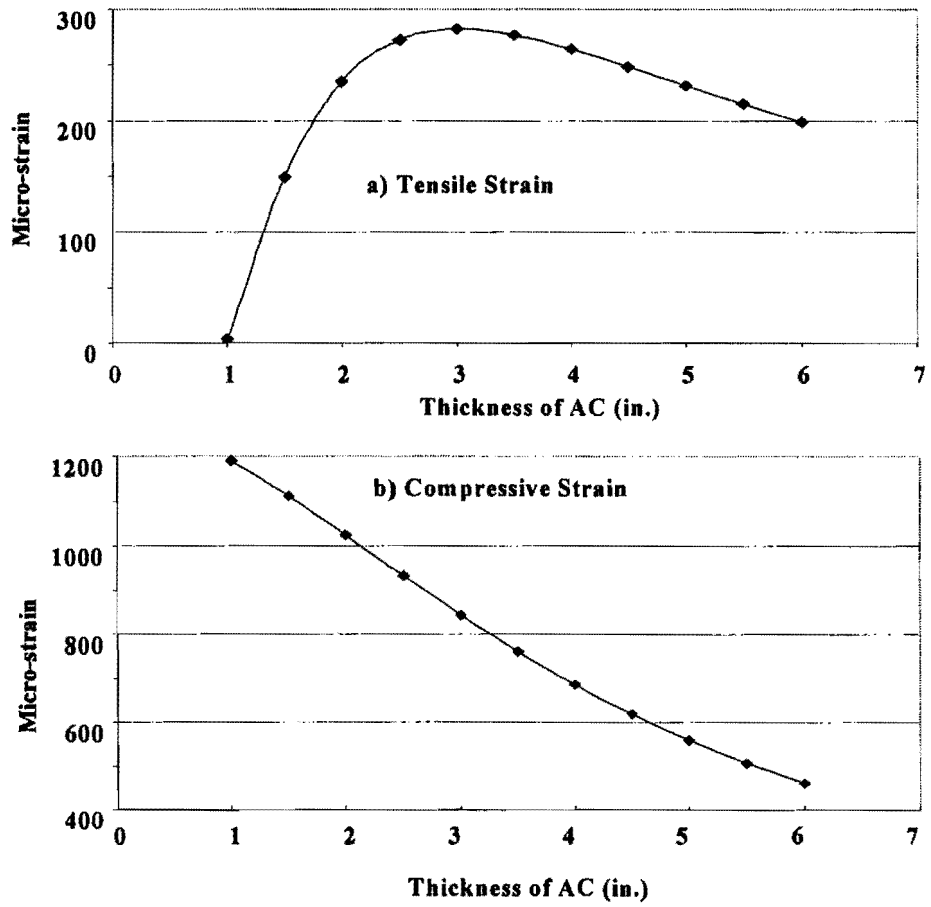


Figure B.3 - Variations in Critical Strains with Thickness of AC

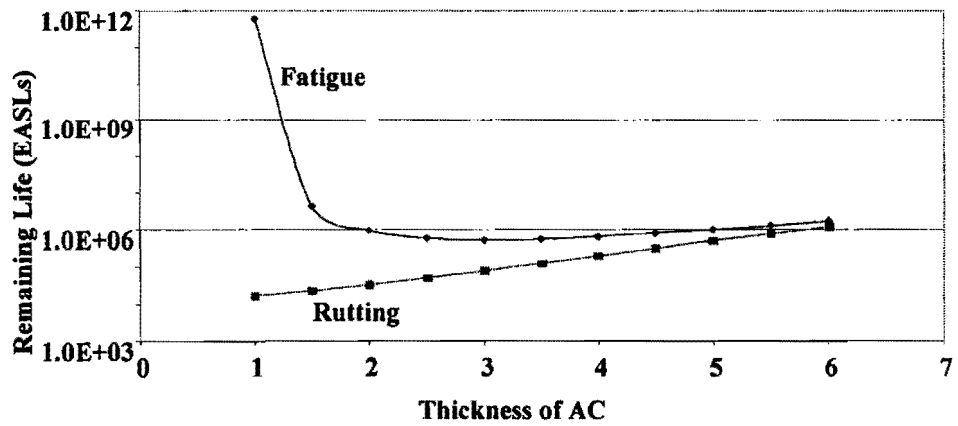


Figure B.4 - Variation in Remaining lives with Thickness of AC

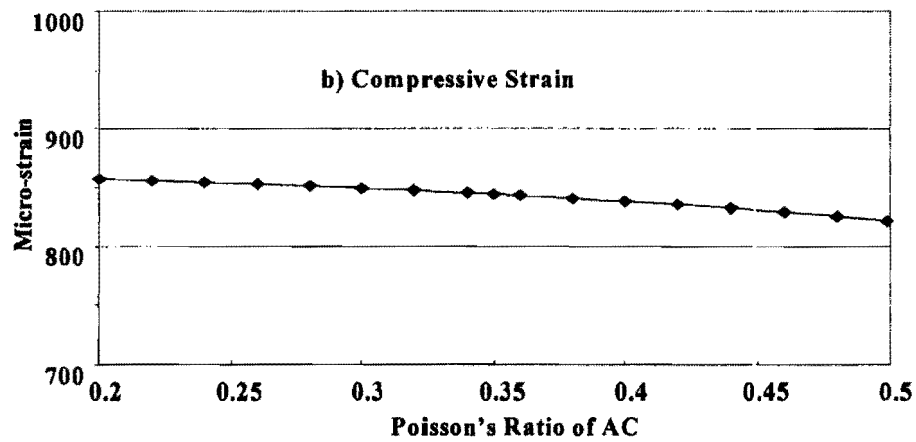
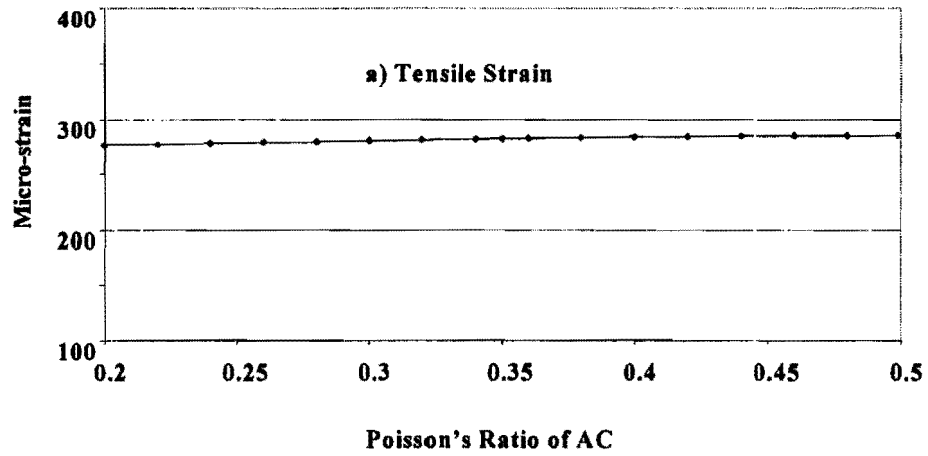


Figure B. 5 -Variations in Critical Strains with Poisson's Ratio of AC

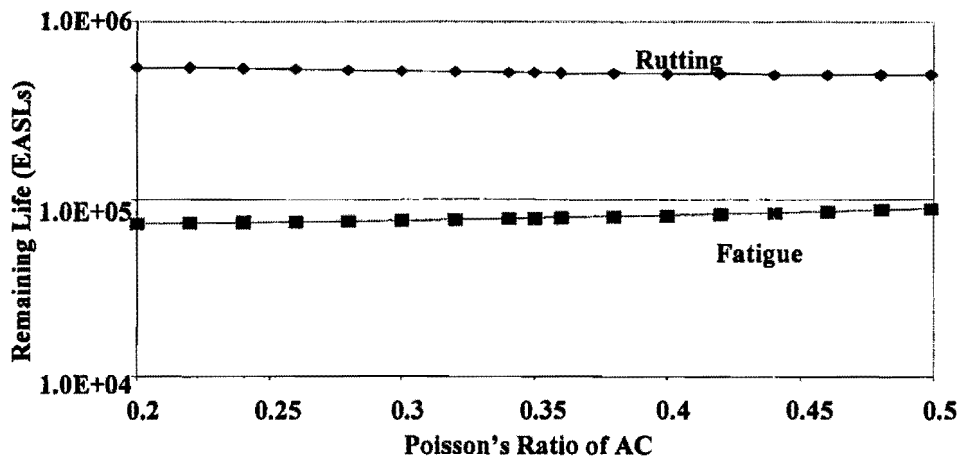


Figure B.6 -Variations in Remaining Lives with Poisson's Ratio of AC

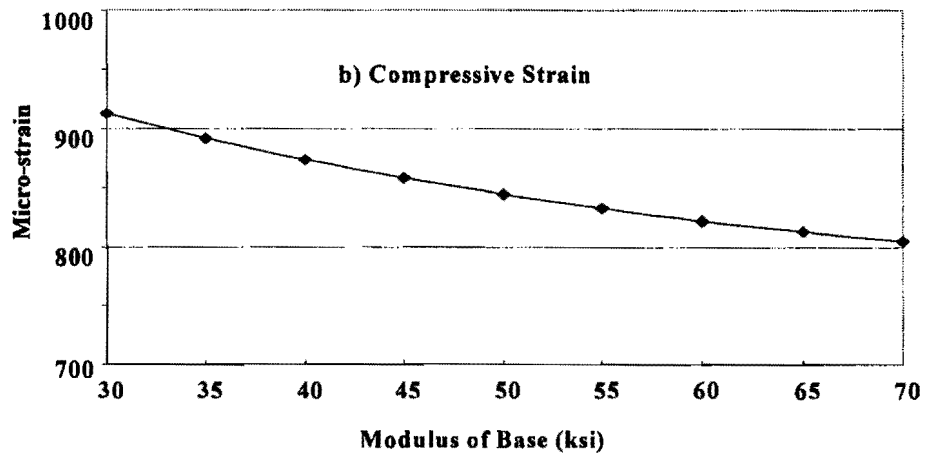
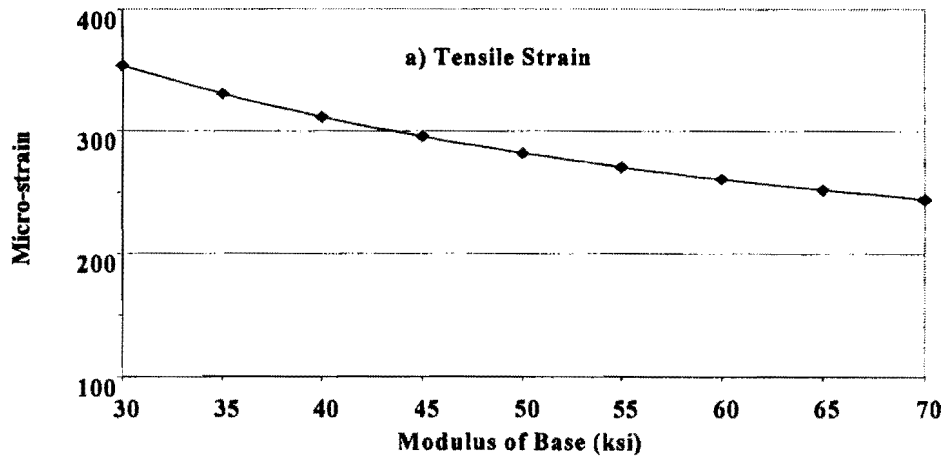


Figure B.7 - Variations in Critical Strains with Modulus of Base

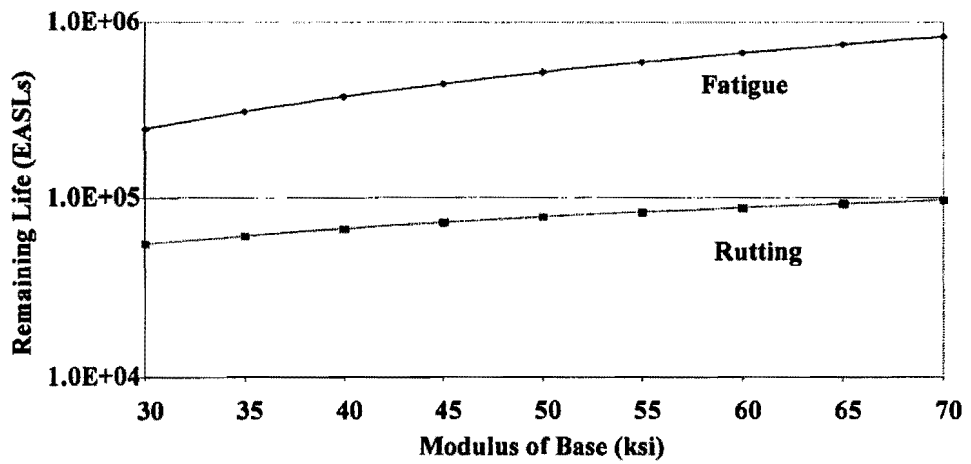


Figure B.8 - Variations in Remaining Lives with Modulus of Base

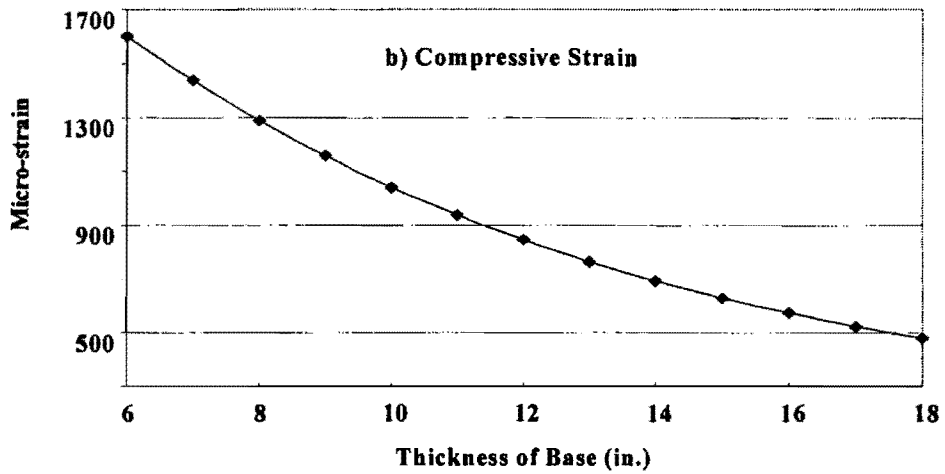
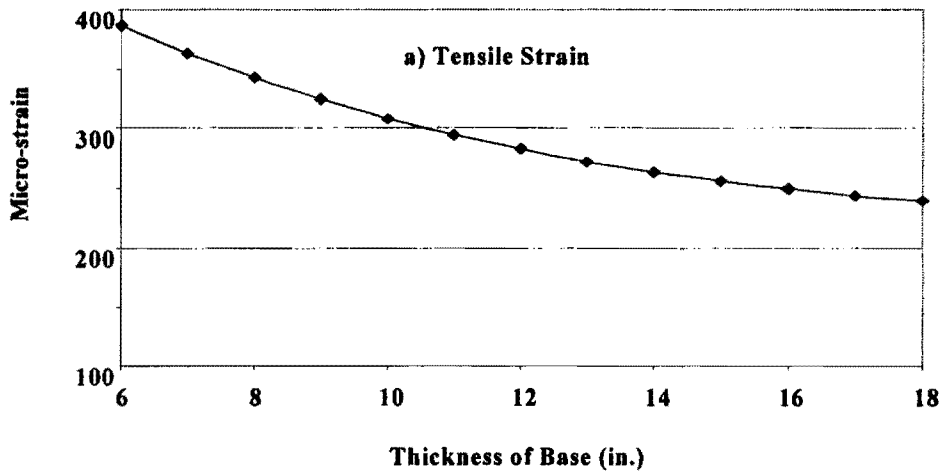


Figure B.9 - Variations in Critical Strains with Thickness of Base

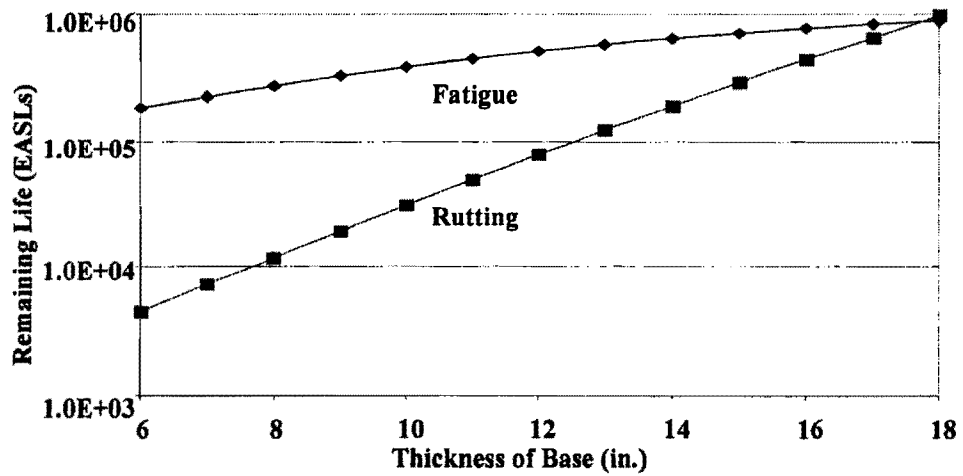


Figure B.10 - Variations in Remaining Lives with Thickness of Base

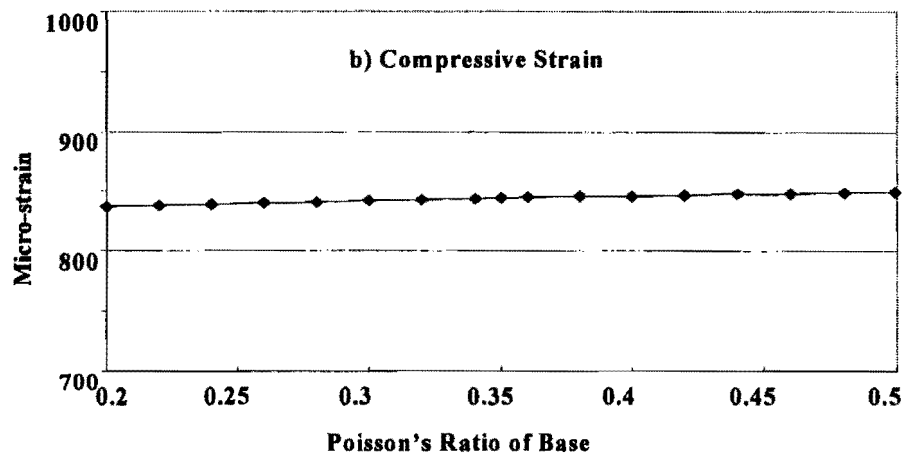
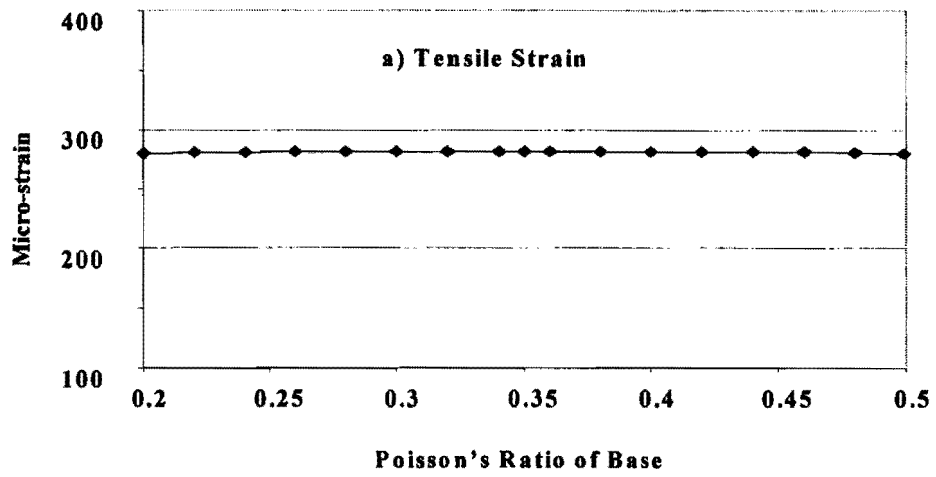


Figure B.11 - Variations in Critical Strain with Poisson's Ratio of Base

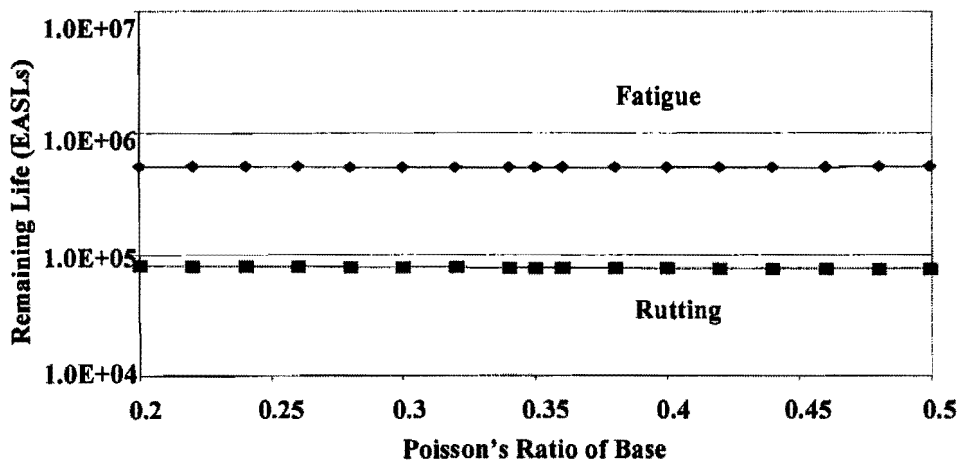


Figure B.12 - Variations in Remaining Lives with Poisson's Ratio of Base

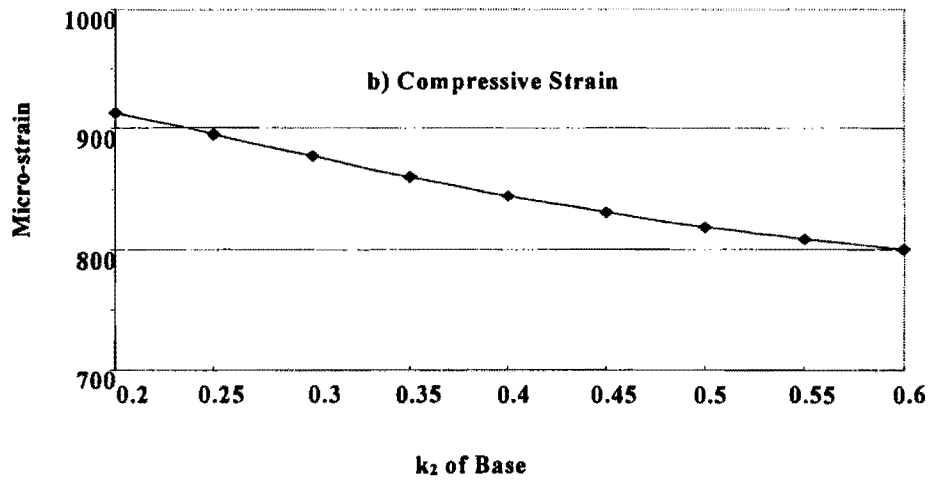
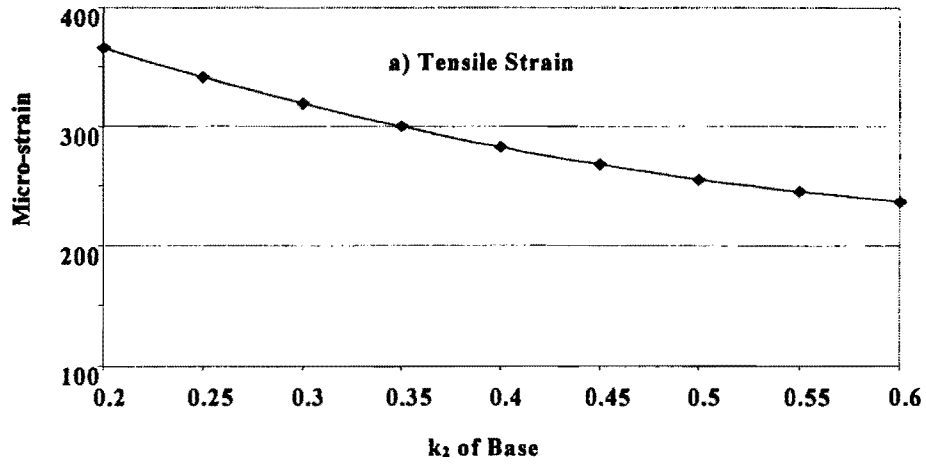


Figure B.13 –Variations in Critical Strains with k_2 of Base

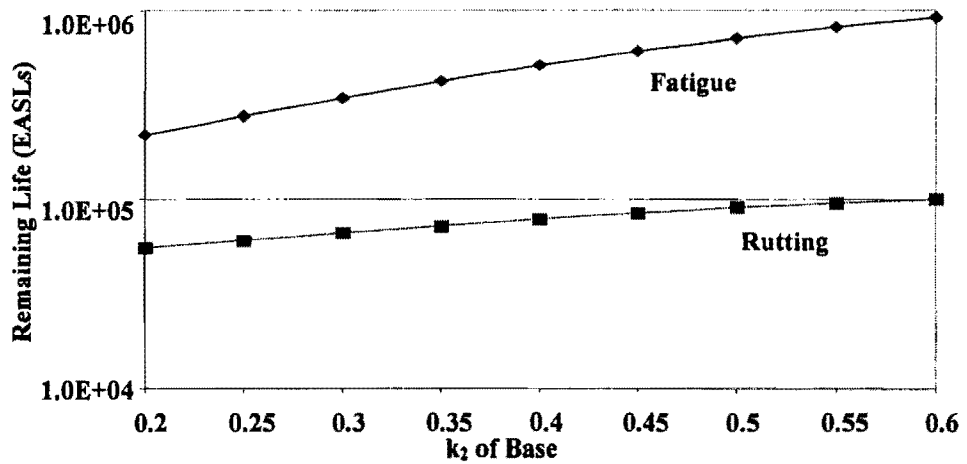


Figure B.14 - Variations in Remaining Lives with k_2 of Base

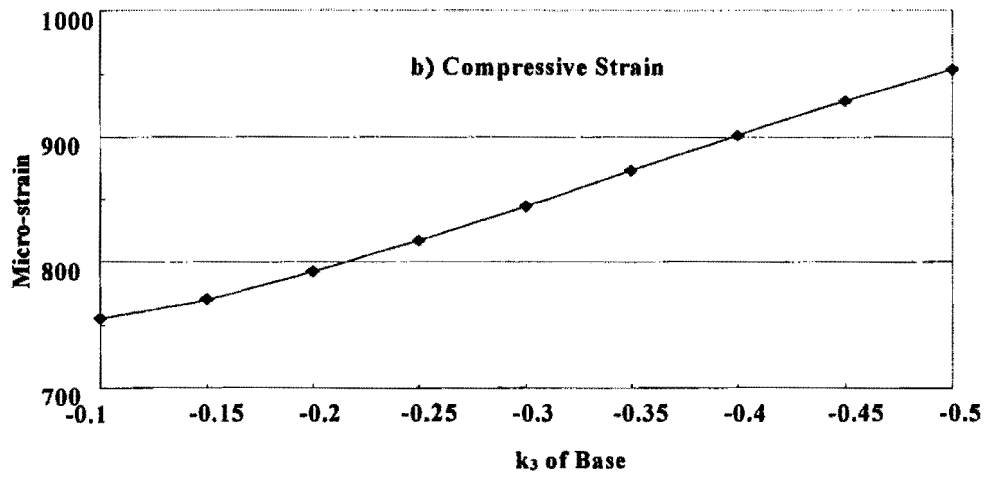
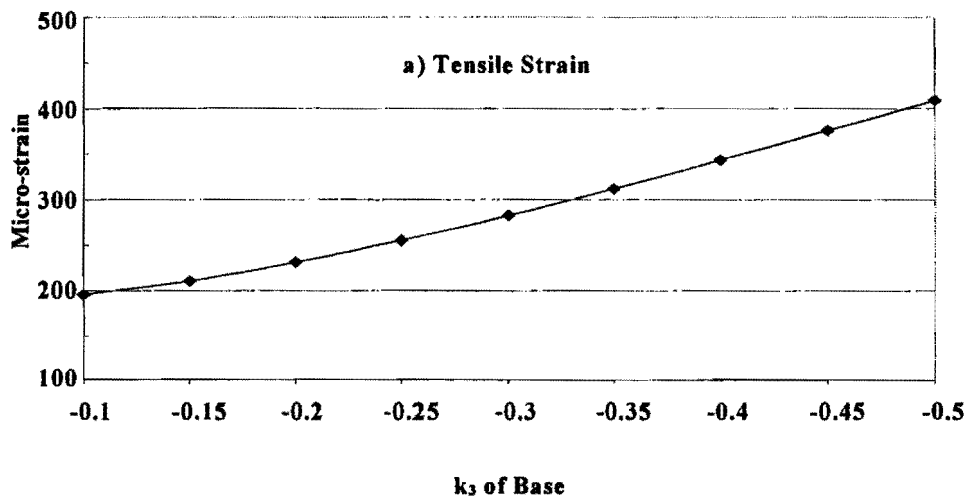


Figure B.15 – Variations in Critical Strains with k_3 of Base

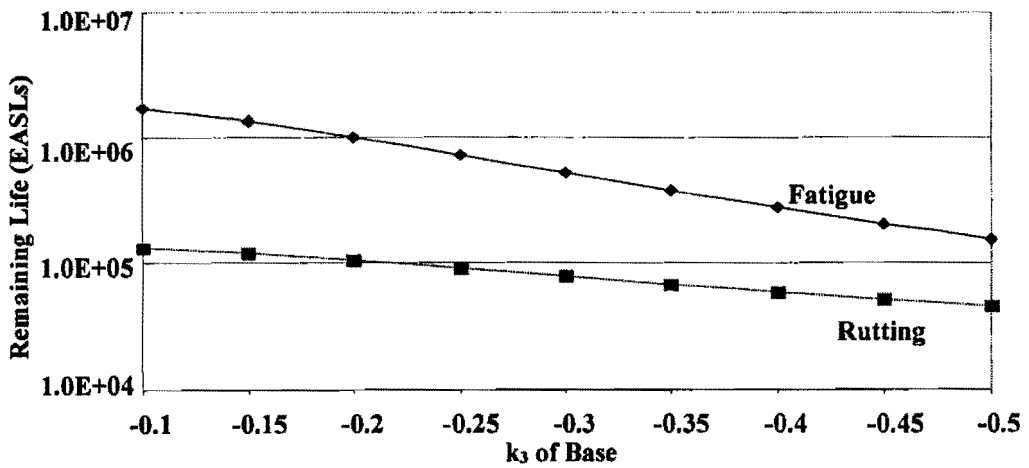


Figure B.16 - Variations in Remaining Lives with k_3 of Base

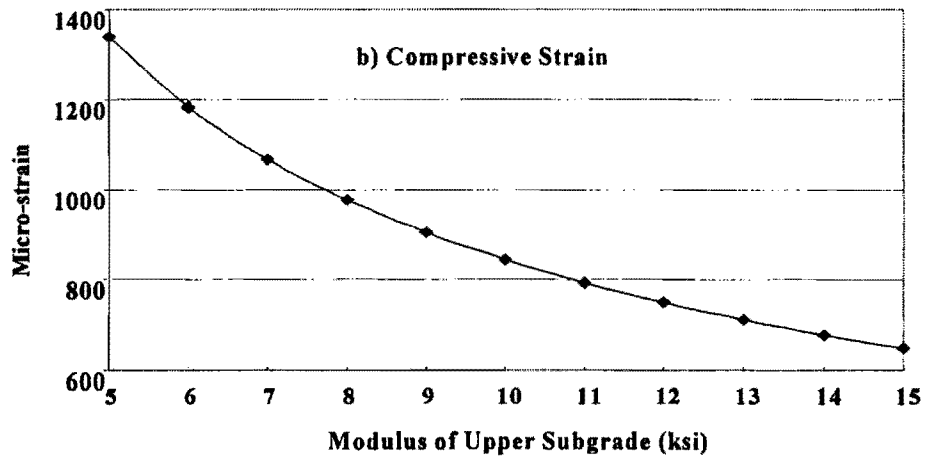
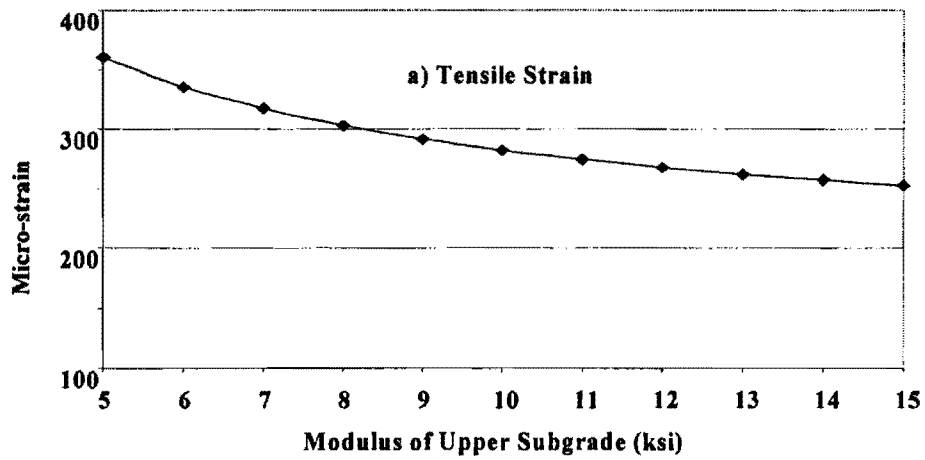


Figure B.17 – Variations in Critical Strains with Modulus of Upper Subgrade

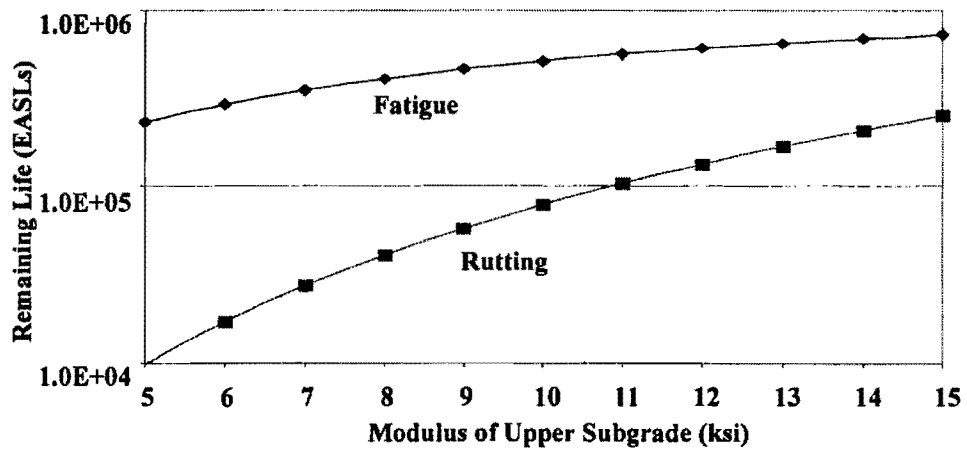


Figure B.18 – Variations in Remaining Lives with Modulus of Upper Subgrade

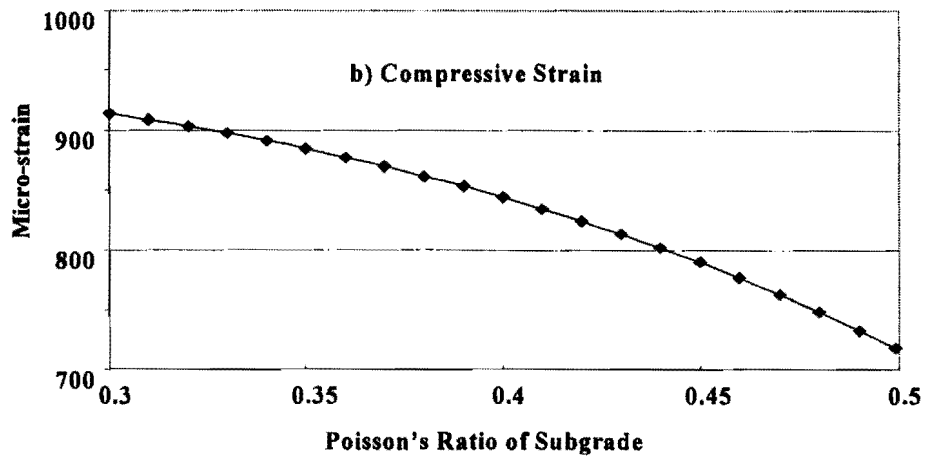
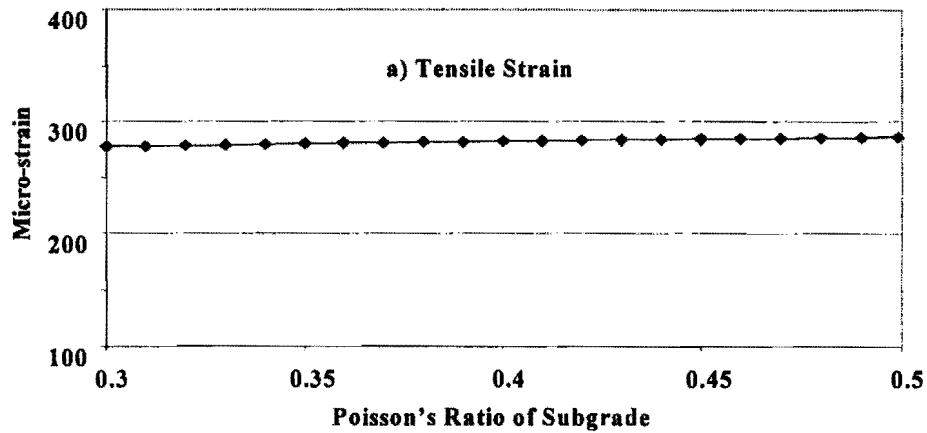


Figure B.19 - Variations of Critical Strain with Poisson's Ratio of Subgrade

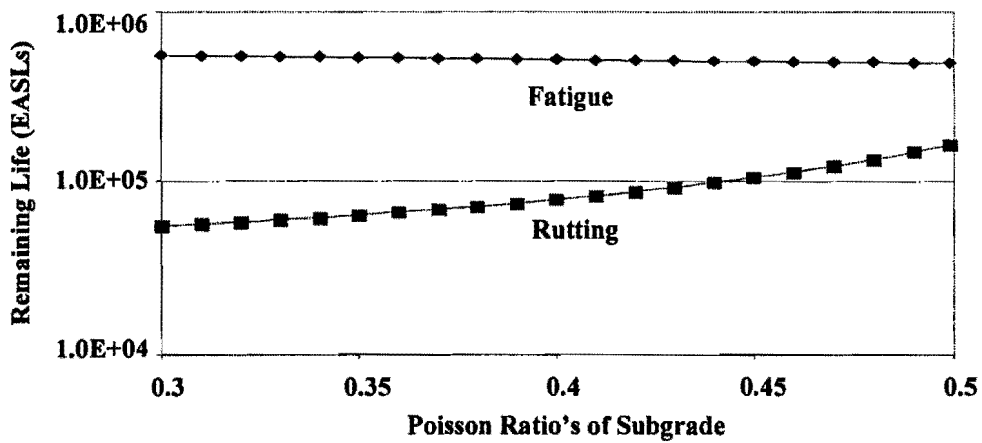


Figure B.20 - Variations in Remaining Lives with Poisson's Ratio of Subgrade

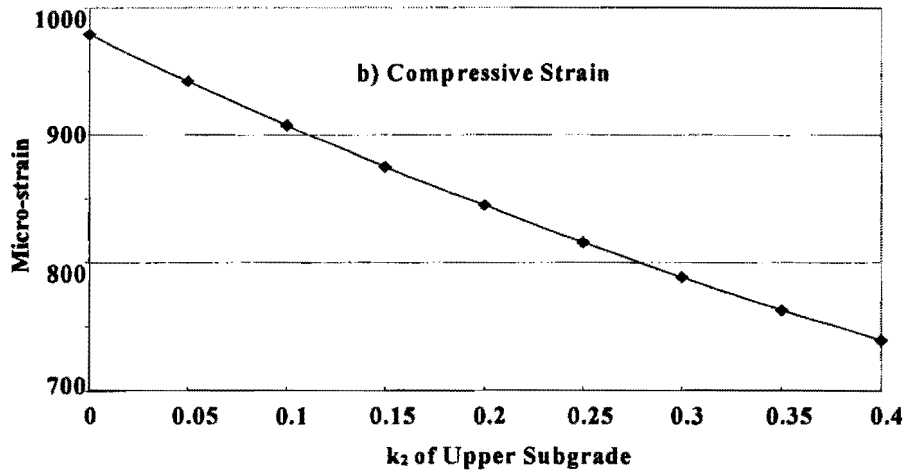
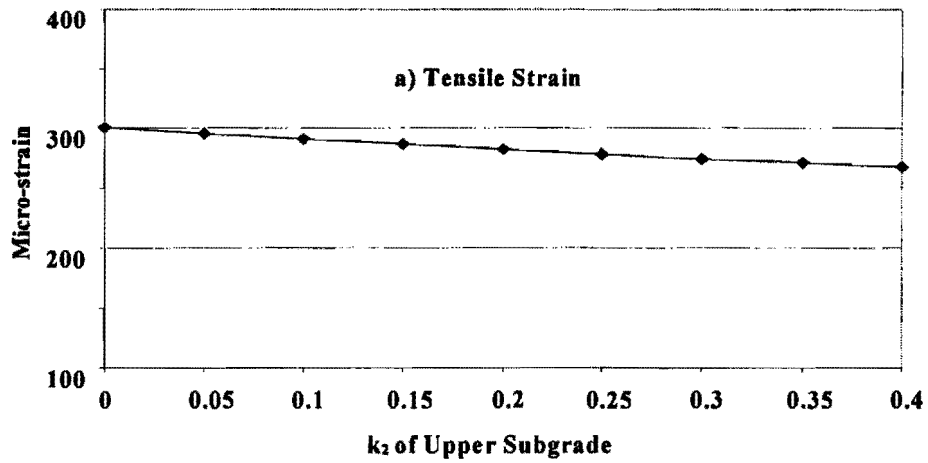


Figure B.21 – Variations in Critical Strains with k_2 of Upper Subgrade

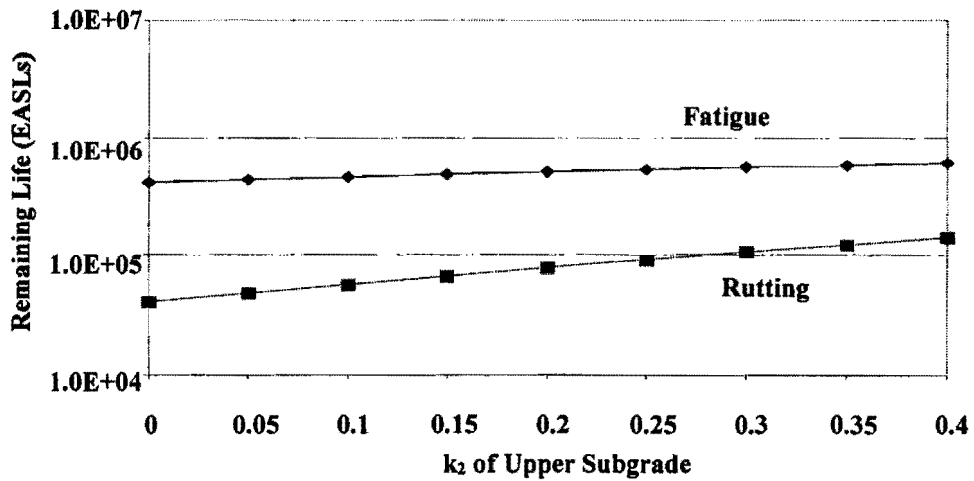


Figure B.22 - Variations in Remaining Lives with k_2 of Upper Subgrade

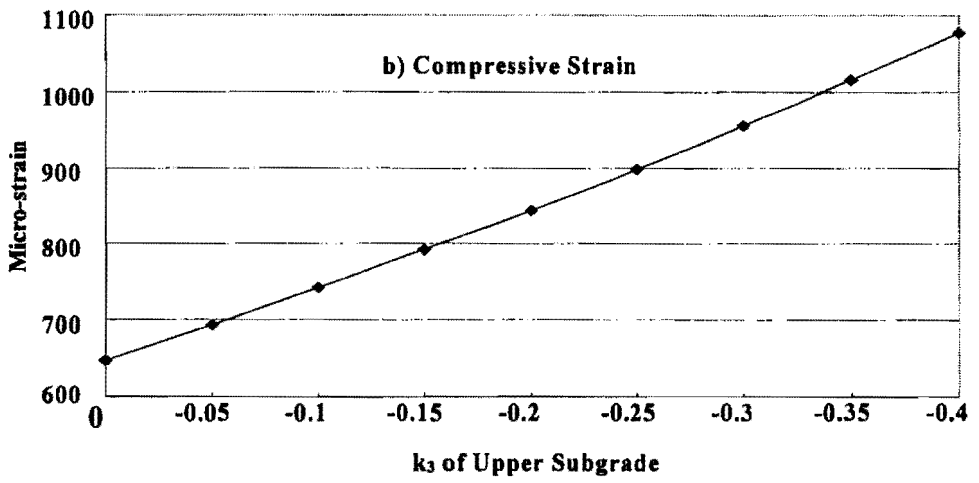
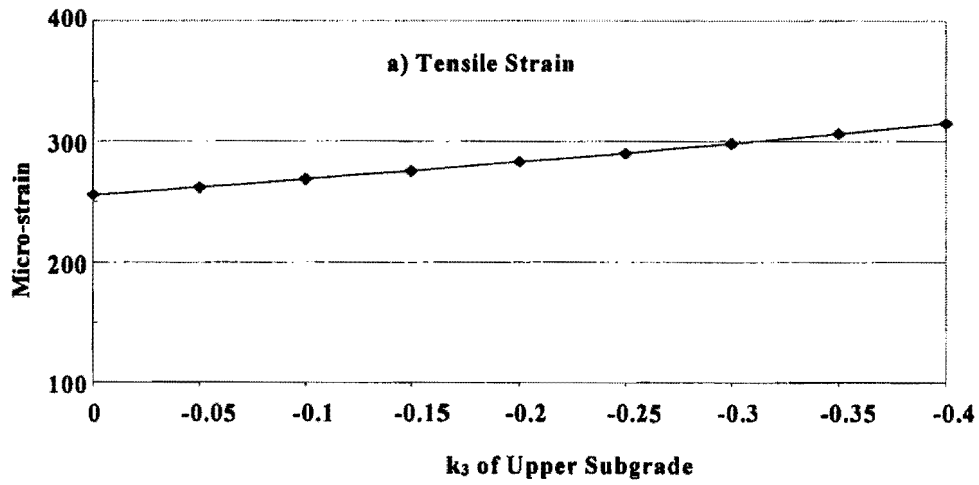


Figure B.23 - Variations in Critical Strains with k_3 of Upper Subgrade

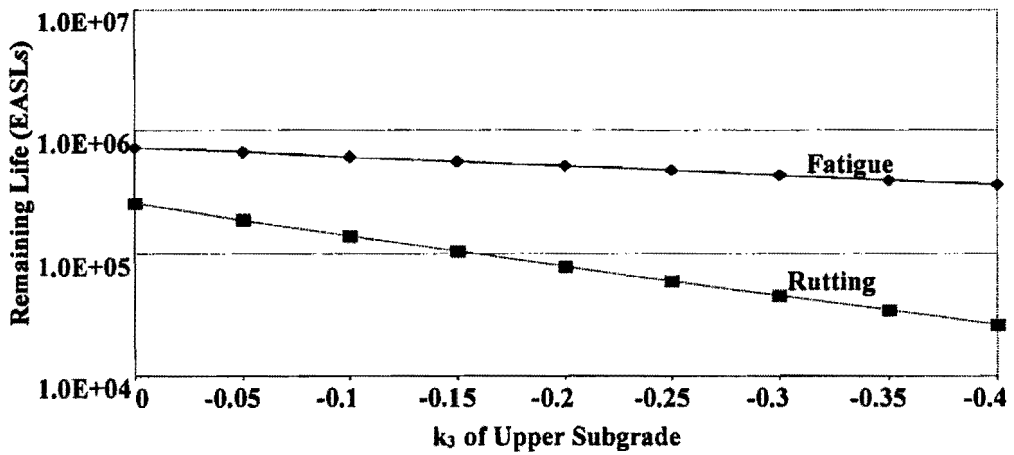


Figure B.24 - Variations in Remaining Lives with k_3 of Upper Subgrade

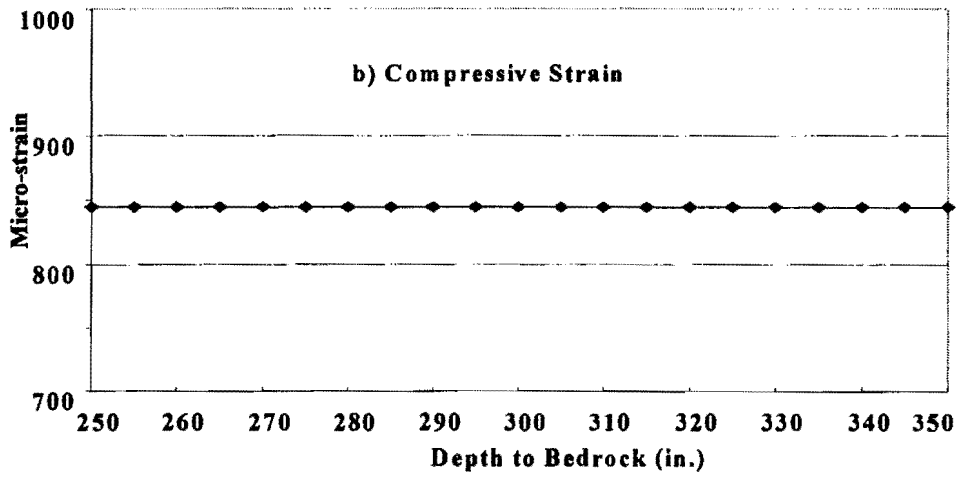
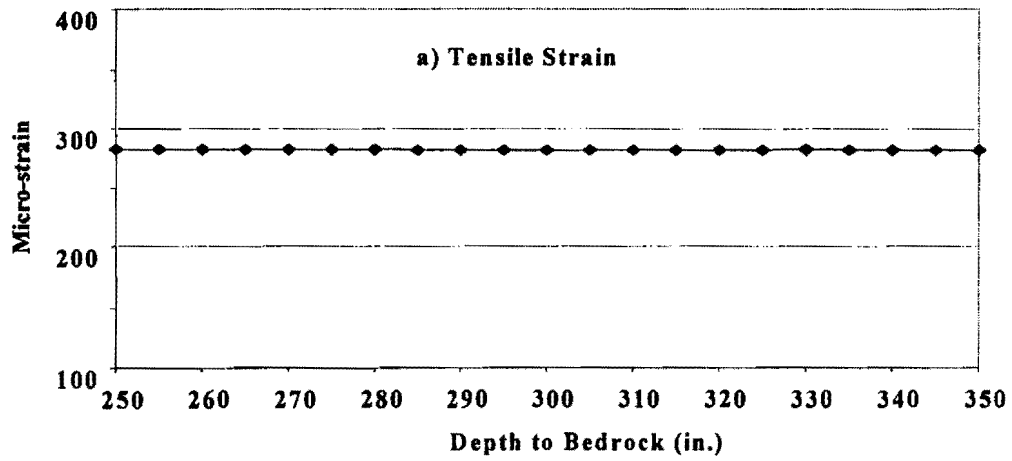


Figure B.27 - Variations in Critical Strains with Depth to Bedrock

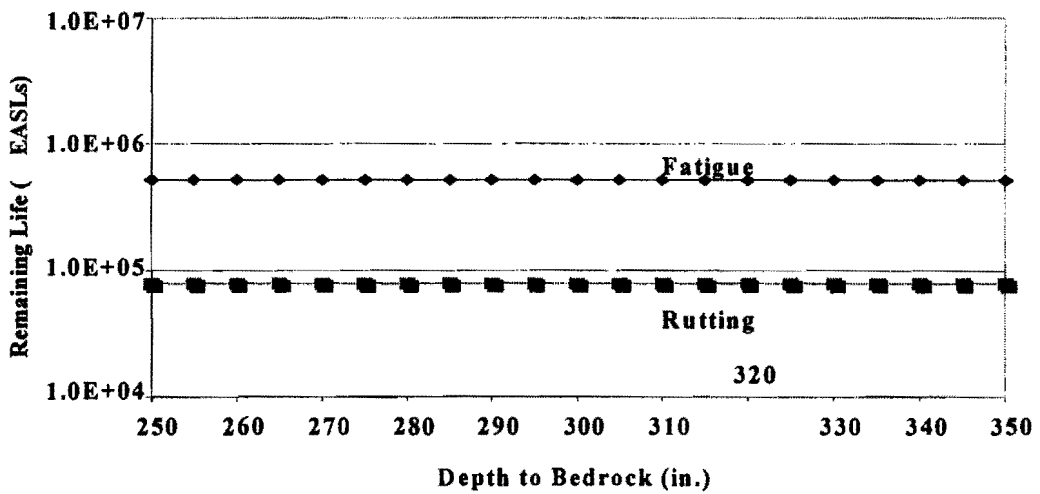


Figure B.28 - Variations in Remaining Lives with Depth to Bedrock

APPENDIX C

**RESULTS OF SENSITIVITY STUDY
UNDER NONLINEAR STATIC MODEL**

1) Properties of AC layer

Table C.1.1 - Variation in Pavement Response with Modulus of AC

Modulus of AC layer	Surface Deflections (milli-inch)							Critical Strains (10 ⁻⁴ in./in.)		Remaining Lives (10 ³ EASLs)	
	Radial Distance (in.)							Tensile ^[1]	Compressive ^[2]	Fatigue	Rutting
(ksi)	0	12	24	36	48	60	72				
300	26.6	15.3	9.1	5.9	4.1	2.9	2.2	2.527	7.184	1154	162
400	25.9	15.3	9.1	5.9	4.1	2.9	2.2	2.579	6.931	845	190
500	25.1	15.1	9.0	5.9	4.1	2.9	2.2	2.537	6.948	737	188
600	24.7	15.2	9.0	5.9	4.1	2.9	2.2	2.453	6.557	704	244
700	24.1	15.1	9.0	5.9	4.1	2.9	2.2	2.359	6.424	703	267
Sensitivity Index								0.18	0.28	1.42	1.48

[1]: Tangential tensile strain at the bottom of the AC layer;

[2]: Vertical compressive strain at the top of the subgrade.

Table C.1.2 - Variation in Pavement Response with Thickness of AC Layer

Thickness of AC layer	Surface Deflections (milli-inch)							Critical Strains (10^{-4} in./in.)		Remaining Lives (10^3 EASLs)	
	Radial Distance (in.)							Tensile ^[1]	Compressive ^[2]	Fatigue	Rutting
(in.)	0	12	24	36	48	60	72				
1	31.1	16.3	9.4	5.9	4.0	2.9	2.2	1.085	9.002	12080	59
3	25.1	15.1	9.0	5.9	4.1	2.9	2.2	2.537	6.948	737	188
5	19.6	13.7	8.8	5.9	4.1	3.0	2.3	2.148	4.859	1275	933
Sensitivity Index								0.86	0.45	23.1	5.9

[1]: Tangential tensile strain at the bottom of the AC layer;

[2]: Vertical compressive strain at the top of the subgrade.

Table C.1.3 - Variation in Pavement Response with Poisson's Ratio of AC Layer

Poisson's Ratio of AC layer	Surface Deflections (milli-inch)							Critical Strains (10^{-4} in./in.)		Remaining Lives (10^3 EASLs)	
	Radial Distance (in.)							Tensile ^[1]	Compressive ^[2]	Fatigue	Rutting
	0	12	24	36	48	60	72				
0.2	25.5	15.2	9.0	5.9	4.1	2.9	2.2	2.461	7.061	815	175
0.35	25.1	15.1	9.0	5.9	4.1	2.9	2.2	2.537	6.948	737	188
0.5	24.7	15.1	9.0	5.9	4.1	2.9	2.2	2.610	6.467	671	259
Sensitivity Index								0.07	0.16	0.25	0.88

[1]: Tangential tensile strain at the bottom of the AC layer;

[2]: Vertical compressive strain at the top of the subgrade.

2) Properties of Base Layer

Table C.2.1 - Variation in Pavement Response with Modulus of Base Layer

Modulus of Base	Surface Deflections (milli-inch)							Critical Strains (10 ⁻⁴ in./in.)		Remaining Lives (10 ³ EASLs)	
	Radial Distance (in.)							Tensile ^[1]	Compressive ^[2]	Fatigue	Rutting
(ksi)	0	12	24	36	48	60	72				
30	28.4	16.6	9.3	5.8	4.0	2.9	2.2	3.168	7.732	355	117
40	26.6	15.8	9.1	5.9	4.0	2.9	2.2	2.814	7.171	524	163
50	25.1	15.1	9.0	5.9	4.1	2.9	2.2	2.537	6.948	737	188
60	24.2	14.7	8.9	5.9	4.1	3.0	2.2	2.381	6.499	908	254
70	23.0	14.3	8.8	5.9	4.1	3.0	2.2	2.076	6.405	1426	271
Sensitivity Index								0.62	0.32	2.34	1.74

[1]: Tangential tensile strain at the bottom of the AC layer;

[2]: Vertical compressive strain at the top of the subgrade.

Table C.2.2 - Variation in Pavement Response with Thickness of Base Layer

Thickness of Base (in.)	Surface Deflections (milli-inch)							Critical Strains (10 ⁻⁴ in./in.)		Remaining Lives (10 ³ EASLs)	
	Radial Distance (in.)							Tensile ^[1]	Compressive ^[2]	Fatigue	Rutting
	0	12	24	36	48	60	72				
6	32.8	19.4	10.4	6.0	3.8	2.7	2.1	3.505	14.086	254	8
12	25.1	15.1	9.0	5.9	4.1	2.9	2.2	2.537	6.948	737	188
18	21.1	12.9	8.1	5.6	4.0	3.0	2.3	2.065	3.877	1451	2561
Sensitivity Index								0.8	2.1	1.9	25.3

[1]: Tangential tensile strain at the bottom of the AC layer;

[2]: Vertical compressive strain at the top of the subgrade.

Table C.2.3 - Variation in Pavement Response with Poisson's Ratio of Base Layer

Poisson's Ratio of Base	Surface Deflections (milli-inch)							Critical Strains (10^{-4} in./in.)		Remaining Lives (10^3 EASLs)	
	Radial Distance (in.)							Tensile ^[1]	Compressive ^[2]	Fatigue	Rutting
	0	12	24	36	48	60	72				
0.2	25.0	15.1	9.0	5.9	4.1	3.0	2.2	2.498	6.744	775	215
0.35	25.1	15.1	9.0	5.9	4.1	2.9	2.2	2.537	6.948	737	188
0.5	25.2	15.2	9.0	5.8	4.0	2.9	2.2	2.692	6.998	606	182
Sensitivity Index								0.14	0.07	0.41	0.33

[1]: Tangential tensile strain at the bottom of the AC layer;

[2]: Vertical compressive strain at the top of the subgrade.

Table C.2.4 - Variation in Pavement Response with Parameter k_2 of Base Layer

k_2 of Base	Surface Deflections (milli-inch)							Critical Strains (10^{-4} in./in.)		Remaining Lives (10^3 EASLs)	
	Radial Distance (in.)							Tensile ^[1]	Compressive ^[2]	Fatigue	Rutting
	0	12	24	36	48	60	72				
0.2	27.6	15.9	9.0	5.8	4.0	2.9	2.2	3.246	7.643	327	123
0.3	26.2	15.5	9.0	5.9	4.0	2.9	2.2	2.841	7.207	508	160
0.4	25.1	15.1	9.0	5.9	4.1	2.9	2.2	2.537	6.948	737	188
0.5	25.0	15.1	9.0	5.9	4.1	2.9	2.2	2.125	6.816	1321	205
0.6	23.7	14.8	8.9	5.9	4.1	3.0	2.2	1.837	6.746	2133	215
Sensitivity Index								0.7	0.2	3.8	0.7

[1]: Tangential tensile strain at the bottom of the AC layer;

[2]: Vertical compressive strain at the top of the subgrade.

Table C.2.5 - Variation in Pavement Response with Parameter k_3 of Base Layer

k_3 of Base	Surface Deflections (milli-inch)							Critical Strains (10^{-4} in./in.)		Remaining Lives (10^3 EASLs)	
	Radial Distance (in.)							Tensile ^[1]	Compressive ^[2]	Fatigue	Rutting
	0	12	24	36	48	60	72				
-0.1	21.9	14.3	8.7	5.9	4.2	3.0	2.3	1.747	6.041	2518	352
-0.2	23.7	14.6	8.9	5.9	4.1	3.0	2.2	2.077	6.696	1422	222
-0.3	25.1	15.1	9.0	5.9	4.1	2.9	2.2	2.537	6.948	737	188
-0.4	27.4	16.0	9.1	5.9	4.0	2.9	2.2	3.097	7.176	382	163
-0.5	29.4	16.6	9.2	5.8	4.0	2.9	2.2	3.609	7.796	231	112
Sensitivity Index								0.7	0.2	3.6	1.3

[1]: Tangential tensile strain at the bottom of the AC layer;

[2]: Vertical compressive strain at the top of the subgrade.

3) Properties of Subgrade

Table C.3.1 - Variation in Pavement Response with Modulus of Subgrade

Modulus of Subgrade	Surface Deflections (milli-inch)							Critical Strains (10 ⁻⁴ in./in.)		Remaining Lives (10 ³ EASLs)	
	Radial Distance (in.)							Tensile ^[1]	Compressive ^[2]	Fatigue	Rutting
(ksi)	0	12	24	36	48	60	72				
6	29.5	17.8	10.5	6.6	4.3	3.0	2.2	3.000	9.317	425	51
8	27.1	16.4	9.6	6.2	4.2	2.9	2.2	2.776	7.735	548	116
10	25.1	15.1	9.0	5.9	4.1	2.9	2.2	2.537	6.948	737	188
12	23.8	14.3	8.6	5.7	4.0	2.9	2.2	2.393	6.117	893	333
14	22.7	13.7	8.3	5.5	4.0	2.9	2.2	2.290	5.584	1032	500
Sensitivity Index								0.5	0.9	1.3	4.1

[1]: Tangential tensile strain at the bottom of the AC layer;

[2]: Vertical compressive strain at the top of the subgrade.

Table C.3.2 -Variation in Pavement Response with Poisson's Ratio of Subgrade

Poisson's Ratio of Subgrade	Surface Deflections (milli-inch)							Critical Strains (10^{-4} in./in.)		Remaining Lives (10^3 EASLs)	
	Radial Distance (in.)							Tensile ^[1]	Compressive ^[2]	Fatigue	Rutting
	0	12	24	36	48	60	72				
0.3	25.0	15.2	9.1	6.1	4.3	3.2	2.4	2.466	7.260	809	154
0.4	25.1	15.1	9.0	5.9	4.1	2.9	2.2	2.537	6.948	737	188
0.5	24.9	14.7	8.5	5.3	3.5	2.4	1.7	2.610	5.699	671	456
Sensitivity Index								0.1	0.7	0.4	5.7

[1]: Tangential tensile strain at the bottom of the AC layer;

[2]: Vertical compressive strain at the top of the subgrade.

Table C.3.3 - Variation in Pavement Response with Parameter k_2 of Upper Subgrade

k_2 of Upper Subgrade	Surface Deflections (milli-inch)							Critical Strains (10^{-4} in./in.)		Remaining Lives (10^3 EASLs)	
	Radial Distance (in.)							Tensile ^[1]	Compressive ^[2]	Fatigue	Rutting
	0	12	24	36	48	60	72				
0	26.3	15.8	9.3	6.0	4.1	2.9	2.2	2.729	7.510	580	133
0.1	25.7	15.5	9.2	5.9	4.1	2.9	2.2	2.661	6.987	630	183
0.2	25.1	15.1	9.0	5.9	4.1	2.9	2.2	2.537	6.948	737	188
0.3	24.7	14.9	8.9	5.9	4.1	2.9	2.2	2.458	6.462	818	260
0.4	24.3	14.7	8.8	5.8	4.1	2.9	2.2	2.397	6.136	888	328
Sensitivity Index								0.10	0.14	0.29	0.77

[1]: Tangential tensile strain at the bottom of the AC layer;

[2]: Vertical compressive strain at the top of the subgrade.

Table C.3.4 - Variation in Pavement Response with Parameter k_3 of Upper Subgrade

k_3 of Upper Subgrade	Surface Deflections (milli-inch)							Critical Strains (10^{-4} in./in.)		Remaining Lives (10^3 EASLs)	
	Radial Distance (in.)							Tensile ^[1]	Compressive ^[2]	Fatigue	Rutting
	0	12	24	36	48	60	72				
0	24.0	14.4	8.7	5.8	4.0	2.9	2.2	2.432	5.190	847	694
-0.1	24.8	14.9	8.9	5.8	4.1	2.9	2.2	2.487	5.987	787	366
-0.2	25.1	15.1	9.0	5.9	4.1	2.9	2.2	2.537	6.858	737	199
-0.3	26.3	15.7	9.2	5.9	4.1	2.9	2.2	2.731	7.577	578	128
-0.4	27.0	16.1	9.4	6.0	4.1	2.9	2.2	2.787	8.319	541	84
Sensitivity Index								0.15	0.25	0.43	2.48

[1]: Tangential tensile strain at the bottom of the AC layer;

[2]: Vertical compressive strain at the top of the subgrade.

4) Depth to Bedrock

Table C.4.1 - Variation in Pavement Response with Depth to Bedrock

Depth to Bedrock	Surface Deflections (milli-inch)							Critical Strains (10 ⁻⁴ in./in.)		Remaining Lives (10 ³ EASLs)	
	Radial Distance (in.)							Tensile ^[1]	Compressive ^[2]	Fatigue	Rutting
(in.)	0	12	24	36	48	60	72				
250	24.9	14.9	8.8	5.7	3.9	2.7	2.0	2.531	6.969	743	185
300	25.1	15.1	9.0	5.9	4.1	2.9	2.2	2.537	6.948	737	188
350	25.3	15.2	9.2	6.0	4.2	3.1	2.3	2.536	6.943	738	189
Sensitivity Index								0.01	0.02	0.05	0.08

[1]: Tangential tensile strain at the bottom of the AC layer;

[2]: Vertical compressive strain at the top of the subgrade.

APPENDIX D

**RESPONSES OF TYPICAL PAVEMENT SECTION
UNDER LINEAR DYNAMIC MODEL**

1) Damping Coefficient $\beta=0.0$

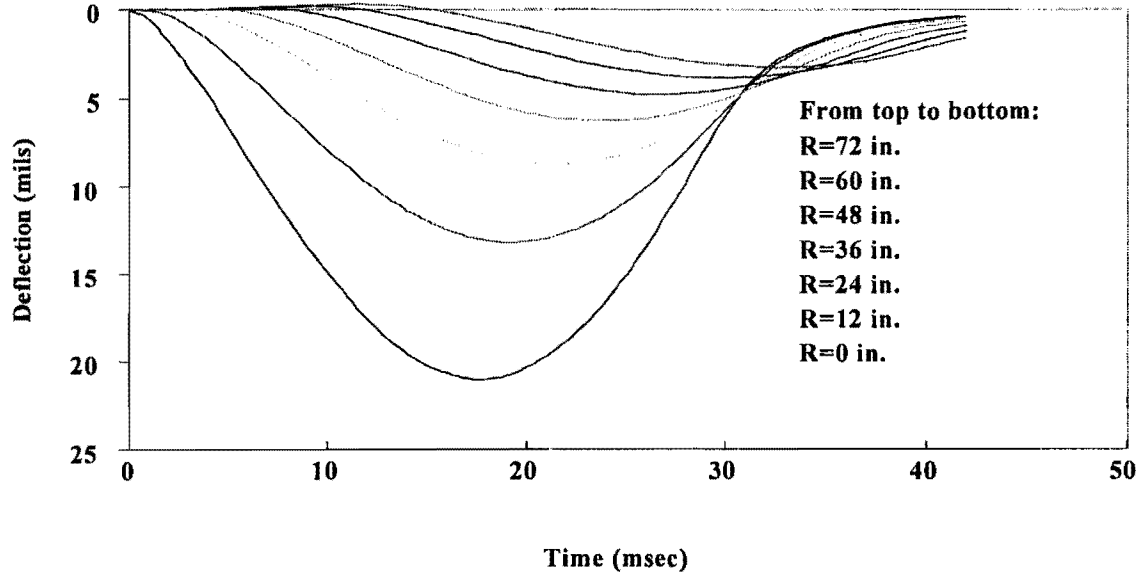


Figure D.1.1 - Time Histories of Surface Deflections

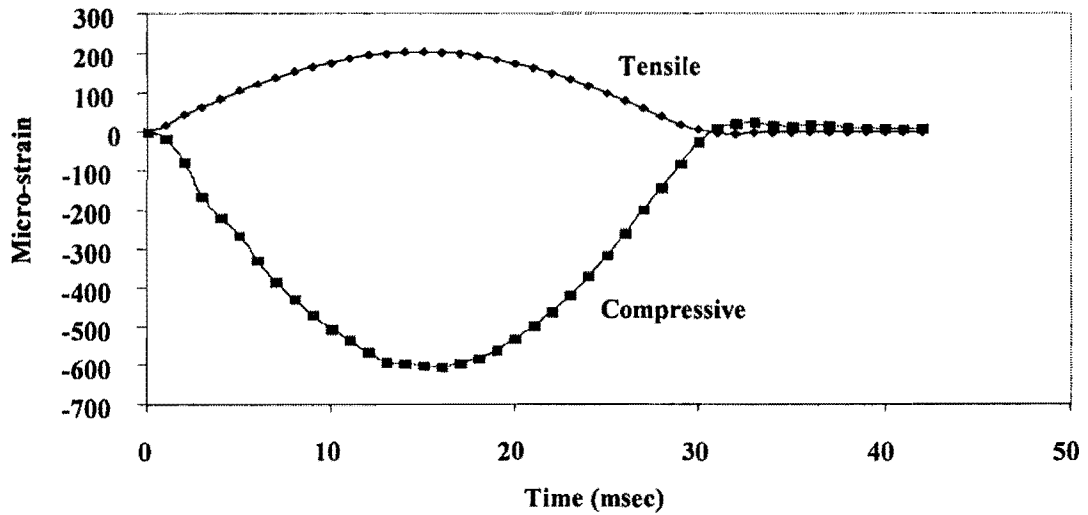


Figure D.1.2 - Time Histories of Critical Strains

2) Damping Coefficient $\beta=0.00114$

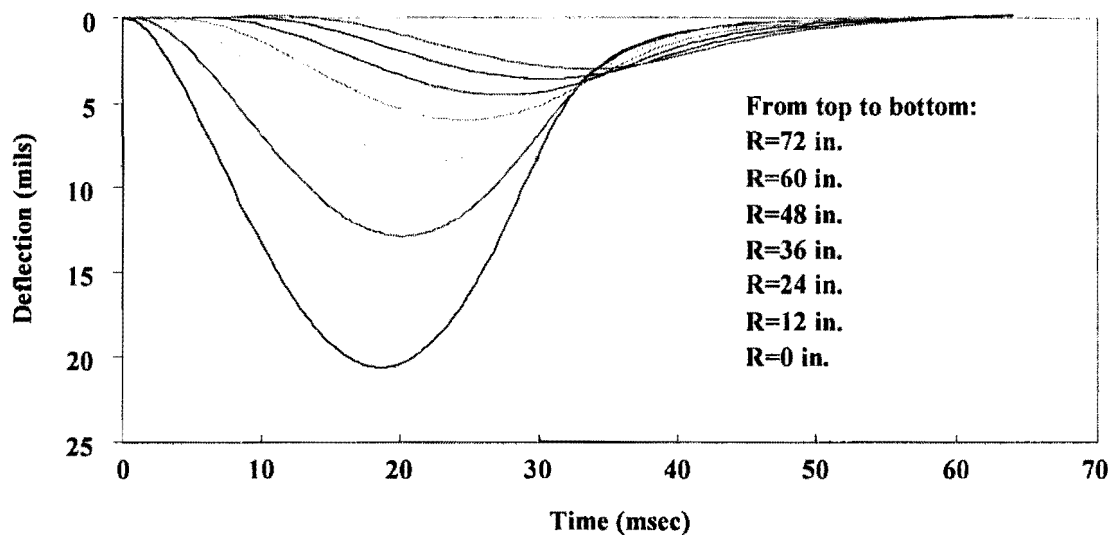


Figure D.2.1 - Time Histories of Surface Deflections

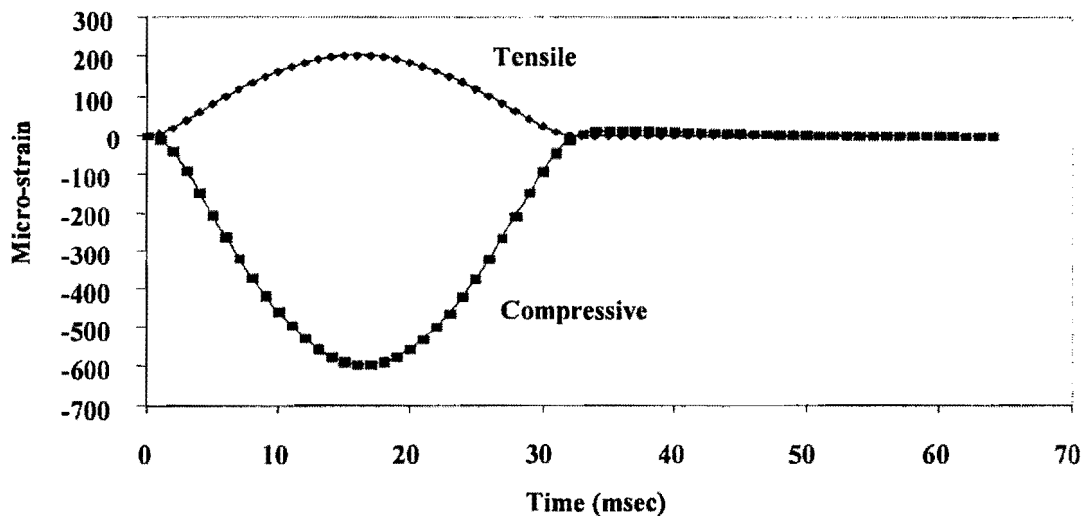


Figure D.2.2 - Time Histories of Critical Strains

3) Damping Coefficient $\beta=0.00228$

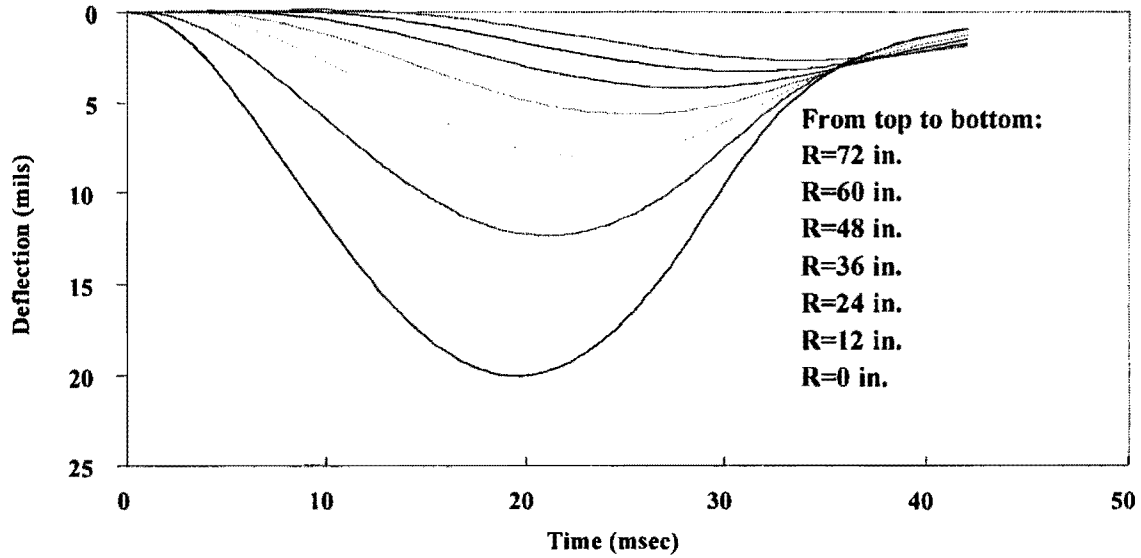


Figure D.3.1 - Time Histories of Surface Deflections

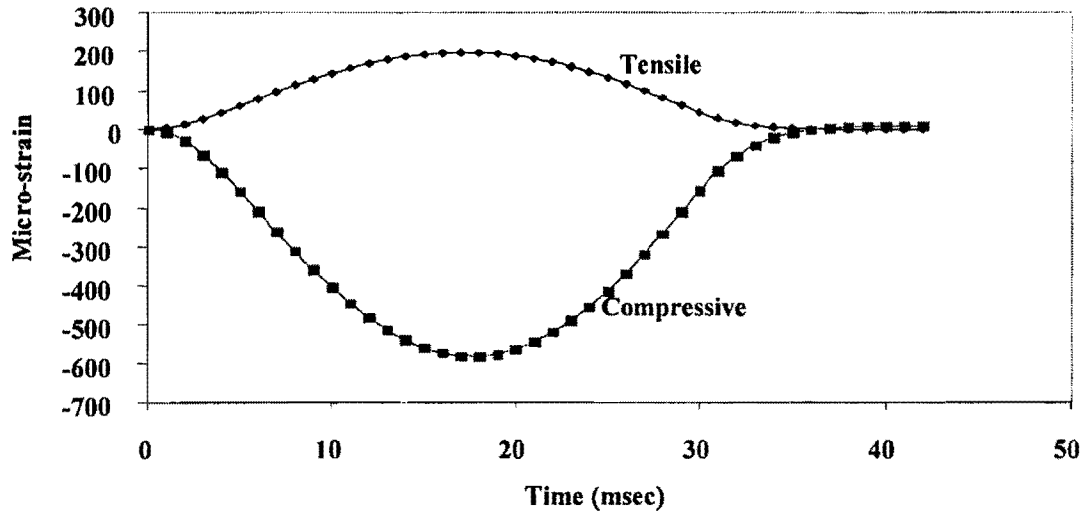


Figure D.3.2 - Time Histories of Critical Strains

4) 75% of Standard Densities

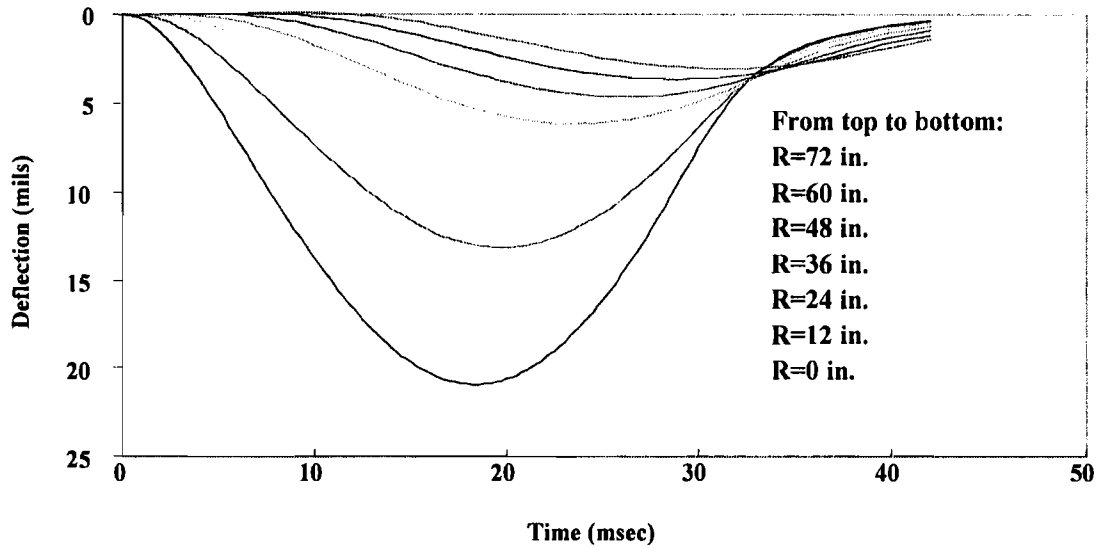


Figure D.4.1 - Time Histories of Surface Deflections

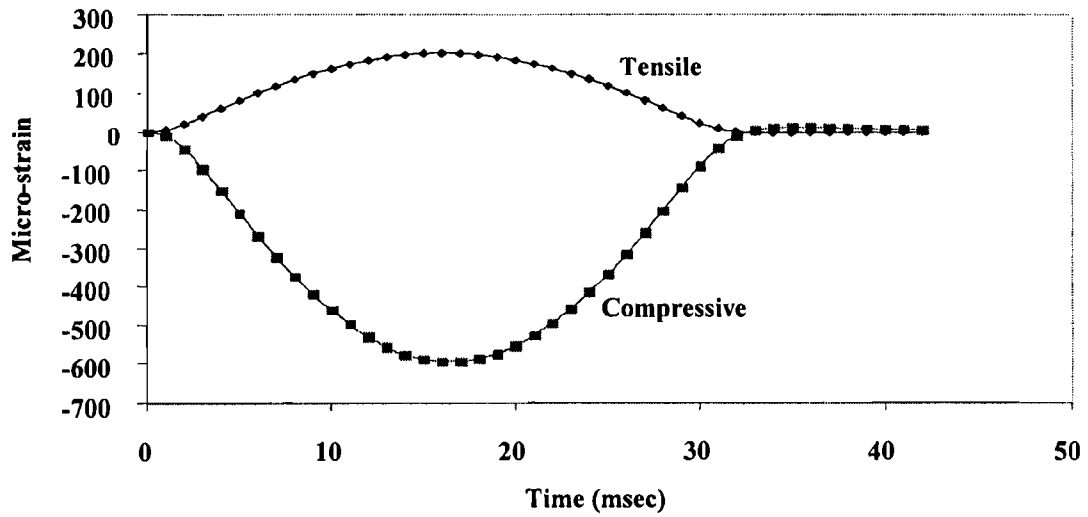


Figure D.4.2 - Time Histories of Critical Strains

5) Standard Densities

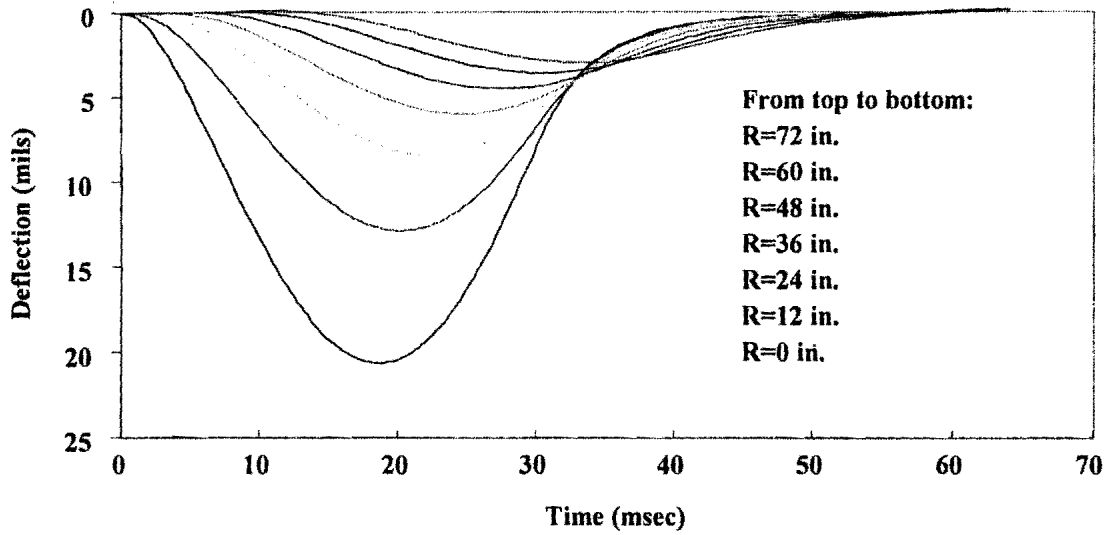


Figure D.5.1 - Time Histories of Surface Deflections

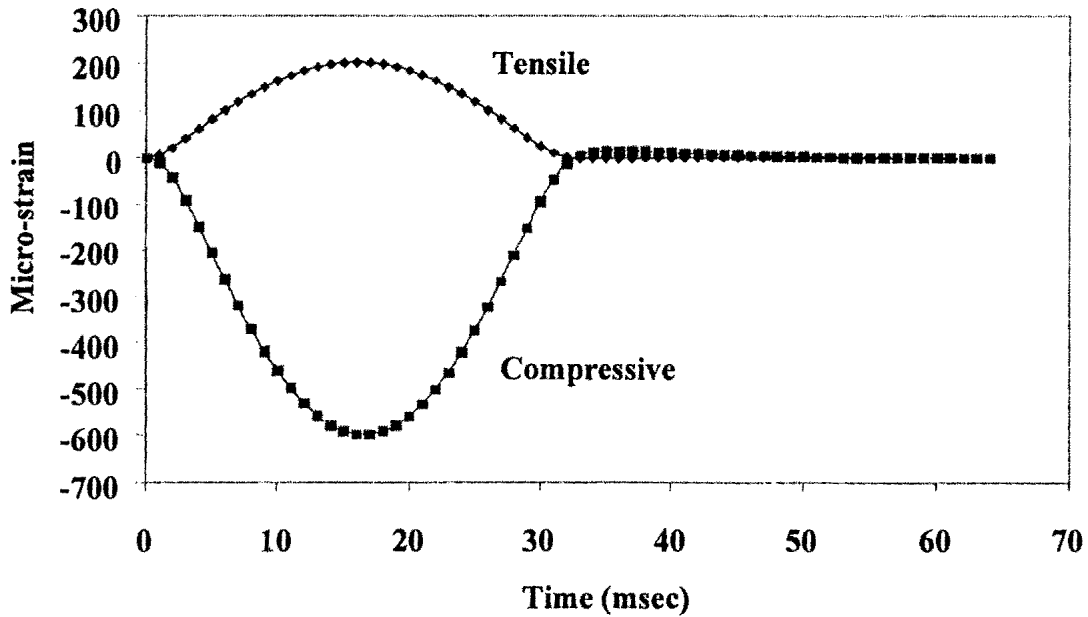


Figure D.5.2 - Time Histories of Critical Strains

6) 125% of Standard Densities

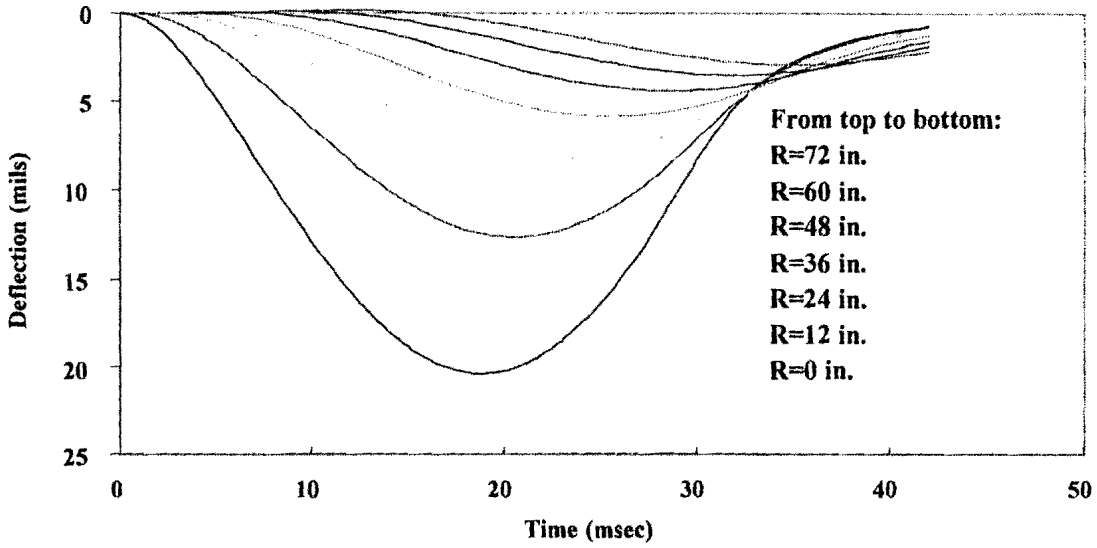


Figure D.6.1 - Time Histories of Surface Deflections

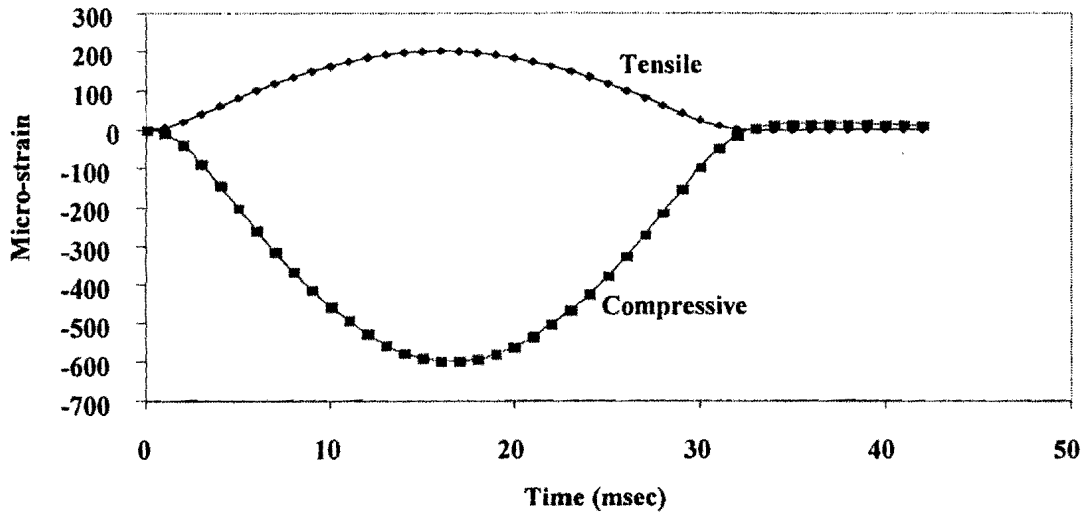


Figure D.6.2 - Time Histories of Critical Strains

APPENDIX E

RESPONSES OF TYPICAL PAVEMENT SECTION UNDER NONLINEAR DYNAMIC MODEL

1) k_2 of Base = 0.2

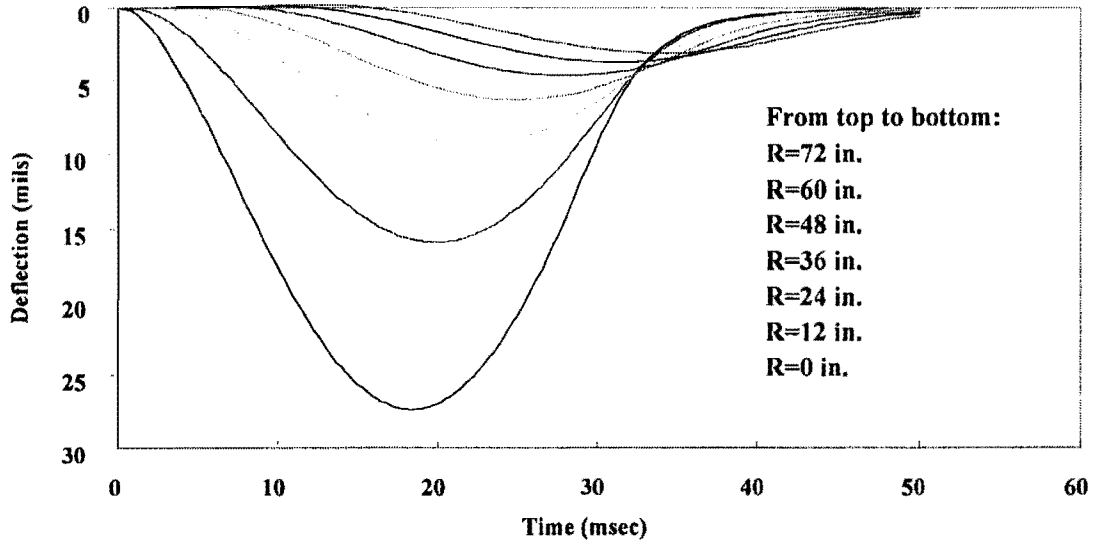


Figure E.1.1 - Time Histories of Surface Deflections

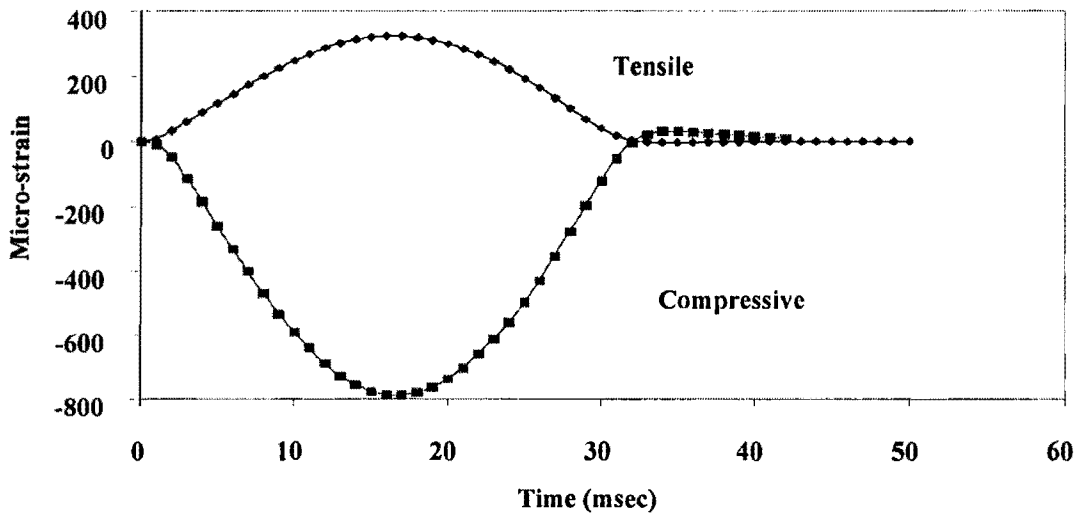


Figure E.1.2 - Time Histories of Critical Strains

2) k_2 of Base = 0.3

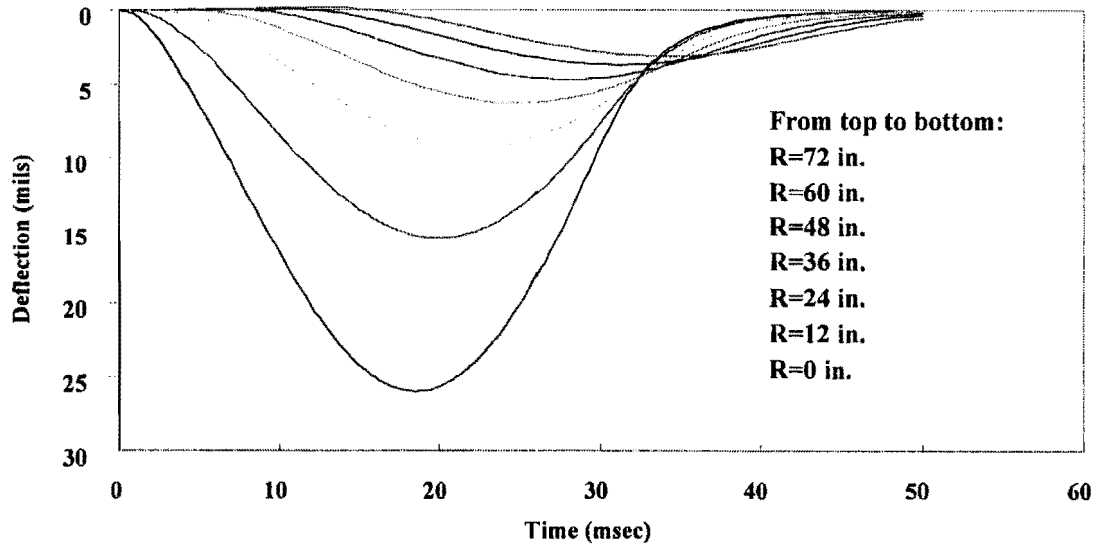


Figure E.2.1 - Time Histories of Surface Deflections

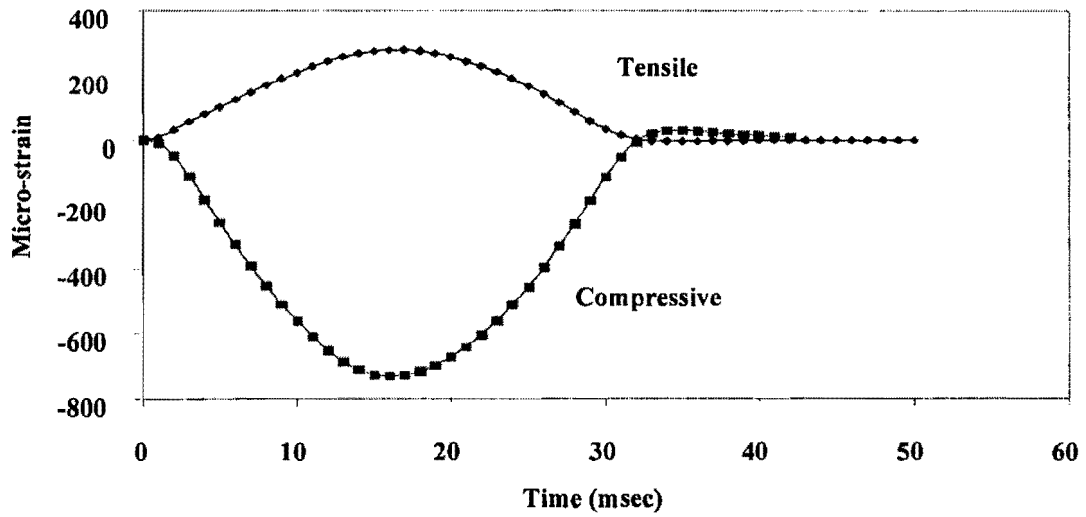


Figure E.2.2 - Time Histories of Critical Strains

3) k_2 of Base = 0.4

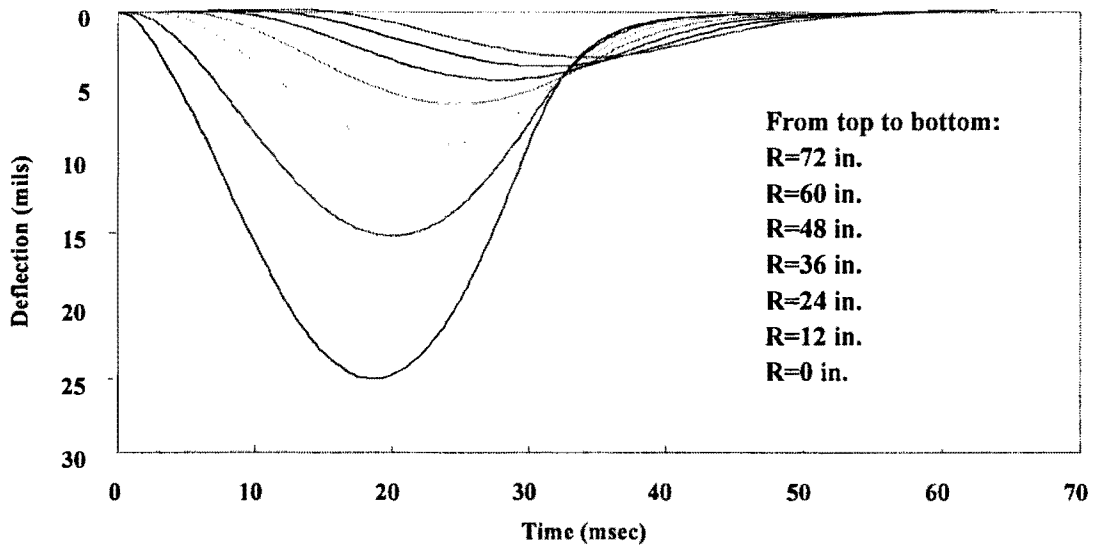


Figure E.3.1 - Time Histories of Surface Deflections

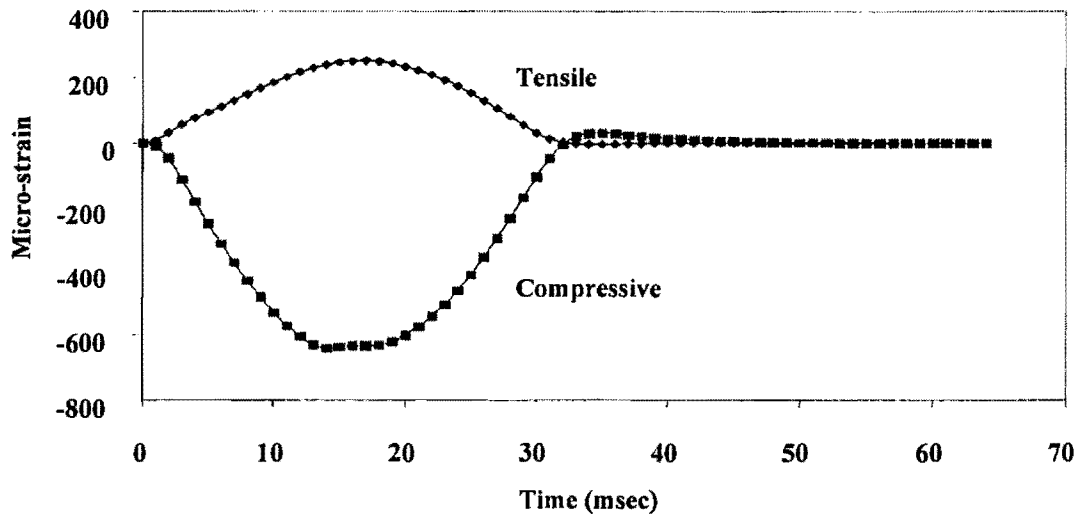


Figure E.3.2 - Time Histories of Critical Strains

4) k_2 of Base = 0.5

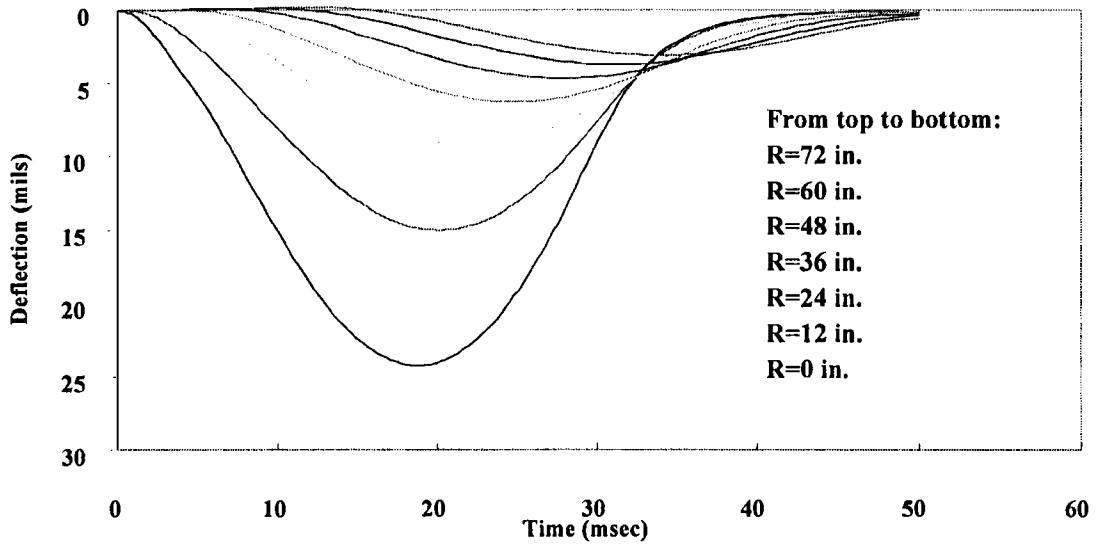


Figure E.4.1 - Time Histories of Surface Deflections

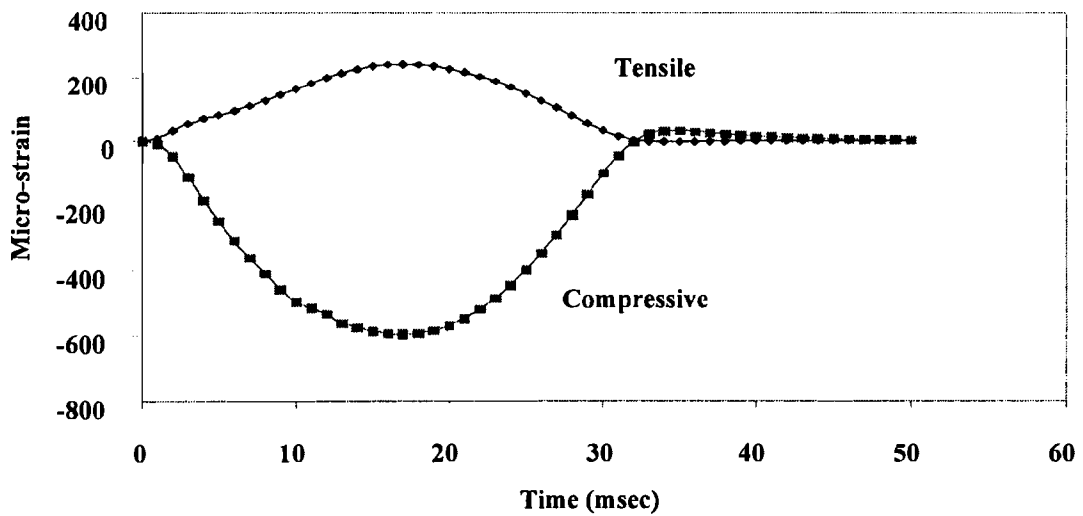


Figure E.4.2 - Time Histories of Critical Strains

5) k_2 of Base = 0.6

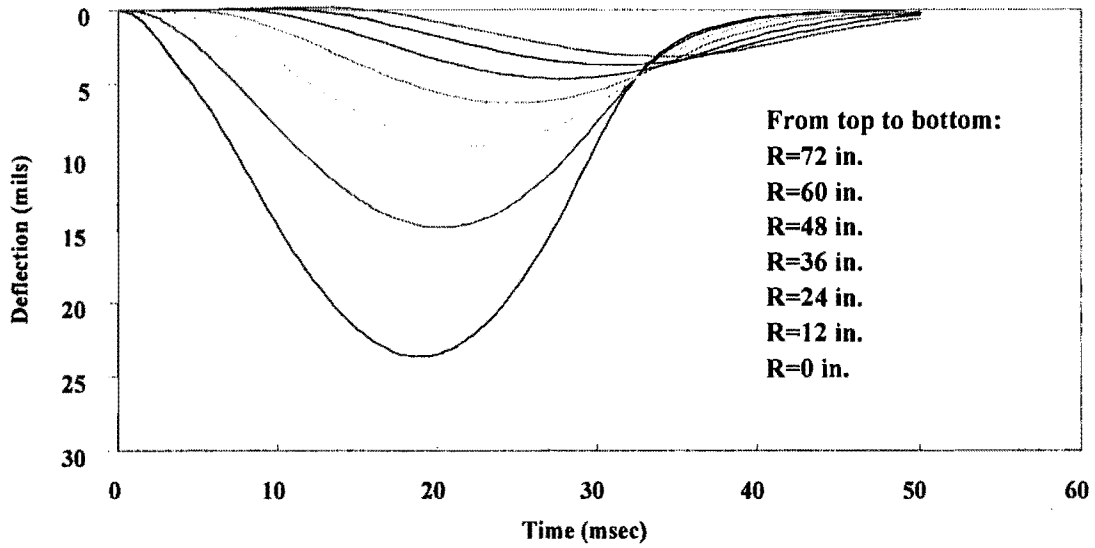


Figure E.5.1 - Time Histories of Surface Deflections

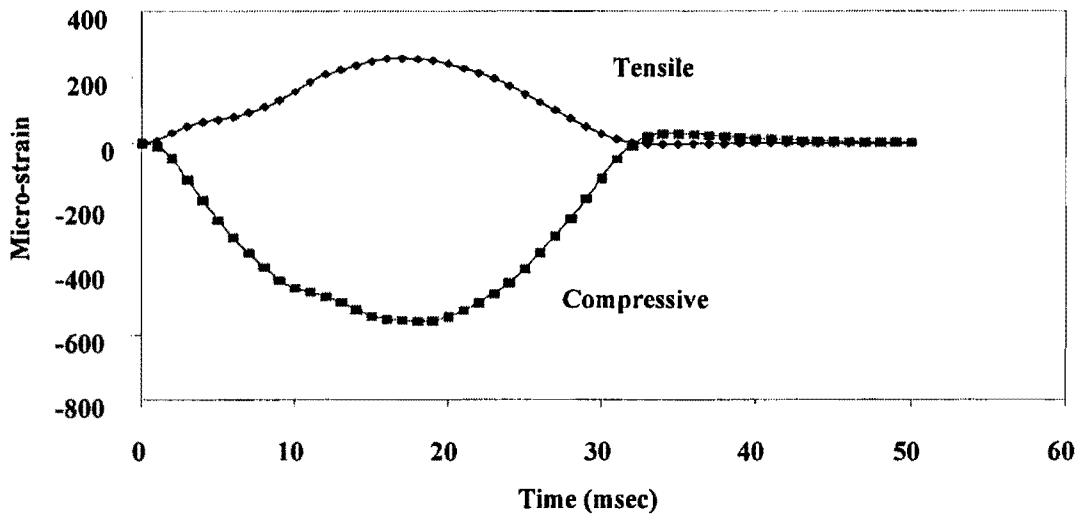


Figure E.5.2 - Time Histories of Critical Strains

6) k_3 of Base = -0.1

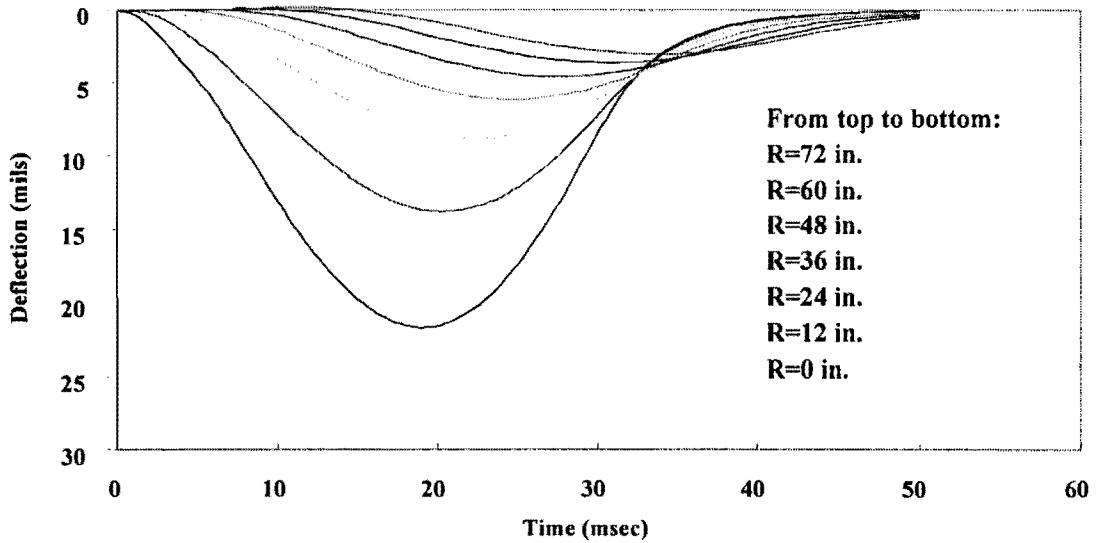


Figure E.6.1 - Time Histories of Surface Deflections

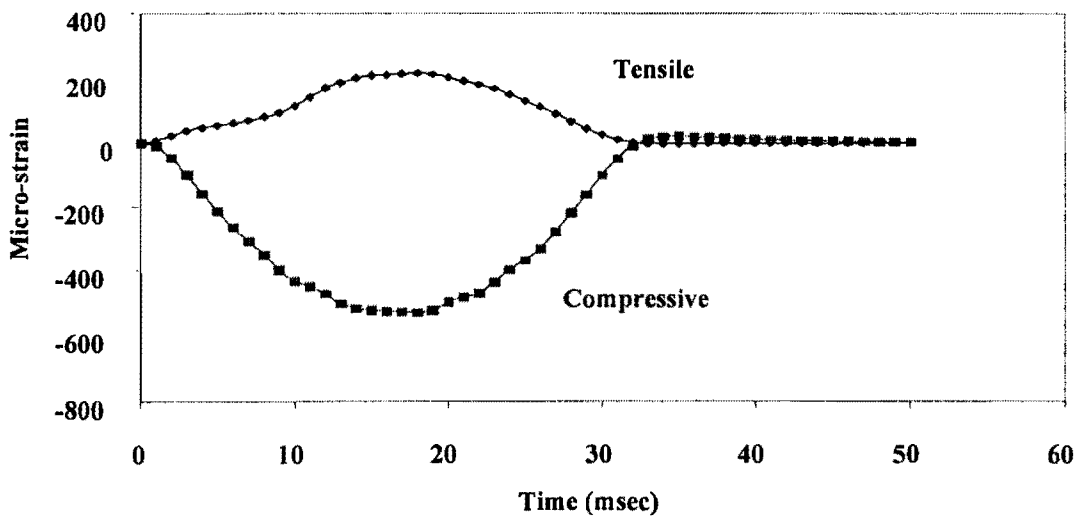


Figure E.6.2 - Time Histories of Critical Strains

7) k_3 of Base = -0.2

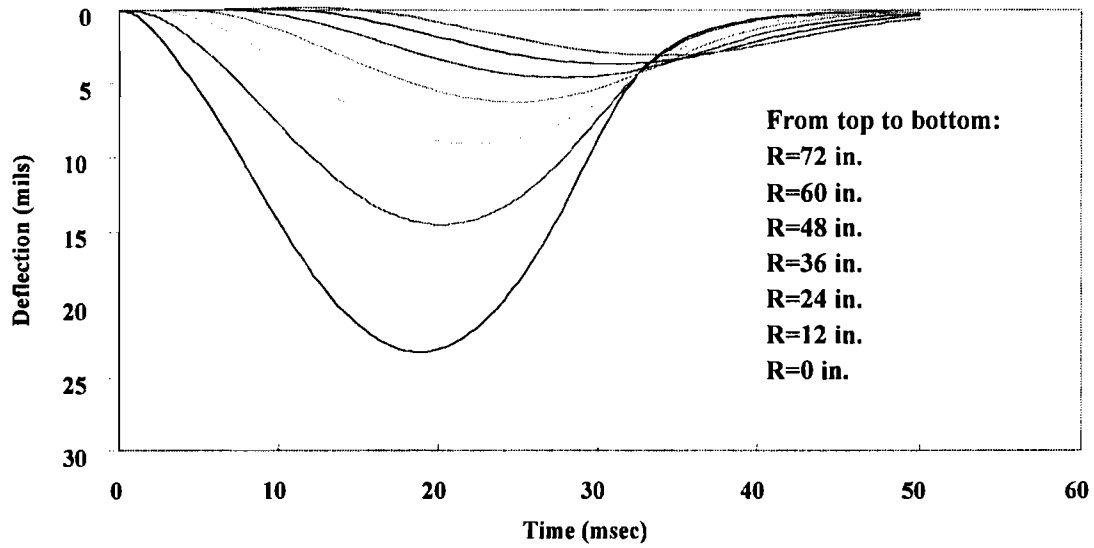


Figure E.7.1 - Time Histories of Surface Deflections

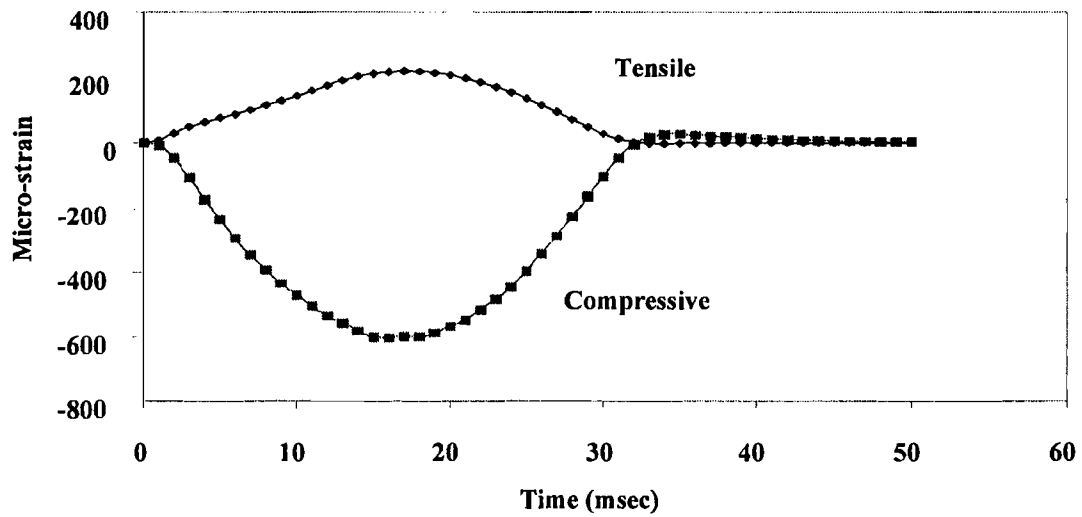


Figure E.7.2 - Time Histories of Critical Strains

8) k_3 of Base = -0.3

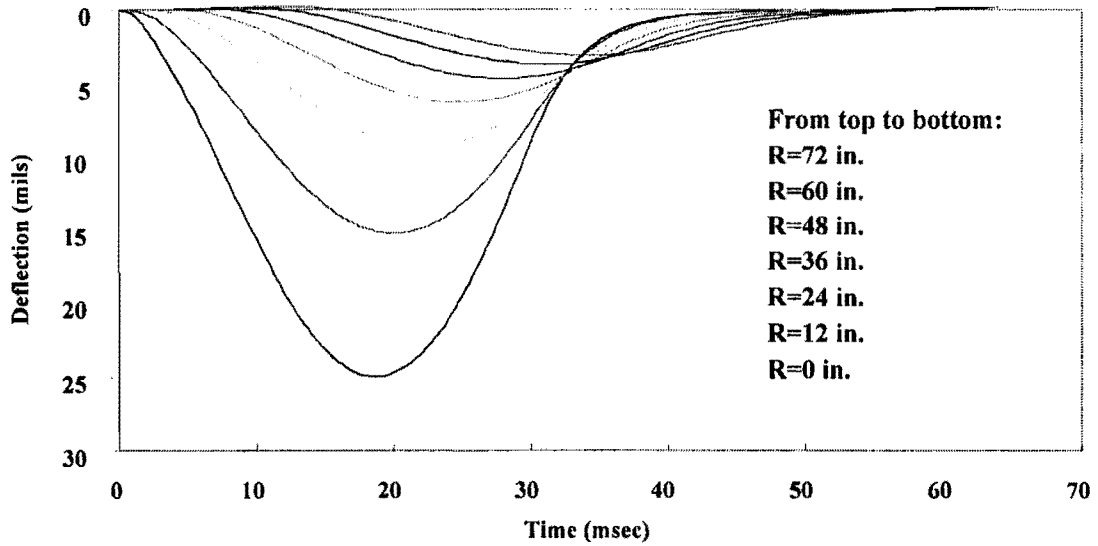


Figure E.8.1 - Time Histories of Surface Deflections

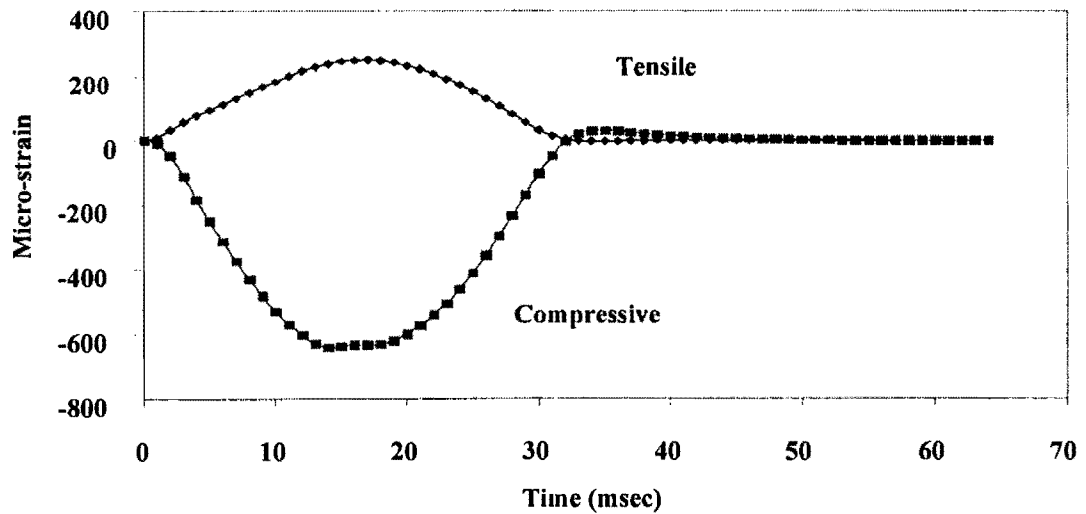


Figure E.8.2 - Time Histories of Critical Strains

9) k_3 of Base = -0.4

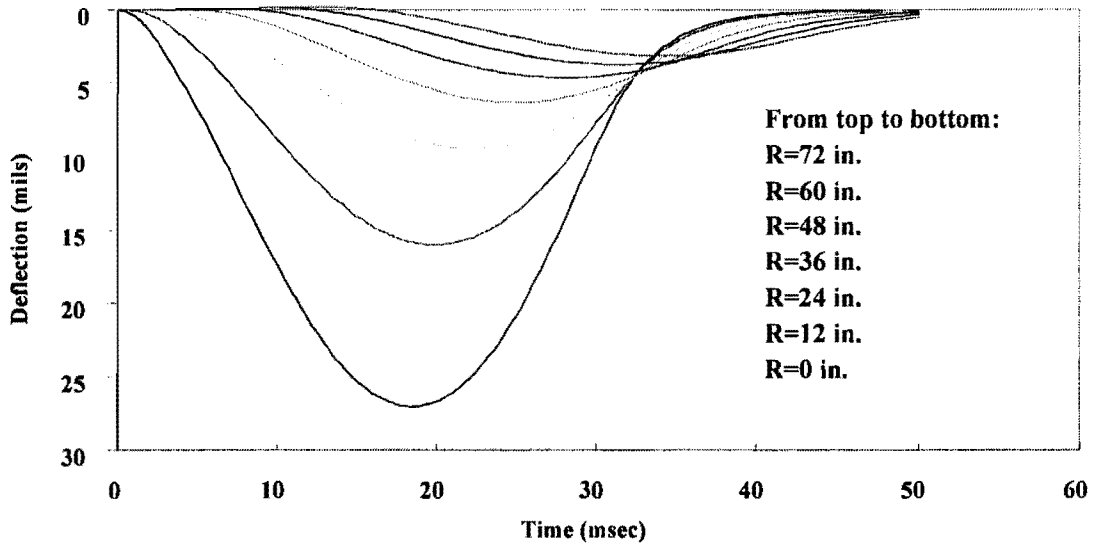


Figure E.9.1 - Time Histories of Surface Deflections

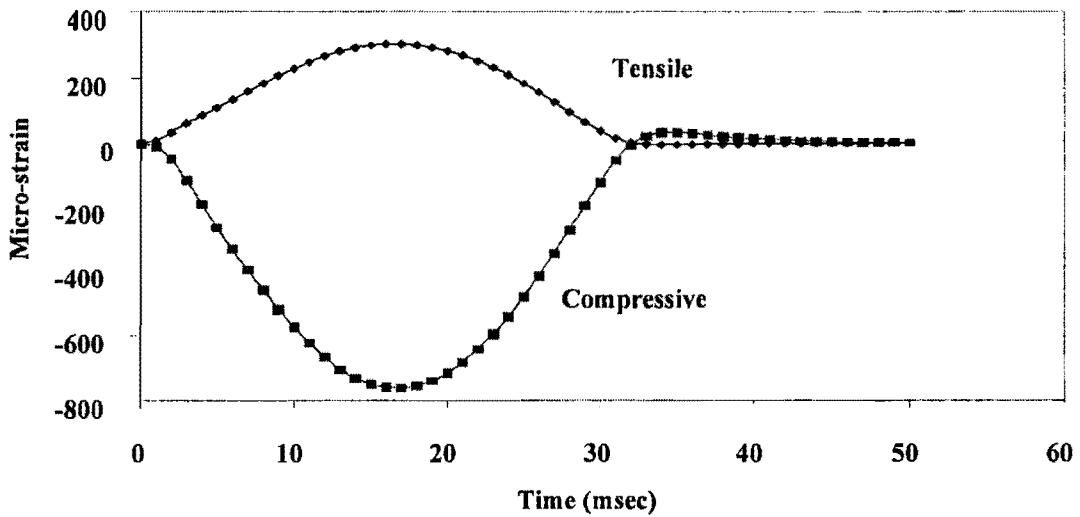


Figure E.9.2 - Time Histories of Critical Strains

10) k_3 of Base = -0.5

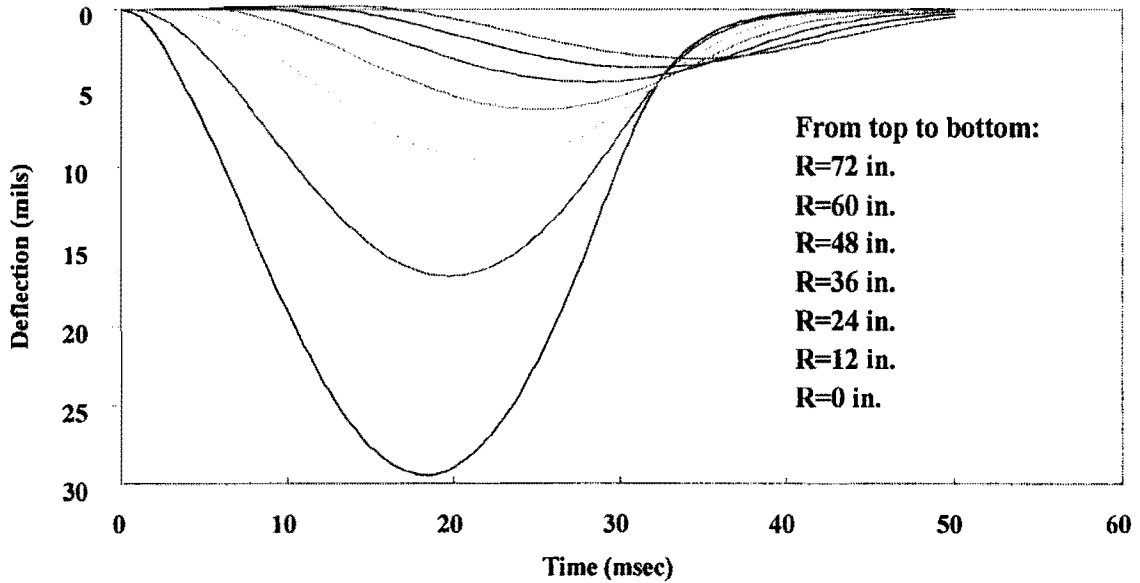


Figure E.10.1 - Time Histories of Surface Deflections

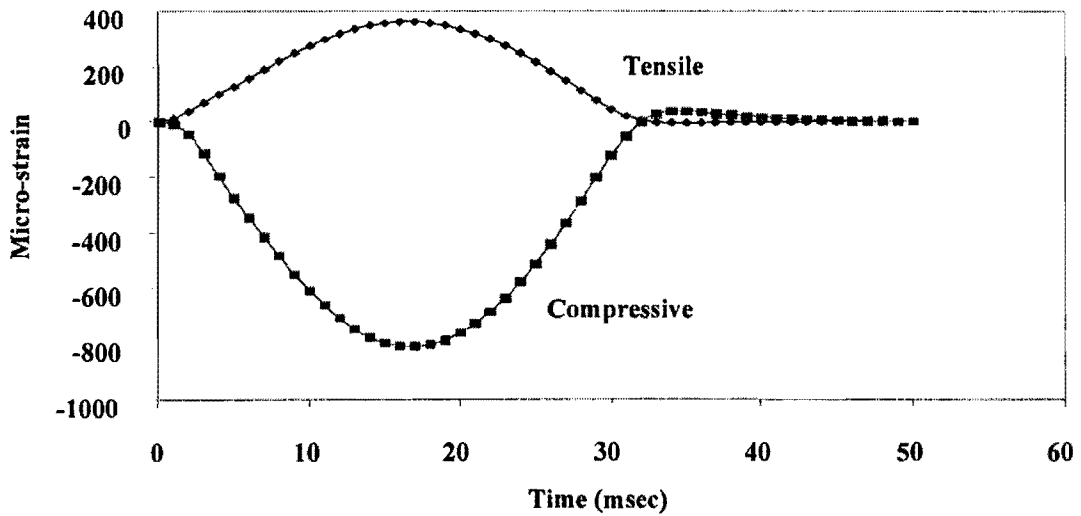


Figure E.10.2 - Time Histories of Critical Strains

11) k_2 of Upper Subgrade = 0.0

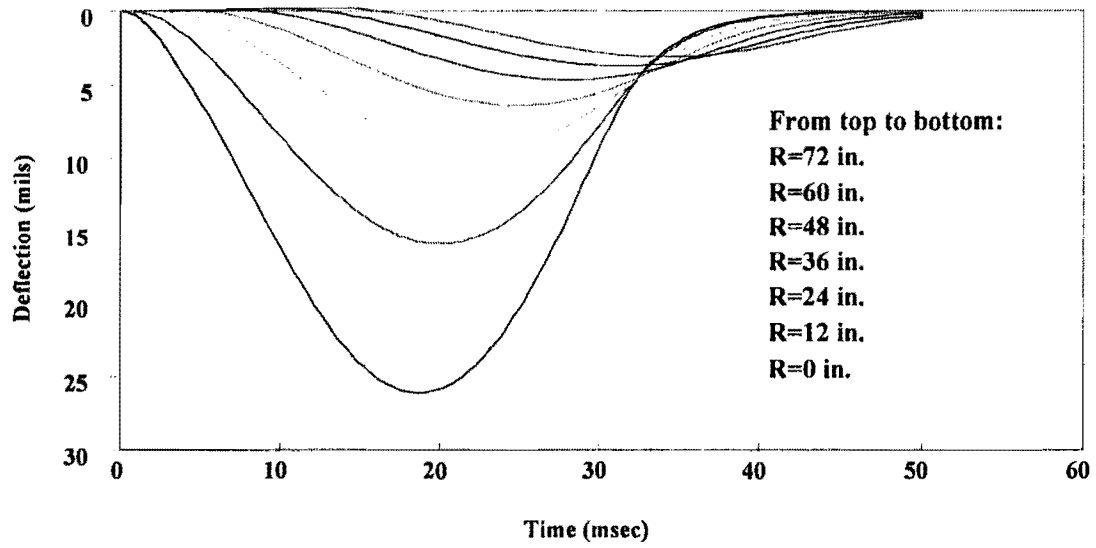


Figure E.11.1 - Time Histories of Surface Deflections

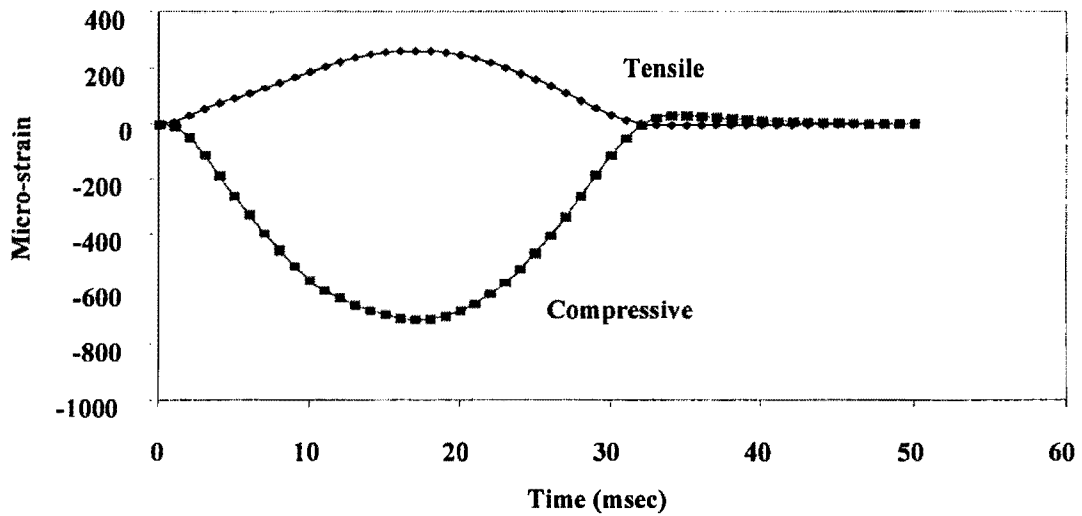


Figure E.11.2 - Time Histories of Critical Strains

12) k_2 of Upper Subgrade = 0.1

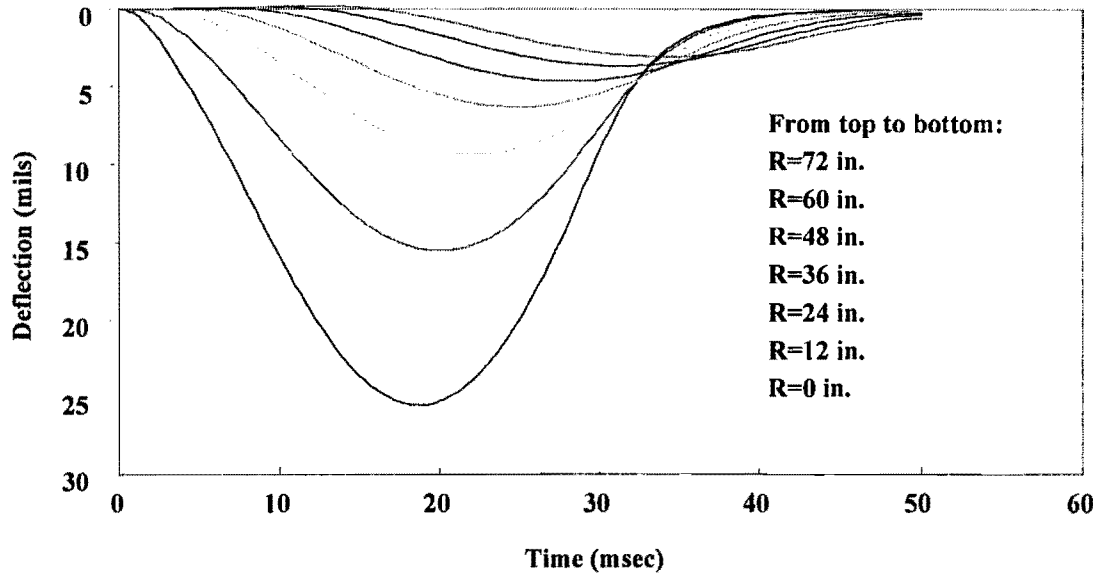


Figure E.12.1 - Time Histories of Surface Deflections

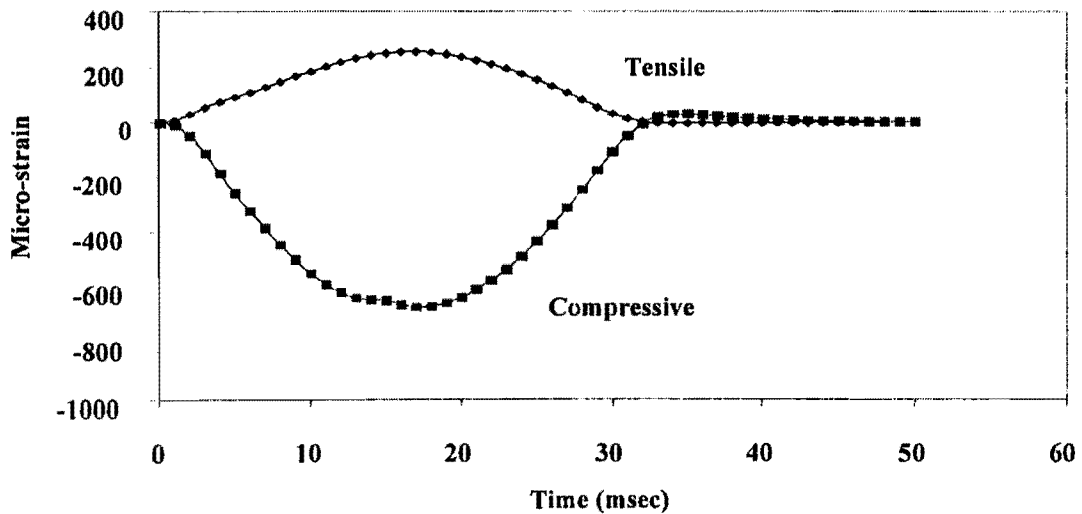


Figure E.12.2 - Time Histories of Critical Strains

13) k_2 of Upper Subgrade = 0.2

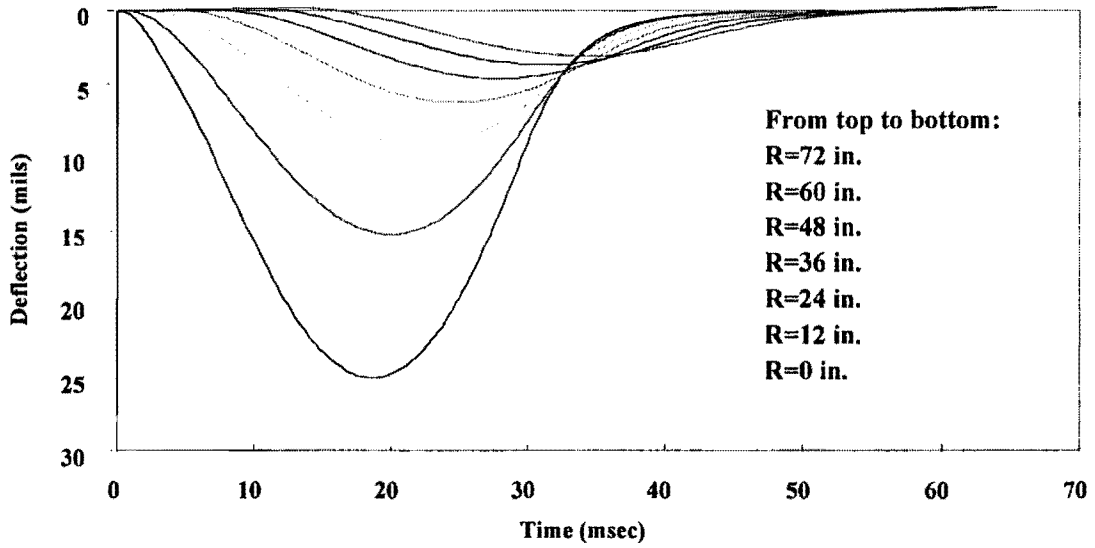


Figure E.13.1 - Time Histories of Surface Deflections

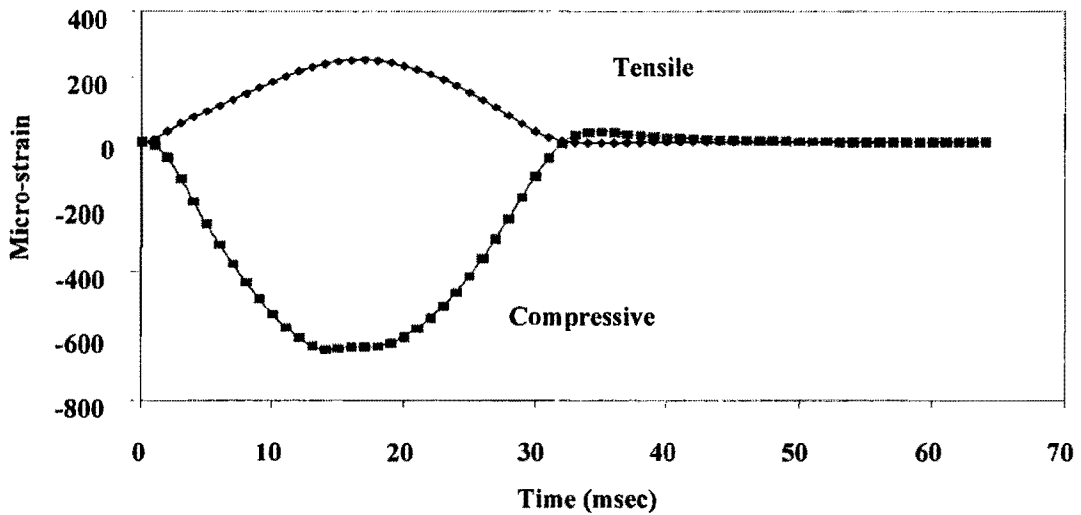


Figure E.13.2 - Time Histories of Critical Strains

14) k_2 of Upper Subgrade = 0.3

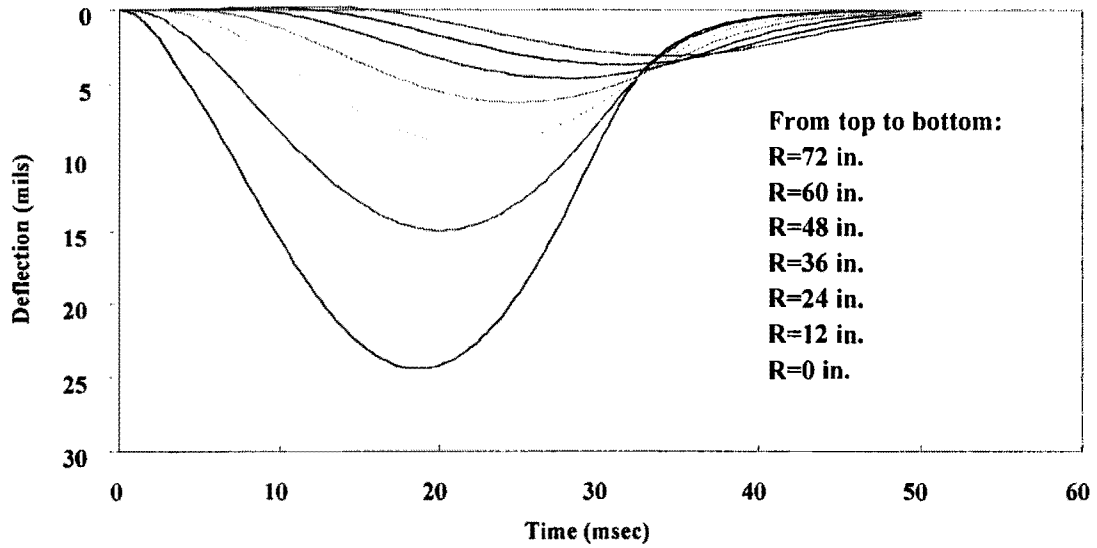


Figure E.14.1 - Time Histories of Surface Deflections

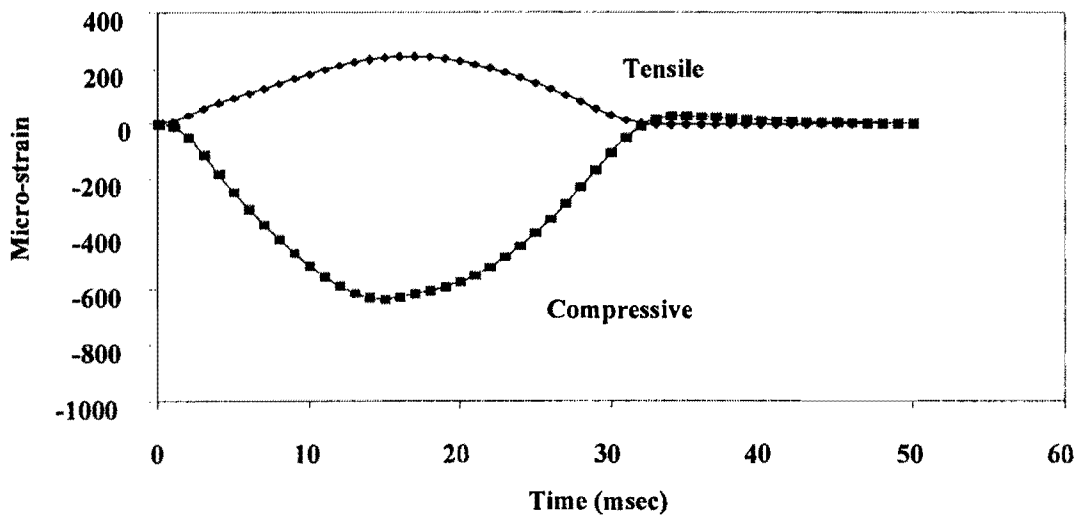


Figure E.14.2 - Time Histories of Critical Strains

15) k_2 of Upper Subgrade = 0.4

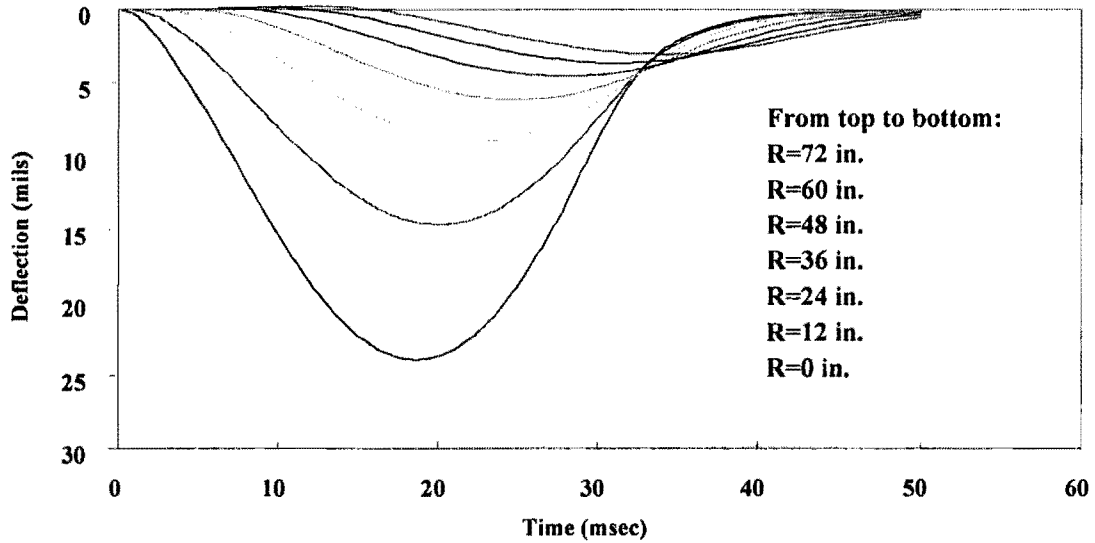


Figure E.15.1 - Time Histories of Surface Deflections

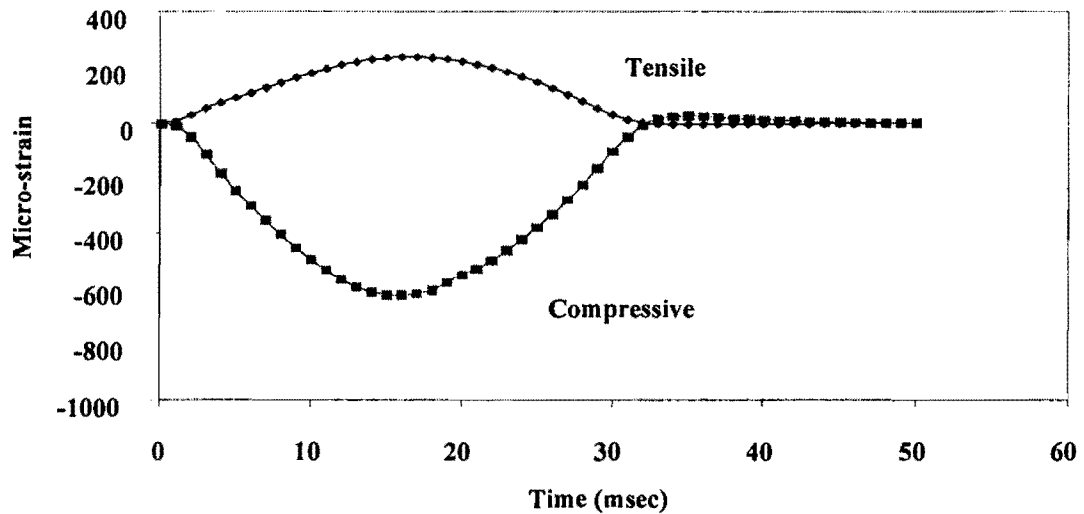


Figure E.15.2 - Time Histories of Critical Strains

16) k_3 of Upper Subgrade = 0.0

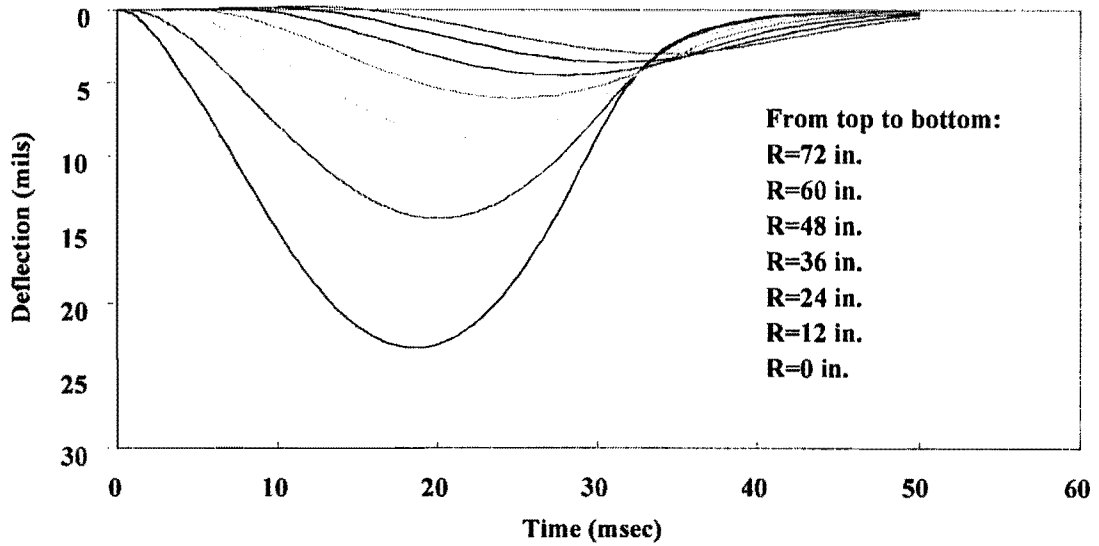


Figure E.16.1 - Time Histories of Surface Deflections

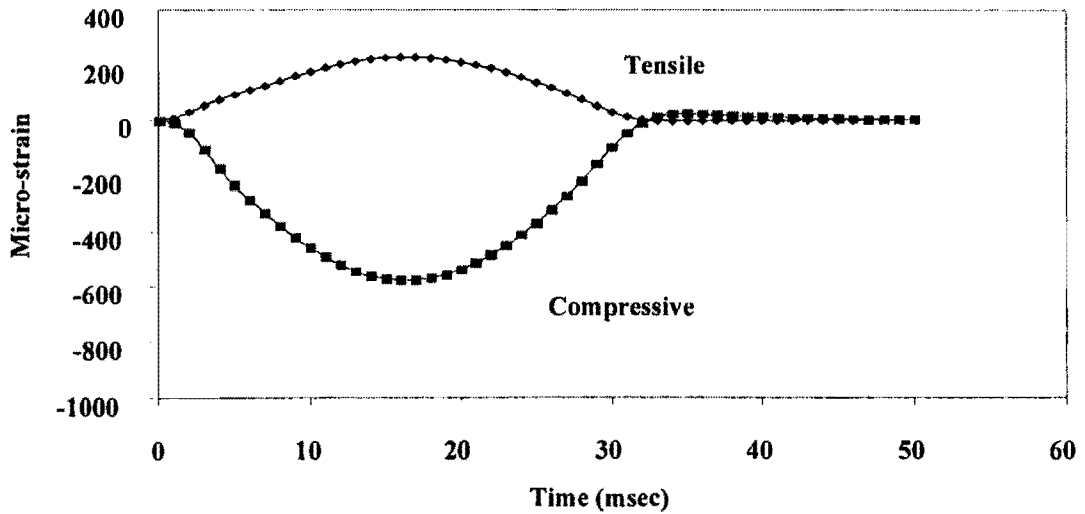


Figure E.16.2 - Time Histories of Critical Strains

17) k_3 of Upper Subgrade = -0.1

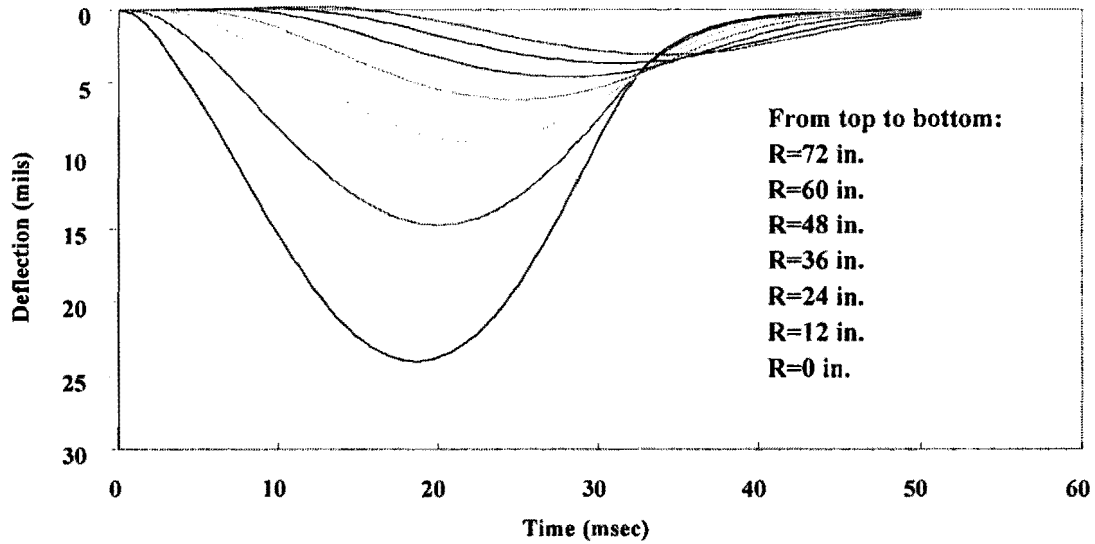


Figure E.17.1 - Time Histories of Surface Deflections

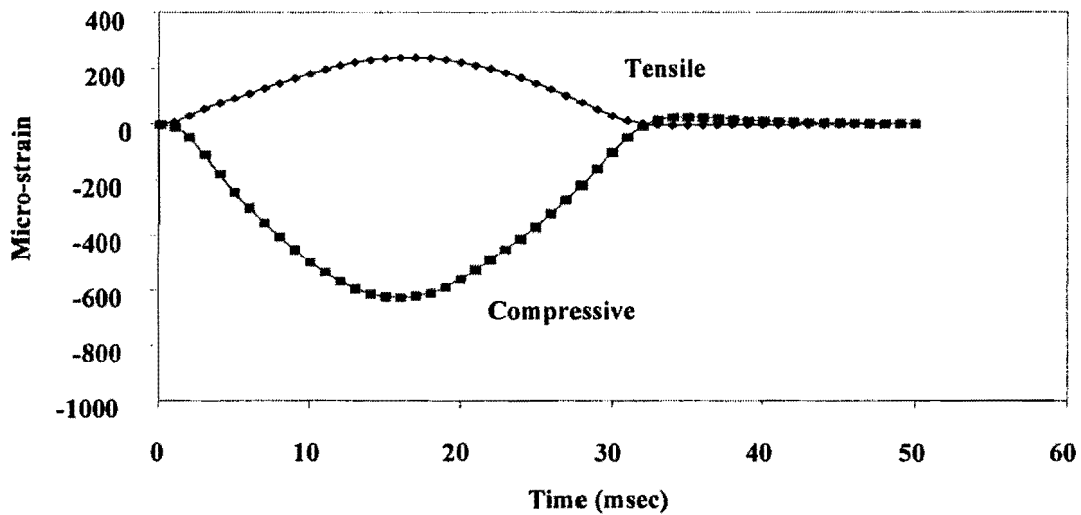


Figure E.17.2 - Time Histories of Critical Strains

18) k_3 of Upper Subgrade = -0.2

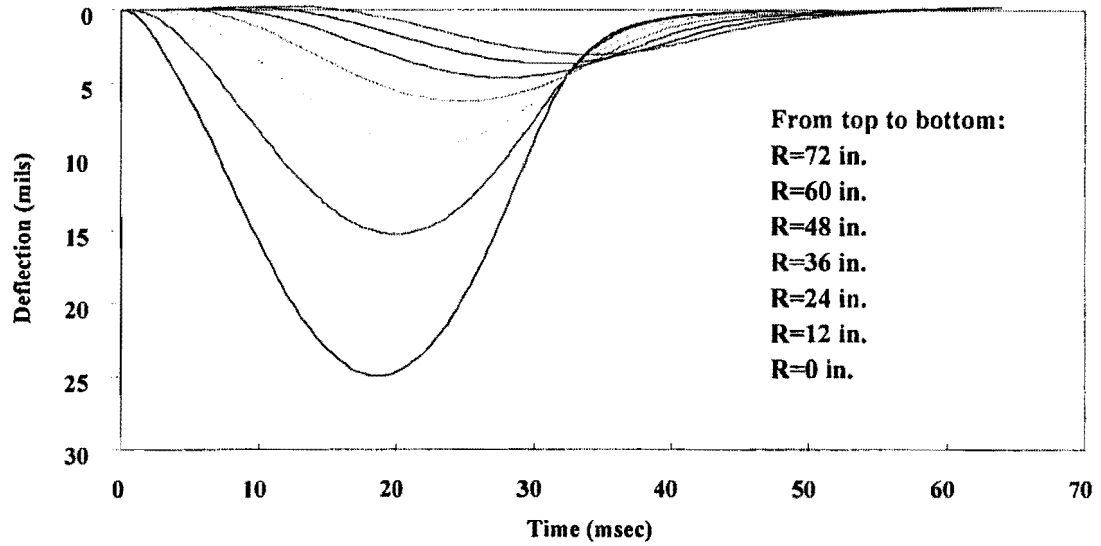


Figure E.18.1 - Time Histories of Surface Deflections

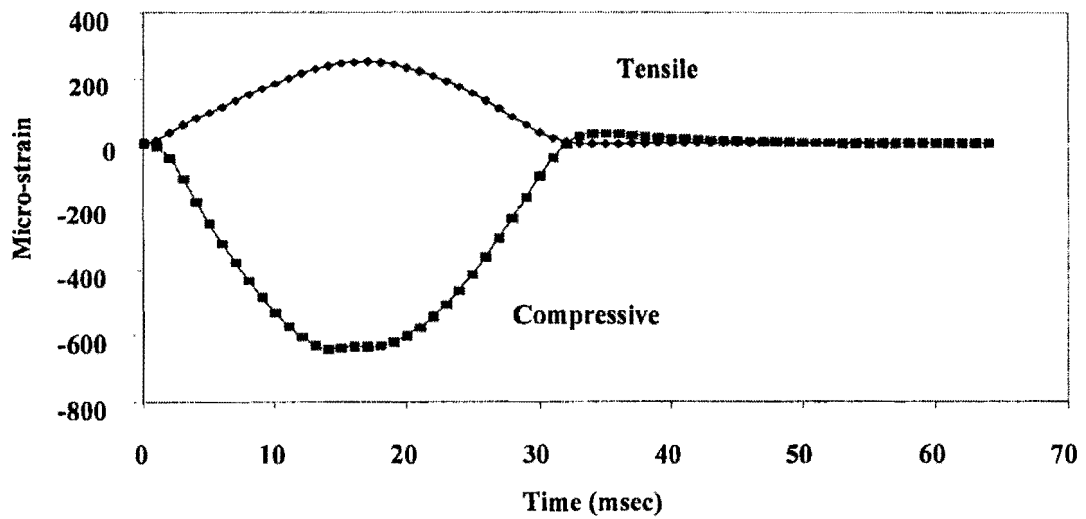


Figure E.18.2 - Time Histories of Critical Strains

19) k_3 of Upper Subgrade = -0.3

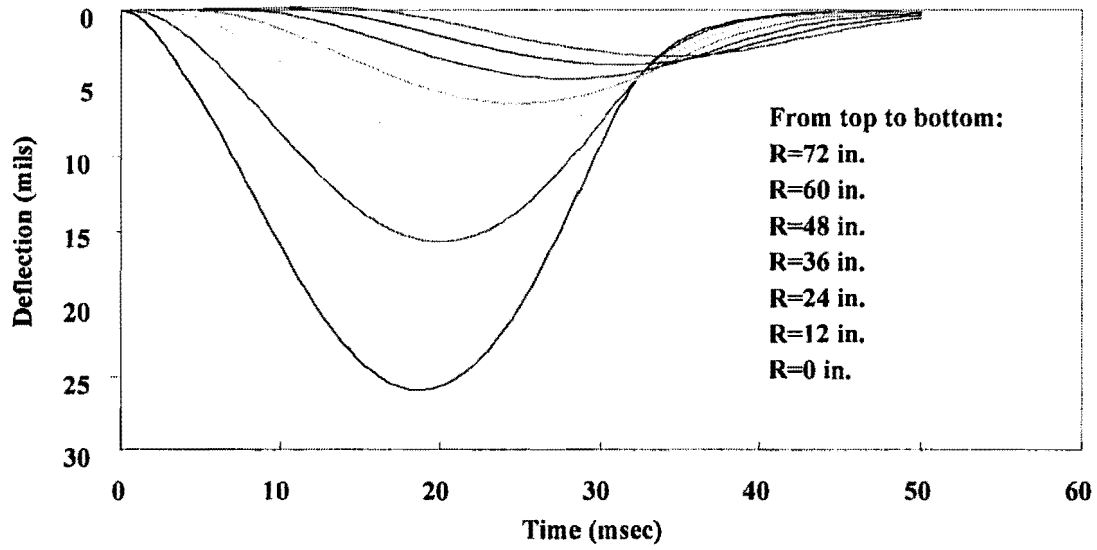


Figure E.19.1 - Time Histories of Surface Deflections

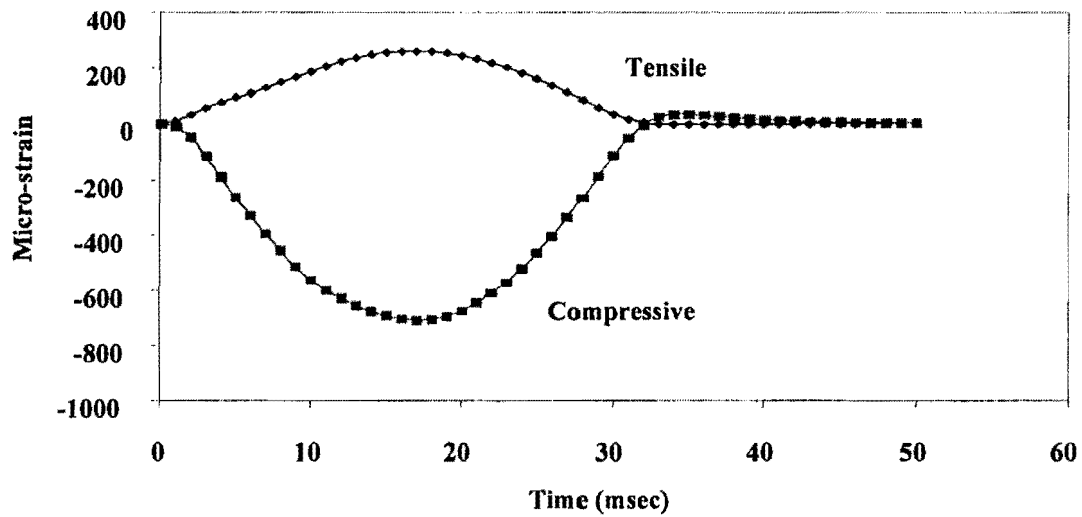


Figure E.19.2 - Time Histories of Critical Strains

20) k_3 of Upper Subgrade = -0.4

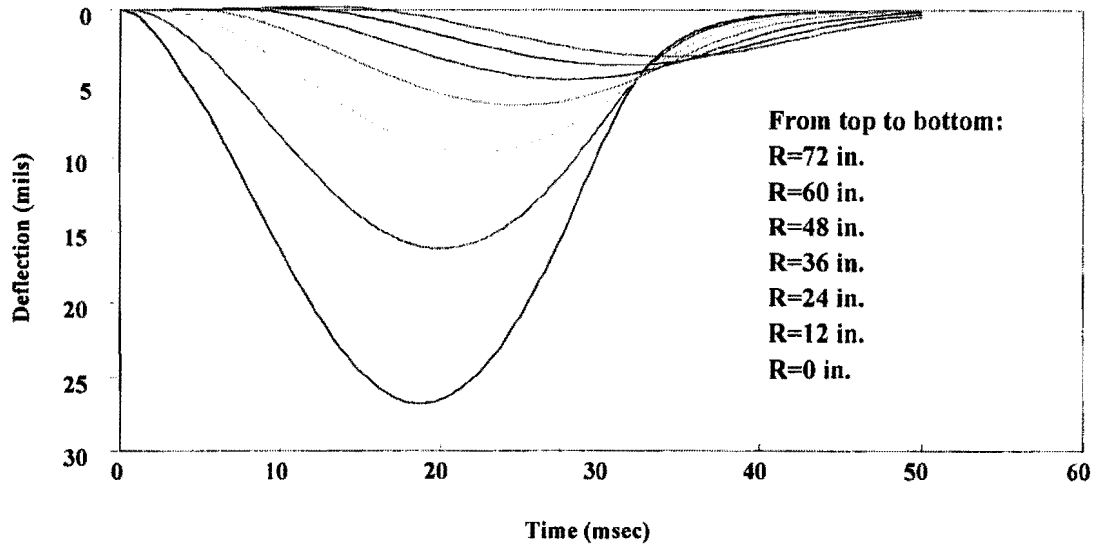


Figure E.20.1 - Time Histories of Surface Deflections

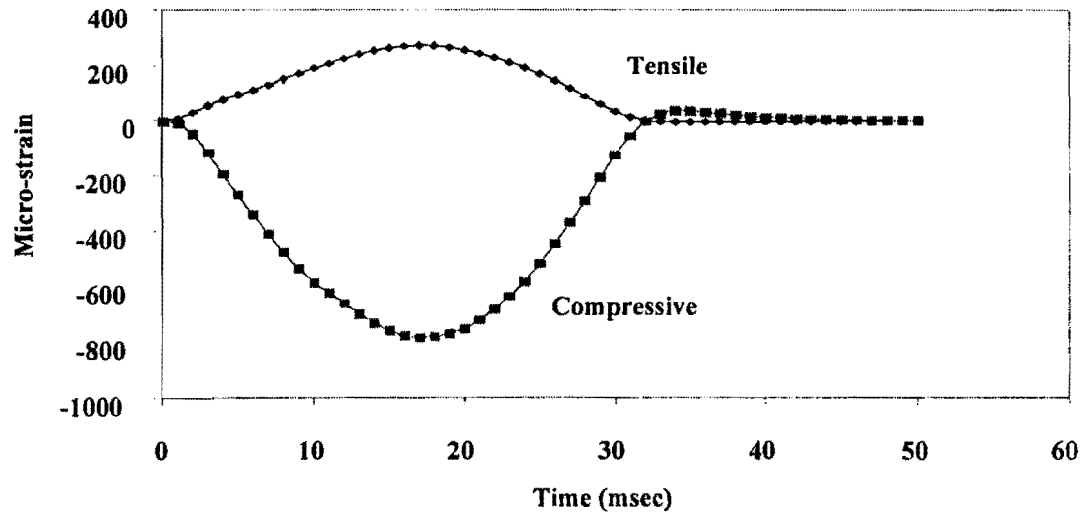


Figure E.20.2 - Time Histories of Critical Strains